Design of a demountable structural glass pavilion

M.Sc. Thesis
Wouter Lasonder

TUDelft

Design of a demountable structural glass pavilion

by

Wouter Lasonder

Thesis Committee

Prof. J. (James) O'Callaghan (Chair)	TU Delft
ir. C. (Chris) Noteboom	TU Delft
Dr. F (Francesco) Messali	TU Delft
ir. K. (Kars) Haarhuis	ABT

voor Frits

Preface

Herewith the thesis 'Design of a demountable structural glass pavilion', a research on structural glass carried out from the perspective of a building engineer. This thesis is written for the completion of the masters Civil Engineering, track Building Engineering with specialisation in structural design at the TU Delft. The final project was carried out from the first full-time day on 08 February 2021, until the oral defence on 30 March 2022, at Delft University of Technology and engineering firm ABT b.v. in Delft.

Fascinated by glass as a building material throughout my bachelors and masters, I decided to set up a project myself for the master's thesis. The research I carried out is comprehensive and, in my opinion, with a representative approach from a building engineer. By keeping the end goal in sight at all time, some points have not been worked out in detail, mainly due to the time span of the project.

On a professional level, I would like to thank my supervisors: James O'Callaghan, Chris Noteboom, Francesco Messali and Kars Haarhuis for their very professional technical and academic guidance. Everyone from ABT / Oosterhoff who helped me after unsolicited Team calls and live sparring sessions, and Martin Bijsterbosch for the effort of printing the 'coffee-cup-hand' detail. Also to the external specialists who helped me by mail and video calls: Wout Hoogendoorn, Christian Louter, Faidra Oikonomopoulou, Ron Kruijs, Mark Spijker, Milan Saleh, Helene van Lookeren Campagne - Bruins and many more; thank you very much. Lastly I am very thankful to Oosterhoff and Quake Innovation for giving Charley, Femke, Casper, Michiel and me the change to start the adventure with connECTOR.

Personally I would like to thank my mom for the support (sorry it took so long). Without my fellow graduate Jim, graduating would have been a lot more boring and difficult (bummer that I still can't beat you at table football). All ABT people at the Delft office thanks for the fun times during work but also at the drinks afterwards. I am very grateful to Max Verstappen for bringing a ray of light in the darkest days of my graduation project last December. Last but not least all many thanks to my family, friends, studymates and (former) housemates of the Spoorsingel, CPT and Vinkenstraat.

Wouter Lasonder
Amsterdam, March 2022

Abstract

Glass is a fascinating material that has also been used as a primary construction material in various remarkable buildings since the last century. Unfortunately, a lot of carbon dioxide is released during the production of glass because of the extreme heat required. The construction industry accounts for ten per cent of global CO_2 emissions. If a focus in this sector is put on recycling, reducing and reusing, emissions can be drastically reduced because of less needed new building material. However, structural glass is currently hardly reused. A second challenge arises with existing demountable structures made of glass like the LocHal: these are not weatherproof, thus unsuitable as sheltered accommodation.

In response to the absence of adequate standardised structural glass building systems, this research project proposes a preliminary design for a modular, transportable art pavilion with an appropriate structural verification. The research question is therefore: 'How can glass be applied as load-bearing material in temporary modular building units to realise easy-to-(dis)assemble, transparent and transportable structures?'.

A case-study is introduced to find an answer to the main research question. The fictive scenario is sketched to design a temporary art pavilion which stands for one to three months in a city centre in the Netherlands. After this period, the pavilion should be demounted and transported to the next destination. The information described here determines the boundary conditions for the design and calculations. The imaginary pavilion is $24\ m$ in length, $10\ m$ in width and $2.5\ m$ in height. The inner walls in the pavilion are retained to create a natural walking path inside. On the short side of the pavilion, doors are inserted as an entrance and an exit. From the available literature, the transportability of the building elements and the requirement for thermal insulation appear to be important preconditions for the final design.

The design is based on four different types of prefabricated building elements: roof panels, wall panels, floor panels and base profiles. The roof panels are of $220\ mm$ thick cross-laminated timber (CLT), in length six or three metres and have a width of $2.5\ m$. The wall panels are of laminated glass, $2.5\ m$ in height and come in two types. Insulated glass units (IGU's) of 6 or $5\ m$ long function as exterior walls. These consist of an outer sheet of $10\ mm$ fully tempered glass, a $15\ mm$ cavity of 90% argon gas and a triple laminated inner panel of $5.10.5\ mm$ heat-strengthened glass. The inner walls are of a composition of $5.10.5\ mm$ heat-strengthened glass. The glass is laminated with a SentryGlas® interlayer of $1.52\ mm$. CLT is also used for the floor panels, now with a thickness of $210\ mm$ and lengths of 6 and $3\ m$. The base is defined by steel 'cap' (RHSFB, lengths of 6 and $5\ m$) and 'hat' (THQ, length of $4.25\ m$) profiles. Both profiles are $265\ mm$ in height.

Roof connections, wall connections and base connections were designed and dimensioned, in total seven different types. The most innovative and structurally interesting joints are two wall connections. These connections consist of a so-called 'coffee-cup-hand' system; titanium elements laminated $30\ mm$ into the middle sheet of the wall panels. The wall panels are checked on maximum deflection and tensile stress, as well as the local tensile stress in the glass and in the SentryGlas® interlayer around the laminated titanium elements. All checks comply with the maximum allowable values described in the Eurocodes and in literature.

The conclusion is that the proposed design, with some enhancements to be made, satisfies the structural-, building physics- and practical requirements as a transportable and a relative transparent building system for structural glass. With this building system, glass can be integrated as a load-bearing material for designs of temporary structures.

Engineers who wish to apply this building system in practice are advised to first enhance the roof connections. For transportation means, the grid-measurements should be decreased by 8% to fit the components in a regular container. For practice, it is also advised to deal with factors such as installations and drainage systems, which were not included in this study. Follow-up research could focus on the adaptability of the building system when the building is used with a more permanent function. In addition, it is mechanically interesting to further investigate how the wall connections interact with each other in a 3D analysis and lab experiments.

Contents

Nomenclature

Abbreviations

Abbreviation	Definition
AN(G)	Annealed non-tempered glass (mainly float glass)
CLS	Collapse limit state
EPDM	Ethylene propylene diene terpolymer - A soft plastic material functioning as interlayer between glass and metal [1]
ESG	Single-pane safety glass (fully tempered)
FEA	Finite element modelling
FT(G)	Fully tempered glass
HDPE	High density poly ethylen
HS(G)	Heat-strengthened glass
IGU	Insulated Glass Unit
- DGU	Double-glass units
- TGU	Triple-glass units
- InsLIP	Insulated laminated inboard pane
- InsLOP	Insulated laminated outboard pane
Low-E	Low-emissioning insulating glass
LTA	Light transmittance value
RHSFB	Rectangular hollow section fabricated beams
SLS	Serviceability limit state
SSG	Structural sealant glazing
THQ	Top hat Q-beams
TSSA	Transparent structural silicone adhesive
TVG	Heath-strengthened glass
u.c.	Unity check
ULS	Ultimate limit state
VSG	Laminated safety glass

Symbols

Symbol	Definition	Unit
E	(Young's) Modulus of Elasticity	$[N/mm^2]$
f_c	Compressive strength	$[N/mm^2]$
f_t	Tensile strength	$[N/mm^2]$
k	Spring stiffness	$[N/mm^2]$
t	Thickness	$[mm]$
α_t	Thermal expansion coefficient	$[-]$
ν	Poisson's ratio	$[-]$
ρ	Density	$[kN/m^3]$

Part I

Introduction

1

Glass and its potential

Humanity has the ability to build structures. To build, you need construction material. It is known that building can be done with concrete, with steel and with timber. But we can also build with glass, a material that is extremely strong in its compressive direction. When glass is applied as a load bearing material, it is called structural glass. In one of the first structural glass project in the Netherlands (Figure 1.1), the potential of structural glass is clearly visible since this was used as an exhibition pavilion for art.

This section provides a brief introduction to relevant topics, then the problem statement is outlined.

Figure 1.1: One of the first structural glass projects in the Netherlands: Sonsbeek pavilion [2]

2

1.1. Introduction of the topic

To understand the problem statement and research objectives, an introduction is given here to elaborate on the basics of glass in structures, circularity and the principles of modular building and demountability.

Structural Glass

Glass has been used for centuries as a material for (drinking) glasses, windows and works of art, but only recently as a structural building material. One of the first examples of the use of structural glass is the Willis Faber and Dumas building from 1970, in which the glass fins support the horizontal forces acting on the building's façade.

What makes glass so fascinating as a building material is its transparency and strength. Although the density of glass is approximately the same as that of concrete, its compressive strength is many times higher [3]. A notable evidence of this material property can be observed in experiments of the load bearing fins at the Co-Creation Centre in Delft. One single fin of $3x12\ mm$ broken glass layers could support the entire 20-ton roof in this scenario [4]. Moreover architects prefer in many projects the beauty of glass over conventional materials, mostly because of its transparency.

Glass breakage is caused by small imperfections, which under concentrated tensile stresses at the origin propagates in larger cracks [5]. This mechanism is the cause of the material's relatively low characteristic bending strength. Several treatments can be implemented to allow greater bending stresses to act on the glass. An example of these strategies is the thermal (or chemical) treatment of glass.

As with constructions made of concrete, steel or wood, the connections in glass structures determine the structural capacity of the entire structure. Glass adds to this that the material is transparent, which means that the connections will most of the time be visible. It can be said that the connections in glass structures control the design.

Towards a Circular Economy

As can be seen from Figure 1.2, the building materials and construction sector is responsible for 10% of the global CO_2 emissions. The need for a greener planet is more present than ever; the transition towards a circular economy is inevitable to reach the Paris climate agreement goals. In the built environment therefore, the demand for sustainable solutions is high.
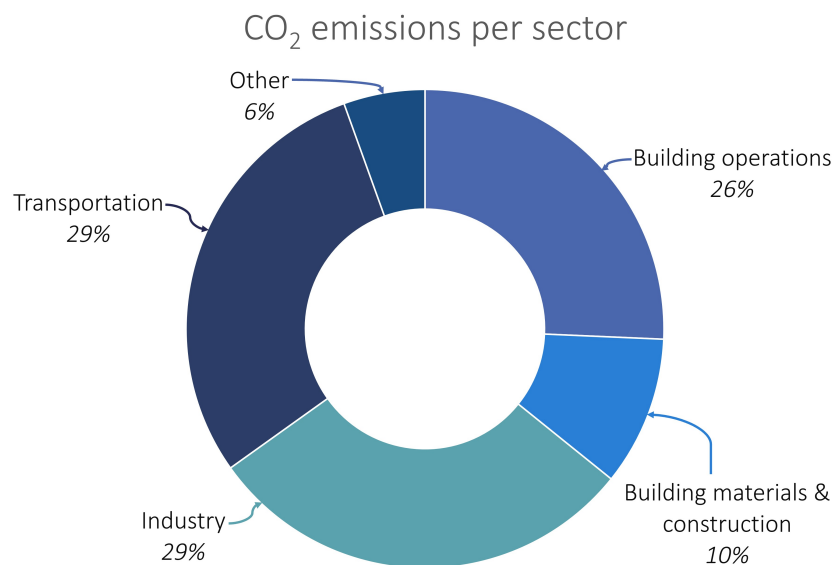
Figure 1.2: Global CO_2 emissions per sector [6]

The term Circular Economy has been widely used for years and is broadly interpreted by many scientists. Kirchherr, Reike and Hekkert gave a definition to the term in 2017 by analysing 114 other definitions which were stated in earlier research and projects [7]. According to the writers, the Circular Economy is often portrayed as a mix of activities that include the words reduce, reuse, and recycle.

In the built environment, this definition means that the use of materials should be reduced to the most optimal level, consideration must be given to the recycling of the materials used and, finally, attention should be paid to the reuse of construction materials or even (parts of) the construction itself. Below an elaboration of the three particular terminologies is given.

Recycle - Despite the fact that glass is infinitely reusable and recyclable, it fails to satisfy high quality standards when recycled and implemented in the building sector [8]. This is the main reason why building glass is almost never recycled and turned into a new glass product [9].

Reduce - The circular economy's reduce principle may very well be observed in the construction industry through material optimisation. In the last 40-50 years, engineers strive for lighter and stronger solutions in the (structural) building industry by making the structures more efficient. Material can be saved in the design of a supporting structure to make it function as effectively as possible. Not only the weight is reduced by this method, the sustainability level of the structure is also simultaneously raised. Material optimisation is done in engineering practice by conducting unity checks on the calculations, and currently also by computational optimisation software tools.

Reuse - Reusing glass is clearly shown in the packaging industry. Beer bottles for example are thoroughly cleaned and subsequently repeatedly reused. These days, there are more and more examples of glass reuse in the construction industry. A window from an old building can be utilised in a new structure; the only concern is that today's building standards must be satisfied. In the Koningskade 4 building in the Hague (the Netherlands), for example, the glass curtain wall facade did not meet todays requirements. The glass panels were for this reason removed and replaced by insulated glass units (IGU's), which satisfy the building norms. Most of the former glass panels were reused at Valkenburg airport, but downcycled presumably as elements in the interior [10].

Modular building and demountability

Modular construction means that prefabricated building components are assembled at the construction site itself. The structure is produced off-site, in factories, and later assembled on the building site. Consequently, modularity in the built environment does not describe a single structure, but a variety of materials and building systems. McKinsey research reports that the terms *prefabrication*, *modular construction*, and *off-site construction* are used in a reciprocal way and account for a broad vision of approaches and systems. The described range varies from single elements that are assembled with standard connections to complete volumes with all installations included. A distinction in the large variety of modular construction levels is made by McKinsey and showcased in Appendix B.1 Figure B.1 [11]. As with glass, the connections in modular building systems are key to the overall structural behaviour, and therefore very important for the design. [12]

The use of modular construction forms has a positive effect on many construction characteristics. This construction method not only assures a more efficient and speedier construction time like shown in the construction of Hotel Jakarta in Amsterdam. 176 Individual cross laminated timber modules were in this case assembled in a period of no more than four weeks. Modular construction also reduces the amount of space required on the construction site and improves building quality control. Contrary to this, due to the rectangular shapes used in modular construction, it may also be claimed that modular building accounts for architectural homogeneity, considered as less interesting shapes. This, according to G. Valle [13], is also the reason that there is a general lack of customisation and flexibility in modular buildings. In addition, there is a limit to the size of the building components due to the transportation limits. Lastly, prefabricated buildings require more effort and detailed elaboration at the design phase, because little can be changed during the executional phase. [11] [12]

Modular
employing or involving a module or modules as the basis of design or construction

Demountable
able to be dismantled or removed from its setting and readily reassembled or repositioned

With the circular economy in mind, the desire for reversible buildings is greater than ever [12]. Demountable structures are, according to the National Operational Guidance [14], built to be quickly assembled and disassembled several times. A fully demountable building is in principle more desirable, looking at its long-term environmental impact, than a non-demountable structure. Demountable construction does not necessarily result in beneficial outcomes. For economic reasons, for example, it may be unprofitable to disassemble a structure and reconstruct it elsewhere. Although a modular demountable building that is able to be constructed and dismantled in different configurations in different places, will take the building environment to a new level of sustainability and flexibility.

1.2. Problem definition

As described in the introduction, the construction world must become more sustainable. This can be done by using sustainable materials like bio-based solutions. But what if materials are desired that are transparent, such as glass? Glass has its challenges on topic of its sustainability, due to the following reasons:

- The production process of glass is energy demanding; high temperatures are needed and thus, glass has a relative high embodied carbon content. Future advancements in the procedure of glass making should preserve the material.
- Structural glass projects are most of the time one-off tailor made projects (see Section 5.1), meaning that the metaphorical wheel has to be reinvented time after time. This fact contradicts the principle of standardisation in the world of structural glass buildings.

A new path will have to be trodden to put structural glass in a new, environmental-friendly light. It is one step in the right direction for sustainable glass projects. Elaborating on the three principles of the circular economy, Reduce, Recycle and Reuse (see Section 1.1), it is possible to see which of these terms are used in new research to make structural glass a little more sustainable.

Recycling of architectural glass is rather difficult when the purity of glass is desired [15]. The fact that glass is transparent is the main reason why architects in some projects have the aesthetic desire to use this material as a construction. More on recycling glass can be found in the 'Glass and Sustainability' section of 5.1.

Reducing the amount of structural glass as much as possible in building projects is mostly taken care of by engineering offices in the optimisation process of the structural design. Previously, this was accomplished by human computations, but there are now a plethora of useful computer tools available. Structures are optimised to the limits required by the construction standards. Furthermore, the innovation in construction materials contributes to the reduction of materials. A structure made out of high strength glass (FT - fully tempered glass), for example, may be built with far less material than standard glass (AG - annealed glass).

Reusing (parts of) structural glass for new construction projects. According to G. Hoogerwaard's thesis about sustainable glass design, demountability plays the biggest role in the design of a glass structure. He argues that demountability should be implemented in the design to improve the sustainability of structural glass designs [16].

A complete building system that standardises the use of structural glass and allows it to be reused could be a general solution to all the sustainability problems and uncertainties regarding structural glass. A research into the possibility of using structural glass as a demountable building system might therefore boost the sustainability of glass use in temporary structures.

2

Goals and methodology

As part of an academic master's thesis, this chapter presents the research definition, methodology and the scope of this research are presented in this chapter.

Figure 2.1: West399 penthouse shows the power of a structural glass facade: bringing outside inside [17]

2.1. Research definition

The project type of this thesis is a qualitative holistic design research. A qualitative research approach makes use of research questions and not of objectives or hypotheses [18]. In this paragraph, the research outline is stated.
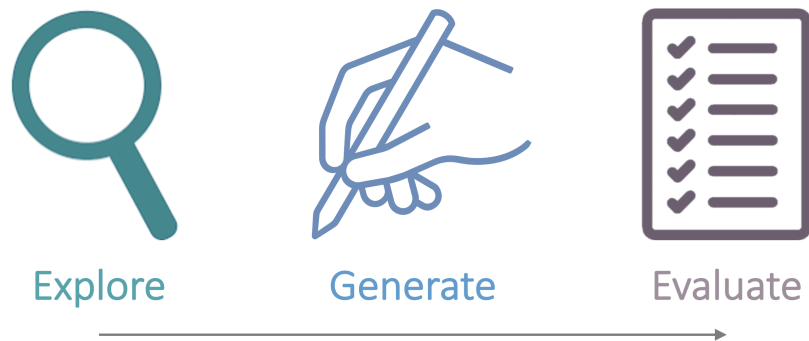
Figure 2.2: The strategy of this research

Throughout the research, the following trinity is at all times kept in mind: *Explore - Generate - Evaluate* (Figure 2.2). This is not only done in the bigger picture (*Explore* the background information, *Generate* ideas and *Evaluate* those afterwards), but also on each small scale decision.

2.1.1. Goals

The following goals together form the framework of this research. The result of this project can help engineers in designing future glass structures in a simple manner that also contributes to the principles of circular economy.

- **Explore** the principles of modular construction and structural glass design (Part II);
- **Generate** a versatile demountable structural glass modular building system (Part III);
- **Evaluate** the potential of the developed building system by verifying its structural-behaviour and -capacity and elaborate on the redundancy, transportability and assembly (Part IV).

2.1.2. Research questions

Below, the research questions are presented per designated part. To begin with, the central question states:

- How can glass be applied as load-bearing material in temporary modular building units to realise easy-to-(dis)assemble, transparent and transportable structures?

Sub-questions help to structure the research and bundle the information needed to answer the main research question:

Part II **Explore** - Theoretical framework:

- What should a building engineer take into account when structurally designing a glass structure? (Chapter 5)
- What are the design principles and constraints that define the design space for a modular demountable temporary visitor pavilion in glass? (Chapter 6)

Part III **Generate** - A temporary exhibition pavilion:

- What type of building elements are present in the design of the pavilion? (Chapter 7)
- What do the different connections physically look like? (Chapter 8)

Part IV **Evaluate** - Analyses:

- How are the stresses from horizontal loads distributed in a wall panel and transferred to a stabilising element? (Chapter 9)
- How is taken care of redundancy if one building element fails? (Chapter 10)
- How is the building system being transported and (dis)assembled? (Chapter 11)

### 2.1.3. State of the art

Structural glass has not yet widely been used as primary construction material for (modular) building solutions. Modules are now more or less constructed by steel, prefabricated concrete and/or a timber frame, whereas glass is mostly used in glazing for windows [12]. The choice of a demountable structure is important for the design decisions taken. The design and utilisation of the connections in particular has a significant impact on this. Besides, the (diss)assembly order and method must be properly considered, whereas for non-demountable buildings this is less important. Examples of demountable modular constructions with the use of glass in it are for example Bouwdeel D(emontabel) and glass hall of Octatube, respectively Figure 2.3a and 2.3b.

Building section D(emountable) is an office building in Delft, consisting of prefabricated and lightweight materials. According to the architects, the building is an exemplary project for building in a circular economy. The building can be disassembled in its entirety, and the components can be easily reused [19]. After the building's lifetime, the office can easily be disassembled. The question remains whether the building will be completely rebuilt afterwards, or whether the materials will be recycled. Of course, economic concerns will play a role in this consideration.

The glass hall, designed by Octatube, was engineered in the beginning for the Beurs van Berlage in Amsterdam. The hall functioned as a music hall for the Dutch Philharmonic Orchestra and demanded high performing acoustic standards [20]. At that time, in 1990, the construction was the first frameless glass construction in the Netherlands. Steel forms the main load-bearing structure in this building, and carries the glass panels [21]. The remarkable fact of the glass hall was that it was fully disassembled, stored and later rebuilt in 2018 in the city of Tilburg. With a few adjustments, such as replacing the glass roof panels with laminated glass, the glass hall is useful for the present time [22]. The structure now serves as a hall for gatherings. [20]
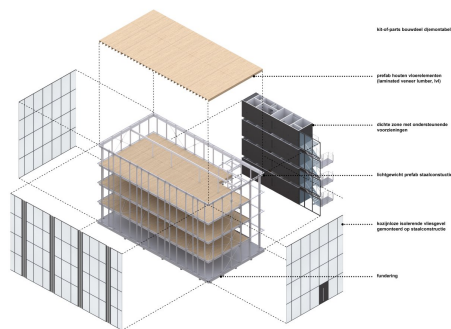
(a) Cepezed's Bouwedeel D(emontabel) [19]

(b) Glass Hall, here in the Beurs van Berlage, from [21]

Figure 2.3: Demountable structures with glass as dominant material

One example of a fully glass structure that has proven to be demountable is the Glaspavilon. The glass building from 1995 by Ulrich Knaack and Thomas Link was built for the 125th anniversary of the Rheinisch-Westfälische Technische Hochschule Aachen [23]. A picture of the connection wall panel - wall panel shows no decent solution for moisture and rain penetration. More technical information about the Glaspavilon can be found in Part II, Section 5.4.

A linear reversible interlocking connection by Oikonomopoulou, researched in 2013, is shown in Figure 2.4b. According to the author, there are several complications involved in the connection regarding the manufacturing precision and the assembling [24]. More on this connection is written in Section 5.4.

(a) Wall panel - wall panel - glass fin connection in the Glaspavilon (1990), from [23]
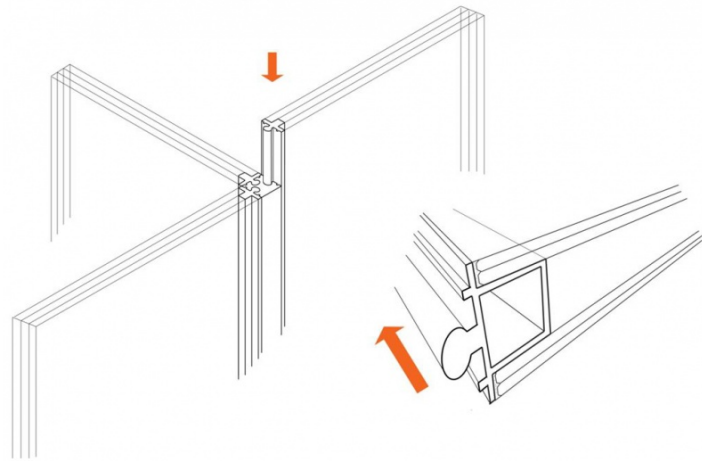
(b) Design for a reversible slender connection system

Figure 2.4: Details of structural glass connections

2.2. Methodology

This section deals with the methodology that is applied to the different sections, distributed over the research questions. By doing investigation in the sub-questions, an answer can be found on the main research question.

> How can glass be integrated as load-bearing material in temporary modular building units to realise easy-to-(dis)assemble, transparent and transportable structures?

2.2.1. Part II - Explore: Theoretical framework

Part II has the literature review as its content and will mainly describe the background theory necessary to make the research successful and has as overall goal to set the design criteria and considerations for the design phase.

What should a building engineer take into account when structurally designing a glass pavilion? (Chapter 5)
Goal: Providing basic knowledge of glass as a material: its origin and history, its production methods and an overview of projects already completed. Besides, a general building physic knowledge is to be gained and the effect of glass on the building physics should be determined.
Methodology: The books *Structural Glass - Design and Construction of Self-Supporting Skins* [3] and the *Glass Construction Manual* [25] will mainly be used to answer the first sub-question. Missing information will be supplemented with content from various webinars, articles and miscellaneous.

What are the design principles and constraints that define the design space for a modular demountable temporary visitor pavilion in glass? (Chapter 6)
Goal: Creating a design area for the modular building system. Some issues will have to be simplified or even be eliminated out of the scope. A well thought-out design area and a list of requirements is key for a smooth design process.
Methodology: The literature of Wurm [3], Schittich [25] and IStructE [26] all give design principles of glass. In addition, the Bouwbesluit [27] provides various requirements with which a temporary structure must comply.

2.2.2. Part III - Generate: A temporary exhibition pavilion

Part III may be called the body of this thesis research. This part embodies the design of the building elements needed for the construction of the temporary pavilion. Besides, it elaborates on the different details, gives a structural verification of the system and goes into depth about structural redundancy. Finally, Part III provides information about transportation and assembly of the pavilion.

What type of building elements are present in the design of the pavilion? (Chapter 7)
Goal: List the different construction elements needed to successfully realise the temporary exhibition pavilion. Describe their main characteristics. The elements should prove the structural safety of the building, in terms of stability and strength.
Methodology: With the list of requirements and the scope of the research in mind, the pavilion is divided into separate building elements. Clear diagrams are used to visualise the force transfer in vertical and in horizontal direction. The dimensions and

properties of the building elements are given.

What do the connections physically look like? (Chapter 8)
Goal: Presentation of detailed drawings of the connections that are required for the building system to function.
Methodology: Inspiration can be retrieved from the literature study and reference projects. For the drawings, computer software is used to visualise the detailing in both 3D and 2D. The locations of the particular joints are additionally pointed out. For the dimensions of the details, the critical forces per detail must be highlighted.

How are the stresses from horizontal loads distributed in a wall panel and transferred to a stabilising element? (Chapter 9)
Goal: Establishing a well-founded analysis of the stresses in a glass wall panel. A local analysis is besides meant to check if the detailing wall to wall is sufficient or should be modified.
Methodology: There is a particular structural verification of the most critical outer wall panels with a non linear analysis and both a linear and non linear analyses of the load transfer in the detail between the walls. These analyses are executed by structural analysis via finite element modeling (FEA).

How is taken care of redundancy if one building element fails? (Chapter 10)
Goal: Not only a structural analysis is made of the pavilion's structural resilience, but also a replacement strategy in the event of collapse of one (part of a) building unit is defined.
Methodology: Describing the secondary load path in case of a failed building element and displaying a step by step method for replacing building components. It is very important to elaborating on the construction method and sequence of the modular building system.

How is the building system being transported and (dis)assembled? (Chapter 11)
Goal: Showing the added value of a modular building system; the transportability and ease of (de)construction.
Methodology: The goal is achieved by demonstrating how building elements fit into a standard container. In addition, it is precisely described how the pavilion is being assembled.

2.2.3. Part IV - Evaluate: Conclusions
What are the building system's main advantages regarding functionality and flexibility? (Chapter 13)
Goal: Evaluation of the pavilion and identifying the potential of the designed building system.
Methodology: Not only describe the power of the building system, but also a critical discussion is stated if the designed building system contributes to more sustainable glass construction.

2.3. Scope

Generating a building system that structurally verifies the Dutch norms is the goal of the research. The study makes use of a holistic design approach that, in practice, means that the details of the design are part of the bigger picture (the modules), which in turn are part of a structure. Thus, the detailed design takes into account the overall picture of the building system.

2.3.1. Focus

The building system in the end will hypothetically give designers the opportunity to realise easy-to-(disassemble), transparent and transportable structures, as was stated in the main research question. Below a clarification of the various terms given.

- Temporary and easy-to-(dis)assemble
  A design criteria that will be kept in mind is that the structure should be easily (dis)assemble and transportable, making the structure location independent. Transportation limits define the maximum sizes of the elements and the demountability criterion will have a significant effect on the connection types used. The easier and quicker it is to disassemble and reassemble a temporary structure, the cheaper, more accessible and more feasible the building system will become.

- Modular building units
  The end project should be modular, implying that the structure consists out of prefabricated elements which are as modules assembled together on the building site [12]. A new building system will be extensively researched which later can be used in different settings to create, for instance, pavilions. It is crucial to keep flexibility in mind, because the exact function of the building to be designed is not known.

- Transparent
  Glass will be used as main construction material for the pavilion. Using glass as load bearing material improves the transparency of the construction. Therefore, particular attention should be paid to the parts that are opaque, as these will attract the viewer's attention. To keep it as transparent as possible, it is important to keep the opaque elements sober and small.

Building physics requirements, glass (supplier) characteristics and modular building principles will hypothetically state the main limitations for the design, they will however not be part of the research's body. Subsequently, these topics are thoroughly studied in the literature review. Later, in Chapter 6, design criteria are listed to define the ultimate scope (or: design area) of the research.

2.3.2. Scope limitations

Out of scope topics are:

- Elaboration on the necessary foundation and settlements;
- Details on services and installations;
- Extensive non-glass element verification;
- Architectural features like doors, colours, light plans etcetera;
- Consideration of costs.

3

Case study

In the time frame of this research project, it is unfortunately not possible to deliver and test a completely verified building system. In order to make a distinction, a case study is set up to limit the range of the thesis. This allows for the creation of unambiguous preconditions later in the project, which define the design area. First, a fictive scenario is sketched as a design problem. Second, a preliminary design for the problem is presented.
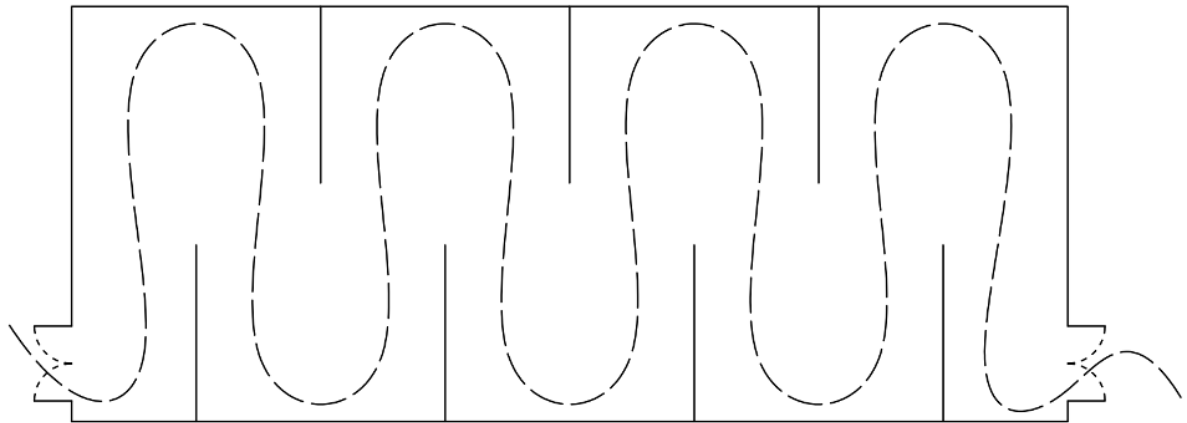

Figure 3.1: Floor plan with a route for the interested visitor

3.1. Scenario

A pavilion is asked to be designed for a commercial travelling sculpture and painting exhibition. The director wants to create maximum transparency of the for the passer-by to feel invited to visit the exhibition. The client defines a desired floor area of around $240\ m^2$ and prefers to have as much open space as possible. She wants to create a visiting experience by making a one-way route through the building. The pavilion should be engineered to travel through the Netherlands. The design should incorporate the ability to be disassembled, transported and put together again in a different inner-city. Eventually, the pavilion should compromise to the building standards in the country on structural and building physical level.

3.2. Physical outline of the pavilion

An impression of the imaginary art pavilion can be found in Figure 3.2. The imaginary pavilion's dimensions are 10 by 24 metres, with an internal height of 2.5 metres. The total surface area of the building will therefore be $240\ m^2$. These dimensions have been established with the demand from the client, and the CoCreation Centre ($17.5 * 26.5\ m$, $6\ m$ high) in mind, as a real comparative structure. On both ends, doors will serve as an entry and exit to the pavilion. The interior walls that have been placed, provide with their placarding a natural walk for the visitor from the entrance on one side of the building, to the exit on the other side. For this reason, the interior walls have been shortened to $4.25\ m$, leaving $1.5\ m$ in the middle on the long axis for a natural walkway.

Figure 3.2: Impression art pavilion
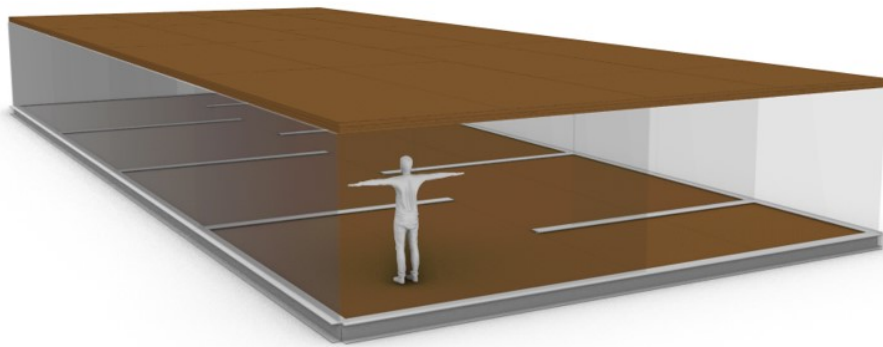
Two different routes for visitors of the pavilion are showcased in Appendix B.1. Route 1 is intended for the more intrepid visitor who wishes to explore every inch of the art show. Route 2 is a speedier route that also demonstrates the presence of a walkway in the middle owing to a shortening of $75\ cm$ of the inner walls. Technical information about the design can be found in Part III.

4
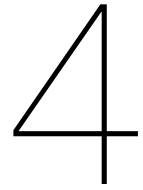
Structure of the report

Literature research, reference projects and the building standards determine the programme of requirements and provide necessary inspiration for the design. The building elements and connections are then technically examined one by one in terms of dimensions and structural and building physics behaviour. Then, by means of computer analyses, the report goes into detail on the structural behaviour of critical outer walls and on the connection between outer and inner walls. This is done by means of linear and non-linear calculation models in the program DIANA finite element analysis. Finally, the failure analysis describes what happens if a building element collapses and the transport and the procedure of building are described.

Three stages define the process of this design project; *'Explore'*, *'Generate'* and *'Evaluate'*. The report's structure will be taken the following structure:

- Part I - Introduction

    - Glass and its potential
    - Objectives and methodology
    - Case study definition

- Part II - Explore: Theoretical framework

    - Theoretical background
    - Design principles

- Part III - Generate: A temporary exhibition pavilion

    - Pavilion design
    - Connection design

- Part IV - Evaluate: Analyses

    - Detailed analysis: IGU's and 'coffee-cup-hand' system
    - Redundancy
    - Transportation and assembly procedure

- Part V - Conclusions

    - Discussion
    - Conclusions
    - Recommendations

Part II

Explore: Theoretical framework

5

Theoretical background

This chapter provides general background information about glass as building material that is useful while developing the building system. Four different topics are explained:

- Glass as building material (Section 5.1)
- Connections (Section 5.2)
- Building physics (Section 5.3)
- Reference projects (Section 5.4)

Figure 5.1: Clamp connections in the facade of the Markthal, Rotterdam [28]

5.1. Glass as building material

Background information about the history of glass and the production technologies is covered in Appendix C. Relevant background about the material itself is described in this section.

What is glass

Construction glass consists mainly of silica, which can be found in pure quartz sand. This type of sand is usually called silicate glass. The silicate glass, together with soda ash, is a crucial ingredient in forming glass. The soda ash (sodium oxide) ensures that the conversion into glass takes place at lower temperatures, making the manufacturing process easier. The addition of calcium oxide as a stabiliser increases the protection against chemicals of the glass to be produced. Finally, to improve the optical properties of the glass, additives can be added to the process. [3]

When the molten material cools, a crystal lattice is formed, with a unique molecule pattern for each glass. The molecules do not have time to reposition by the quick cooling down process. In contrast to structural wood, for example, glass is an isotropic material - its mechanical properties are orientationally and directionally independent. Glass is considered a "super-cooled" liquid due to its amorphous appearance at the molecular level. [3]

Properties

Glass is a brittle ceramic material and does not exhibit plastic deformation behaviour, which means that the material is not capable of transmitting high peak stresses. This means that the glass cannot redistribute the loads, coming from an external force, in a plastic manner [1]. Hence, possible peak stresses should be avoided by carefully designing the details. Moreover, glass cannot absorb large amounts of energy. The reason why glass is rather brittle is that surface defects easily lead to crack growth. Consequently, the actual tensile strength of glass is much lower than its theoretical value (about 100 times!). [29]

	Glass		Steel		Concrete		Wood	
	Sodalime	Borosilicate	S235	S355	C30/37	C50/60	C18	GL24h
ρ $[kN/m^3]$	25	22.5	78.5	78.5	25	25	3.2	3.8
E $[GPa]$	73 (AN) 70 (HS/FT)	63	210	210	33	37	9	11.6
f_t $[N/mm^2]$	4.5	8.3	235 (yield strength)	335 (yield strength)	2.9	4.1	// 11 ⊥ 0.4	// 16.5 ⊥ 0.4
f_c $[N/mm^2]$	50 - 200 [3] & [30]	93	235	335	30	50	// 18 ⊥ 2.2	// 24 ⊥ 2.7
ν $[-]$	0.23	0.20	0.30	0.30	0.20	0.20	n/a	n/a
α_T $[10^{-6}K^{-1}]$	9	3.3	12	12	10	10	n/a	n/a

Table 5.1: Material property comparison between most used glass, steel, concrete and wood species, data gathered from Eurocode 3 (Steel), 4 (Concrete) and 5 (Timber), Wurm [3] and Springer's Handbook of Glass [31]. See Nomenclature for symbol elaboration.

Glass type	Characteristic bending strength $f_{b;k}$ $[N/mm^2]$
AN	45
Enameled HS	45
HS	70
Enameled FT	75
FT	120

Table 5.2: Bending strength of sodalime glass types [31]

The mechanical properties of glass (Soda-Lime glass) can be found in table 5.1. Be aware that the tensile strength of glass depends on many factors [3], like:

- Load duration and conditions
- Pane size
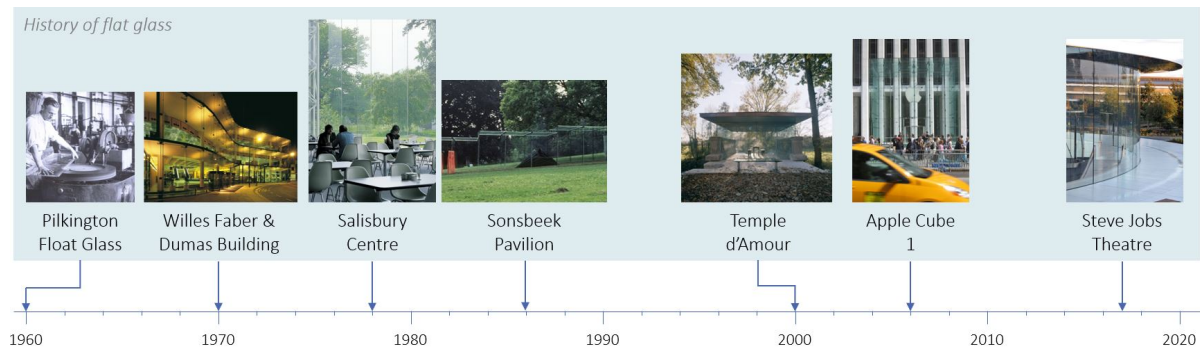- Pane age (important for the durability)
- Type of glass

Figure 5.2: History of flat glass, for a complete overview together with cast- and extruded glass, see Appendix B.2

- Surrounding air moisture content

The article of F. Veer [32] concludes that there are significant differences in the glass composition from different suppliers, which are due to the change in temperature of the glass. These differences can cause problems such as optical distortions and uneven toughening of the glass [32]. Table 5.1 shows characteristic values of glass, both sodalime and borosilicate, compared to conventional materials.

Glass and sustainability

Theoretically, glass can be recycled indefinitely by remelting the material. In practice, however, this sustainable property of glass is not widely applied. Only a small percentage is recycled today, mainly by the glass bottle and container industry. Most of the glass that is thrown away cannot be recycled because of the current quality standards of the glass trade [8], with high demands on the appearance (iron content) of the glass. Moreover, problems arise in recycling laminated glass with interlayers that cannot be properly separated from the glass [33]. There are project in which the glass is being reused for various purposes, like in the Koningskade project in The Hague (earlier mentioned in the Introduction in Part I), however in that project the glass appears to be downgraded in its future of its lifecycle.

Glass as load-bearing element

Since the excavations at Pompeii, we know that glass was already used as a window in Roman times. A window must be able to withstand wind loads and can therefore be considered a structural element. However, windows are considered secondary structures [34]. This chapter looks more closely at the use of glass as a primary load-bearing element.

As can be seen from the history of glass in the figure in Appendix B.2, glass was ignored as a primary load-bearing material for a very long time. According to Wurm [3], this phenomenon was due to the steel institutes and companies. Wurm also states that glass is still developing its own form language and is still dominated by the tectonics of steel construction.

Float glass

About 90 percent of glass use in the construction industry is float glass [3]. Today, more than 70% of flat glass is used in new buildings or in the renovation of building skins, the other part is mainly used as packaging material [3][8]. A brief history of float glass as structural material can be found in Figure 5.2.

The production of float glass is one large linear process. Silica, soda, limestone and other raw materials go into the furnace. These are combined and heated to about 1600 degrees Celsius to reach a molten glass state. Then the molten glass floats on a bath of tin (about $1100°$), which causes the glass to take on a linear thin shape due to the controlled mechanical drive. The glass leaves the tin bath at about $600°$. The glass is thereafter annealed in a special cooling unit and further cooled with air to room temperature. Finally, the glass rolls through machines that check its quality, after which the glass is cut into the desired format. [35]

Cast glass

Glass is cast by pouring molten glass into moulds and allowing it to cool down. Three-dimensional structures of glass can subsequently be produced in theoretically any shape [36]. An additional advantage of this glass production method is that it can be used in a reasonably easy way to recycle waste glass [8].

Cast glass blocks are widely used in projects as partition walls, but until recently were not used as load-bearing elements. The Crown Fountain (2017) in Chicago is an example of a cast-glass project in which the bricks act as the dominant load-bearing structure. Two years later, in Madrid, the Atocha Memorial was unveiled. Together with researchers from TU Delft, 'Crystal Houses' was built in the centre of Amsterdam, pushing the boundaries of structural cast glass building [36]. A history of cast glass in building projects is displayed in the figure in Appendix B.2.
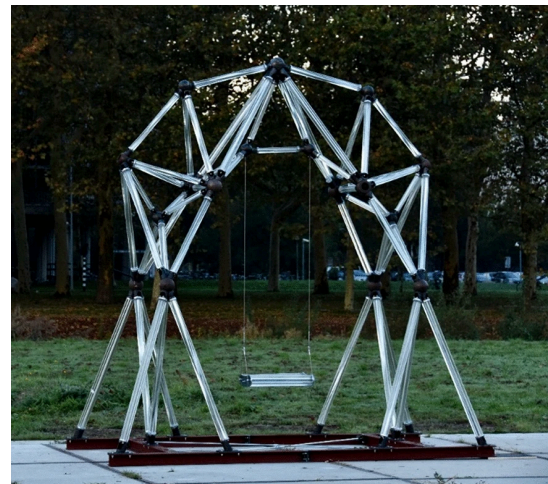
Extruded glass

As with the production of float glass, the process of making extruded glass begins with the mixing of the raw materials in a mixer, which makes the substance homogeneous. The mixture is then processed into a paste by a screw extruder. Next, the honeycomb die ensures that the glass comes out of the machine as a linear rod and is cut to size at the end. [37]

The glass truss bridge is an example of an extruded glass construction and is located on the Green Village of the TU Delft campus. In 2016 a design competition was held for the design and engineering of the bridge and a year later the bridge was built. Glass diagonals form a Warren truss and act as a supporting structure for the bridge deck. The diagonals consist of six $20\ mm$ glass rods with a $12\ mm$ steel rod in between [34]. The bridge proved to be structurally safe when a group of 60 people walked across the structure.

The glass swing immediately explains its own name. The swing is made up of similar lattice elements to the glass lattice bridge; a steel rod within bundled glass columns. The bundles are connected by 3D-printed steel or the thermoplastic polyester PETG. The glass swing was optimally designed by parametric design and engineering, using modern calculation software. Complicated dynamic loads result from the function of the structure, showing that glass can also be structurally applied in rather irregular situations. [34].

(a) Glass truss bridge, from [38]

(b) Glass swing, from [39]

Figure 5.3: Extruded glass structures

Treatment of glass

Glass can be treated by thermal or chemical processes and finally laminated to meet safety requirements. Functional coatings, or thin-film coatings, are applied to the surface of float glass to treat the material, i.e. change the optical properties of the glass.

Thermal treatment

Heat-strengthening *(HSG)* and (fully) tempering *(FTG)* is done by (rapidly) cooling down the glass after production. The residual stresses that are formed by this process in the glass improve the bearing capacity and influence the breakage pattern in particular modes [3]. Fully tempered glass, for example, breaks into much smaller pieces than non-thermally strengthened glass.

In the case of structural use of tempered glass panes, the manufacturer is advised to test the glass by the heat soak method, a destructive test. Possible Nickel-Sulfide inclusions are being traced, which might be the cause for fragmentation of the glass [40]. The method of Nickel-Sulfide inspection of [41] showed that less than 1.7% of the 1000+ tested glass panels had these imperfections. Glass company *Guardian Glass* claims that not the heat soaking method might not be fully effective [42], but in 2018 was found that heat soaking testing is more reliable than previously stated [43].

Lamination of glass

At the end of the manufacturing process, glass should be laminated to reach the safety requirements as load-bearing material. This is done by placing two or more panes of glass on top of each other with in between a interlayer. Laminated panels are labeled with types of code to clarify its composition. To illustrate, 12.12FT means that two layers of fully tempered glass are laminated.

Laminated glass is an example of so-called safety glass. This type of glass is characterised by the fact that it does not immediately collapse in the event of an impact load, such as a passer-by with a hammer. The softer, binding interlayer that laminated glass possesses keeps the collapsed glass in place by the bond to the unharmed panel(s).

Insulated Glass Units

Laminated glass should not be confused with isolated glass units (IGU's). The glass panels in IGU's are separated by a distinct gap, meant to increase the insulating capacity of an IGU. An IGU can be used with double glazing (DGU) or even triple glazing (TGU). Main properties of IGU's are the type of glass, type and placement of coatings if applied, the width of the cavity, the type of gas filling and the edge seal.

When there is a pressure on the exterior of a panel (e.g., wind or climate load), the airtight cavity in an IGU must balance with that particular pressure. This phenomenon is also known as isochoric pressure. The size of the spacer in the glazing must be able to withstand the resulting pressure in the cavity. The cavity will no longer be airtight and will lose its insulating capability if the spacer cannot support the stresses induced by the pressure in the cavity. According to NEN 2608, there is no need to take isochoric pressure into account if the shortest side of the IGU is longer than one metre. As a result, the phenomena of isochoric pressure appears to be limited to smaller-sized, unbent windows only. Climate load experiments are executed in Stratiy's paper [44] to offer further technical information on this issue. [45]

Laminated glass panes can also be used in insulated glass units. The cavity in between glass panes is usually between twelve to sixteen millimeters and filled with argon or krypton gas, although 100% air can also be used. By implementing gases such as Argon and Krypton, the circulation in the cavity is better counteracted, thus reducing the release of heat by convection by these molecules from one glass pane to the other. [45] [3] [46]

5.2. Connections

This section distinguishes between connections in glass projects and modular construction connections. Only the most relevant connection typologies for the case study are discussed. The rest is elaborated on in Appendix C, as stated below:

- Glass connections

    - Embedded laminated connections
    - Continuous linear support connections (shown in appendix Section C.2)
    - Clamp connections (shown in appendix Section C.2)
    - Friction connections (shown in appendix Section C.2)
    - Bolted connections (shown in appendix Section C.2)
    - Adhesive connections (shown in appendix Section C.2)

- Interlocking connections
- Glass interlocking systems (shown in appendix Section C.2)
- Modular connections
- General
- Modular interlocking connections (shown in appendix Section C.2)

Glass connections

Connections and restraints have a critical role in the design of 3D structures. This is, on the one hand, due to when the structure is subject to extreme loads over the design life, on the other hand, due to the possible interaction between single glass components and other structural members. Connections between multiple glass components is one of the main principles of glass engineering [1]. The connection design in (structural) glass facades can be of enormous complexity, as can be seen in the detail of the Apple Store Westlake in Hangzhou (Figure 5.5).

In the existing literature, a subdivision is made into different types of glass connections, but a general distinction is lacking. The various subdivisions are highlighted in Tables C.1, C.2 in Appendix C.2 and 5.3 here.

Connection type	Category	Sort
Force	Friction grip	Clamping plate (point fixing)
		Clamping rail (linear)
Mechanical interlock connections	Contact Connection	Linear blocks
		Punctiform blocks
		Bearing bolt connection
Adhesive connection	Adhesive	Adhesive point fixing
		Linear adhesive (SG)

Table 5.3: Connection typology of Wurm [3]

Embedded laminated connections

A more recent innovation on topic of non-penetrating connections in glass is the laminated connections. [49]. An example of such embedded connection is the connection typology used in an Apple Store staircase, which was already patented in 2003, shown in Figure 5.6a.

More recent embedded connection research [49] show that laminated connections are efficient load transferring elements. In this research, a 6-10-6 glass composition was used with an embedded stainless steel element in the middle recessed glass layer. This metal insert was bonded to the glass with a SentryGlas® layer. At the bottom of the laminated connection, a strut-and-tie behaviour of stressed can be recognised during the in-pane load transfer, shown in Figure 5.6b.

In a later research, Bedon and Santarsiero describe the numerical analysis of the full-scale test of glass beams with laminated connections. Using finite element modelling is a proper alternative to time- and money-consuming experiments. Their research validated detailed finite element models with results from experimental tests. Three type of embedded connections were investigated (Figure 5.7). [51]
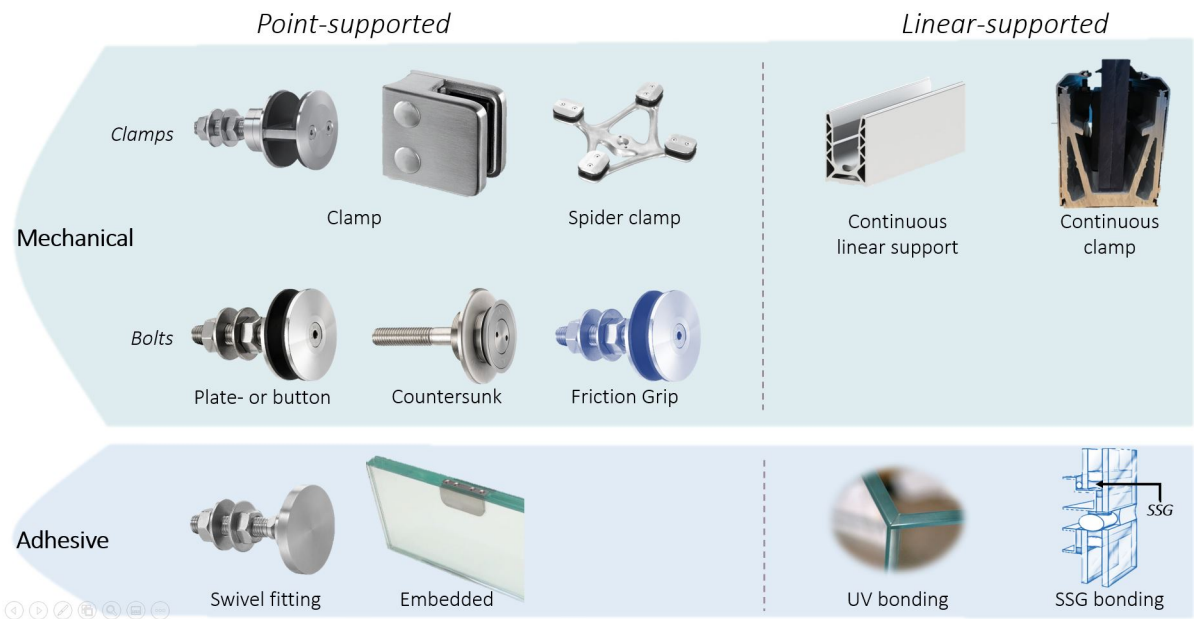
Figure 5.4: Overview glass connections, for more elaboration, see Appedix figures B.4 and B.5

Figure 5.5: Detail of the Apple Westlake Store, in which the complexity of a glass detail at the top bracked facade can be seen, information from[47] , image from [48]

(a) Detail of the 2003 embedded connection [50]

(b) In-pane load transfer mechanism during monotonic testing [49]

Figure 5.6: Laminated connections

Figure 5.7: Composition of the three different embedded connections from Bedon and Santarsiero [51]

Modular connections

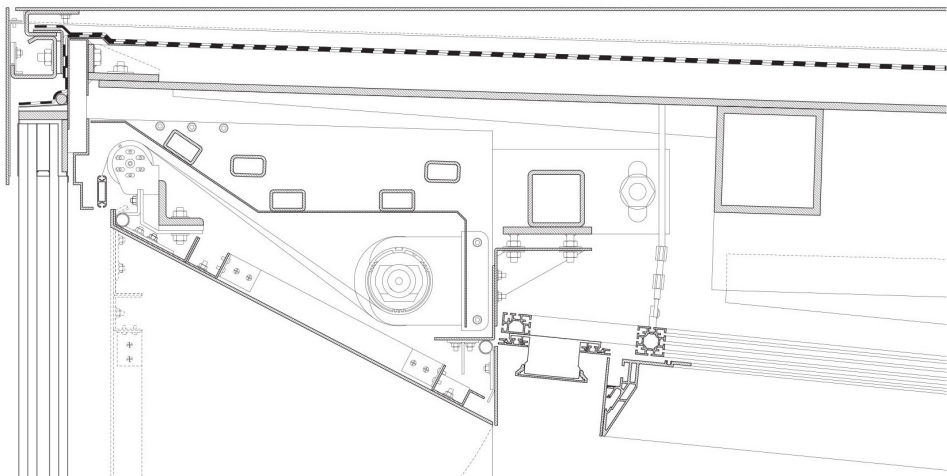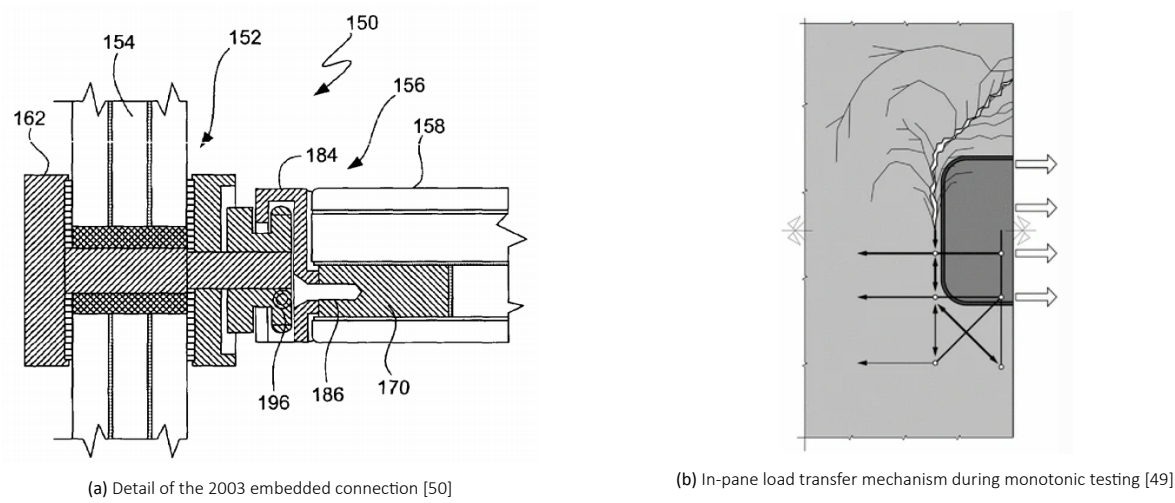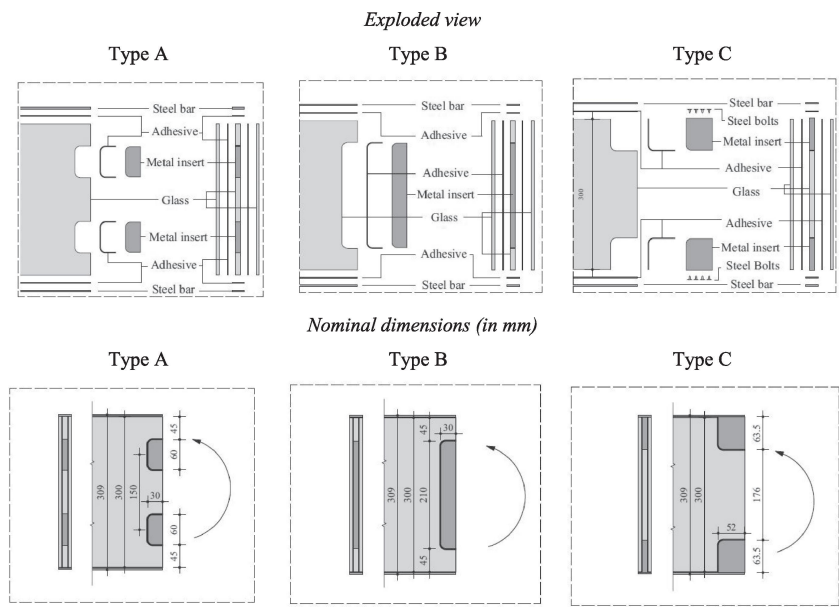Post - World War II, East Germany had a severe housing shortage of around 1.4 million units. As a result, a government-driven housing plan was introduced in politics to solve this problem. This was a unique chance for the USSR to turn East Germany into a communist model state. The design philosophy behind this mega plan was that people needed a house (apartment) to live in, without useless decorating elements. The slogan at the time became 'Build better, cheaper and faster'. [52]

Subsequently, mass-produced housing projects were initiated, for which experts travelled to France to study precast systems. Precast concrete elements proved to be the answer to the housing problem not only in the DDR, but throughout much of Europe. In the years that followed, this Krushchev-inspired construction technique became the norm in East Germany. The identity of architects is gradually translated into standardised building systems. It was relatively simple to design a building using these methods without the involvement of architects. The subsequent technological development of more powerful construction cranes made it possible to assemble even larger prefabricated elements on the building site. [52]

(a) Mass-housing in Marzahn, East-Berlin [53]   (b) A dwelling made out of recycled concrete panels [54]

Figure 5.8: Transformation from mass-house production to more human residential areas

After the fall of the Wall in 1989, there was a mass migration from East to West Germany of about 2.8 million people. Following the massive housing scarcity, the former DDR suddenly had a substantial surplus of homes. The large housing blocks that had been built were partially dismantled and transformed into residential areas of three to four levels high, in a more humane form than the communist building style of before. [52]

The physical transformation from large residential buildings to more friendly housing, such as that seen in Germany, has demonstrated that prefabricated concrete construction offers several advantages. The concrete parts proved to be of great quality when reused, because they were manufactured in a factory rather than on-site. Furthermore, the utilisation of prefabricated pieces was a significant benefit over mass home deconstruction, with its 'demolition' being the reverse process of construction. The deconstruction site had relatively little debris, and the disassembled elements were commonly repurposed in future projects, as seen in Figure 5.8. [52]

The history described above marks an important point in the development of modular, prefabricated construction. Whereas the preceding section focused on the employment of standardised concrete elements and their reuse, now the focus is put on various modular building connection concepts.

Modular construction is possible on every level. As mentioned earlier, a report by McKinsey provides a subdivision into the scales and complexity in which modular construction can take place (image in Appendix B.1). With this extensive subdivision and timber construction principles, three different levels of modularity are qualitatively subdivided and compared with their capacity for transportablity, (dis)assembly, transparency and replacement. The three levels, increasing in the number of individual parts, are named linear, surface and volumetric. The overview is visually shown in Figure 5.9.

Modular building has a sincere effect on the design of the structure's connections. Lacey et al. [12] divides the connections in modular structure into three categories: inter-module, intra-module and module-to-foundation (Figure B.6 in Appendix B.2). Here, the author gives the advantages and disadvantages of various techniques for realising these connections. It should be clear that the welded variants are not desirable when the particular connection has to be demountable.

Figure 5.10 shows the possible inter-module connections in modular steel buildings. Although not especially meant for modular glass construction, these connection typologies might give engineers crucial insight in modular construction. It is important to understand the structural behaviour of the inter-modular connection types. all connection types are bolted but differ in force-displacement and moment-rotation bearing regarding structural behaviour. [55]

Lacey et al. emphasise the important factors of inter-modular connections, they state that attention must be paid on the:

- compactness;
- ease of on-site installation;
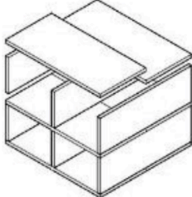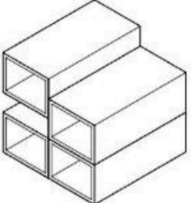- tolerances, and;
- demountability.

Figure 5.9: Different levels in modular building units with their characteristics

	Linear '1D'	Rectangular '2D'	Volumetric '3D'
Transportability	Efficient use of space when structure is demounted. Light building units.	Since the units are (almost) 2D, the building system can be stacked in an efficient manner.	The building units will be very heavy. No efficient use of the space, large residual space.
(Diss)assembly	Much effort to diss(assemble) the structure, many connections.	Adequate ease of (de)mountability. Clear number of connections.	Very quick (diss)assembly of a whole structure, few connections.
Transparency	Many connections could mean less transparency. Connections draw attention of passers-by.	Transparency can be relatively high. Consider linear intermodule connections carefully.	Large transparency can be reached by glueing glass panes internally.
Replacement	Ease replacement of possible broken building components.	Moderate ease of replacement when one component fails.	Complete replacement of one module is necessary in case of failure of only one component.

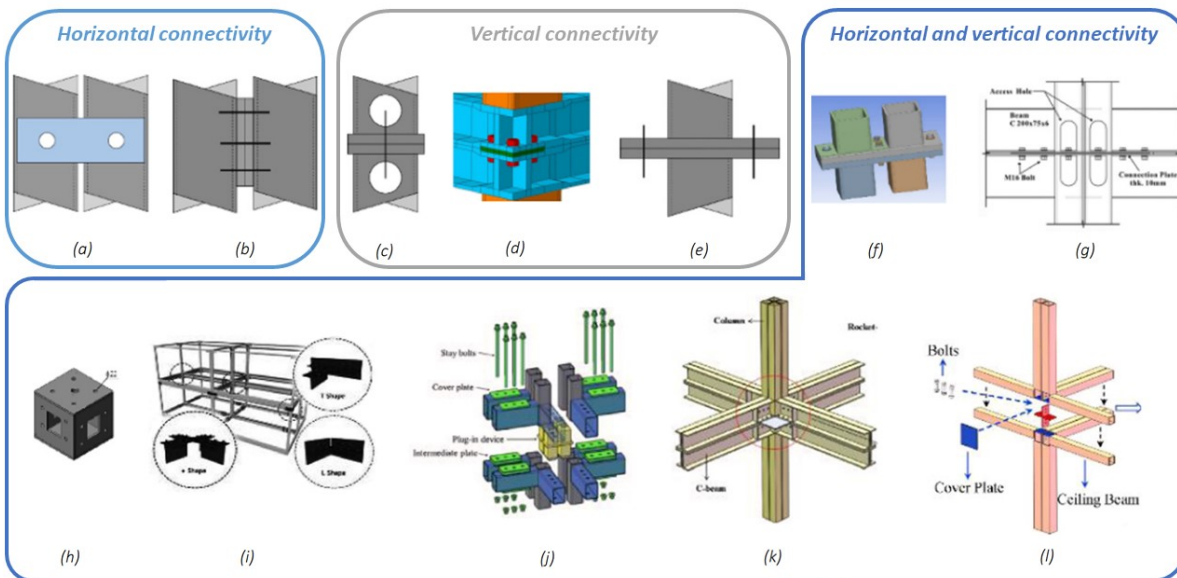Figure 5.10: Existing inter-modular steel connections, (a) Tie plate; (b) Bolted side plate; (c) Bolted end plate; (d) Bolted connection; (e) Bolted end plate 2; (f) Bolted end plate (complex); (g) Bolted connection plate; (h) Steel bracket; (i) Steel bracket 2; (j) Bolted connections with plug-in device; (k) Bolted connection with rocket-shaped tenon; (l) Bolted connection with welded cover plate, from [55]

5.3. Building physics

The basic float glass undergoes mostly one or multiple processing stages to optimise the material characteristics. This is also done for several building physics requirements when using glass as construction material [3]. Examples for these necessities are solar or pure aesthetic demands like colour effect. This section describes some requirements the designer has to keep in mind regarding the building physics of a building. The text is based on thorough building physic literature research which can be found in Appendix C.3.

Findings Building Physics

AGC glass provides a calculator on its website that allows the engineer to model a glass composition of his own choosing. The calculator is capable of calculating the main building physics parameters of the specific composition. These parameters, regarding light, solar energy, heat and sound are shown in Table C.6. The writer has modelled multiple glass compositions in the machine, building up a small database and subsequently comparing different glass units. The main findings are as follows:

- The treatment of glass does not have influence on the building physical values (AN/HS/FT).
- The iron content in the glass does have impact on the light transmittance and the solar energy transmittance, but not on light reflection, shading coefficient nor the thermal and sound transmission.
- The thickness of the laminated glass panes does not significantly change the building physic values (it slightly decreases all variables).
- The type of interlayer has no effect on the U_g value of the glass composition. Relative to a PVB interlayer, an EVA interlayer gives smaller values for light transmission, total solar energy transmittance and shading coefficient, while the SentryGlas® layer gives an increase in these values.
- The type of gas present in a cavity between two glass panels does not influence the building physics parameters related to light and energy. However, it does influence the heat convection from the outer panel to the inner panel, when applying the gas in a relative small cavity. Because of the common practice of employing a 90% argon gas in the cavity, using another gas (for instance ordinary air) is more complex and expensive of manufacture. As a result, employing argon as a cavity gas is suggested. [45]
- The larger the cavity, the lower the thermal transmittance value. However, it has very little to no influence on the other building physic values.
- Insulating glass units with lamination on the outside (e.g.: 12.12.15(Air).8) have a significantly lower total solar energy transmission and shading coefficient than the same IGU but with lamination on the inside.
- The application of a Low-E coating in IGU's drastically reduces the solar energy transmission, shading coefficient and thermal transmittance. In addition, it causes a small decrease in light-transmittance and -reflection.

One can imagine that a laminated composition in glass is relatively less economical than a single panel, as is the application of a low-E coating in IGU's, for example. Table 5.4 shows indicative prices for glass compositions. These values are, for comparison, based on compositions with a width of 2000 mm and a height of 3000 mm. The prices shown in the table are consumer prices (exclude vat) and are only intended to give the reader a rough impression of the cost ratios.

Name	Glass composition	Approximate price [$€/m^2$]
Single glass	8(AN)	40
IGU	6(AN).12(AR).8(AN)	55
HR++	6(AN).12(AR).foil.8(AN)	60
Thermally toughened	8(FT)	65
Laminated	8.8(AN)	140
Laminated & thermally toughened	8.8(FT)	175

Table 5.4: Rough estimation of costs for different glass compositions, based on a $2x3$ metre $8mm$ panel, data composed of [56] and [45]

5.4. Reference projects

A diverse mix of reference projects, not all of them contain structural glass, can be seen as the base for the technical inspiration of the reversible art pavilion. The following is a list of the projects discussed in this section and what the main purpose of studying them is. Less relevant projects are elaborated on in appendix Section C.4.

CoCreation Centre Delft, 2020 - Has a façade that also functions as a stability element
Glass busstops - Ordinary structures that rely on a clear (diss)assembly procedure
Glaspavilon Aachen, 1995 - A reversible pavilion out of structural glass elements (shown in Appendix C)
Interlocking connectors and toggles - Topic related, completed research (shown in Appendix C)

CoCreation Centre Delft

The CoCreation centre in Delft is situated in the TU Delft's Green Village, which is exempt from construction regulations. This is the location where new construction concepts can be implemented. The structure, which measures $lxbxh = 2.5x13.5x6\ m$, is used as a large meeting room ($A = 300\ m^2$) for the Green Village.

(a) Render of the CoCreation Centre

(b) Mechanical scheme for horizontal loads
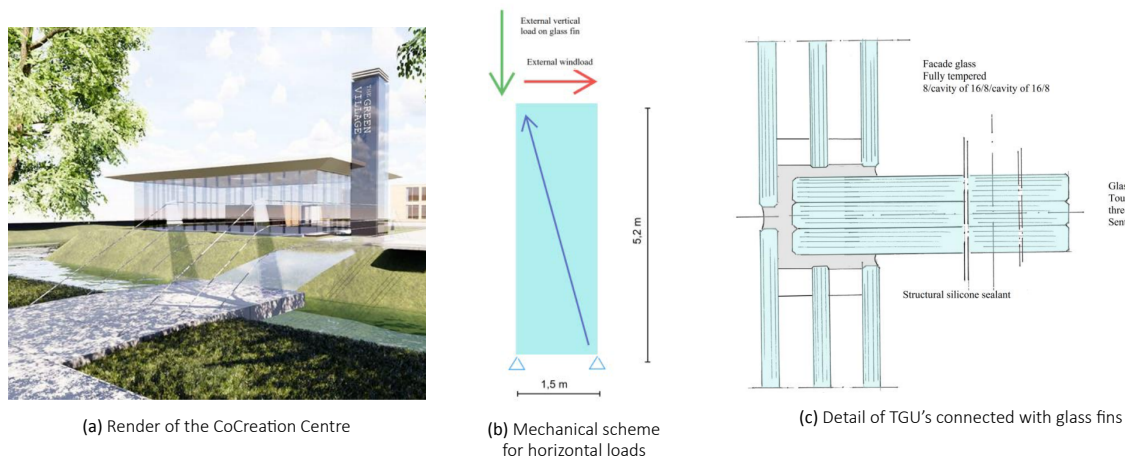
(c) Detail of TGU's connected with glass fins

Figure 5.11: CoCreation Centre [57]

Due to budget constraints, the triple glass façade (consisting out of Triple Glazing Units - TGU) was considered to be a stability element, with the glass fins serving as columns. This meant that the glass stability brackets and the glass span were no longer required. TGUs are typically over-dimensioned and, as a result, relatively less sustainable than ordinary facade panels. The insulated glass units are also utilised as stability components in the CoCreation Centre project. As illustrated in Figure 5.11b, the external wind force acing on the structure is transferred via the panels to the foundation. [57]

The connection between the triple glass and the glass fins consists of a structural silicone sealant which has to transfer the vertical component of the windload. The research by Krom, Veer, Riemens and Hoogendoorn [57] showed that the triple-laminated glass fin had to cover such a surface area with the silicone that it was designed as shown in Figure 5.11c. This structural depth is based on the vertical stresses and the allowable stress of $0.14\ mm^2$ for the silicon sealant. [57]

Glass bus shelter assembly

Public transport passengers are often offered accommodation during the waiting period. At bus stops, this is frequently in the appearance of a shelter. Since reversibility is essential in temporary buildings, the R-net bus stops (without swivel fittings) serve as inspiration for the design of the glass pavilion. Furthermore, the R-net stops created by FromAtoB Public Design are modular. This allows for nearly any design, from a modest tiny bus shelter ($4.6\ m$) with solely a bench, waste bin, lean-to's and an information display to elongated copies ($15.1\ m$) with multiple of those components (Figure 5.12). The depth of the shelter can vary in $1.20\ m$, $1.55\ m$ and $1.80\ m$. [58] [59]

The roof glass is made of either single or laminated glass. The wall glass has only two different widths and is never divided horizontally. The panels are printed and contain a horizontal bar to prevent fall-through of passers-by. Besides, the glass is protected with a protective edge at the bottom. [59]

The bus stop amenities are built into the construction of the shelter. This comprises lighting, electrical connections, and other features. The materials used to construct the shelter are sturdy enough to endure at least 15 years in a public outdoor environment. The ease of maintenance of the building elements was also a key design consideration. To prevent pollution for example, the glass is spaced about $70\ mm$ from the ground at the bottom.[59]

The order of construction (Figure 5.13) is fundamental. First and foremost, the foundation is made (1). The uprights are then installed on top (2). The wall and roof glass panels are subsequently installed on the uprights and secured with a rubber profile
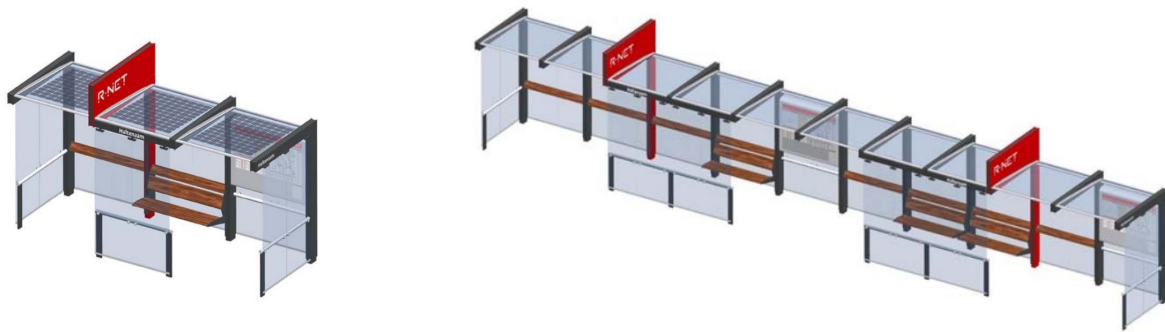
Figure 5.12: Modular R-net bus shelters: from small to large [59]
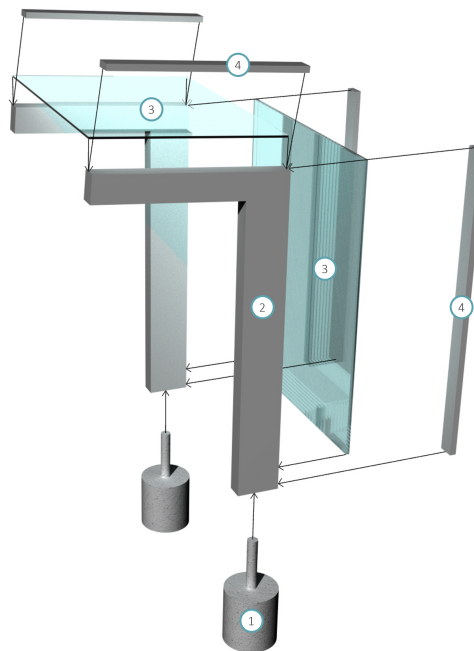
Figure 5.13: Assemblage sequence of a buss shelter *[own image]*

(3). The entire assembly is sealed with an aluminum click strip (4), after installing the electricity cables and drainage. After that, the furnishings, passenger information, and edge protection are installed (not on image).

In the event that a glass panel fails due to, for example, vandalism, this element can easily be replaced. The uprights' metal snap frame, in which the glass panel is mounted, must be temporarily removed. The damaged glass panel is then removed and replaced with a new one. The aluminum snap frames are again reinstalled, and the shelter is ready to be used as bus stop anew. [59]

5.5. Conclusion theoretical background

Above mentioned literature research enables the possibility to answer the sub-question *'What should a building engineer take into account when structurally designing a glass structure?'*, together with the lesser relevant literature review in Appendix C. The answer to this question is divided into three parts out of four literature research themes: on topic of glass as a building material, connections and based on reference projects.

- Glass
  Glass is an extremely strong material in the compressive direction, but significantly weak in the tensile direction. Peak stresses in glass must be prevented.

- Connections
  Bolted connections are very feasible when demountability is an important design criterion. However, bolted connections are disadvantageous when used in insulated glass units. Glued connections are not convenient for disassembly. A great potential lies in laminated connections.

- Reference projects
  Experiments with the glass fins of the CoCreation Centre in Delft still show an extreme load carrying capacity when all glass layers are broken. This fact is important to keep in mind when considering a failure strategy for buildings with glass.

  The assembly of a buss shelter is simple but very cleaver. Replacement of building components of buss shelters can be carried out very easily due to the assembly technique.

6

Design principles

Chapter 6 lists various building codes and guidelines to be incorporated in the design (Section 6.1). The design situation is sketched regarding the safety class and load factors and combinations (Section 6.2). Also, the principles of an ideal building system and a list of requirements (L.o.R.) is presented (Section 6.3) as starting point for the design phase.
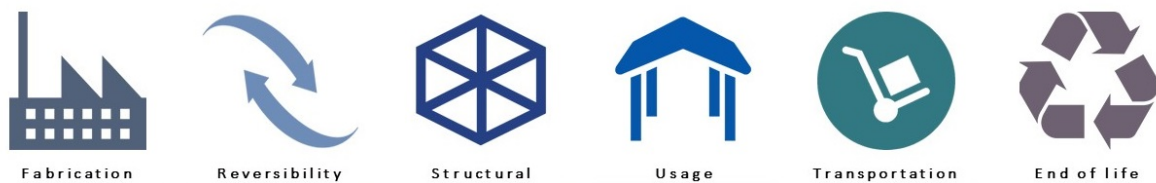

Fabrication   Reversibility   Structural   Usage   Transportation   End of life

Figure 6.1: The different lifecycle phases used for the list of requirements

6.1. Building codes and guidelines

The following building codes are to be followed during the design.

- **NEN-EN 1990** Basis of structural and geotechnical design
- **NEN-EN 1991-1-1** Actions on structures - General actions
- **NEN-EN 1991-1-3** Actions on structures - Snow loads
- **NEN-EN 1991-1-4** Actions on structures - Wind loads
- **NEN2608**: 2014 Glass standards

  The official new glass code, Eurocode 10 (2020-XX-XX) is still being drafted. In 2005 the idea came to make a universal code for glass because of the increasing demand in glass structures. Until the new code is in place, the EU member states will use their own national codes. [60]

- **NEN-EN 12600**: Glass in building - Pendulum test - Impact test method and classification for flat glass
- Tolerances:
    - **NEN-EN 572-2(:1994)** Float glass
    - **NEN-EN 12150-1** Heat strengthened glass
    - **NEN-EN ISO 12543-5** Laminated glass
- **Bouwbesluit 2012**: Energy performance codes

  The Dutch Bouwbesluit is a national code that states regulations regarding safety, health, usability, energy efficiency and the environment of buildings. [27]

- **Brancherichtlijn Betrouwbaarheid Glasconstructie**

  A Dutch handbook for assessing the reliability of a glass structure. The Fine & Kinney approach is thoroughly detailed.

6.2. Safety class, load factors and load combinations

For the structural calculations, the idea of the structure, the possible functions, the use and the loads define the relative magnitude. This section describes all this for the sake of calculation.

Consequence class 2 (CC2) is accurate regarding the demountable art pavilion. According to the Eurocode, *'Medium consequence for loss of human life, social or environmental consequences considerable'* defines the class. Although the pavilion is not large and can be evacuated quickly, the social impact of a possible failure is significant. After all, the pavilion will be situated in the heart of historic cities and will draw a lot of attention. CC2 prescribes a K_{fi} factor of 1.0.

The **design lifetime** of the structure is set on 50 years, even though the pavilion is meant to stay at a location around 3-6 months. The building elements however need to resist the influence of being assembled and disassembled over and over again, meaning a larger design lifetime is applied.

Load combinations are shown in Table 6.1. The ultimate limit state (ULS) combinations are used for ensuring the strength and stability, the serviceability limit state (SLS) combination is used for checking the deflection limits and the failure analysis. Maximum allowable stresses are dependent on the structural material. Maximum allowable deflections are stated in Table 6.2.

Combination	Permanent factor	Variable factor	Description
ULS-0	1.35	$1.50 * \psi$	*Rel. low self-weight, not normative*
ULS-1	1.20	1.50	*Strength and stability*
ULS-2	0.90	1.50	*Strength and stability: uplift wind*
SLS	1.0	1.0	*Deflections and failure*

Table 6.1: Possible load combinations

Value	Requirement	Description
$u_{slabs;max}$	$\leq l/250$	Maximum deflection slabs
$u_{glass;max}$	$\leq l/100$	Maximum deflection edge of glass pane
$u_{dia;max}$	$\leq l_{dia}/65 \leq 50$	Maximum deflection middle of glass pane

Table 6.2: Deflection requirements

6.3. Starting points for the design

Some preconditions are outlined in order to design a building system that is well-founded and as real as possible. Starting with the principles for the most ideal building system, the list of requirements is then drawn up.

6.3.1. Ideal building system

The ideal building system is defined by three terms:

- Transparent
  By using glass as a building material, the transparency of the buildings to be realised is raised by definition. The ideal building system strives to exude the strength of structural glass, and it is critical that transparency will be also reflected in the connections. This means that thick, opaque line connections should be avoided. Transparent connections are the obvious choice, although slim opaque connections can also improve the effect of transparency when used with large-sized glass panels.
- Variable / Adaptable
  To combat conventional, also dull, construction solutions, the most suitable building system has to be variable. The modular building approach already allows for a significant deal of construction freedom. Nonetheless, cube-shaped modules, for example, are less likely to result in interesting and exciting building shapes. The choice of the level of modularity and the design of the connections will have a significant impact on this ideal.
- Weather- and waterproof
  The fictive use of the pavilion, as described in the scope, will be a transportable art pavilion. For the comfort of the visitors, in conjunction with the building rules and the knowledge obtained from the literature research, the building system should not allow the outside climate to enter the structure.

6.3.2. Requirements

In order to develop a well-founded building system, it is wise to keep a context in mind in order to define various preconditions. The scope of this research was discussed earlier in section 2.3 of Part I. When combined with the literature review, the scope offers a specified structure for the requirements list. Along these lines, predefined values for loads can be incorporated in the strength and stability analysis.

The immediate purpose of the list of requirements is to define the boundary conditions of the final design. The list is divided into two levels, the upper level which are hard requirements and the lower level which can be considered as wishes.

Hereafter, six distinct themes have been identified, into which the requirements and desires have been grouped. These themes were developed on the basis a Life Cycle Analysis (LCA) and include the following concepts: Fabrication, Reversibility, Structural, Usage, Transportation, End-of-life (Figure 6.1).

1. Fabrication
Upper-level requirements

- The modules must be of high quality to withstand a lifetime of at least 50 years.

Lower-level requirements (wishes)

- It would be ideal if the glass composition is as clear as possible in order to demonstrate the strength of structural glass.

2. Reversibility
Upper-level requirements

- The system should be as basic as possible, with an emphasis on a small number of unique parts.
- Easy to (diss)assemble, so no special machinery required. The instruction must be understandable for every craftsman.

Lower-level requirements (wishes)

- Only dry solutions, i.e. no temporary 'wet' injection mortar or structural sealant glazing.

3. Structural
Upper-level requirements

- Vertical balance: Glass panels support the roof, the panels are subsequently carried by a steel beam foundation.
- Horizontal balance: The roof and side panels provide stability for the entire structure.
- Non glass-penetrating connections should be applied to avoid peak-stresses.
- The structure should not collapse after a single vandalism assault (Fine & Kinney method).

Lower-level requirements (wishes)

- The components' relative displacements will have to be accommodated by the joints. In such a way that weather tightness is maintained and the coupling system functions as a constrain.

4. Usage

Upper-level requirements

- According to the building physics literature research, the U-value must be below 4.1 W/m²K.
- The height must be greater than 2.1 meters. [Bouwbesluit]
- The pavilion should contain at least two exits for the visitor's safety.

Lower-level requirements (wishes)

- It is preferred that no light at the roof enters the building to make the visitor's experience as pleasant as possible.
- The structure should be aesthetically pleasing, emphasising the power of glass regarding its transparency.
- It is preferable for fire safety reasons if the pavilion just has one level.

5. Transportation

Upper-level requirements

- All parts must fit inside a common container (6100x2440x2590mm) to facilitate the ease of transport.
- Because the elements will be relocated often, they must be fall-proof. This necessitates the use of edge protection for the glass.

Lower-level requirements (wishes)

- The most efficient use of container space boosts transportation productivity. 2D components, for example, make optimal use of available space.

6. End of life

Upper-level requirements

- The various elements should all be easily replaceable.

Lower-level requirements (wishes)

- Zero waste after the lifetime of the building system.

6.4. Conclusion design principles

The research question *'What are the design principles and constraints that define the design space for a modular demountable temporary visitor pavilion in glass?'* can be answered following the information of this chapter.

The calculations of this research have to satisfy several Dutch building codes. The imaginary pavilion is regarded as consequence class 2 with a design lifetime of 50 years. The load combinations are stated: checks on strength should be computed with $ULS - 1 = 1.20 * G_k + 1.5 * Q_k$, in case of uplift wind $ULS - 2 = 0.90 * G_k + 1.5 * Q_k$ and for the deformation and failure analyses $SLS = 1.0 * G_k + 1.0 * Q_k$.

A list of requirements is created with the life-cycle of the pavilion in mind. Six categories are determined with higher-level requirements and lower-level requirements (wishes): fabrication, reversibility, structural, usage, transportation and end-of-life. Most important requirements that have a significant influence on the design are:

- According to the building physics literature research, the U-value must be below 4.1 W/m²K.
- All parts must fit inside a standard container ($6000x2440x2600\ mm$) to facilitate the ease of transport.

With the design principles in mind and the literature study in the next Part, substantiated choices can be made for the design of the pavilion.

Part III

Generate: A temporary exhibition pavilion

7

Pavilion design

The first chapter of Part 3 focuses on the next stages after setting the List of Requirements (LoR). These comprise the starting points for the reference pavilion with dimensions. Finally, all of the required construction elements are enumerated and shown.
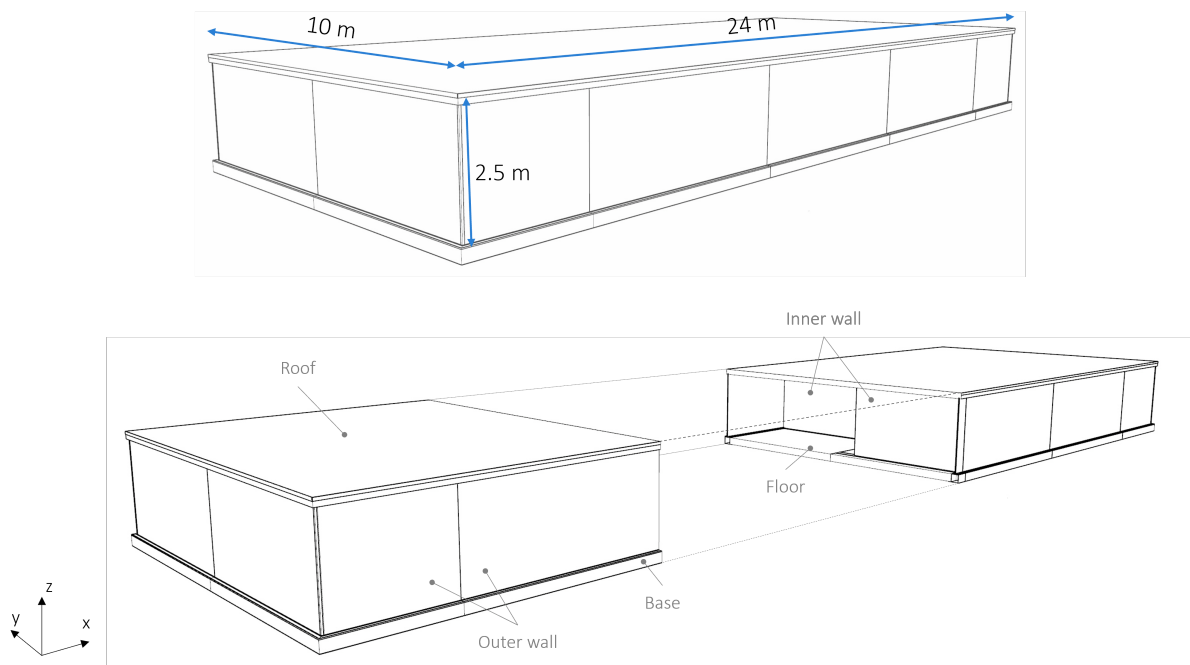

Figure 7.1: The pavilion's dimensions and a split version

7.1. Structure

Dimensions, elevations and sections are shown here. The stability system is elaborated in the next section and properties and the physical outline of the different building elements are showcased in Section 7.1.

The pavilion's construction consists of a wooden roof and floor, glass walls and a steel base (Figure 7.2).
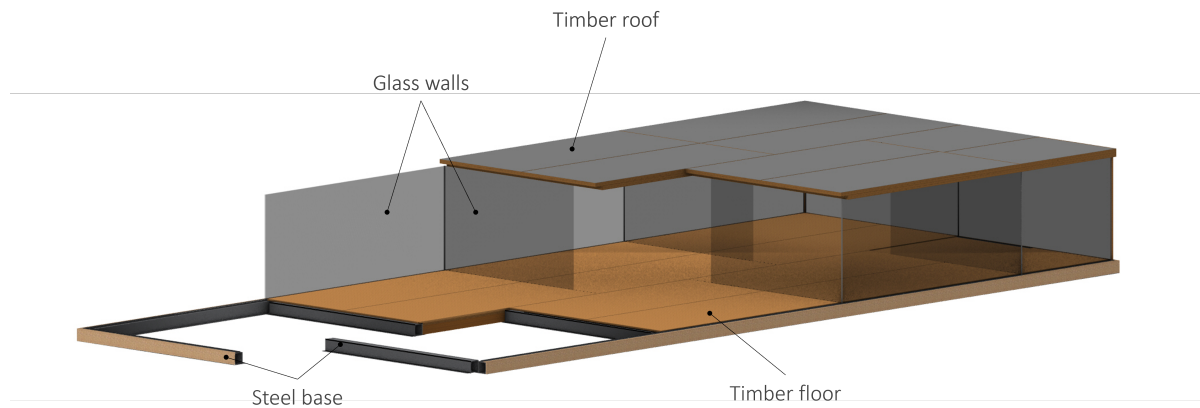

Figure 7.2: Structure of the pavilion - cut off version to show the structural elements
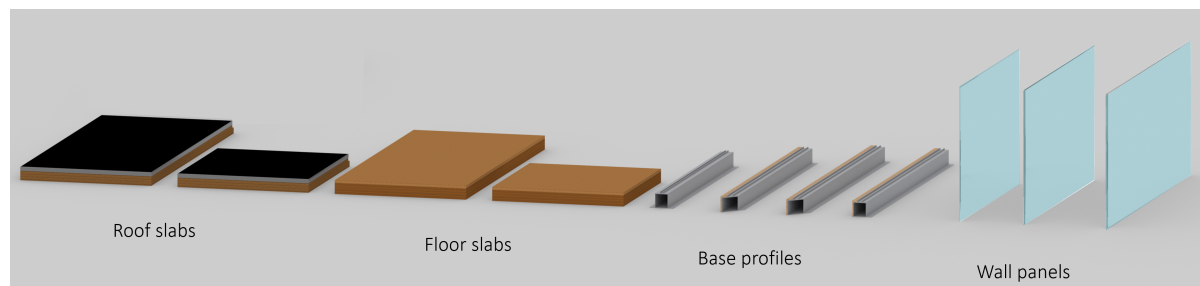

Figure 7.3: All building elements, Table 7.1 lists the properties

The general design of the building system is composed out of the elements in Table 7.1. It may be subdivided into the '*2D: rectangular*' concept of the literature review on modular building. The system's structural modular components (roof, walls and floor) are made up of very thin cuboids. The elements will look practically two-dimensional on the size scale due to their dimensions, therefore the categorisation under the 2D system of the modularity principle. The reason for this relatively thin structural elements is the requirement for transportability of the system as a whole. Loading the thin cuboids into a conventional container will be easy and efficient in this manner.

Connecting the four building elements leads to the creation of a building. Chapter 8 of this part showcases the connection typologies which need to be used. The next section here describes every particular building element in the following structure:

- Physical outline
- Structural representation
- Building physic characteristics

Element	Material	t [mm]	L [mm]	b [mm]
Roof	Bitumen layer DERIX L-160/5s	164	6000 3000	2500
Wall	Glass	48 *10(FT)-15(Ar)-5.10.5(HS)* 23 *5.10.5(HS)*	6000 5000 4250	h = 2500
Floor	Dry screed DERIX CLT LL-210/7s	298	6000 3000	2500
Base	RHSFB265 THQ265	h = 265	6000 5000	b$_0$ = 240 b$_u$ = 345 (RHSFB), 450 (TQH)

Table 7.1: Structural elements needed for construction

7.1.1. Roof

Physical outline

The chosen material for the roof slabs is timber, CLT (cross-laminated timber) in particular. This is the result of the general architect's aesthetic desire; the combination of glass and wood is highly valued. Furthermore, CLT is constructed of wood, a bio-based product, and has a more appealing appearance than traditional roof slabs like concrete.

The roof consists of slabs that are $2.5\ m$ in width. The length of the plates are for the pavilion 6 and 3 meters. Maximum CLT sizes are up to 3.5 by 16 meters (StoraEnso [61]), meaning that there is no need for splice lamination of the CLT plates.

Four rows of CLT slabs lay in the width of the pavilion. In the length, one half of the building has another grid than the other half, as can bee seen in Figure 7.6. From the perspective of the map, the upper half has two times four slabs of $6x2.5\ m$ in a row and the lower half two times three slabs of $6x2.5\ m$, with on both ends two times a slab of $3x2.5\ m$.

The exact sizes of the panels are determined by the connection system that is employed. The detailed design has ensured that there will be recesses in the CLT roof panels. This decision results in a 50-millimetre overhanging roof on the pavilion's exterior. The overhanging CLT roof system increases the aesthetics of the connection, causing a more seamless transition from the outside to the inside..

Structural representation

With knowledge of various initial load and span values, the DERIX design guide is an useful tool for determining a first thickness of CLT. The engineer needs know if the slab will be utilised as a roof or a floor structure, as well as the permanent- and snow load. Furthermore, the way of spanning (in two, three, or four directions) and the length of the span are crucial to know.

The values acquired from the pavilion's (structural) design are shown in Table 7.2 and are as follows. The kind of construction is roof, the mode of span is on two supports (one-directional) and the span length is six metres. The permanent load is expected to be $0.75\ kN/m^2$ and is derived from the load of the permanent roof components other than the CLT. In order to maintain a high level of flexibility in the usage of the construction system, the value of $0.75\ kN/m^2$ is on the conservative side. Furthermore, when the normative variable load is considered, the live load of $1.0\ kN/m^2$ acting on the roof (see Appendix D) is greater than the computed snow load of $0.56\ kN/m^2$. Once again, a conservative approach is applied on the live load by choosing the $1.10\ kN/m^2$ value for snow load in the DERIX design table.

Type of structure	Roof
Type of span	One-directional
Length of span	$6\ m^2$
Permanent load	$0.75\ kN/m^2$
Variable load	$1.10\ kN/m^2$

Table 7.2: Input for the DERIX determination of required CLT roof slab

The minimum required type of CLT slab can now be extracted from the DERIX design table. This leads the designer to the L-160/5s plate; a five-layer cross-laminated board of $160\ mm$ thick with an apparent fire resistance of R90. See Table 7.3 for characteristics.

It is assumed for the structural verification that the roof works as one large infinitely stiff area for the force transfer of the horizontal wind loads. This approximation is on the non-conservative side. Therefore, careful conclusions should be taken when evaluating the unity checks of the connections.
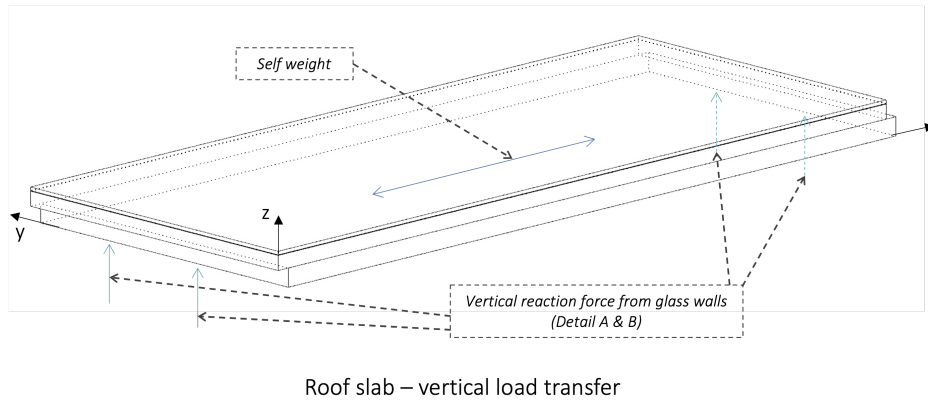
Roof slab – vertical load transfer

Figure 7.4: Vertical load transfer in a roof slab

Roof slab – horizontal load transfer in x-direction   Roof slab – horizontal load transfer in y-direction
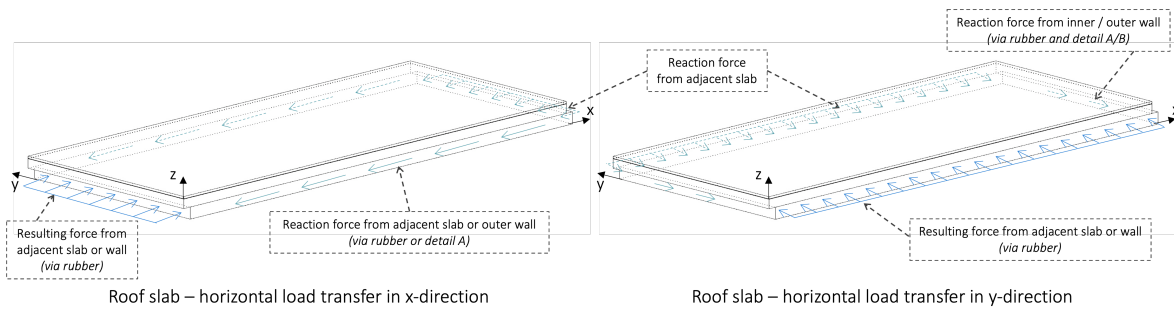
Figure 7.5: Horizontal load transfer in a roof slab in x- and in y-direction

Building physic characteristics

On top of the CLT plates a damp- and a water resistant layer should be applied. A basic bitumen layer is applied for this purpose (the damp layer is not shown in the drawings). A small calculation is done to investigate if an insulation layer in the roof slab is needed. The U-value of the total composition should be below $4.1\ W/m^2K$. The λ value of CLT is 0.13, according to Greenspec. It can be concluded with the calculation shown in Formula 7.1 that no insulation is required in the roof slabs. Extensive heat analysis on the detail wall-roof are shown in Appendix B.5.

$$R_m = d/\lambda = 0.22/0.13 = 1.69\ [m^2K/W]$$
$$U - value = 1/R_m = 1/1.69 = 0.59 \le 4.1\ [W/(m^2K)]$$

(7.1)

Type	Nominal strength [mm]	Structure of plates	Self-weight $[kN/m^2]$	Layers
L-160/5s	160	$\|40\|\overline{20}\|40\|\overline{20}\|40\|$	0.72	5

Table 7.3: Details of the chosen CLT roof-slab. Characteristics from DERIX.
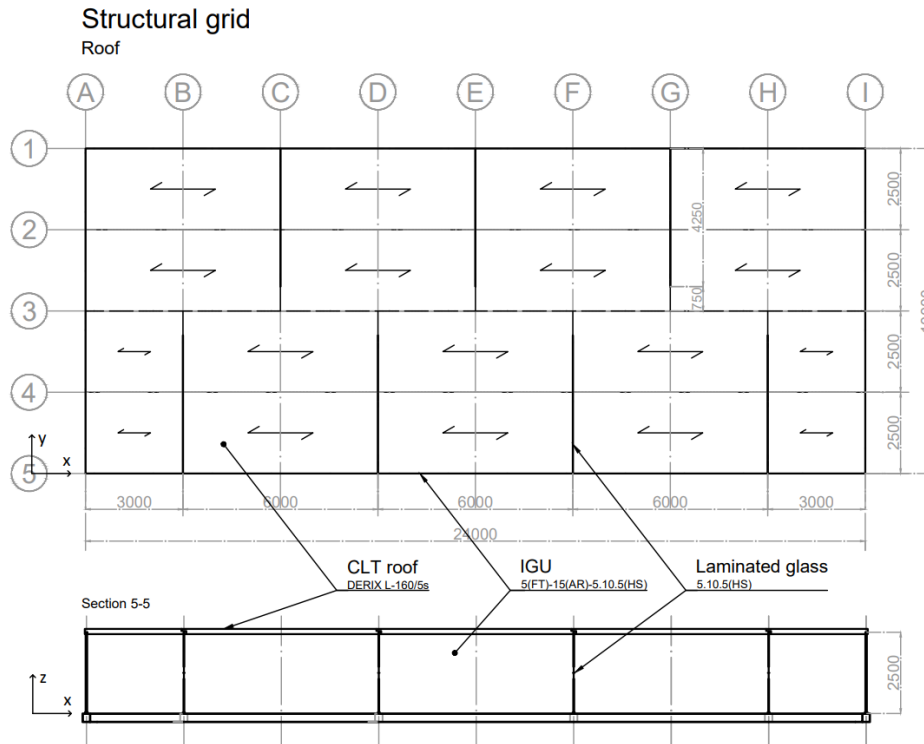

Figure 7.6: Structural outline of the roof

7.1.2. Glass panels

The glass wall panels are the most important elements of the structural system and overall architecture. These building components are particularly the motivation for this thesis research and thus play a significant role in the design. The goal is therefore to demonstrate the power of structural glass through the design of the building system.

Physical outline

There are two distinct composition of panels: outer wall panels of $6x2.5$ and $5x2.5$ meters and inner wall panels of $4.25x2.5$ meters. They all do not exceed the Jumbo panel sizes (see literature review), and fit in a regular transportation container. In two of the IGU's on the short side of the pavilion, openings are present for the installation of doors. These cutouts, however, are not shown in the structural grid of the pavilion (Figure 7.13) and are not considered in the further structural design, as they cause irregularities in the force distribution.

Soda lime glass will be used in this project since it is the most common and relative cheapest glass, with a predictable structural and physical behaviour. The other main possible type of glass, borosilicate glass, is a better option in cases with require for a higher thermal shock resistance. Owing to the fact that the case study is situated solely in the Netherlands, this, more pricey, material property is not required.

Furthermore, low-iron glass was chosen for the fictional pavilion. Low-iron glass gives the impression of the material being more translucent. The walls of the pavilion will have a less blue haze. The decision for low-iron glass is based on the focus intended to demonstrate the power of structural glass application. Due to the lack of vertical structural opaque building parts, the CLT roof will appear to float in the air with low-iron glass.

Another advantage of this sort of glass is that it soothes the transition from inside to outside and vice versa. The effect for the pavilion visitor is that, despite the relatively low ceiling, the visit to the pavilion is experienced as more pleasant because of the spaciousness. The people inside experience a 360-degree view to the outside, which is only theoretically obstructed by the presence of art items and people. Apart from that, the effect for passers-by is that they can easily take a look at the art

collection inside the pavilion. As a result, more tourists are likely to be enticed inside. More information on low-iron glass, the reader is referred to Part II.

The chosen configuration for the IGU's (outer walls) is $10(FT) - 15(Ar) - 5.10.5(HS)$, marking together with the interlayers a total nominal distance of approximately $48\ mm$ (with interlayers). The outer panel is $10\ mm$ thick, whereas the cavity in the IGU is $15\ mm$ in diameter and filled with 90% Argon gas. The laminated side is formed by three panels, respectively 5, 10 and $5\ mm$ thick glass panels which are bonded by a $1.52\ mm$ SentryGlas® interlayer.

The choice of SentryGlas® originates from the intermediate layer's exposure to the outside air. The intermediate layer is in constant touch with the outside air during the construction's disassembly and reassembly. In these conditions, an alternative PVB intermediate layer will absorb moisture, however a SentryGlas® layer would not [62]. Furthermore, based on past study, the choice of this interlayer type is based on the connection design. In the following chapter, this will be explained in further detail.

The weight of the insulated glass unit will be $78\ kg/m^2$, meaning the $6x2.5\ m$ panel has a self-weight of $78 * 6 * 2.5/1000 = 1.17\ kN$ and the $5x2.5\ m$ panel has a self-weight of $78 * 5 * 2.5/1000 = 0.98\ kN$.

The inner wall panels are made out of a 5.10.5(HS) composition. These elements do not need elaboration on the insulating capacity, since they are placed at the inside of the pavilion. Like the IGU, these panels have a SentryGlas® interlayer of $1.52\ mm$. The inner wall panels eventually weigh $53\ kg/m^2$, resulting in a self-weight of $53 * 4.25 * 2.5/1000 = 0.56\ kN$.

The large size of the glass panels, both exterior and interior, means that undesirable deviations occur during the process of lamination. In a perfect world, the three laminated panels would fall perfectly on top of each other, without any deviation in the plane of the panels. However, this will not be the case in practice.

With large panels of this sort, tolerances of up to $6\ mm$ are possible. This pavilion's detailed design, on the other hand, is unable to accommodate this order of magnitude tolerance. The manufacturer of the laminated glass is explicitly requested to keep the tolerance as small as possible, in any case no more than $2\ mm$. Previous structural glass projects have proven that this wish can be met. However, the tight tolerances are not designed with in the connection design.

Structural representation

The laminated side of the IGU (**5.10.15(HS)**) is necessary to function as a structural glass unit. The IGU may be strong enough when applied as a single panels with a cavity in between. However, in the event of the structural panel collapsing, there is no way of reducing the forces. This means that the entire side panel fails, an event that certainly needs to be avoided. This is also mentioned in the NEN-EN 2608 standard and listed on the 'Kenniscentrum Glas infosheet' [63]. It specifies that the impact side of an insulating glass floor-separating wall must be composed of at least laminated glass according to NEN-EN 12600. Isochoric pressure is not accounted for, since the shortest side of the panels is in any case larger than one meter (NEN-EN 2608, article 6.2.1).
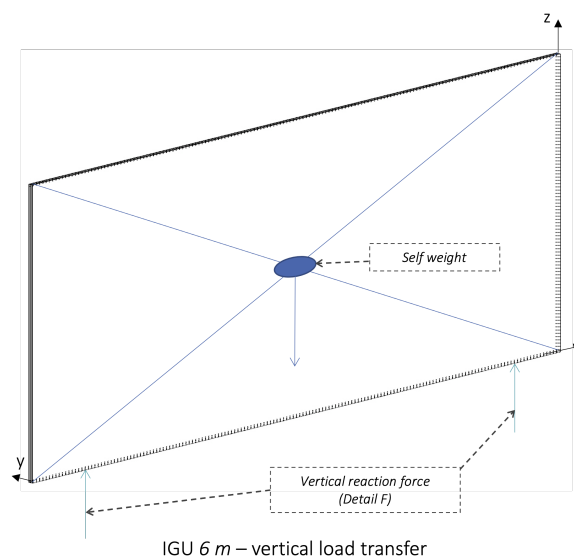

IGU $6\ m$ – vertical load transfer

Figure 7.7: Vertical load transfer in an IGU on the long side. Note: no roof is carried by the $6\ m$ IGU's
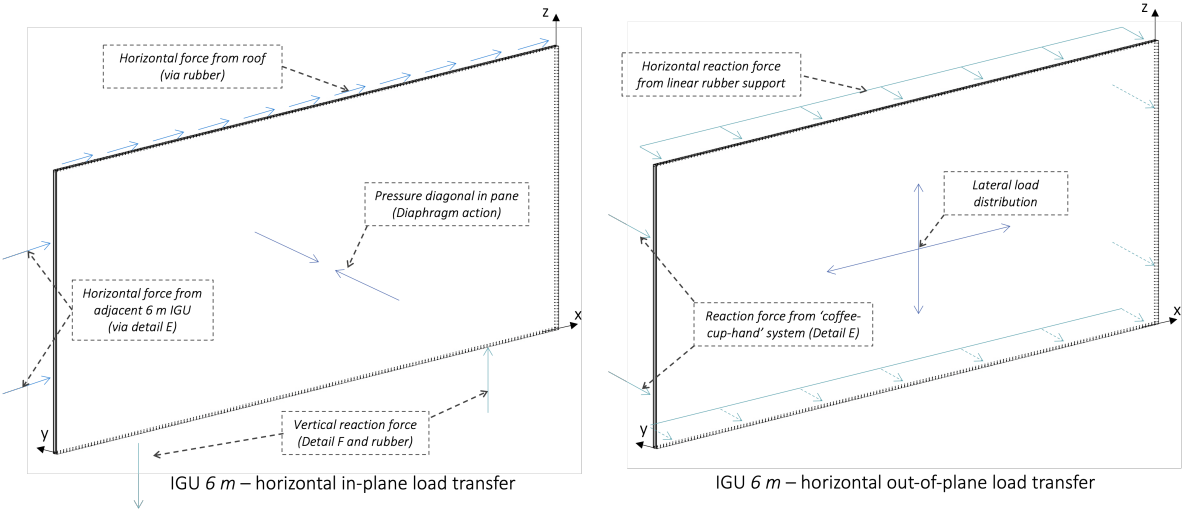
Figure 7.8: Horizontal load transfer in an IGU on the long side

Building physic characteristics

For the outer wall panels, the U-value for thermal insulation must remain below 4.1, as previously stated (Part 1 Chapter 6). According to the AGC Glass configurator, this limit cannot be satisfied with laminated glass alone. This necessitates the use of an insulated glass units as wall panels (IGU). A quantitative study was carried out using the AGC Glass configurator to compare different glass compositions based on building physics requirements. The results can be found in Section 5.3 of Part II (Literature review).

10(FT)-15(Ar)-5.10.15(HS) composition	
Light transmittance [τ_v]	82%
Total solar energy transmittance [g]	79%
Light reflection external [ρ_v]	15%
Light reflection internal [ρ_{vi}]	14%
Shading coefficient [SC]	0.91 -
Thermal transmittance [U_g]	2.4 $W/(m^2 K)$

Table 7.4: Building Physic characteristics of the glass composition (AGC)

The characteristic values regarding building physics are showcased in Table 7.4, and its terms are elaborated in the literature review (Part II, Section 5.3). The U-value (thermal transmittance) is the most important value, which is also included in the requirements package.
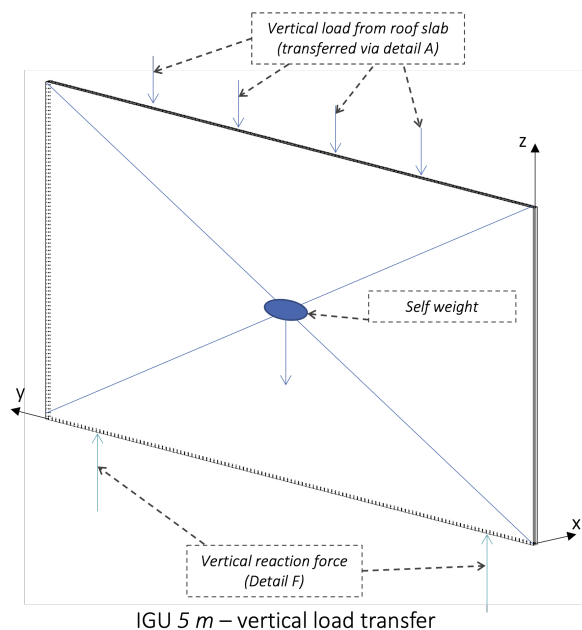
IGU *5 m* − vertical load transfer

Figure 7.9: Vertical load transfer in an IGU on the short side

7.1.3. Floor

Physical outline

The floor consist out of a DERIX CLT LL-210/7s plate with a $88\ mm$ dry screed on top and comes in the same length and width as the roofplates: length of 6 or 3 meters and width of 2.5 meters, the same dimensions and layout as the roofslabs. The main difference compared to the roof slabs is that the CLT DERIX floor slabs are slightly thinner, as well as that they are supported on the entire width of the panels at both ends (Figure 7.13).

The addition of the floor with the dry screed, together with the choice of the base profiles, enabled the design to establish an uniform floor over the entire surface of the pavilion. The places where the outer and inner walls are attached to the base profile can seemingly be eliminated in this way.

Structural representation

Similar to the roof slab determination, the floor slabs' minimal thickness is based on the design tables of DERIX. The starting points are listed in Table 7.5 below, in the same method as the roof slabs. Different now is that the minimum required vibration value is used, which is stated as a minimum of $8\ Hz$ for buildings with a temporary visitor function in the Netherlands.

Type of structure	Floor
Type of span	One-directional
Length of span	$6\ m^2$
Permanent load	$1.0\ kN/m^2$
Variable load	$5.0\ kN/m^2$
Natural frequency requirement	$S > 8\ Hz$

Table 7.5: Input for the DERIX determination of required CLT floor slab

The permanent load for the floor is expected to be around $1.0\ kN/m^2$ and is based on the load of the permanent floor components other than the CLT, mainly the dry screed layer and possible installations. The possible live load is put on $5.0\ kN/m^2$, which has been formulated by the Eurocode (Congregation area class C3, according to Chapter D).

The minimum required type of CLT slab can once again be extracted from the DERIX design table. This leads the designer to the LL-210/7s plate; a seven-layer cross-laminated board of $210\ mm$ thick with an apparent fire resistance of R90. Contrary to the roof slabs, no recesses are made into the floor slabs, so no additional thickness is needed to reach the equivalent strength and stiffness in the plates. See Table 7.6
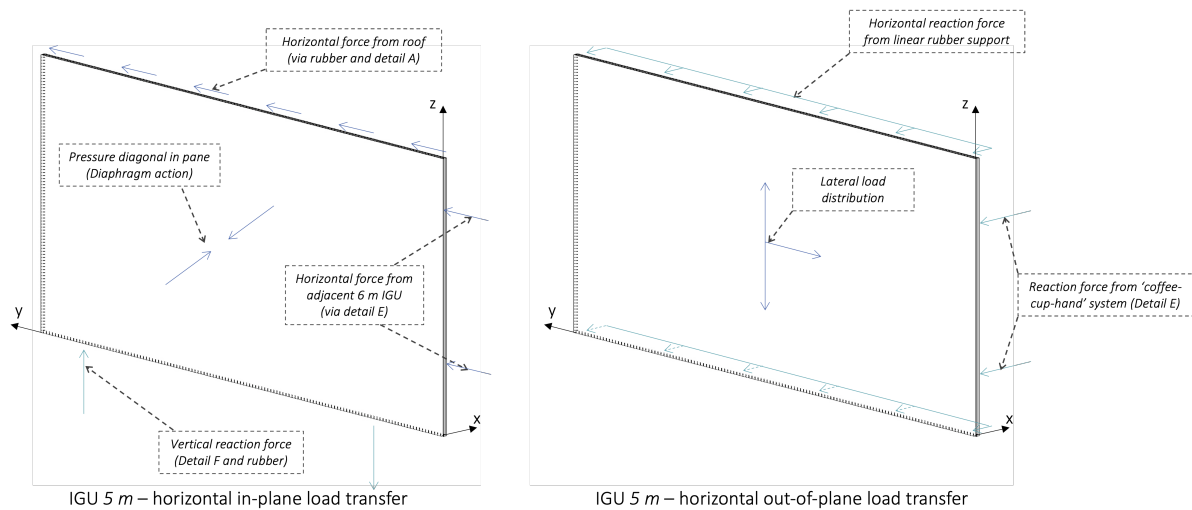
IGU *5 m* – horizontal in-plane load transfer   IGU *5 m* – horizontal out-of-plane load transfer

Figure 7.10: Horizontal load transfer in an IGU on the short side

Type	Nominal strength $[mm]$	Structure of plates	Self-weight $[kN/m^2]$	Layers
LL-210/7s	210	|30||30|$\overline{30}$|30|$\overline{30}$|30||30|	0.95	7

Table 7.6: Details of the chosen CLT floor-slab. Characteristics from DERIX design tables.

Building physical characteristics

No additional insulation is necessary for the insulating capacity the CLT contains itself, looking at Equation 7.2. Detailed heat analyses are executed on the floor detail in the next chapter, Chapter 8.

$$R_m = d/\lambda = 0.21/0.13 = 1.62\,[m^2 * K/W]$$
$$U - value = 1/R_m = 1/1.23 = 0.62 \leq 4.1\,[W/(m^2 * K)]$$

(7.2)

7.1.4. Base

As the pavilion to be referred to will not be permanently in one place, it is important to devise a simple solution to transfer the forces to the ground. The chosen solution are steel 'hat'-beams (THQ265) that are placed at the locations below the inner wall panels, and steel 'cap'-beams (RHSFB265) at the locations beneath the IGU's. These locations are tactically chosen in order to transfer the forces from the structural glass wall panels to a linear equal base.

The floor slabs will be placed on the bottom flanges of the steel profiles, the design will subsequently give the visitor the impression that the steel base beams are integrated in the floor elements. Not only for aesthetic reasons this is done, but also to avoid an even smaller inside storey height than the height of the glass panels ($2.5\,m$). To prevent peak stresses in the glass, there should be a soft connection between the steel and the glass, which the rubber in between will take care of. Two steel plates will be welded on top of the 'hat'- and 'cap'-beams to create a shoe in which the glass panels can be placed. The glass is placed on two HDPE blocks of $50\,mm$ long each, to make sure the forces in the glass are transferred at a distance from the outer edges. For more info on these blocks, see Chapter 8.

Assuming that the places where the building system is to be installed are not perfectly straight and level, an intermediate solution is required so the steel profiles can be placed according to plan. The steel beams are supported in several places by concrete slabs. The support is such that critical deflection, lateral bucking and other mechanisms do not have to be taken into account. The elaboration of the support is beyond the scope of this study, as well as possible occurrences of sag due to geo-technical reasons.
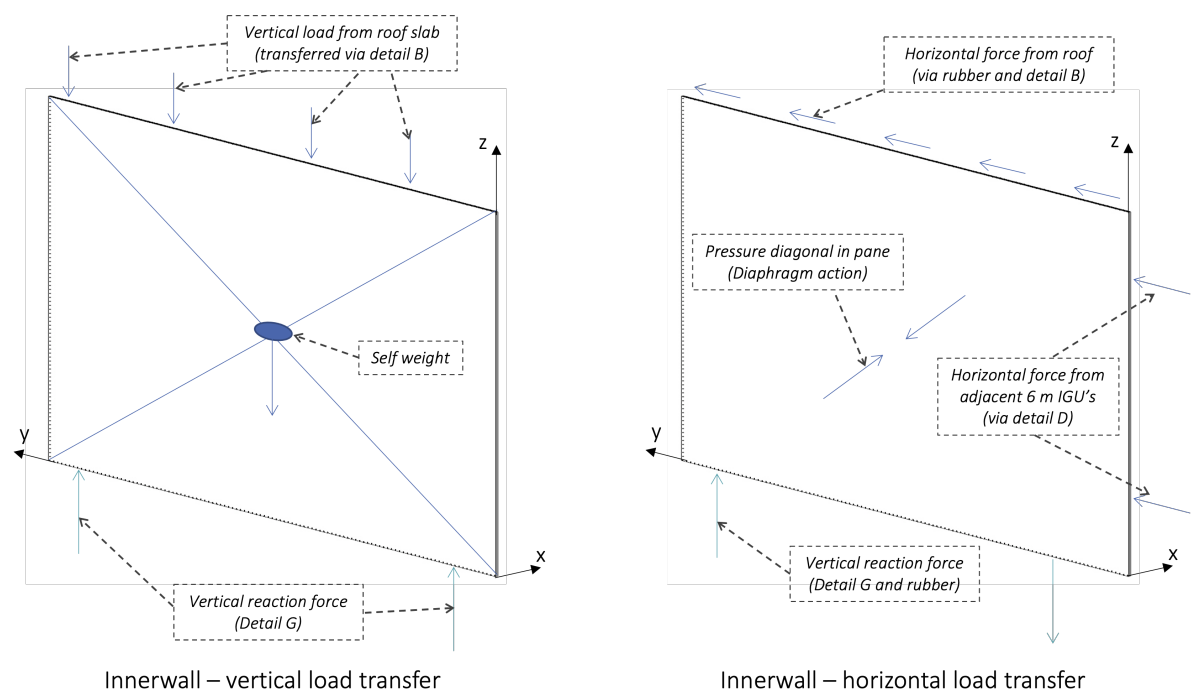
Innerwall – vertical load transfer

Innerwall – horizontal load transfer

Figure 7.11: Vertical and horizontal load transfer in an inner wall
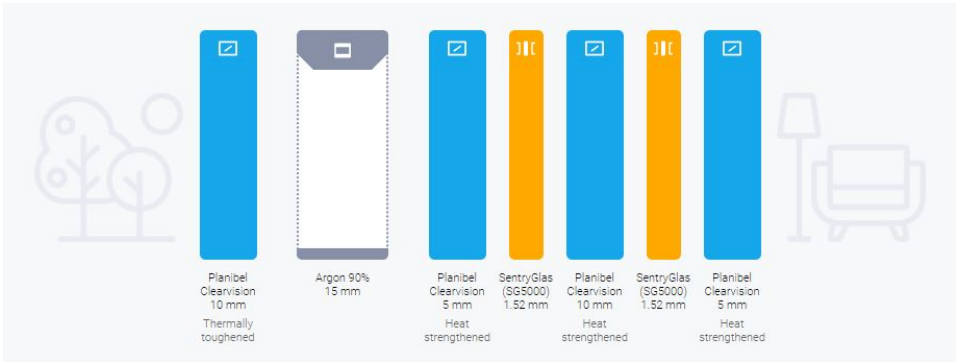

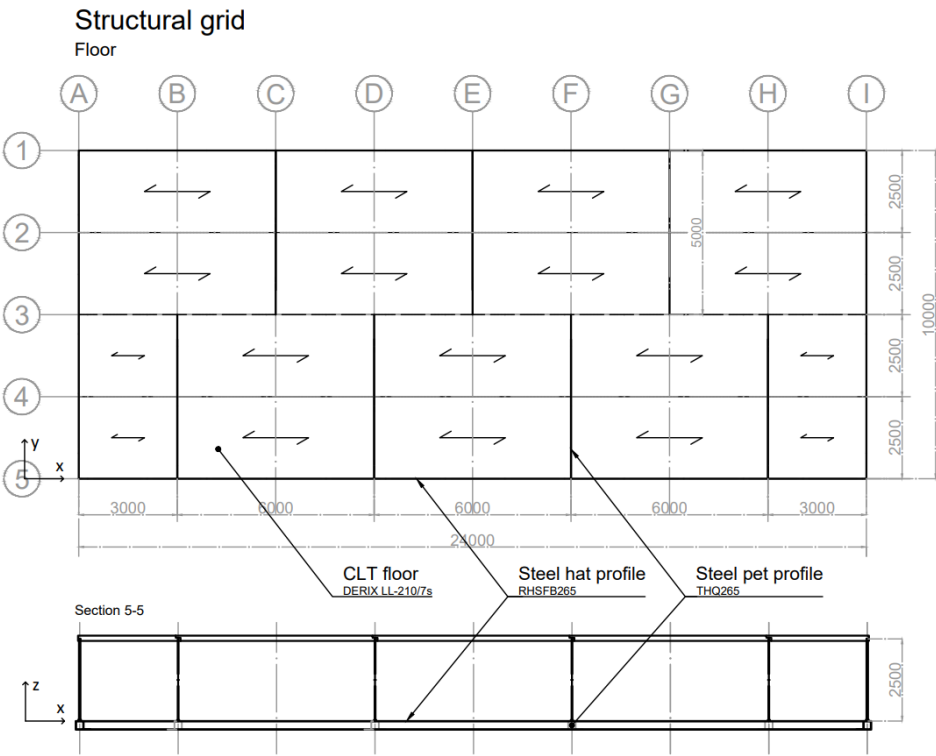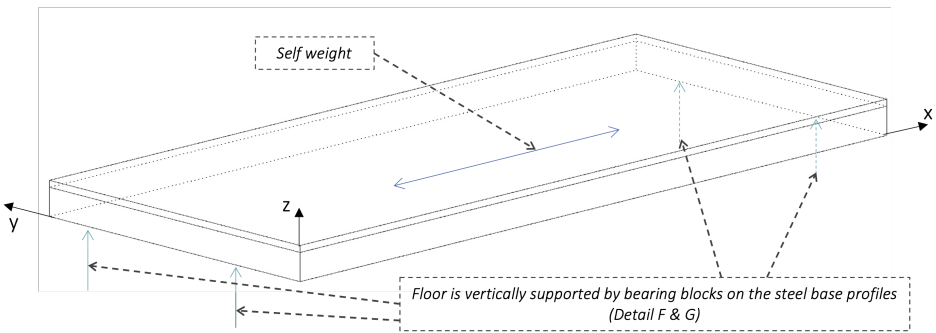**Figure 7.12:** Input composition in the AGC Glass configurator

Figure 7.13: Structural outline of the ground floor

Floor slab – vertical load transfer

Figure 7.14: Vertical load transfer in a floor slab

7.2. Stability

The stability strategy is discussed in this section. Ensuring stability is crucial for the transfer of horizontal loads.

Together with the creation of the building system's design, identification of potential forces in the structure and how they'll be transferred to the base is done. With this approach, a design framework for the details of the connections can be generated and with calculations design forces can be quantified.
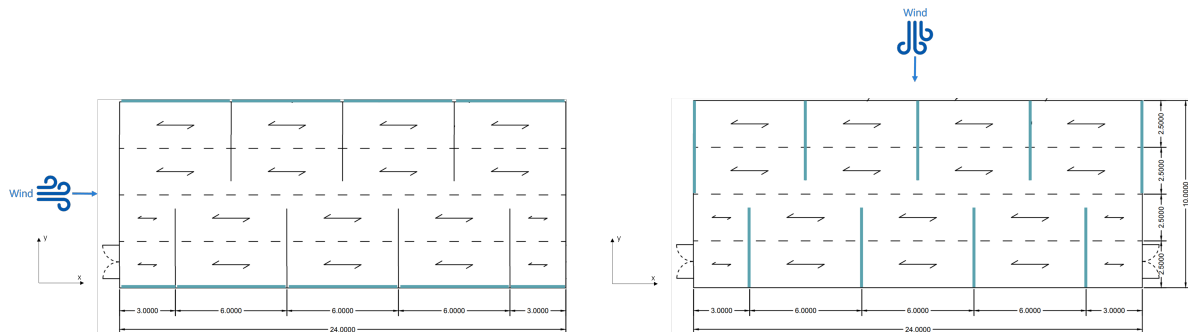

Figure 7.15: Stability strategies with wind coming from x- and y-direction. Stabilising walls shown in blue.

The calculations for wind loads are performed according to NEN-EN 1991-1-4 and performed in Appendix D.

7.2.1. General

The force applied on the side panel is distributed equally to the top and bottom of the IGU, and this **horizontal force** needs to be transferred to the base. The steel I-profile foundation transfers the part that goes to the bottom. The part that is led to the top is led to the roof via the connection. The roof subsequently transfers the load to one (or more) wall panels that are parallel to the wind direction. This implies that the detail connecting the roof with wall panels must transfer longitudinal shear force. Via diaphragm behaviour of the wall panels, the lateral loads are transferred to the base.

7.2.2. x-direction

The stability in x-direction is guaranteed by the IGU's on the long side of the pavilion, thus the wall panels that are placed in the direction of the x-axis in the figures.
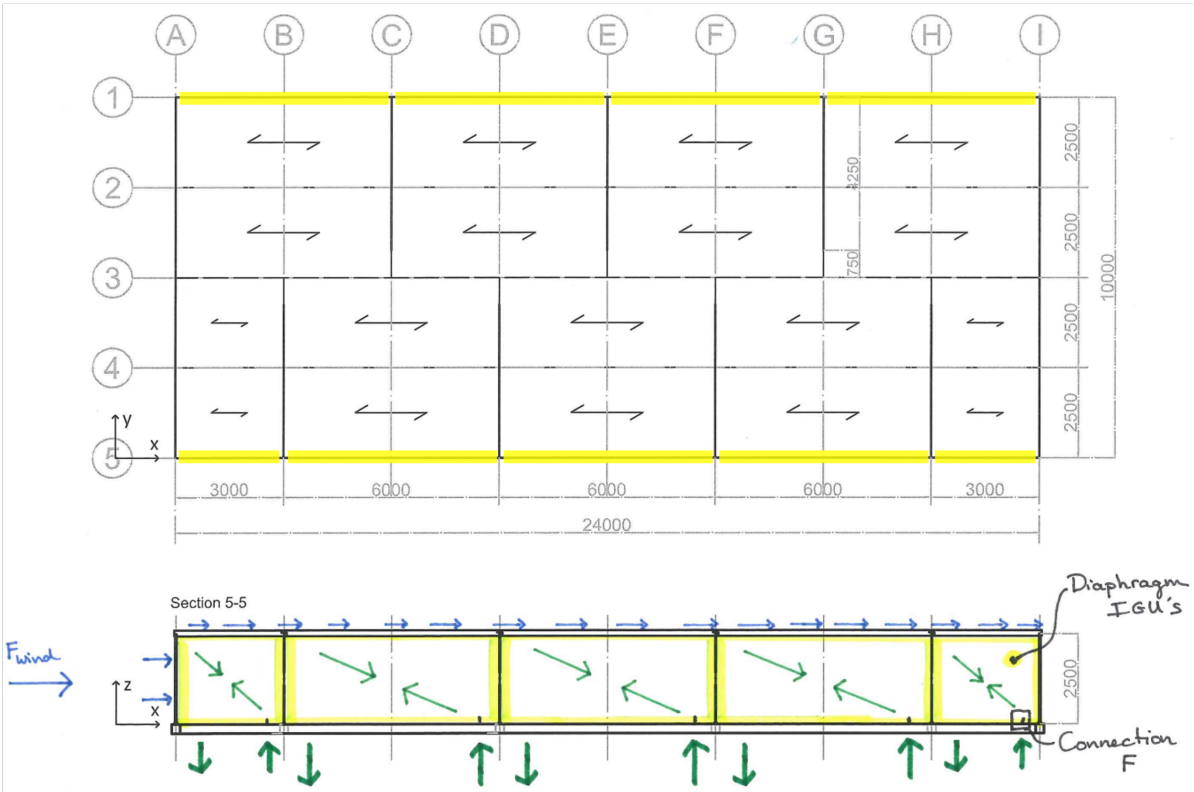

Figure 7.16: Stability system in x-direction

7.2.3. y-direction

The two entrances (cut-outs in the glass with doors in it), both at the short sides of the building, are not considered in the structural analysis. It is therefore assumed that the pavilion on the short sides consists of both two IGU's of 5 metres wide by 2.5 metres high. The IGU's on the short side, as well as all inner wall panels, function as stability element in y-direction.
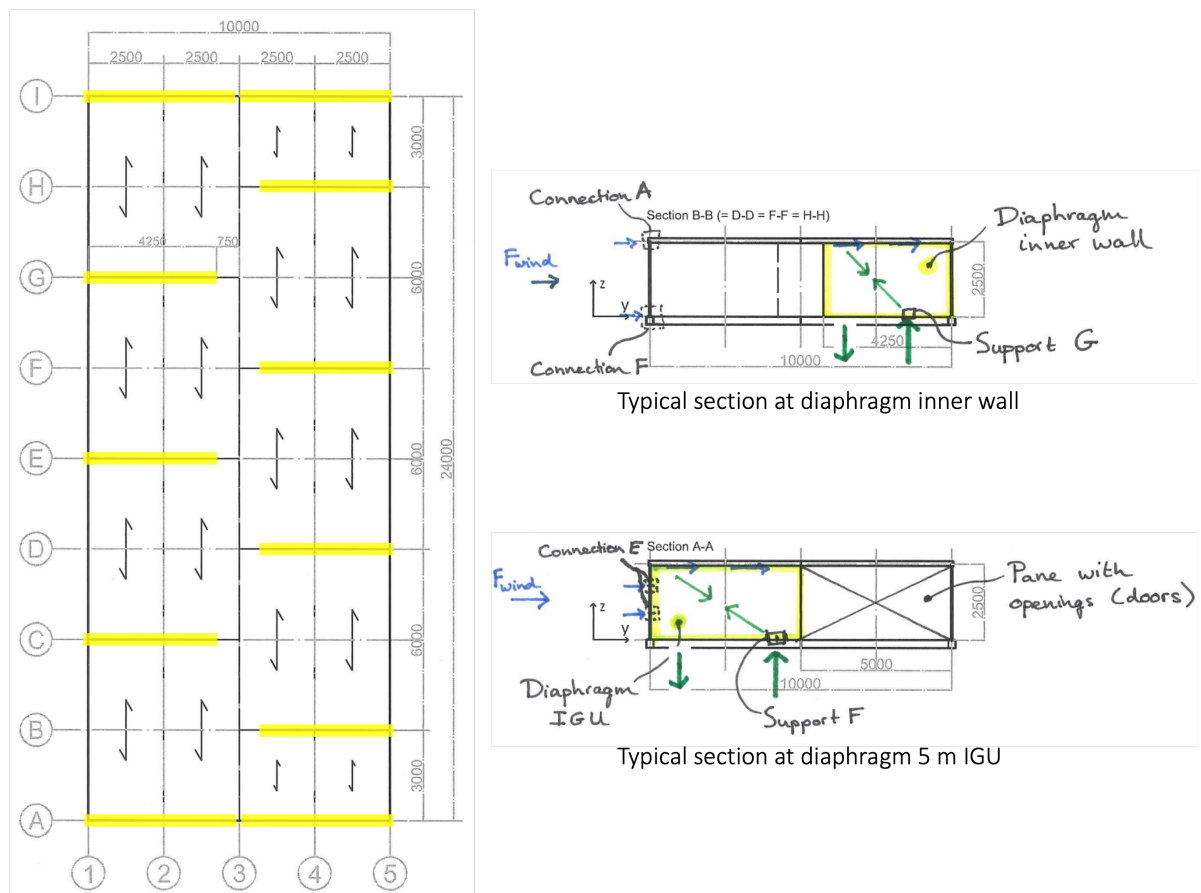

Typical section at diaphragm inner wall

Typical section at diaphragm 5 m IGU

Figure 7.17: Stability system in y-direction

7.3. Conclusion of the pavilion design

'What type of building elements are present in the design of the pavilion?' is the research question corresponding to this chapter. Timber roof slabs, glass wall panels, timber floor slabs and steel base profiles define the different building components needed for the realisation of the pavilion. Stability in x-direction is guaranteed by the outer wall panels on the long side; stability in y-direction is dependent on the short-side IGU's and the inner wall panels.

8

Connection design

The elements that transfer loads to the base via the building elements are the connections. The actual purpose of these joints, besides from keeping the structure wind and waterproof, is to connect the main building elements with each other.

Figure 8.1 lists all the different connections, divided into *'linear'* and *'corner'* connections. This chapter gives a description of the linear type of connections that are present in the design of the imaginary pavilion and so, in the building system. Corner connections are situated in every corner of building elements. These will not play a key structural role in the transfer of forces. Therefore they are not designed and so, not described in this chapter. However, the corner connections are important for sealing the building and so, making it weather-tight.

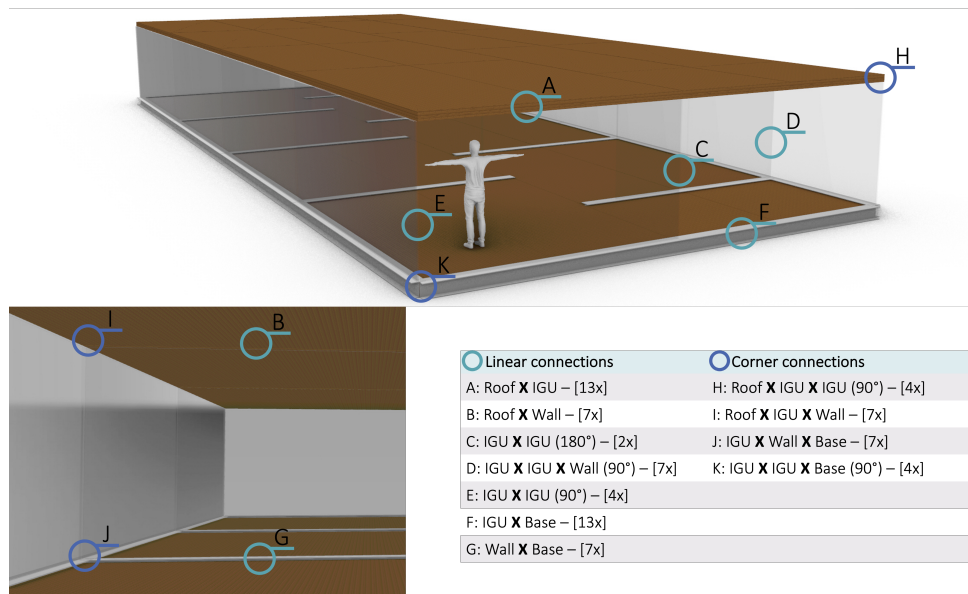| Linear connections	Corner connections
A: Roof **X** IGU – [13x]	H: Roof **X** IGU **X** IGU (90°) – [4x]
B: Roof **X** Wall – [7x]	I: Roof **X** IGU **X** Wall – [7x]
C: IGU **X** IGU (180°) – [2x]	J: IGU **X** Wall **X** Base – [7x]
D: IGU **X** IGU **X** Wall (90°) – [7x]	K: IGU **X** IGU **X** Base (90°) – [4x]
E: IGU **X** IGU (90°) – [4x]	
F: IGU **X** Base – [13x]	
G: Wall **X** Base – [7x]	

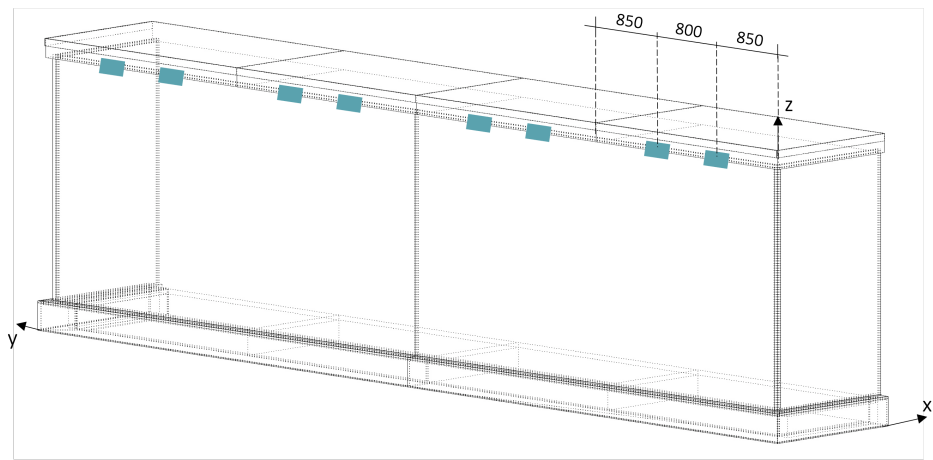Figure 8.1: The different type of connections

Appendix E contains a preliminary study for the design of the final connections. This prior work was based on a comparison of three distinct connection methods, which eventually inspired and inspired the detailed design in this chapter. Next, a lot of inspiration and knowledge is gained from the theoretical background (Chapter 5).

The connections will be described by means of three parts:

- Position of the joint
- Forces needed to be transferred by the connection (following from Appendix D)
- Physical outline of the element and dimensioning

8.1. A: roof to outer wall

Connector A is positioned between the roof and the outer wall panels, the IGU's. There are 4x4 such joints located in the pavilion (4 IGU's of $5\ m$ present with each 4 top connections required). It should be noted that on top of the $6\ m$ IGU's, no connection A is present. Along the top of the $6\ m$ IGU's, the notch in the CLT is present with the rubbers to transfer the horizontal loads.

Locations of connection type A on grid section A-A

Figure 8.2: Locations of connection type A showed in green

For type A, the forces to be transmitted are different on the long (x) and short (y) sides of the pavilion. The inner wall panels, the roof and the base transfer the pushing and suction wind loads on the long side, the y-elevation. On the short side (x-elevation), three sides work together to absorb the load: the side (IGU's in x-direction), the top (roof), and the bottom (base). In summary, the type A connection should be able to transfer the roof's dead weight, upward wind force, and horizontal wind force in both directions.

Table 8.1 shows the design forces for connection A. These forces are determined by the critical loads put on the pavilion, as elaborated on in Appendix D.
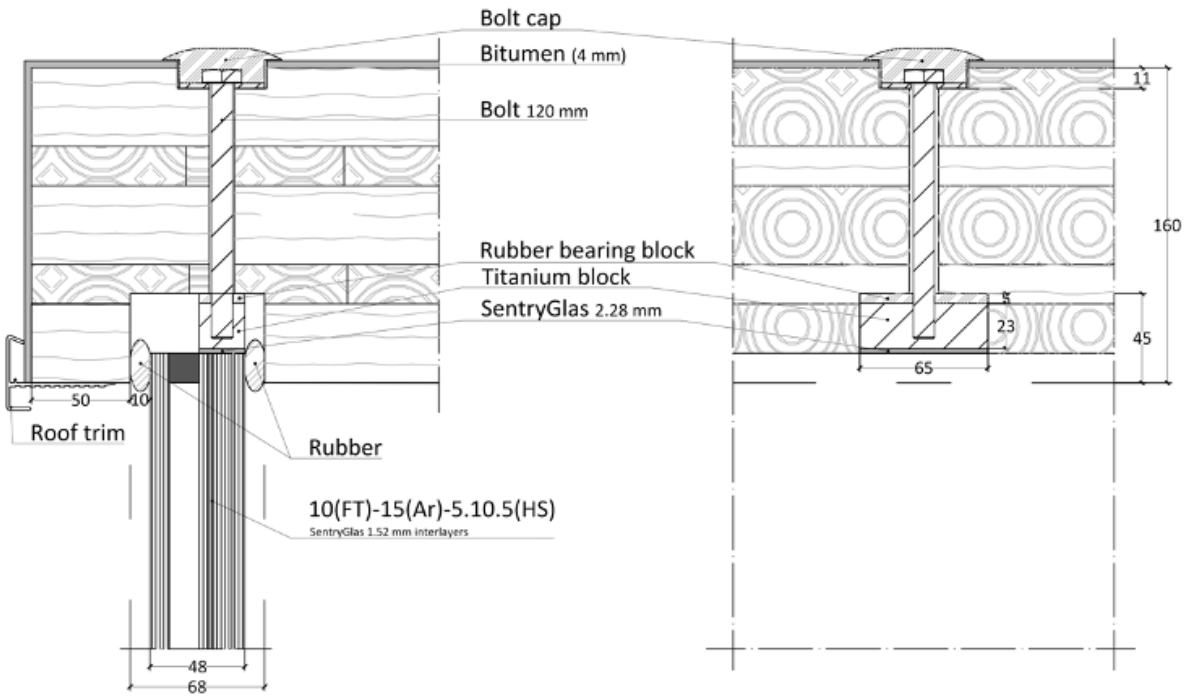

Figure 8.3: Connection type A

Local axis	Forces [kN]		
	x	y	z
A	+0.98	+0.40	+0.95
	-1.35	-0.40	-8.46

Table 8.1: Design forces connection A

As shown in Figure 8.3, detail A consists of the roof slab laid on top of the IGU. By gluing a metal element to the top of the laminated part of the outer wall, the roof element can be bolted on. The bolt is screwed into the block from the top, through the roof. To make the connection watertight, the bolt will also simultaneously fasten an aluminium profile to the roof, on which an inverted U-profile can then be clicked, a kind of bolt cap. In the opening between the IGU and the roof element on the outside, there will be a pushing gasket to make this connection type water and wind tight.

The uplift wind force acting on the connection of $0.95\ kN$ (Table 8.1) will not cause stresses higher than the assumed tensile strength in the SentryGlas® of $5\ N/mm^2$ (see Equation 8.1).

$$\sigma_{t;d_S G} = \frac{F_d}{A} = \frac{950}{20 * 55} = 0.86 \leq 5 N/mm^2 \tag{8.1}$$

In Appendix D.4.1 elaboration is made on the compressive stresses perpendicular to the grain in the CLT slabs. With a unity check of 1.30, the connection seem to not meet the safety requirements, meaning a redesign of the connection should be made. In the recommendations (Part V, Chapter 14) it is stated what should be changed in the design of connection A and B.

8.2. B: roof to inner wall

Connection B is positioned between the roof and the inner wall panels, the laminated glass panes. Seven inner walls are present in the pavilion, which means that there are 28 connections of type B in the pavilion (each inner wall panel has 4 B-connections on top.
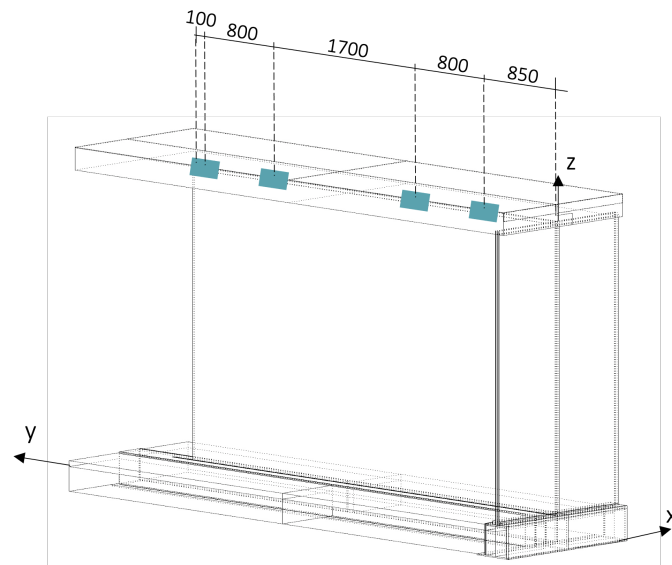
Locations of connection type B on grid section B-B

Figure 8.4: Locations of connection type B showed in green

Two roof panels are connected with an inner panel via connection B. In both a downward and upward direction, the joint must transfer the vertical weight from the roof to the laminated glass. As the horizontal stability of the pavilion in longitudinal direction is also achieved with the roof, the connectors type B have to transfer this force from roof panel to roof panel. It is not necessary to convey this force to the inner panel.

	Forces [kN]		
Local axis	x	y	z
B	0	+0.40	-19.90
		-0.40	

Table 8.2: Design forces connection B

The L-shaped ends of the roof panels make it simple to stack two on top of each other. These are simply supported on an inner wall panel and fastened with a bolt in the same method as connection type A. This bolt will be screwed through the roof panels into a metal block that is attached on the laminated glass composition. To guarantee that the connection is waterproof, an aluminium click profile will here also be added to the top of the roof panel. Figure 8.5 shows the design of this connection type.
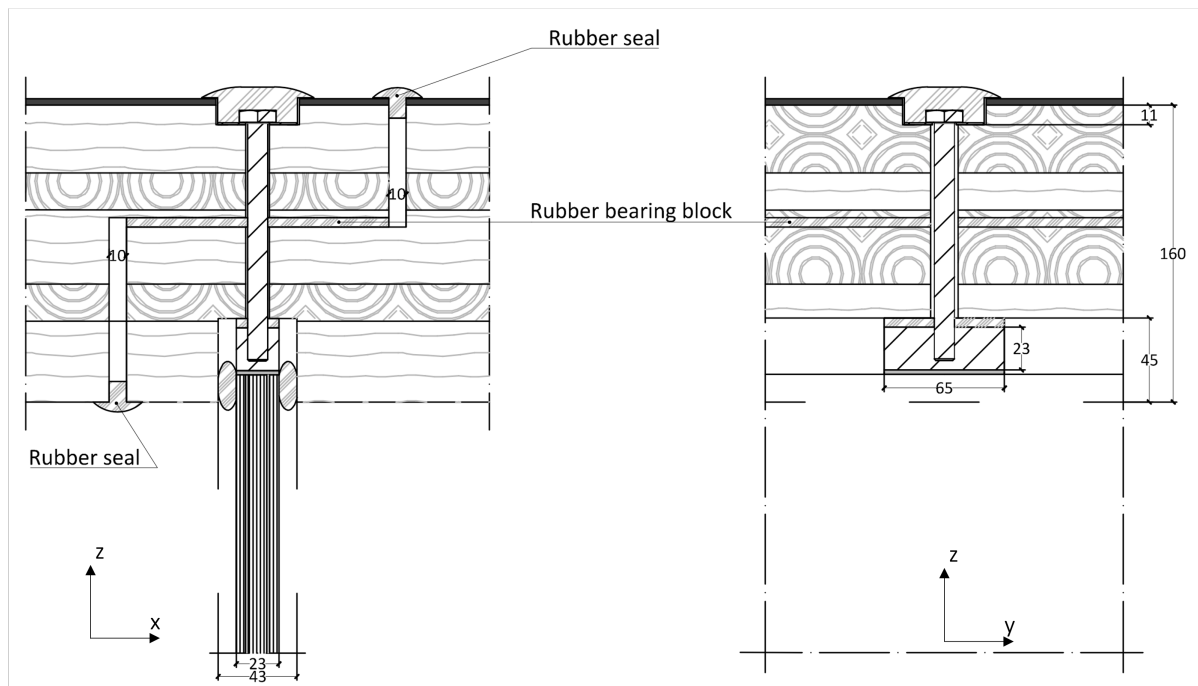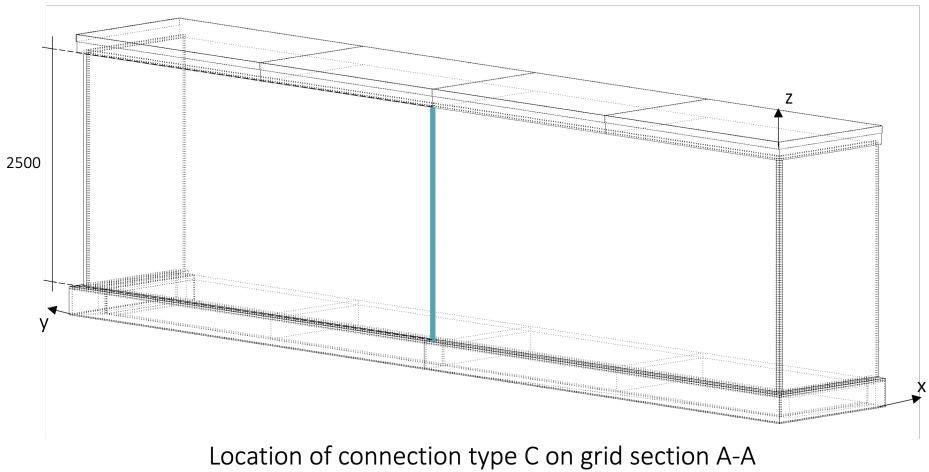
Figure 8.5: Connection type B

In type A, the stress perpendicular to the fibre direction proved to be too great, and this is also the case for type B. The unity check for connection B results in 2.61, twice as high as for connection A due to a roof area twice as large as connection B has to bear. As with A, recommendations for a redesign of the connection are given in Chapter 14 of Part V.

8.3. C: outer wall to outer wall (straight)

At the short sides of the pavilion, connection type C connects the two IGU's. These connectors have a length of 2.5 meters, which is also the height of the outer glass panels.

Location of connection type C on grid section A-A

Figure 8.6: Locations of connection type C showed in green

Connection C is primarily used to keep the glass panels on the pavilion's short side weatherproof connected. The horizontal wind force is transferred via the other three sides of these panels. As a result, no force is transferred through this link.
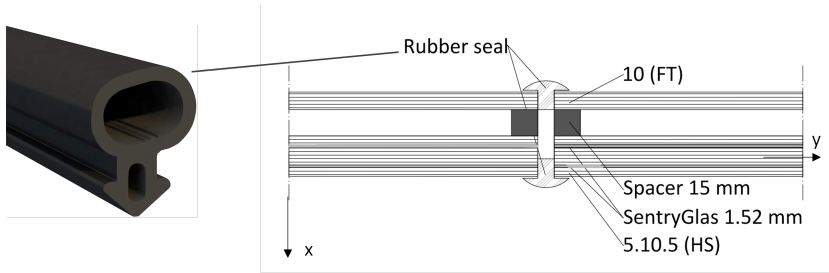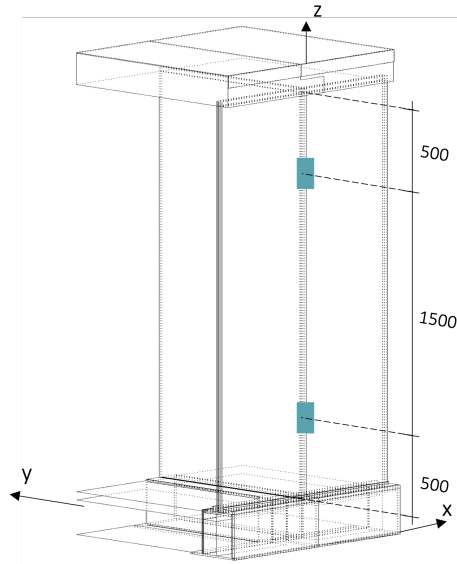

Figure 8.7: Connection type C

There are pushing gaskets on both sides of the joint, the outside and the inside, which guarantee the water and wind tightness of the pavilion. The rubber on the inside could possibly function as an installation and electricity shaft.

	Forces [kN]		
Local axis	*x*	*y*	*z*
C	0	0	0

Table 8.3: Design forces connection C

## 8.4. D: outer wall to outer wall to inner wall

Connector D, like connection type C, links two insulated glass units, but here on the pavilion's long side connection the $6\ m$ IGU's. In addition, there is an inner panel positioned at a 90 degree angle to the IGU's. At seven positions in the pavilion the IGU to IGU to inner wall connection is needed at two positions along the height, resulting in a total of $7x2 = 14$ connections D.

Locations of connection type D on grid section B-B

Figure 8.8: Locations of connection type D showed in green

This joint is to transfer the horizontal force of the wind on an outer panel to an inner panel that is perpendicularly placed. The IGU's should be simply supported at the sides, by details D and E, to behave like a hinge support.
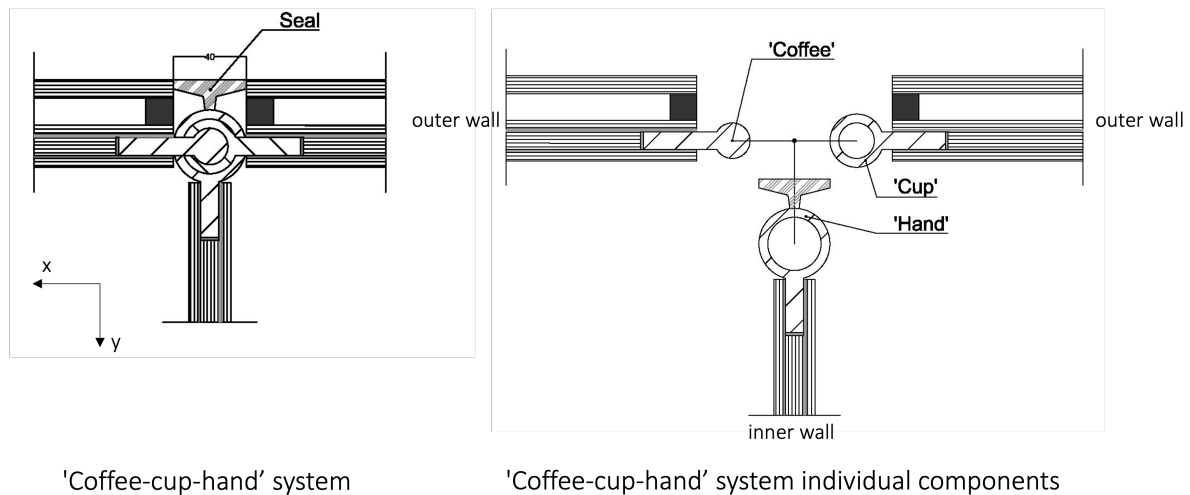
'Coffee-cup-hand' system   'Coffee-cup-hand' system individual components

Figure 8.9: Connection type D

Connection D is showcased in Figure 8.9. A hinge-looking connection is the starting point for connection type D. An element is attached to an insert in the insulated glass that links the panel to the other panel. This works via the novel 'coffee-cup-hand' design principle: one side of the joint has an insert with a hollow conical shape, the other insert contains a solid shape that fits exactly into the conic. The latter is considered the 'coffee' and the hollow conical shape the 'cup'. Another titanium element

	Force [kN]		
Local axis	*x*	*y*	*z*
D	+1.13 -4.73	0	0

Table 8.4: Design forces connection D

is laminated in the inner wall panel, the 'hand' of the connection system. This component has the appearance of a ring into which an IGU's 'coffee-cup' is subsequently put. Between the inner panel and the two outer panels there is a pushing gasket to avoid the contact of glass on glass and to neatly conceal the detail. The measurements of the 'coffee-cup-hand' system are shown in Appendix B, Figure B.7 and the technical substantiation for the dimensions are described in Appendix D.5. The final dimensions for the glass panes and laminated elements are shown here in Table 8.5.
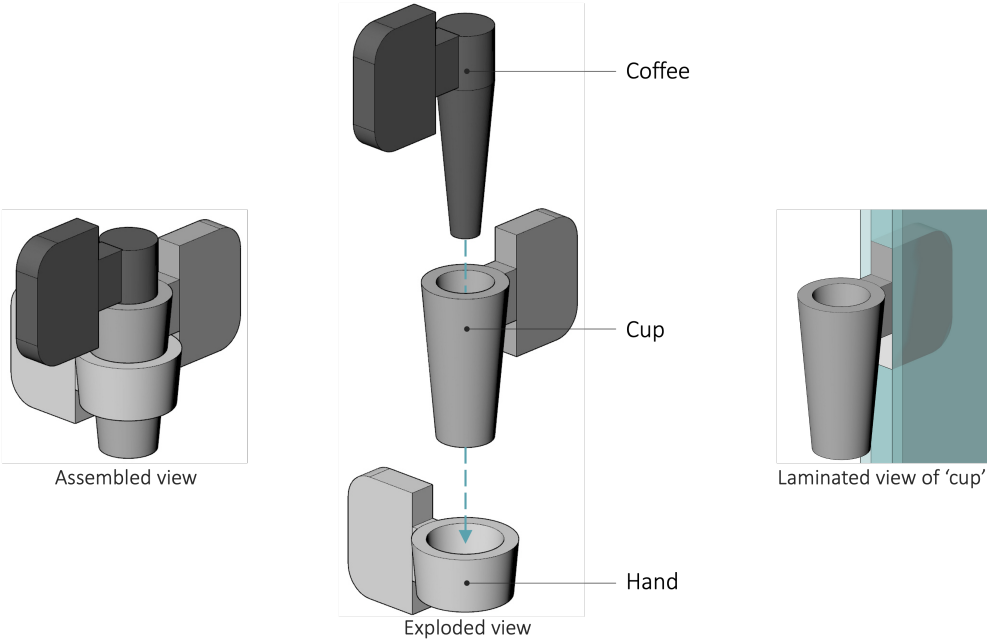

Figure 8.10: Connection type D outlook, measurements in Appendix B, Figure B.7

Description	Symbol	Value		Unit
Outer pane thickness	$t_{t_p;1.3}$	5		mm
Inner pane thickness	$t_{t_p;1.3}$	10		mm
Depth element	d_e	30		mm
Height element	h_e	45		mm
Distance a	a	10		mm
Distance b	b	20		mm
Amount of elements	n_e	2		-
Unity check	u.c.	0.24	0.99	-
Wind direction on glass pane		*push*	*suc*	

Table 8.5: Final dimensions of the laminated part of the 'coffee-cup-hand' system. Visualisation in Figure B.7, Appendix B.

8.5. E: outer wall to outer wall (corner)

The pavilion is enclosed in the corners by connecting element E. This requires eight connection units, two in each corner. This element joins two perpendicular IGU's with a 90 degree angle.
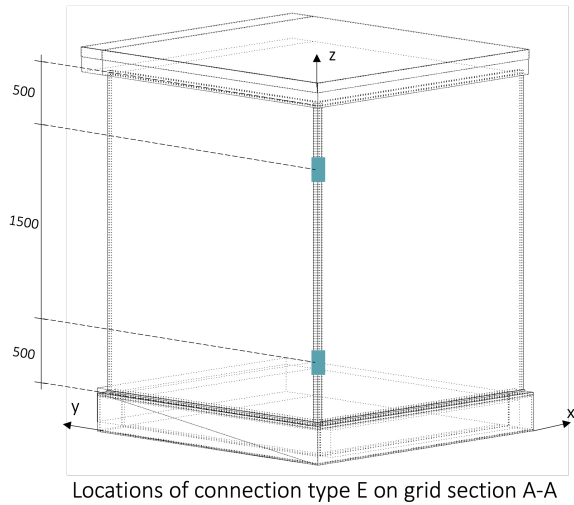

Locations of connection type E on grid section A-A

Figure 8.11: Locations of connection type E showed in green

As with connection D, the connection type E should transfer the horizontal wind loads on the IGU's of the longer side to the perpendicular outer wall panels of the shorter side. This connection should also behave schematically as a hinge.
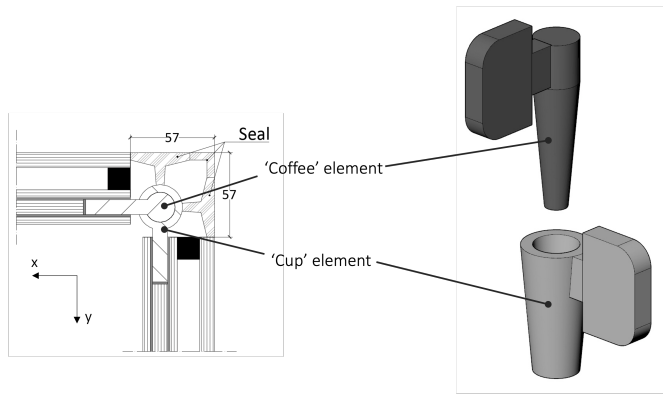

Figure 8.12: Connection type E

Local axis	Forces [kN]		
	x	y	z
E	+1.06 -1.06		0

Table 8.6: Design forces connection E

Connection E is oriented at a 90 degree angle (see Figure 8.12). A hollow conical form ('cup') should be on one IGU's insert, while a solid conical shape ('coffee') should be on the other IGU's insert. The difference with connection C is that attention must be paid to the sealing of the connection, the fixing of the wind and water tightness. An L profile should be placed on the exterior. On the interior, there is a pushing gasket whose primary function is to prevent peak stresses in the glass from being conveyed by contact between the two outer panels.

8.6. F: outer wall to base

Connection type F links the IGU to the base at the bottom of the outer wall. 13x2 of these will be required (13 IGU's present with each requiring 2 base connections), similar to connection A, with a length of 6 meters on the long side of the pavilion and 5 meters on the short side.
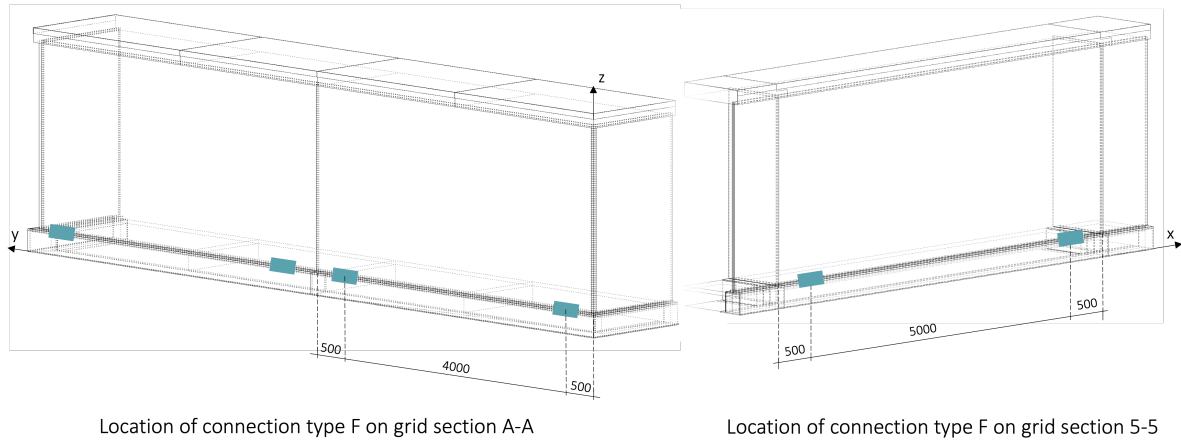

Location of connection type F on grid section A-A

Location of connection type F on grid section 5-5

Figure 8.13: Locations of connection type F showed in green

The connection from the outside to the base serves to keep the IGU's in place. These connections also ensure that the downward vertical force of the pavilion's own weight is transferred to the ground. This is not only the weight of the roof and the outer panels, but also the weight of the floor on the short sides of the pavilion's base. It is calculated that the wall panels are heavy enough to prevent possible uplift due to wind forces on the roof, see Appendix D.4.5.
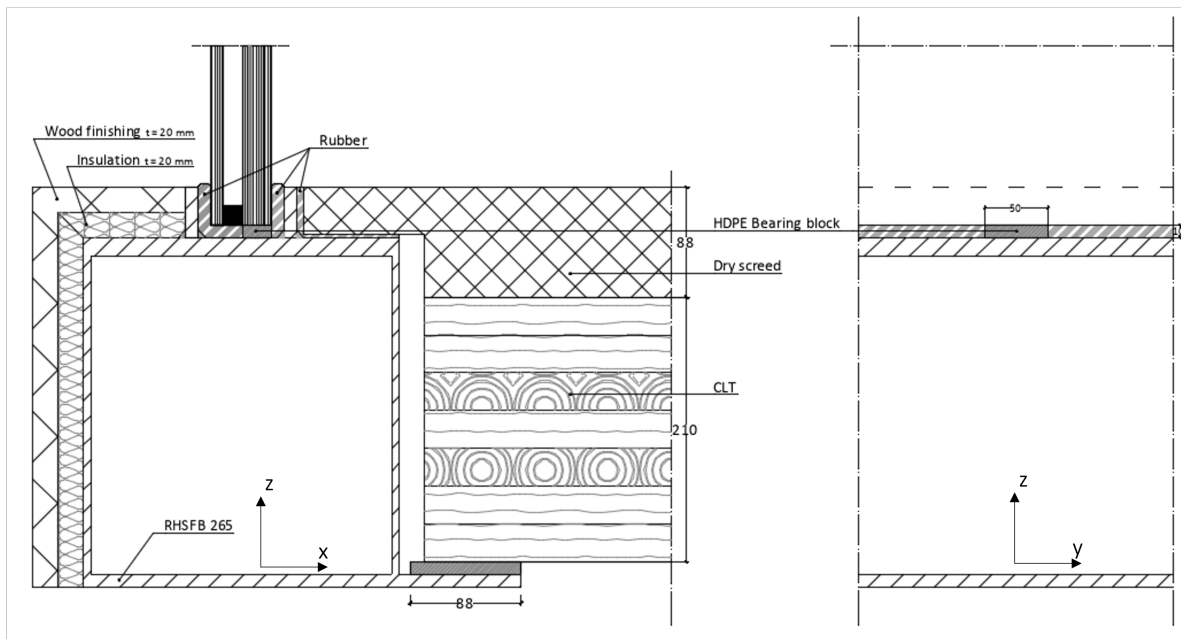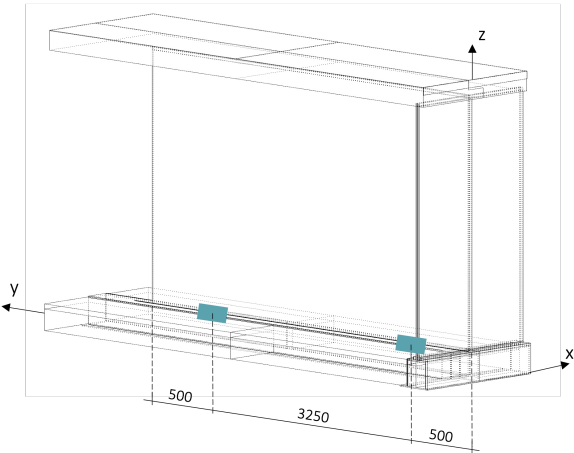

Figure 8.14: Connection type F

Figure 8.14 shows that connector type F consists of a steel 'cap' profile. On this profile, two steel plates are welded that form a shoe into which the outer wall panels can be inserted. The steel profiles at the pavilion's four corners are cut at a 45 degree angle to avoid colliding with one another. Rubber is glued in the U-profile of the steel shoe so that the glass does not come into direct contact with the steel. To avoid condensation on the steel, the profile is filled with insulating material on the outside. The floor slabs are placed on the inside of the profile, on the bottom flange.

	Forces [kN]		
Local axis	*x*	*y*	*z*
F	+2.37	+2.04	-14.08
	-2.88	-2.04	

Table 8.7: Design forces connection F

8.7. G: outer wall to base

The last variety of connection is found at the bottom of the pavilion, connecting the inner wall to the base. Seven times two pieces of this type are required (seven inner walls with each two base supports needed), with a length of $5\ m$ each. The interesting thing about this connection is that the inner walls are only 4.25 meters long, therefore the connection over its length will not exactly be the same.

Locations of connection type G on grid section B-B

Figure 8.15: Locations of connection type G showed in green

Similar to connection type F, G transfers the vertical forces from the internal walls and floors to the substrate. Any upward force from the wind must be counteracted.
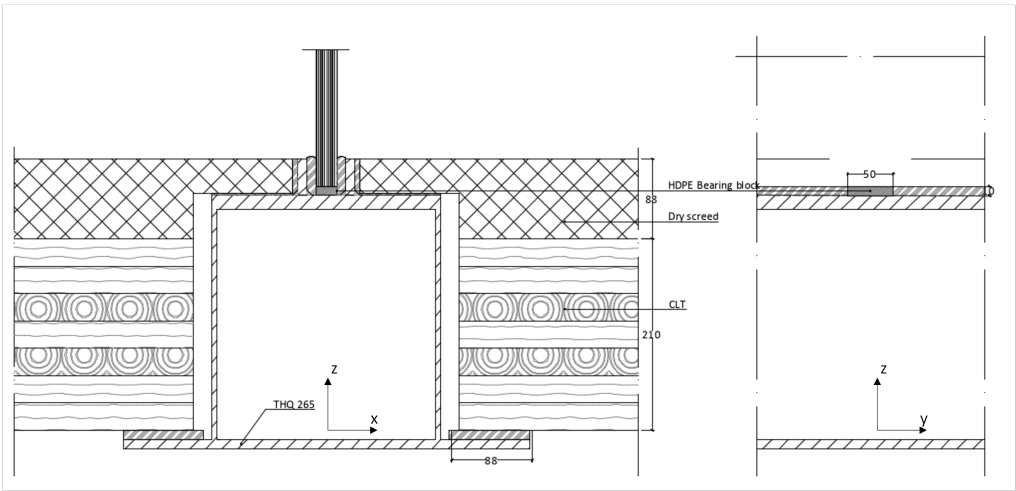

Figure 8.16: Connection type G. For dimensions of detail G, check detail F (Figure 8.14 which is similar, but misses the left 'foot'.

	Force per meter [kN]		
Local axis	*x*	*y*	*z*
G	0	1.45	-34.60

Table 8.8: Design forces connection G

The last connecting element is type G, the connection between an inner panel and the base. It will not consist of a 'cap' profile as in connection F, but of a steel 'hat' profile. This is chosen for the purpose of placing the CLT floor plates on both sides of the wall on the profile. Similar to F, a base consisting of two steel plates with a rubber on top will be welded to this steel profile. The inner panel can be placed in this shoe, as shown in Figure 8.16.

8.8. Conclusion of the connection design

The question *'What do the different connections physically look like?'* can be answered after the connection design. The connections present are as follows:

- Roof connections

    - A: roof to outer wall
    - B: roof to inner wall

- Wall connections

    - C: outer wall to outer wall
    - D: outer wall to outer wall to inner wall
    - E: outer wall to outer wall (corner)

- Base connections

    - F: outer wall to base profile
    - G: inner wall to base profile

The longitudinal connection between the roof slabs is not included in the design.

The forces that the connections have to transfer are shown in Table 8.8. Note that connection C does not have to transfer any forces, this joint is only present for the weather-tightness of the pavilion.

Local axis	Maximum force per connection *[kN]*		
	x	*y*	*z*
A	+0.98 -1.35	+0.40 -0.40	+0.95 -8.46
B	0	+0.40 -0.40	-19.90
C	0	0	0
D	+1.13 -4.73	0	0
E	+1.06 -1.06		0
F	+2.37 -2.88	+2.04 -2.04	-14.08
G	0	1.45	-34.60

Table 8.9: Forces per connection

A novel joint type is designed for connections D & E. The so-called 'coffee-cup-hand' sytem is based on interlocking titanium elements, each of which is laminated $30\ mm$ into a glass panel.

Part IV

Evaluate: Analyses

9

Detailed analysis: IGU's and 'coffee-cup-hand' system

Chapter 9 describes the procedure for finite element analysis of two critical outer wall panels first. One five meter long panel, situated on the short side of the pavilion, is examined and one six meter long panel on the long side of the pavilion. The analysis of the wall panels is performed parallel, with in general images on the left side of the paper the short IGU and on the right side the long IGU. Later detail D is examined in detailed structural analysis. All structural analyses are executed with finite element software DIANA FEA.

Prior to the computer modelling, clear goals of the analysis to be performed should be determined. Next, the model is set up by first defining the geometry and its material properties. Mesh properties are next to be determined. Thirdly, the boundary conditions should be implemented, i.e. the supports. The loads can subsequently be applied to the model. DIANA then needs to know the type of analysis. Before analysing the model, expectations are given to later check if the model corresponds to the situation in real life. Afterwards, the analysis can be run and a verification of the validity and interpretation should be given. In short, the sections in this chapter have the following structure:

- Introduction
- Goal of the analysis
- Model Setup

    - Geometry and properties
    - Boundary conditions
    - Loads
    - Analysis type

- Expectations
- Results
- Limitations of the model

9.1. Outer wall panels

The two types of exterior walls present are analysed in finite element software. The first is the IGU of 5x2.5 metres, situated on the short side of the pavilion positioned in the y-direction of the coordinate system. The second is the IGU on the long side of the pavilion, measuring 6 by $2.5\ m$ and positioned along the x-direction of the coordinate system. The figures below show the location of the analysed outer wall panels with visualisation of the wind suction force acting on the elements. The depicted IGU's are chosen after detailed hand calculations on the forces acting on the panels (see Appendix D).
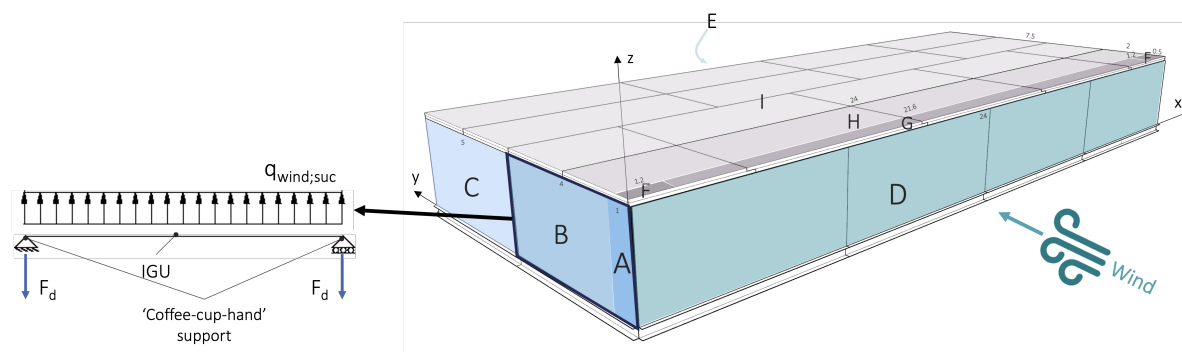

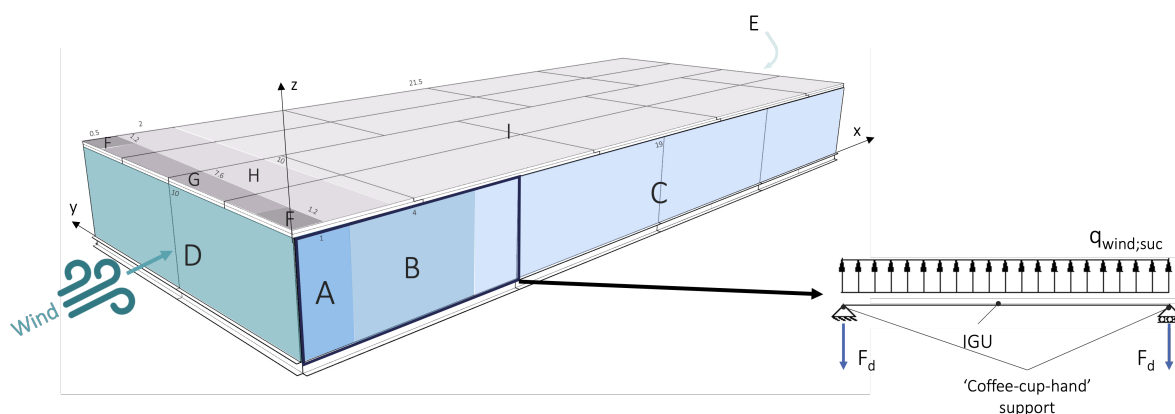Figure 9.1: Location and situation of the $5\ m$ long outer wall panel

Figure 9.2: Location and situation of the $6\ m$ long outer wall panel

9.1.1. Goal of the analysis

The main purpose of the numerical analysis of the two insulated glass units is to check these two most critical panels for deflection and tensile bending stress. For the latter, stress distribution near the supports are key to explore.
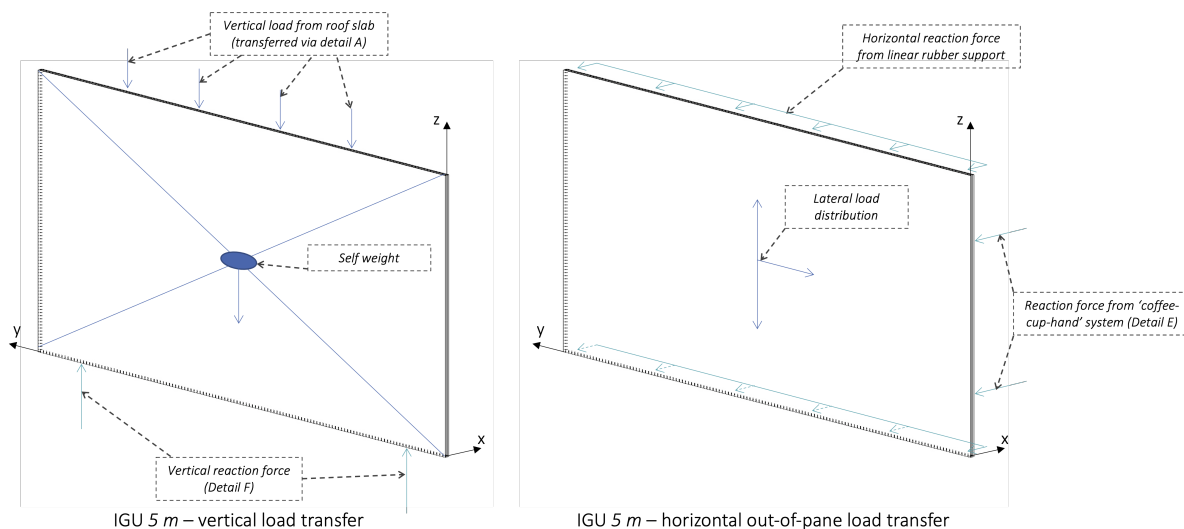

IGU *5 m* – vertical load transfer   IGU *5 m* – horizontal out-of-pane load transfer

Figure 9.3: Vertical and horizontal load transfer of the $5\ m$ IGU

IGU *6 m* – vertical load transfer   IGU *6 m* – horizontal out-of-pane load transfer
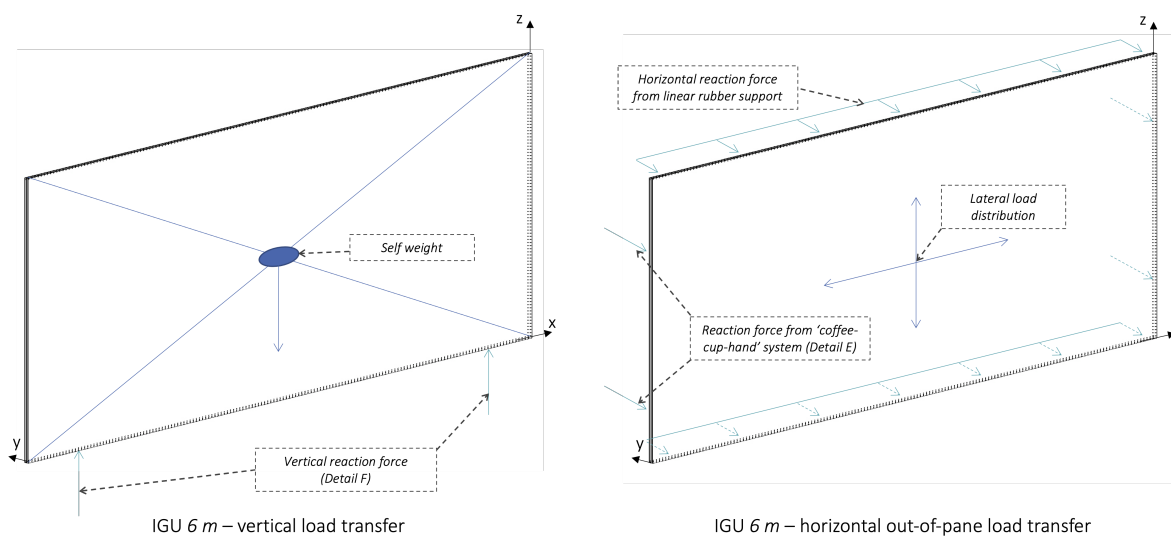
Figure 9.4: Vertical and horizontal load transfer of the $6\ m$ IGU

The difference of the two panels is the load transfer, showcased in Figures 9.3 and 9.4. The load transfer is explained before in Chapter 7. Horizontal in-plane loads are not considered in the numerical analysis.

9.1.2. Model setup

Geometry and properties

The panels are divided in multiple zones, representing the different wind loading zones from Appendix D. The glass panels have a thickness of $19.3\ mm$, which is the equivalent glass thickness for the selected glass composition in ULS phase. Later, if needed, this thickness can be changed to $19.2\ mm$ (the equivalent SLS glass thickness) in case of a critical deflection check.
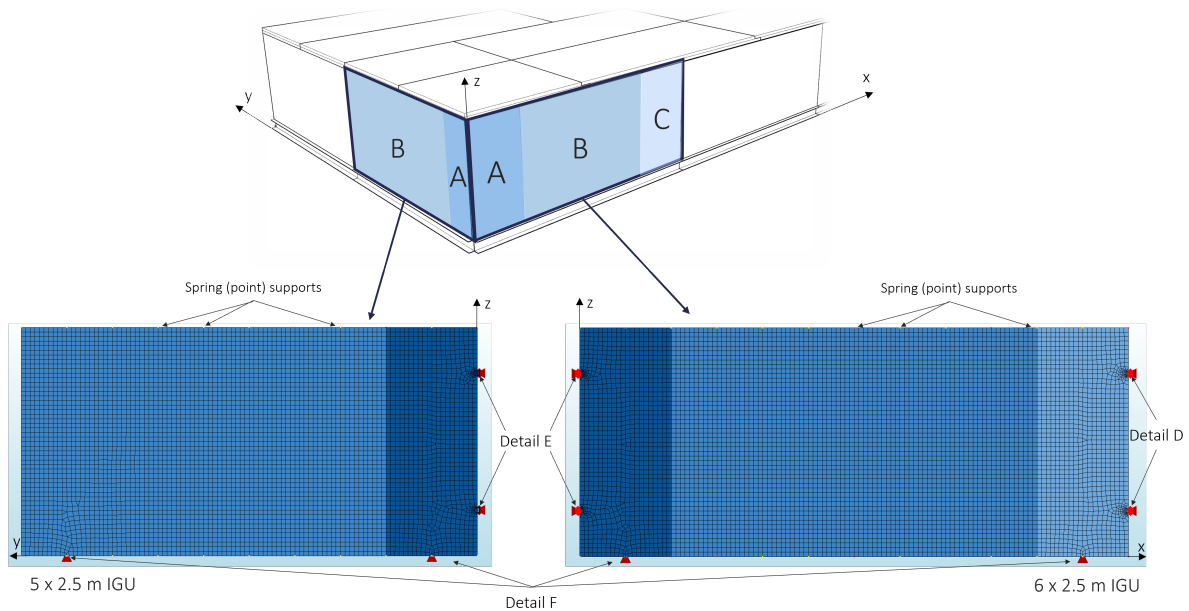
Figure 9.5: Geometrical input of the finite element model with supports

The glass thickness is smaller at the position of details D and E. Here, a titanium element (the 'coffee-cup-hand' system is laminated in the middle pane of the glass composition. The glass thickness at this position is set at $2 * 4.8 = 9.6\ mm$ (the combined equivalent thickness of two $5\ mm$ glass panels, assuming full shear interaction). The thickness of the titanium element is subsequently put on $10\ mm$, and its dimensions for the model are shown in Figure 9.5.

Material	Young's Modulus [MPa]	Poisson's Ratio [-]	Mass density [kg/m^3]
Glass	70000	0.23	2500
Titanium	106000	0.34	4260

Table 9.1: Material properties input in DIANA

The properties of the inserted materials are shown in Table 9.1.

Boundary conditions

The boundary conditions of both models are based on the supports, i.e. the details shown in Chapter 8 before.

At the bottom of the panes, $500\ mm$ from the outer corners, a vertical support is added. This line support of $50\ mm$ resembles detail F from Chapter 8 and supports the glass in z-direction, shown in Figure 9.5 and 9.6. The line is assigned to a material with an relative high stiffness.

As shown in the detailing, the insulated glass units are supported on the entire upper and bottom edge by rubber. This rubber is modeled in the finite element software by boundary springs every $0.5\ m$, even though it is considered as a linear support in the real situation. The springs have a stiffness of $0.5\ N/mm^2$ and are able to be indented $5\ mm$ on both sides, so in the model out of pane. By constraining the springs to be pushed more than $5\ mm$, relative high stiffness for larger elongation is implemented using a force-elongation diagram (Figure 9.7). For this reason, a **nonlinear analysis** has to be performed.

At the position of the titanium element (Detail D and E), the glass sheets and the titanium sheet are in the model regarded as
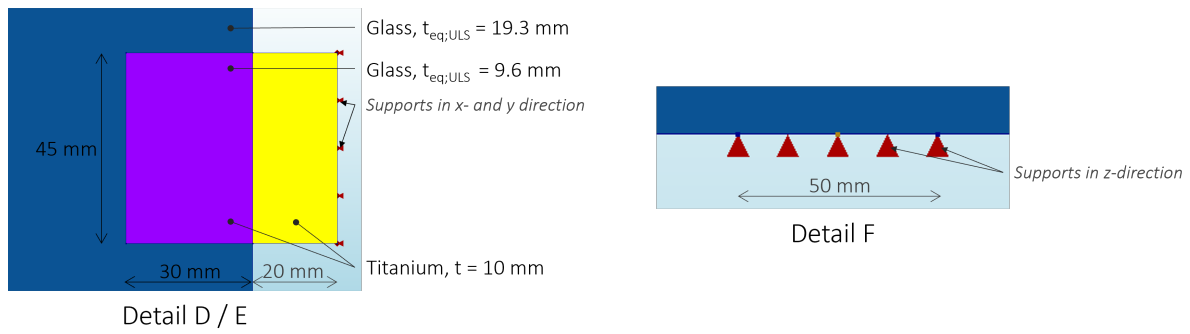
Figure 9.6: Definition of the supports in the model, detail D/E and F
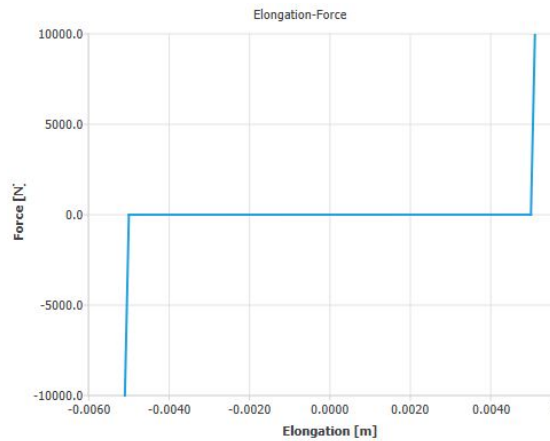

Figure 9.7: Force-elongation diagram for the out-of-plane springs at the upper and lower edge of the IGU's

full-interacting (default in DIANA FEA). The titanium element is on the outer edge supported in x- and y direction, as shown in Figure 9.5 and 9.6.

Loads

The loads defined in the model are shown in Figure 9.8. The self weight of the panel is automatically taken care on by the program. Wind loads are defined according to Figure 9.8 and Appendix D. The effect of the possible internal pressure coefficient $(+0.2 \, kN/m^2)$ (characteristic value) is taken into account.

The wind loads shown in Figure 9.8 are design loads. This makes the load combination that was implemented in the model $ULS_{model} = 1.2 * q_g + 1.0 * q_{w;d}$. For deflection analyses the combination changes to $SLS_{model} = 1.0 * q_g + (1.0/1.5) * q_{w;d}$.

Analysis type

For the reason of the nonlinear spring behaviour at the upper- and lower-edge supports, a structural nonlinear analysis is needed to be executed. The load steps performed are of a 0.05 step, marking 20 steps in total using a regular Newton-Rapson iteration method. A parallel direct sparse solution method is applied. In the table below (Table 9.2), the difference between analysing between SLS and ULS are showed.

Limit state	SLS	ULS
Laminated equivalent glass thickness $[mm]$	19.2	19.3
Load combination	$1.0 * q_g + (1.0/1.5) * q_{w;d}$	$1.2 * q_g + 1.0 * q_{w;d}$

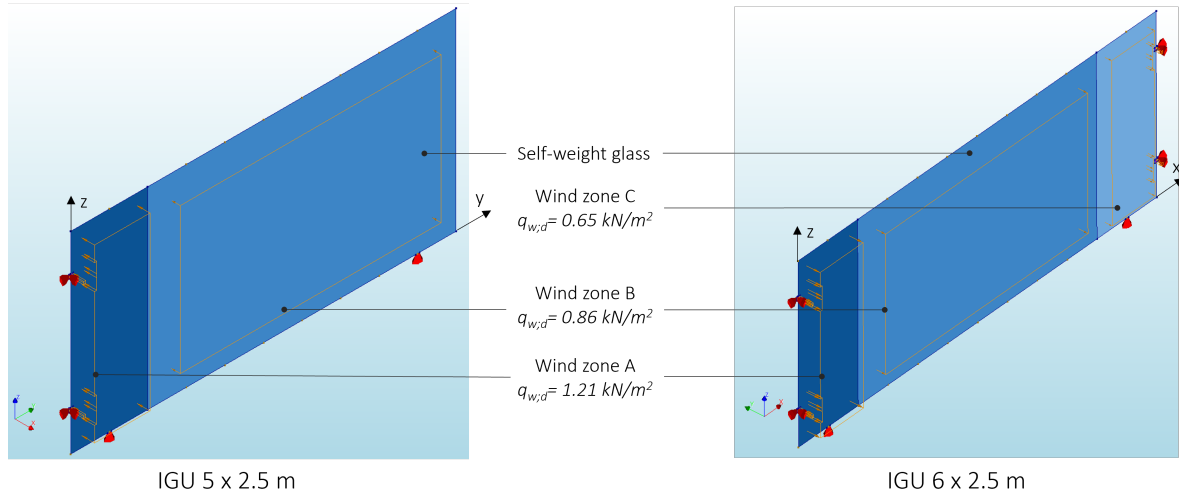**Table 9.2:** Difference of SLS and ULS analyses

Figure 9.8: Loads in the FEA model

9.1.3. Expectations

To check whether the outcome of the finite element model corresponds to simple hand calculations, the following factors are computed:

- SLS: Maximum deflection of the panel, w_{max}
- ULS: Maximum stress in the panel, $\sigma_{Ed;max}$
- ULS: Total vertical support reaction, R_v

Deflection and stress

Table 18 of NEN6720 (Figure 9.9) shows equations for predicting the maximum moment in a slab, based on a uniformly distributed load (out-of-plane). Yang [64] gives an additional equation to calculate the deflection of a simply supported slab (Equation 9.1.
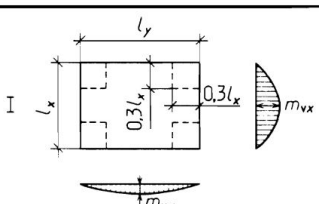
$$w = 0.001 \frac{p_{d;SLS} * l_x^4}{EI} \tag{9.1}$$

Figure 9.9: Table 18 of NEN6720 shows a calculation method for bending moments in a simply supported slab

With these equations, a prediction can be made for the result outcome of the finite element model for the IGU of $6\ m$ long. With a length ($'l_y'$) of $6\ m$ and a height ($'l_x'$) of $2.5\ m$, $l_y/l_x = 2.4$, the coefficient for the moments m_{vx} and m_{vy}, and deflection can be calculated by linear interpolation of the values of Table 18 of NEN6710 (Figure 9.9). These computed coefficient values are shown in Table 9.3.

The p_d value in the moments- and deflection equation is considered to be the wind load acting on the IGU, and equally distributed. Taking the average of the wind load zones and their magnitude, a value of $(1 * 1.21 + 4 * 0.86 + 1 * 0.65)/6 = 0.88\ kN/m^2$ is used. This is the design value, including the load factors for ULS and the internal pressure coefficient. For the prediction of the deflection w, this value is multiplied by $1.0/1.5$, making $p_{d;SLS} = 0.59\ kN/m^2$.

$$I = \frac{8}{12} t_{pl;SLS}^3 = \frac{8}{12} 19.2^3 = 4799\ mm^4 \tag{9.2}$$

Equation	Coefficient needed with $l_y/l_x = 2.4$
m_{vx}	107.4
m_{vy}	24.2
w	10.88

Table 9.3: Linear interpolated values for calculation of moments and deflection of a simply supported slab

Symbol	Value	Unit
m_{vx}	590.7	Nmm/mm^1
m_{vy}	133.1	Nmm/mm^1
w	0.76	mm

Table 9.4: Expected values based on the calculation theory of NEN6720 and Yang

Based on the assumption of full shear interaction of the laminated glass panes of the IGU, the maximum stress would be according to Equation 9.3. Following the same assumption for the shear interaction, the moment of inertia, I, is calculated according to Equation 9.2. The latter value is needed for the calculation of the maximum deflection (Equation 9.4).

$$\sigma_{Ed} = 1.5 \frac{M}{t_{pl}{}^2} = 1.5 * \frac{590.7}{19.3^2} = 2.38 N/mm^2 \tag{9.3}$$

$$w = 0.001 * \frac{p_{d;SLS} * l_x^4}{EI} = 0.001 * 10.88 \frac{0.59 * 10^{-3} * 2500^4}{70000 * 4799} = 0.76\ mm \tag{9.4}$$

Total vertical support reaction

The total vertical reaction is based on the self-weight of the panel, since no external vertical forces are applied on the $6\ m$ long IGU. See Equation 9.5 for the calculation of the expectation. The weight of the insulated pane is not taken into account since this panel is not inserted in the DIANA computations.

$$F_v = \rho_{g;glass} * t * b * h = 25 * 0.02 * 2.5 * 6 = 7.5\ kN \tag{9.5}$$

9.1.4. Results

All iterations went converging, no problems were found during the analysis. The results are split up in three sections corresponding to the checks:

- Deflection
- Principle tensile stress
- Vertical reaction force

Deflection

The IGU on the short side of the pavilion shows a maximum value of $12.5\ mm$ (Figure 9.10 for the results of deflection in the x-direction (out-of-plane). On the left-hand side, in the middle of the panel, this maximum deflection is located. The deflection is maximum at the left side of the panel because no support in x-direction is located on that edge, only the seal of connection C (Chapter 8, detail C).

The upper and bottom edge of the glass element show in the numerical analysis a deflection with a maximum value of $5\ mm$. This result satisfies the expectations and demonstrates that the model functions with the inserted springs. The spring supports on these edges represent the rubbers on the top and bottom of the panels, with an assumed maximum deflection of 5 millimetres. The deflection at the 'coffee-cup-hand' systems (detail E) on the right edge of the left panel in Figure 9.10 is, and should be, $0\ mm$.
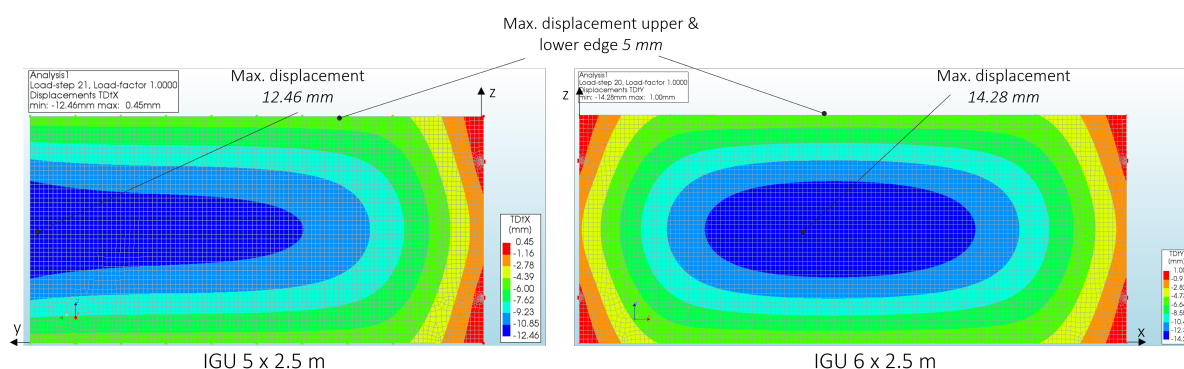

Figure 9.10: Results of the out of pane deflections

The right side of the image resembles the out-of-plane deflection of the $6\ m$ long outer wall. The analysis of the IGU here results in a maximum deflection of $14.28\ mm$. The value occurs at a place just left from the center of the plane, due to the different wind zones. The strongest wind suction zone (dark blue zone in the right image of Figure 9.8), is located on the left side of the panel.

The upper and bottom edge of the glass element result in this model in $5\ mm$, similar to the IGU of $5\ mm$. Likewise, the out-of-plane deflection at the 'coffee-cup-hand' systems (detail D and E) on the outer edges are $0\ mm$.

Not only the maximum deflection of the $6\ m$ long outer wall needs to be retrieved, also the deflection in the middle of the element is of interest to check the hand-calculated expectations. The deflection in the center of the panel, according to the computer analysis, is $14.12\ mm$ in y-direction.

Principle tensile stress
For retrieving the principle tensile stresses in the glass, the titanium elements are eliminated from the result diagrams.
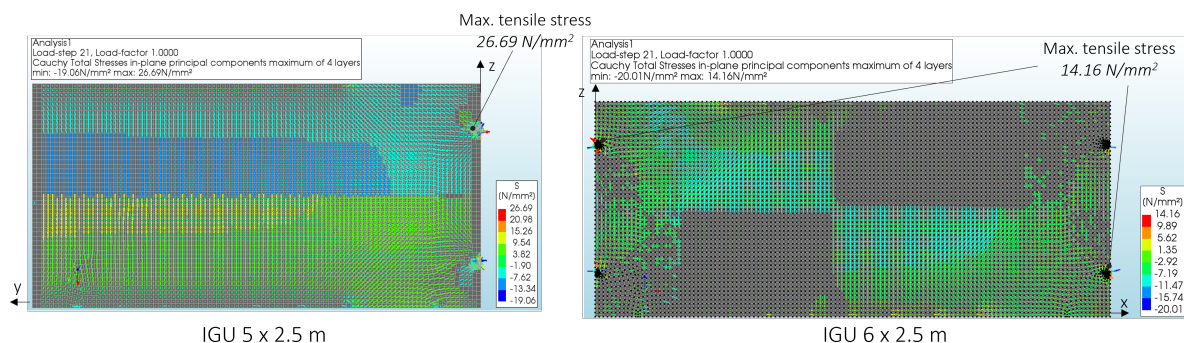

IGU 5 x 2.5 m   IGU 6 x 2.5 m

Figure 9.11: Results of the principle tensile stresses in the glass

The shorter IGU shows a maximum principle tensile stress if $26.69\ N/mm^2$, at the location of the upper 'coffee-cup-hand' element (detail E). At this location, the modelled glass is thinner because the titanium element is situated where normally the middle glass plate is laminated in. Together with the introduction of forces from the connection element, the highest tensile stress occur at this location.

A maximum principle tensile stress of $14.16\ N/mm^2$ is situated at the upper left connection of the $6\ m$ outer wall panel. Like the $5\ m$ IGU, the glass is modelled $10\ mm$ thinner due to the presence of the titanium connection element. The perceived stress here is lower than in the $5x2.5\ m$ model since the glass panel in this situation is supported in y direction at both ends.

The principle tensile stress at the middle of the panel is relatively lower than the maximum stress at the place of the 'coffee-cup-hand' system. With hand calculations based on a simply supported slab, an expectation was drawn up in order to compare the result with the model's outcome. The numerical FEA analysis gives a maximum principle tensile stress of $3.18\ N/mm^2$ in the centre of the panel.

Support reaction

The vertical support reaction is analysed to check the validity of the model. The mesh size used at the locations of the vertical supports (connection type F) makes it necessary to add up the thee particular results for every single support. Then, the result is added to the results of the other vertical supports and the total vertical support reaction is determined.
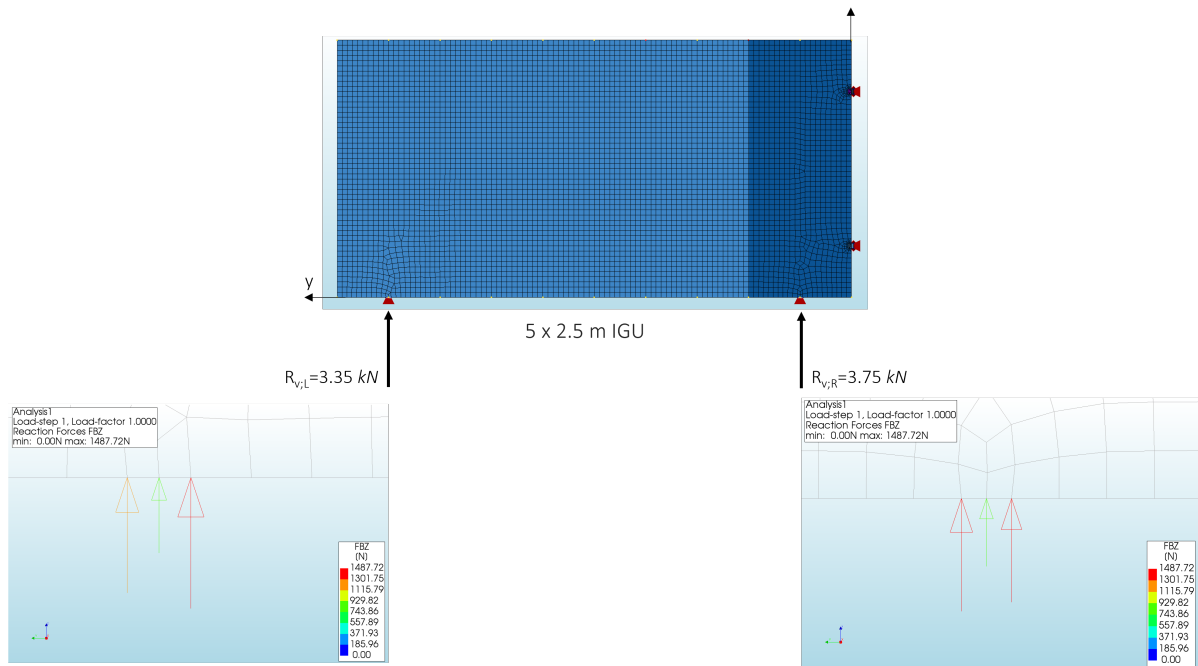

Figure 9.12: Results of the $5\,m$ IGU vertical reaction forces

As Figure 9.12 shows, the total vertical support reaction of the $5\,m$ outer wall panel is $3.35 + 3.75 = 7.10\,kN$. It appears that the numerical model shows an approximate 20% larger vertical support reaction in the base connection on the right. Simple calculations did not expect this significant difference. The titanium elements, which in this model are placed on the right side of the panel, contribute with a $0.96\,N$ to the load on the right support (based on the self-weight of the titanium elements). The support reactions of the $6\,m$ long IGU however, do not show a difference in their magnitude. The forces at the supports in z-direction of both $4.26\,kN$ result in a total vertical reaction force of $8.52\,kN$. There is no difference in the weight of the panel owing to the fact that the model is perfectly symmetrical. In horizontal direction however, the wind load is not distributed equally over the width. The horizontal behaviour does not influence the symmetry of the vertical equilibrium.
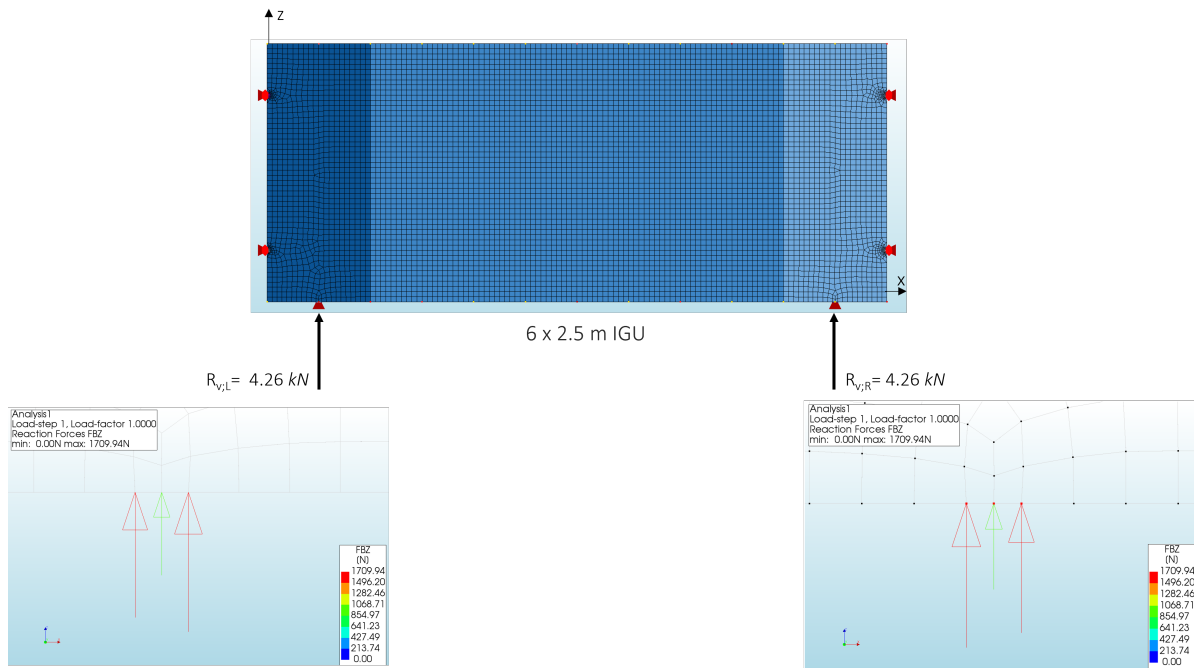
Figure 9.13: Results of the $6\ m$ IGU vertical reaction forces

9.1.5. Limitations of the IGU modelling

There are several limitations of the finite element models.

- The mentioned calculation methods for predicting the deflection and moments in the $6\ m$ IGU are a simplification of the real situation. The method is considered slightly more conservative than the due to the rubber supports along the edges, and the supports at detail D. Figure 9.14 compares the supporting conditions out-of-plane of the calculations with the model in DIANA FEA.

- In real-life support F is able to support the glass in a manner that no extreme peak stresses will occur by the use of an HDPE block. For sake of simplicity however in the model this line support is regarded to be infinitely stiff.

- The titanium element of details D and E is laminated in the glass and not moment-resistant connected like in the model. For this reason, the distributed stresses are expected to be slightly different in real life.

- The load resulting from the roof slabs via detail A is not implemented in the model of the $5\ m$ IGU. This force is not regarded as a large influence on the behaviour of the glass panes. However, it will have an effect on the support reactions in detail F. The upward wind force acting on the roof will cause a decrease in the support reaction, the downward dead- and live load will cause an increase in the support reaction.
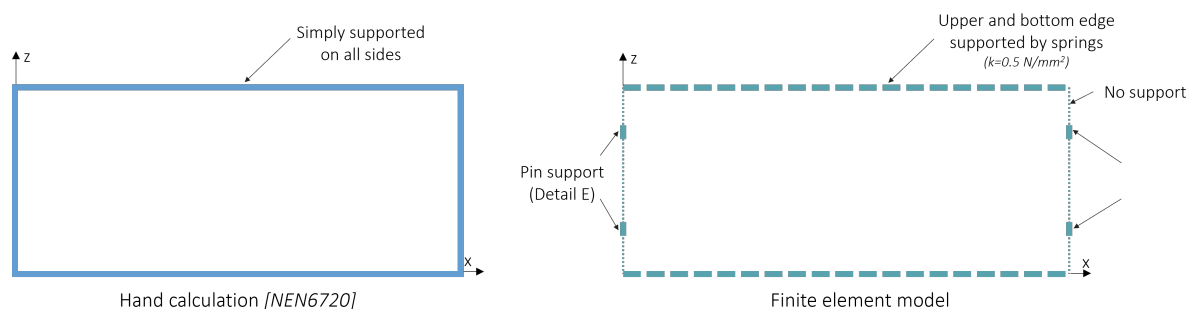

Figure 9.14: Comparison of supports calculation model versus finite element model

9.2. Coffee - cup - hand detail (Detail D & E)

Two of the details, connection D and E, contain the 'coffee-cup-hand' system. These details are being examined thoroughly. This specific type was chosen to be analysed because of its relative novel connection method. There is preliminary research on laminated joints in glass (Santarsiero, 2017 [49]), although no published assessments of the glass composition as in this study have yet been conducted.
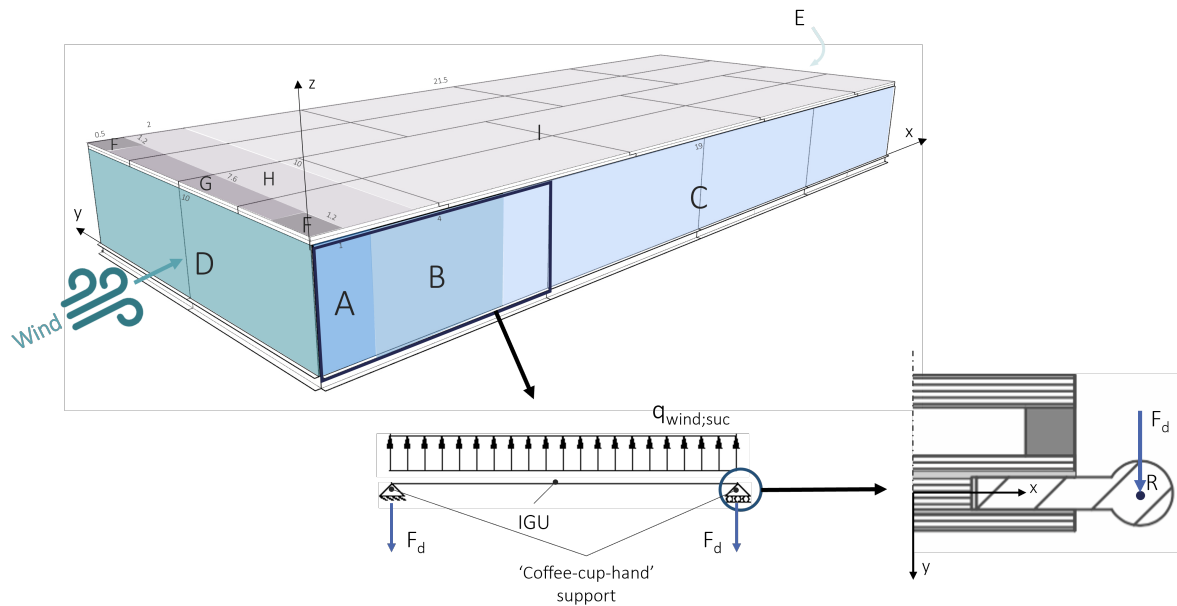

Figure 9.15: Location of the critical detail to analyse

Figure 9.15 shows the location of the detail that is analysed. That is at the location at which the resulting force from the wind suction on the IGU is largest. With wind coming from x-direction (as shown in the figure), the highest reaction forces from the 'coffee-mug-hand' system appear to be in the designated IGU, at the zones with the highest wind suction force. Connection D and E are subsequently responsible for the load transfer from the outer wall panels to the adjacent stabilising walls

9.2.1. Goal of the analysis

The main purpose of this detailed analysis is to investigate whether some specific failure mechanisms of connection D could occur, under the most critical wind suction load that is acting on the connected outer wall panels. The detail is being examined on the following:

- Distance 'a' (See Figure 9.16 below; to check if the assumption in the detailed design (see Chapter 8 of this part) is valid
- Pressure and tension zones in the SentryGlas®
- Principle tensile stress in the SentryGlas
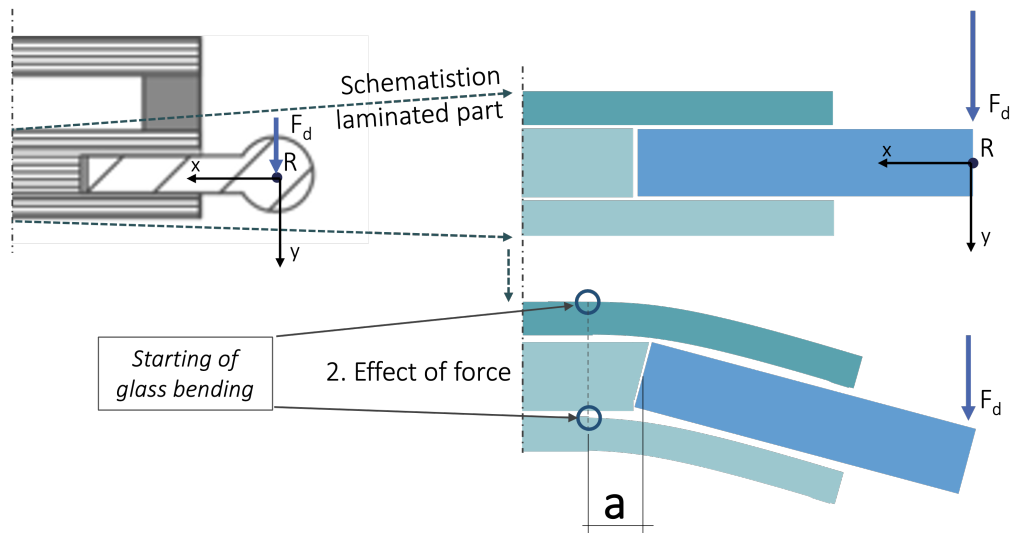- Principle tensile stress in the glass

Figure 9.16: Distance 'a', for more explanation of the determination, see Chapter 8 section 'Detail D'

9.2.2. Model setup

Geometry and properties

A laminated titanium element in the glass composition of an IGU is cropped at the centre of rotation (see 'R' in Figure 9.16). This centre of rotation is where the resultant force of the stabilising wall, holding the outer wall (IGU) in place, comes into play. The titanium element is shown in dark grey in Figure 9.17. Like determined in the previous chapter, the titanium element has a thickness of $10\ mm$, an embedded depth of $30\ mm$ and a cantilevering length of $20\ mm$ (until the centre of rotation). The depth (in z-direction) is the height of the titanium element of 45 millimeters. The inserted properties of the titanium are showed in Table 9.5.
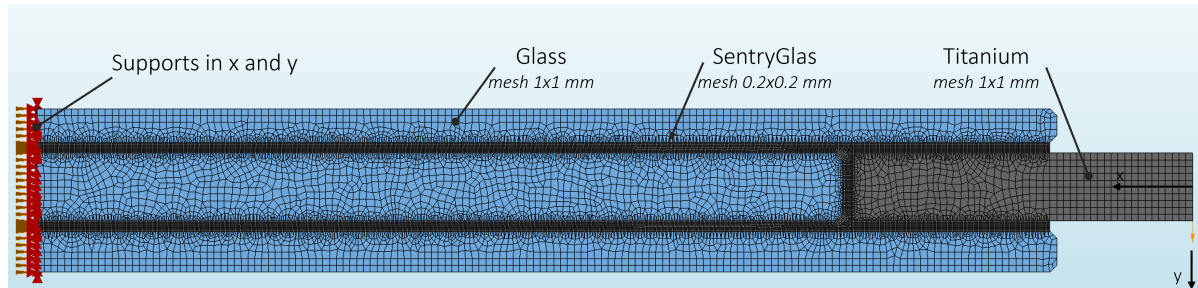

Figure 9.17: Geometrical input of the finite element model with supports and designated differing mesh sizes

The titanium element is bonded into the laminated glass composition. All laminates are executed with $1.52\ mm$ SentryGlas®, and shown inbetween the elements in dark-blue in Figure 9.17. The mesh of the SentryGlas® (mesh of $0.2x0.2\ mm$) is chosen to be smaller than the meshes of the glass and the titanium (mesh of $1x1\ mm$), since the bond is to be more precisely analysed. The depth of the SentryGlas® is in the model equal at every location and put on $45\ mm$, to simplify the model for 2D calculations. Used SentryGlas® material properties are shown in Table 9.5.

Material	Young's Modulus [N/mm^2]	Poisson's Ratio [$-$]	Mass density [kg/m^3]
Glass	70000	0.23	2500
Titanium	106000	0.34	4260
SentryGlas	612	0.449	0

Table 9.5: Inserted material properties in the finite element model

Three glass panes are shown in Figure 9.17 in light blue. The glass panes thicknesses correspond to the 5.10.5 composition of the laminated panel of the insulated glass units. The $10\ mm$ insulating pane on the outside of the composition is not taken into account for the computer simulation. The pane would have a positive effect on the outcome of the stresses (relatively smaller tensile stresses in the glass), since the force would be carried by both of the panels. The glass modelled has also a depth of $45\ mm$, but in real life a depth (global height) of $2.5\ m$.

As to be seen in Figure 9.17, the glass composition is not modeled at its entire length of $6\ m$. For computations and sake of simplicity, the model only implements $150\ mm$ of glass. From trial-and-error, this length is chosen so that the moments and forces from the supports are not affecting the mechanical behaviour of the materials in and around the titanium element.

Boundary conditions

The model is supported on the left side in Figure 9.17 by hinged linear supports in x and y direction. Owing to the beforementioned simplification of the model (glass length), the designated supports need to be modelled to create the most thrust worthy mechanical behaviour at the location near by the end of the glass (Figure 9.17, right hand side).

Load

At the end of the modelled titanium element (in real-life at the centre of rotation of the 'coffee-cup-hand' system), a force of $4.73\ kN$ is applied. The magnitude is determined by thorough wind calculations (see Appendix D), and showcased in Figure 9.18. The load of $4.73\ kN$ includes the load factor for variable (/ wind) load of 1.5.
Self-weight of the materials is not applied as a load since this factor is acting in out-of-plane direction of the model. It will subsequently not have an effect on the results of the finite element analyses in this section.

Analysis type

A nonlinear analysis has been performed to model the interface between the titanium element and the SentryGlas® for the check on the locations of compression and tension of the titanium element on the glass. For this check interface elements are implemented in between the titanium and SentryGlas® (see *'Results: Locations of compression / tension of the titanium*
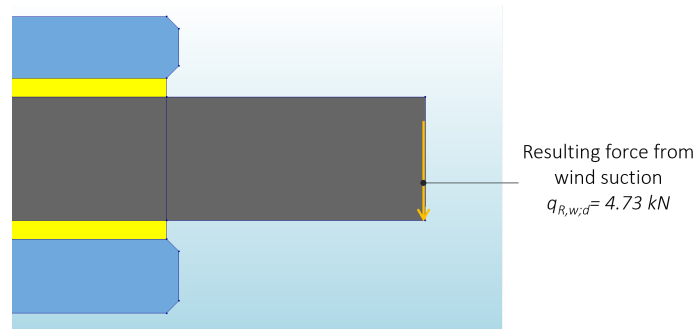
Figure 9.18: Resulting load from wind suction acting on the end of the titanium element in the model

element on the glass'). In addition, with a nonlinear analysis the behaviour of increasing stresses after each load step can be checked and verified. The latter could be an advantage to check whether the supports at the other side of the model do not influence the mechanical behaviour of the locations that are analysed (the locations around the titanium element).

9.2.3. Expectations

Three expectations of the model are stated:

- Distance 'a'
- Locations of compression / tension of the titanium element on the glass
- Tensile stress in the glass

Distance 'a'

As depicted in Figure 9.16, distance 'a' is the distance from which the bending in the glass starts until the beginning of the titanium element. The distance affects the magnitude of the moment in the glass and so on, the possible critical tensile stresses in the glass. The dimensions of details D and E (the 'coffee-cup-hand' system) were derived from the optimisation procedure which stated a unity check of 0.99 for maximum tensile stress in the glass. An assumption was made for the distance 'a' during the design of the details in the previous chapter. The length was first put on $10\,mm$ with in the optimisation procedure another option of $5\,mm$ to derive what the effect would be. In the end, distance 'a' was set on $10\,mm$.

In case of correct finite element modelling, the distance 'a' can be derived from the place at which the maximum principle tensile stress in the glass to the titanium element. If this distance is relatively close to $10\,mm$, it can be said that the assumption for 'a' in the design phase was reasonable and, so on, the dimensioning of the 'coffee-cup-hand' system.

Locations of compression / tension by titanium elements

In any case when a force is applied on the titanium element, a reaction will occur in the SentryGlas® bonding and in the glass panes. What is expected to happen is shown visually in Figure 9.19.
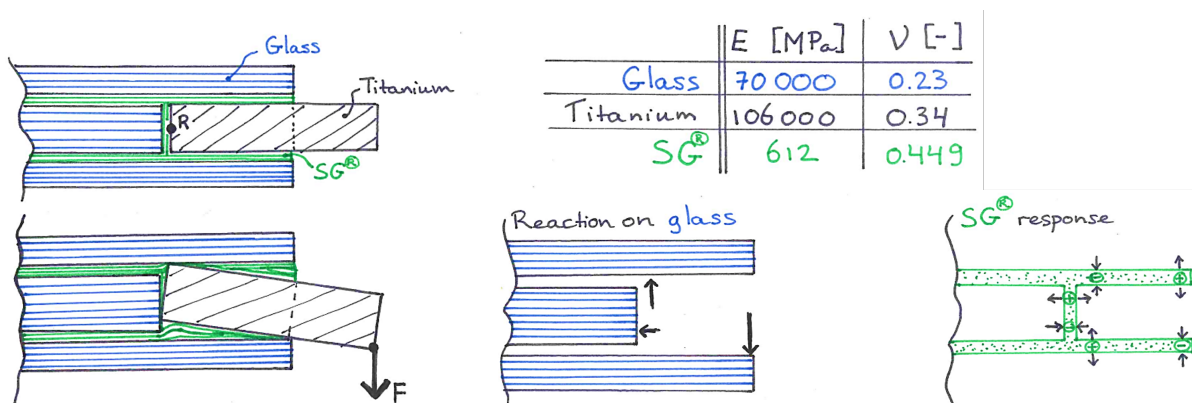

Figure 9.19: Expected locations of compression and tension in the SentryGlas as a result of a force on the titanium element

First, a look is taken at the different stiffnesses (E-modulus) of the various elements in the composition and how they related to one another. The titanium and the glass are relatively much stiffer than the SentryGlas® bond (ratios ±1:170 and 1:115 respectively). As a simplification, it can be said that the SentryGlas® will deform first and significantly higher stresses must occur for the glass and titanium to deform. In the Figure it is therefore shown that only the SentryGlas® will deform in cases of a significant low force on the titanium element.

Under an applied load (force F), the titanium element will rotate as a rigid element in the glass composition. This behaviour enables the glass to create reaction forces (Figure 9.19) at the positions where the titanium element now is closer to the glass than in a non-loaded situation. Bottom-left in the figure, it is showcased how the SentryGlas® will react on this glass-titanium behaviour, as a relatively flexible material.

Tensile stress in the glass

As described earlier with the determination of distance 'a', the maximum expected tensile stress in the glass is derived from the optimisation procedure of detail D in chapter 8. The optimisation was focused on having a unity check (u.c.) (close to) 0.99 for the maximum tensile stress ($f_t = 36.7 \ N/mm^2$) in the glass. The result of over 1700 variants was indeed $u.c. = 0.99$ with a maximum tensile stress of $36.46 \ N/mm^2$.
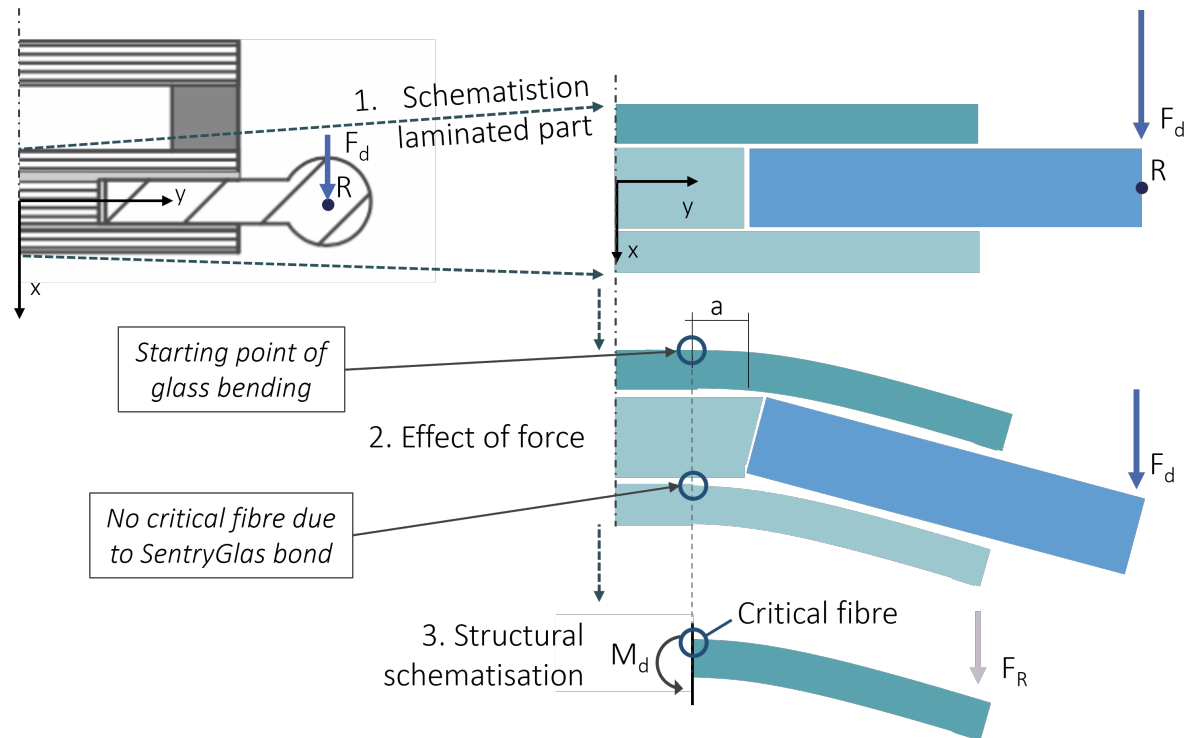
Figure 9.20: Procedure for the expectation of the location with the highest occurring tensile stress in the glass

The stress of $36.46 \ N/mm^2$ that, according to the optimisation study, is situated in the glass, is a relative conservative number because of the simplifications mentioned in the previous chapter. For the finite element model a significant lower stress is expected because of the non-critical $5 \ mm$ thick glass pane that will additionally transfer stresses from the titanium element.

9.2.4. Results

Distance 'a'

Out of the results of the finite element model, the principle tensile stresses can be extracted. These are determined at the local level, as the tensile stresses in the glass surrounding the titanium element are considered. The tensile stresses in the titanium element itself, and the stresses near the bearings are therefore not considered.
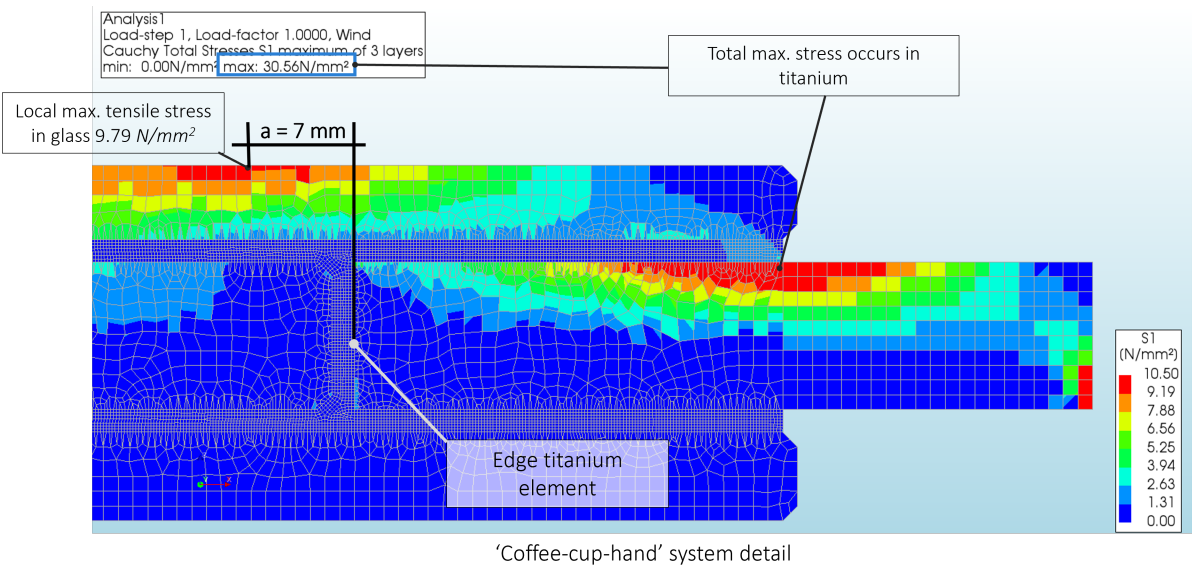

'Coffee-cup-hand' system detail

Figure 9.21: Result of the distance 'a' determination (deflection not shown to retrieve the straight distance)

The distance 'a' is the distance from the location of the highest principle stress in the glass to the equivalent position of the edge of the titanium projected on the upper glass edge. The value was crucial in the calculation and optimisation of the dimensioning of the 'coffee-cup-hand' details.From detailed node selection and measurements in DIANA, distance 'a' results in $7\ mm$, as shown in Figure 9.21.

Locations of compression / tension by titanium elements

To check at which positions tension and at which positions compression takes place between the titanium element and the SentryGlas®, interface elements are added along these edges. The interface elements behave as no-tension with shear stiffness reduction elements; for the reason of retrieving only the compression- and tension areas on the edges.

Figure 9.22 showcases the zones in the interface with tension stresses in red. The locations of compressive stress are shown in blue.
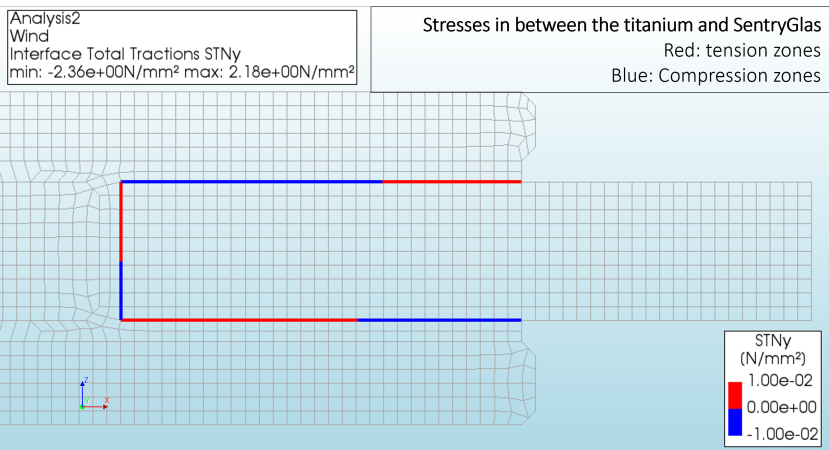

Figure 9.22: Result of the locations of compression / tension in the interface titanium - SentryGlas®

Tensile stress in the glass

The principle maximum tensile stress in the model appears to be situated at the support (uppermost-left of Figure 9.17). However, this stress is not of interest for the analysis due to the simplification of the model; the modelled supports are not even present in the design of the pavilion.

The maximum tensile stress around the insert is, as previously described, located in the outermost fibre at the top of the laminated glass sheet. According to the model, this principle tensile stress is $9.8 N/mm^2$ (Figure 9.23).

Analysis1
Load-step 1, Load-factor 1.0000, Wind
Cauchy Total Stresses S1 maximum of 3 layers
min: 0.00N/mm² max: 26.98N/mm²

Max. tensile stress in glass occurs at supports (not shown)

Local max. tensile stress in glass 9.79 N/mm^2

S1
(N/mm²)
10.50
9.19
7.88
6.56
5.25
3.94
2.63
1.31
0.00

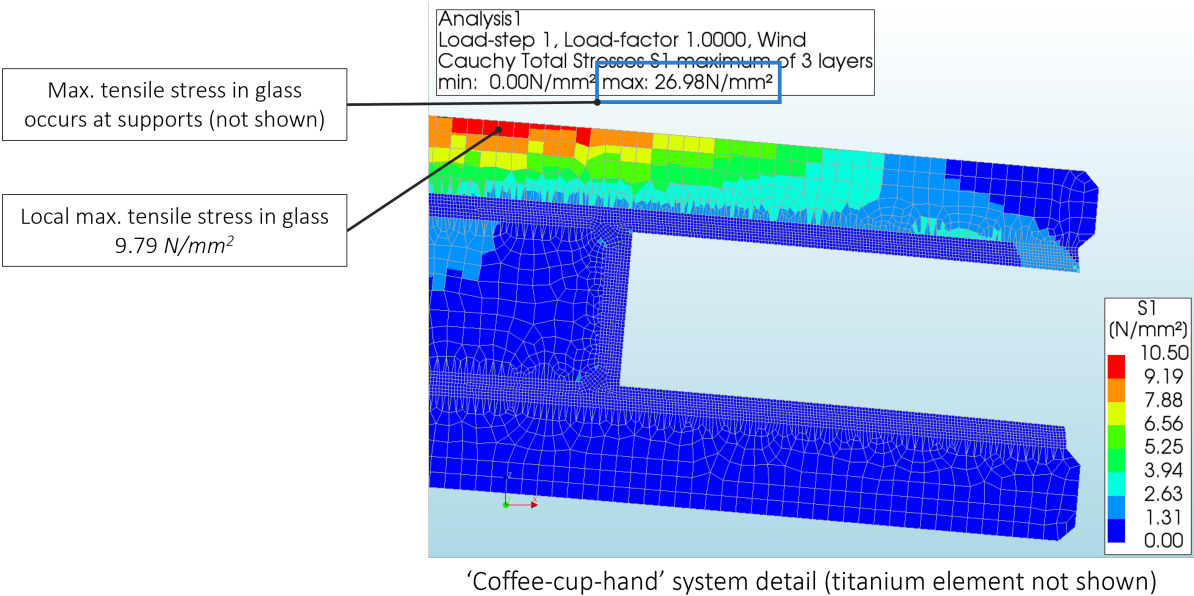'Coffee-cup-hand' system detail (titanium element not shown)

Figure 9.23: Results of the maximum tensile stresses in the glass around the 'coffee-cup-hand' system

The occurring principle tensile stress in the glass is significantly smaller than the expected value of $36.5 \ N/mm^2$. A reason could be that the approximation in the optimisation study is based on different values than used in the FEA model. Another possibility is that the AutoStudy parameters and calculations are based on the behaviour of a clamped beam, whereas the finite element model contains supports relatively far away from the maximum stress in the glass.

With a maximum tensile strength of 36.7 for the applied glass in this project, the unity check results in $9.79/36.7 = 0.27$.

Tensile stress in the SentryGlas®

As can be seen from Figure 9.23 on the right, the maximum principle tensile stress in the SentryGlas® occurs at the outermost position where the interlayer meets the embedded element. A singularity in the model's result was found at the bottom right corner of the SentryGlas® bond, depicted in Figure 9.23.

It is assumed that tensile stresses in the SentryGlas® should not exceed $5\ N/mm^2$. The model gives us, apart from the singularity, a maximum principle tensile stress in the interlayer of $2.70\ N/mm^2$. The unity check subsequently marks the value of $2.70/5 = 0.54$. Possible delamination because of excessive tensile stresses in the bond itself are unlikely to occur.
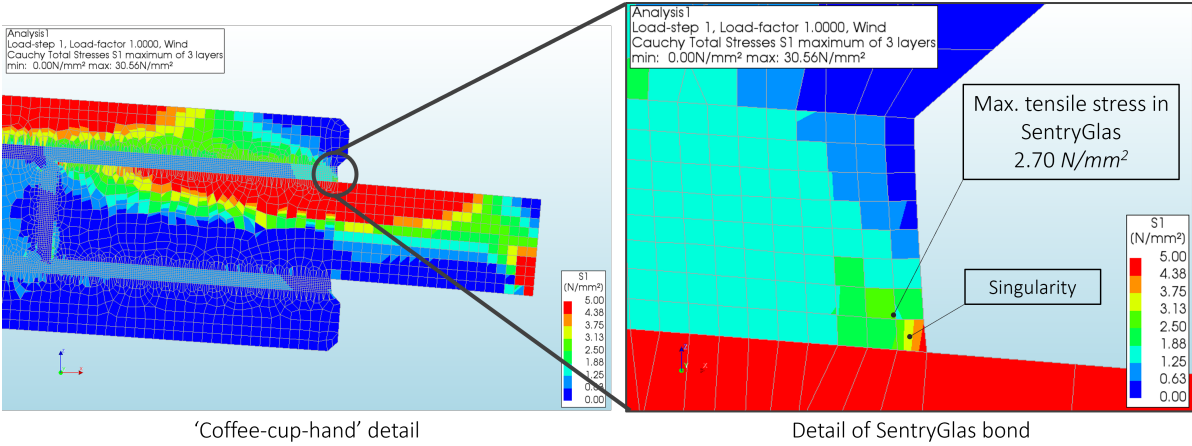

'Coffee-cup-hand' detail Detail of SentryGlas bond

Figure 9.24: Results of the principle tensile stresses at detail D in the SentryGlas® interlayer. The scale limit is for clarity modified to a maximum of $5\ N/mm^2$.

9.2.5. Limitations of the 'coffee-cup-hand' modelling

The finite element model is a simplification of the real-life situation. Below a summation of the limitations of the computer model:

- Detail D is placed in the design in two places along the height of the glass panels; both $500\ mm$ from the ends. The titanium element there is $45\ mm$ in height. The finite element model is two-dimensional and only assumes an equal height of all defined elements (glass sheets, SentryGlas and the titanium), while in reality the glass and SentryGlas are located over the entire height. This affects the stress distribution in the glass and SentryGlas: in a 3D model these stresses will be smaller.
- The simplification of only modelling the laminated part of an insulated glass unit makes the outcome of the results more conservative, since the stresses resulting from the wind force acting on the glass pane will be distributed over more glass plates.

9.3. Conclusion of the detailed analysis

To answer the research question *'How are the stresses from horizontal loads distributed in a wall panel and transferred to a stabilising element?'*, a look is considered to make at the finite element result diagrams of the Chapter for a visual representation. The numerical result is described here, structured in the insulated glass units and the 'coffee-cup-hand' detail.

9.3.1. Insulated glass units

Two IGU's are examined which, from hand calculations, need to transfer the largest horizontal force. One outer wall panel on the short side of the pavilion ('5 m *IGU*'), the other one on the long side of the pavilion ('6 m *IGU*').

Symbol	Expectation	Model	Unit
w_M	0.76	14.12	mm
σ_M	2.38	3.18	N/mm^2
R_v	7.5	8.52	kN

Table 9.6: Expected values (based on the calculation theory of NEN6720 and Yang[64]) compared to the model results for the 6 m IGU

In Table 9.6, hand computations of the '6 m *IGU*' are compared to the numerical model in DIANA, with as main reason to check their validity. It can be retrieved from the table that the finite element model shows different, less favourable, numbers than the human computations. Several limitations state that this could be due to the simplification of the panel (slab) as a simply supported slab, whereas in the model the out-of-plane supports are significantly more complex.

The vertical support reactions of both solution strategies are more in line with each other. The panel in the computer model seems to create a higher vertical load (self-weight) than the hand-calculated panel, although the same value for material weight was taken into account.

Symbol	5 m IGU	6 m IGU	Unit
w_{max}	12.46	14.28	mm
$\sigma_{t_p;max}$	26.69	14.16	N/mm^2
R_{vtotal}	7.1	8.52	kN

Table 9.7: Results of the IGU finite element modelling

Both IGU's are checked for deflection and tensile stress, as these can be critical. Table 9.7 shows the results. The maximum out-of-plane deflection is in the 5x2.5 m IGU reaches 12.46 mm, in the 6x2.5 m IGU the maximum deflection is 14.28 millimetres.

Chapter 6 of Part II stated the limit for deflections in glass panes. The 5 m IGU deflects most on its edge, where the norm states $u_{glass;max} \leq l/100 = 2500/100 = 25\ mm$. The SLS unity check for the 5 m panel is then $12.5/25 = 0.50$. The deflection in the larger IGU is situated in the middle of the glass pane (norm: $u_{dia;max} \leq l/65 = 6000/65 = 92.3 \leq 50\ mm$), marking a unity check of ($14.28/50 = 0.29$). The SLS unity checks subsequently concludes that both IGU's satisfy the norms for serviceability.

The ultimate limit state results include the maximum principle tensile stress. The tensile stress should not exceed the tensile strength of the glass ($\sigma_t = 36.7\ N/mm^2$) to stay in safe boundaries. The apparent maximum principle tensile stress of 26.69 N/mm^2 at the location of the upper 'coffee-cup-hand' system of the 5 m IGU gives a unity check of $26.69/36.7 = 0.73$. Therefore, the ULS requirements are satisfied in the design of both IGU's.

9.3.2. 'Coffee-cup-hand' system

The possible most critical 'coffee-cup-hand' connection (detail D and E) is being checked on its load transfer to the laminated glass panes. The expectations and the model's results are listed in Table 9.8.

The first check is on the distance determined during the design of the 'coffee-cup-hand' connection. Distance 'a' was there important in the prediction of the possible maximum moment, and so the tensile stress in the glass. 'a' was put on 10 mm in the design phase and the starting point for the final dimensions of the titanium elements.

Numerical analysis demonstrated that distance 'a' measured 7 mm. A footnote has to be placed because of the applied mesh-size for the glass plates of $1x1\ mm$, so a possible error of 1 mm could in real situations occur. Nevertheless, the assumption for distance 'a' in the design phase seemed plausible and finite element modelling proofed that the 10 mm even is on the safe side (higher distance 'a' means higher tensile stresses in the glass).

The locations of the expected compression and tension zones in the interface of SentryGlas®-titanium are very much corresponding to the results of the finite element model. Although no prediction was made for the specific lengths of the zones, it is stated that the titanium element behaves like expected in the glass-SentryGlas® composition.

Symbol	Expectation	Model	Unit
Distance a	10	7	mm
$\sigma_{t_p;\,glass,\,max}$	36.46	9.79	N/mm^2
$\sigma_{t_p;\,SG,\,max}$	-	2.70	N/mm^2

Table 9.8: Expectations and results of the 'coffee-cup-hand' finite element modelling

On the upper edge of the outer laminated glass plate, a maximum principle tensile stress of $9.79 \ N/mm^2$ is present according to the DIANA FEA results, marking a unity check of $9.79/36.7 \ = \ 0.27$. The prediction of the stress ($36.46 \ N/mm^2$) is significantly higher than the numerical model shows. The large difference shows that the simplifications in the computer model are more conservative than the ones implemented in the hand calculations. However, a statement can be made that the hand calculations did not include a detailed 3D analysis as well. Further 3D modelling development is necessary to extract more trust worthy results.

It was noted that tensile stresses in the SentryGlas® should not exceed $5 \ mm^2$. The highest principle tensile stress in the SentryGlas® is situated in the upper layer, on the right side close to the titanium element. The tensile stress appears to be $2.70 \ N/mm^2$ and makes the ULS unity check $2.70/5 = 0.54$.

All in all, it can be stated that a significant large deviation takes place in between the 'human' (hand-calculated) model and the computer model. The supports in the design of the IGU panels seem to be too complex for checks by hand. Regarding the 'coffee-cup-hand' connection, many simplifications are made both in the hand calculations and in the finite element model.

10
Redundancy

The structural design of buildings must account for the possibility of a building element collapsing. In the event of completely collapse of a building element, a second structural load bearing route must be established. The elements that must carry these additional weights may be estimated using a load factor of 1.0, instead of the 1.2 for permanent- and 1.5 for live-actions.

This section describes the structural redundancy of the pavilion by analysing the events of failure of the building components. Also, a replacement strategy is presented per element. The redundancy study does not cover the steel base profiles (RHSFB265 and THQ265). It is safe to presume that they are sufficiently robust, moreover the elements are not exposed to passers-by.
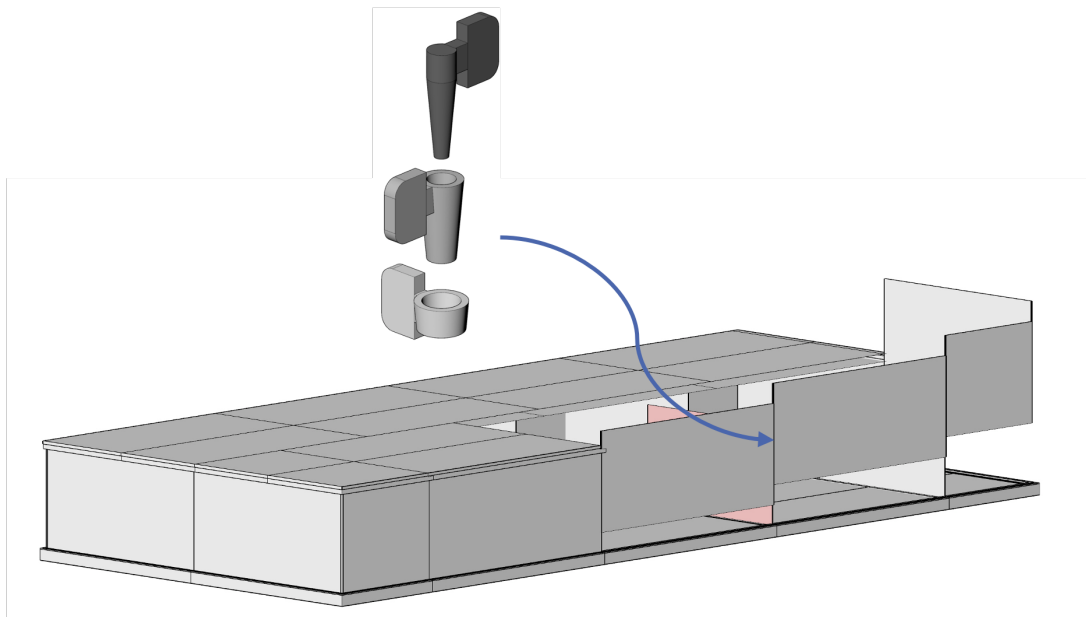

Figure 10.1: Point of attention for the replacement strategy of an inner wall

10.1. Failure of a roof panel

The roof panels are simply supported on the glass panels, meaning if a slab would fail, it will not impact the vertical load bearing path.

However, the horizontal stability of the pavilion is partly subject to the roof. If a roof panel fails, the horizontal forces coming from the wind must be redistributed. But in the x-direction, this is not a severe issue since the wall panels, which partially transfer horizontal force to the roof, are not dependent on a single roof panel. The roof panels are 2.5 metres wide, while an IGU is 5 metres wide on the short side. In this situation, the horizontal forces may be readily redistributed over the other roof panel, the perpendicular wall panel on the side and the steel base profile.

Whenever there is a horizontal load from the y-direction, the force distribution will be different than in the x-direction. Not only is the structural design different, but a roof panel is fixed horizontally on the pavilion's long side (y-direction) throughout the complete length of an IGU. As a result, if a side roof panel fails, the entire horizontal bearing path at the top of the IGU is lost. Horizontal forces should now be redistributed throughout the sides (D- and E-joints) and bottom (the base profile).
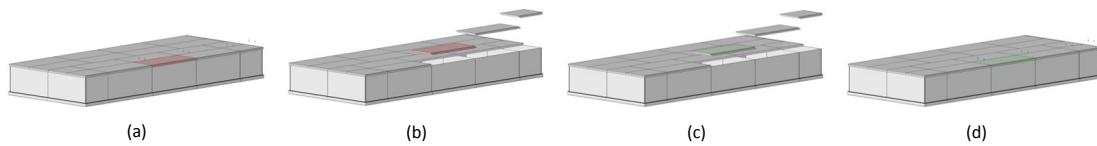

(a)   (b)   (c)   (d)

Figure 10.2: Replacement strategy of a roof panel

As soon as a roof panel fails during use of the pavilion, it should be replaced by a new one as soon as possible. This is done by first dismantling the old panel by loosening the screws of the panels that need to be disassembled (Figure 10.2a) and removing the corresponding seals in between the roof slabs. The slab is subsequently lifted from its place (Figure 10.2b) and the replacement roof panel is placed on the location of the old one (Figure 10.2c). The same bolts are then used to secure the whole the glass wall panels (Figure 10.2d), presuming the bolts have not failed. Finally, rubber seals are pressed into the joints between the new and old slabs, restoring full functionality to the pavilion.

10.2. Failure of a wall panel

The glass wall panels are a very important part of the pavilion. They not only serve as a key structural element, but they also highlight the visual impact of glass as a building material. A damaged panel would strongly invalidate this theory, so it is important to set up an accurate failure analysis for the transparent building elements.

By using the Fine & Kinney method from NEN2608 (Annex D), a risk estimation can be made (*RS*). The estimation is based on calamities, in this case study, 'the man with the sledge hammer'. Three factors are included in the calculation of the risk assessment: the probability of the calamity occurring (*WS*), the degree of exposure (*BS*) and the consequence of failure of the element (*ES*). If the *RS* value is above 400, complete breakage of the structural element should be incorporated. If $70 < RS < 400$, the structural element calculations should include the possibility of lateral breakage on two sides and if the risk *RS* is smaller than 70, lateral breakage on one side could be happening (Table 10.1).

Risk	Damage to structural element
RS <70	Lateral breakage on one side
70 <RS <400	Lateral breakage on two sides
RS >400	Complete breakage of the structural element

Table 10.1: Table D.1 from NEN2608: Determination of the damage risk (Fine & Kinney method)

$$RS = WS * BS * ES \tag{10.1}$$

10.2.1. Failure of an inner wall panel

Inner wall panels function as a vertical load bearing element. On the laminated panels, roof slabs are attached. A complete failure of an inner wall panel thus would be very inconvenient, meaning the vertical forces need to be redistributed to other construction elements. This scenario however is very unlikely to occur because of two reasons.

First, the interior walls are three-layer laminated. A vandal who tries to break the wall on both sides with a hammer, for example, will only be able to reach the inner panel from the end side ($10\ mm$ wide). Secondly, the glass is of a heat strengthened (HS) composition, which means that if the glass breaks, it breaks into larger pieces that can still work together as a whole when laminated. The glass fins of the CoCreation Centre on the TU Delft's Green Village (see Literature Review, page 27) showed a magnificent structural capacity with even all three glass layers broken. It can eventually be assumed that no complete failure of the inner wall will arise.

The Fine & Kinney's *WS* factor, the probability of damage, of an inner wall panel is set to be only possible in the long term ($WS = 1$). The exposure of the inner wall is daily, since an art pavilion will not be open during the night, visitors (and possible vandals) will be able to reach the element during daytime. The *BS* value is then 6. Lastly, in case of complete failure of an inner wall, the forces of the roof will be redistributed, so only the inner wall itself will collapse. A person standing in the vicinity hypothetically could get minor injuries from the event. The Fine & Kinney's *ES* value is then put on 7. According to Equation 10.2.1, the *RS* value is below 70 and 400, meaning that lateral breakage on one side is the determined damage.

$$RS = 1 * 6 * 7 = 42 \tag{10.2}$$

Only one outer panel would be harmed based on the risk analysis above. The other two panels are examined for possible buckling. The calculation method works the same as the earlier structural verification of the component, but now with load factors of 1.0 and an equivalent glass thickness of $12.3\ mm$. This results in a design load of $9.78\ kN$ per unit length (Equation 10.3) and a critical buckling load of $0.85\ kN$ per unit length (Equation 10.4). The unity check results in 0.10. As this value is far below the safe limit of 0.99, the theoretical conclusion can be drawn that the panel would not be subject to buckling. Since the inner sheet of the wall panel will still be laminated to the outer panels during breakage, the calculation can be regarded as significant conservative.

$$F_{\text{d}} = b * (1.0 * g + 1.0 * q_{\text{L}})$$
$$= 6 * (1.0 * 0.63 + 1.0 * 1.0) = 9.78 \, kN/m^1 \tag{10.3}$$

$$F_{\text{cr}} = \frac{\pi * EI}{(n * l)^2}$$
$$= \frac{\pi^2 * 70000 * 1240.58}{(1 * 2500)^2} = 137.13 \, kN/m^1 \tag{10.4}$$

$$u.c. = \frac{F_d}{F_{\text{cr}}} = \frac{9.78}{0.85} = 0.10 \tag{10.5}$$

The technique for replacing an interior wall panel is rather extensive. First, the bolts and seals of the roof are removed (Figure 10.4a). The roof panels are then lifted out of place (Figure 10.4b) and temporarily moved elsewhere. The pavilion's outer panels must next be removed (Figure 10.4c). Because of the detailing (connection D and E), the outer wall panel on the short side needs to be removed first, since this panel is on one edge not structurally connected to the next one. Up to and including the damaged panel, the following exterior panels are removed in the sequence. It is important that all connected panels to the failed inner wall panel should be removed. The detailing of the connection (detail D) is such that the laminated titanium element on the inner wall is the first to be installed and the last to be removed. This particular outer panel can be replaced (Figure 10.4d) by a new laminated one (Figure 10.4e). Then the insulated glass units are put back in place (Figure 10.4f) and the roof is mounted on the pavilion (Figure 10.4g). Finally, all bolts and seals are put back into position (Figure 10.4h), and the pavilion can function again.
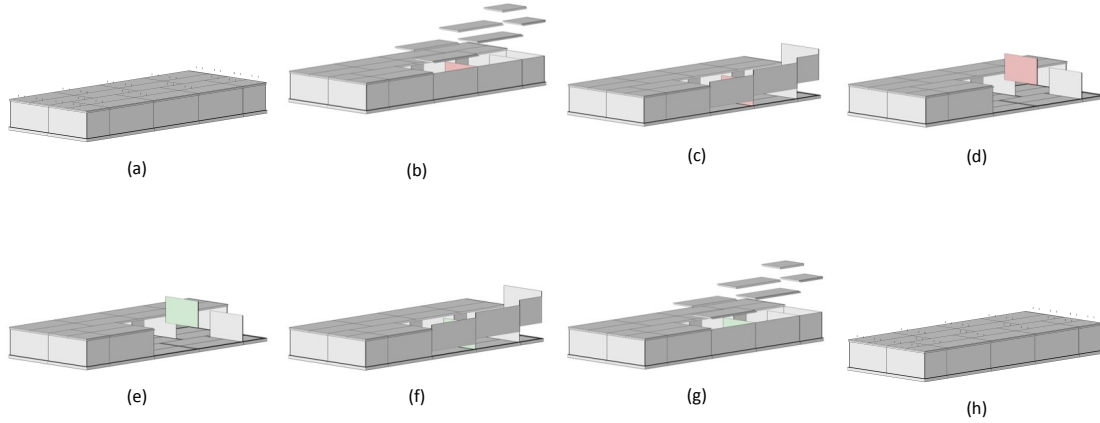

Figure 10.4: Replacement strategy of an inner wall panel

10.2.2. Failure of an outer wall panel (IGU)

Outer wall panels function as the pavilion's envelope and as horizontal stability elements. On the short side of the pavilion, the IGU's have the additional function as vertical load bearing element, since the roof panels are mounted on top. On the laminated side panes, roof slabs are attached similar to the inner wall panels. A complete failure of an IGU thus would be mean that not only the vertical and horizontal forces need to be redistributed to other construction elements, but also that the inside of the building becomes outside. This scenario however is very unlikely to occur because of the following reason.

The IGU's are on the inside laminated glass panes (exactly the same as the inner wall panels). On the outside, a cavity is present with an additional pane of $10 \, mm$ fully tempered (FT) glass. A vandal who tries to break the wall from the inside of the pavilion shows the same scenario as the inner wall panels. When this person tries to break the insulated glass unit from the outside, the outer non-laminated panel will fail first. A fully tempered panel has a significant higher tensile bending strength than heat strengthened glass panels. The vandal will less likely to break the panel than a single pane from the inner wall. Nonetheless, if the person does succeed in breaking the element, the panel will be completely collapsing. Fully tempered glass has the tendency to break into little fragments, whereas this panel is not laminated, the panel will eventually fail as a whole. In case the vandal has broken the outer pane, the glass unit transfers to having the same composition and will behave the same as the inner wall panels.

The Fine & Kinney's *WS* factor, the probability of damage, of the IGU's is set to be unusual yet possible ($WS = 3$) since no extra safety measures are incorporated on the outside of the pavilion. The exposure of all outer walls is constant, since passers-by will be able to reach the element both during the day and night ($BS = 10$). In case of complete failure of an outer wall on the short side, the forces of the roof will be redistributed. A person standing nearby could theoretically get minor injuries from

the collapse. The *ES* value is then put on 7. According to Equation 10.6, the *RS* value is between 70 and 400, meaning that lateral breakage on two sides is the determined damage.

$$RS = 3 * 10 * 7 = 210 \tag{10.6}$$

The element does not demand to be computed on its buckling strength, since the buckling check of a damaged inner wall panel seemed to be on a very safe side. Additionally, the outer walls bear less load in the vertical direction. Contrary, an outer wall should be calculated with only the inner panel on the laminated side functioning as the only load bearing element according to the risk analysis above. However, since this inner sheet will still be laminated to the outer panels during breakage, the panel is expected not to buckle.
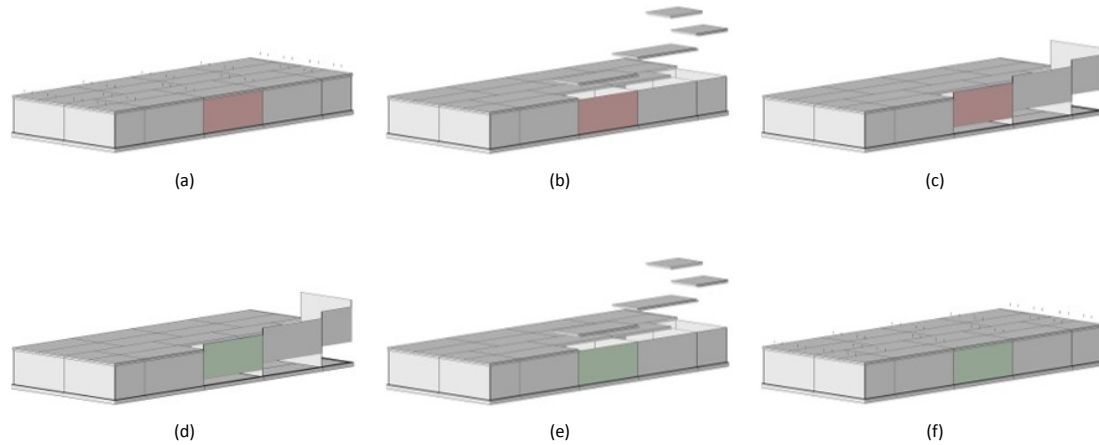

Figure 10.6: Replacement strategy of an outer wall panel

Replacing an external wall is comparable to replacing an internal wall, but somewhat simpler. Once all bolts and seals have been removed (Figure 10.6a), the roof panels may be pulled out of position (Figure 10.6b). The insulated glass panel adjacent to connection C, on the broken panel's side, is removed next. Afterwards the outer panels are disassembled one by one (Figure 10.6c), and the damaged panel can be replaced with a new one (Figure 10.6d). Following that, the demounted glass panels can be installed again. The roof panels are placed (Figure 10.6e) and finally the seals and bolts seal everything neatly (Figure 10.6f).

10.3. Failure of a floor slab

The floor slabs are simply supported on the base profiles and carry the load of the pavilion's visitors and the art installations. No extraordinary loads are expected for the floor slabs. Besides, failure of a floor slab would not have large consequences. If one floor slab fails, visitors and art installations will approximately fall 10-20 centimeters (height of the base profiles plus the height of the substructure). No secondary load bearing path is applied to the floor slabs.
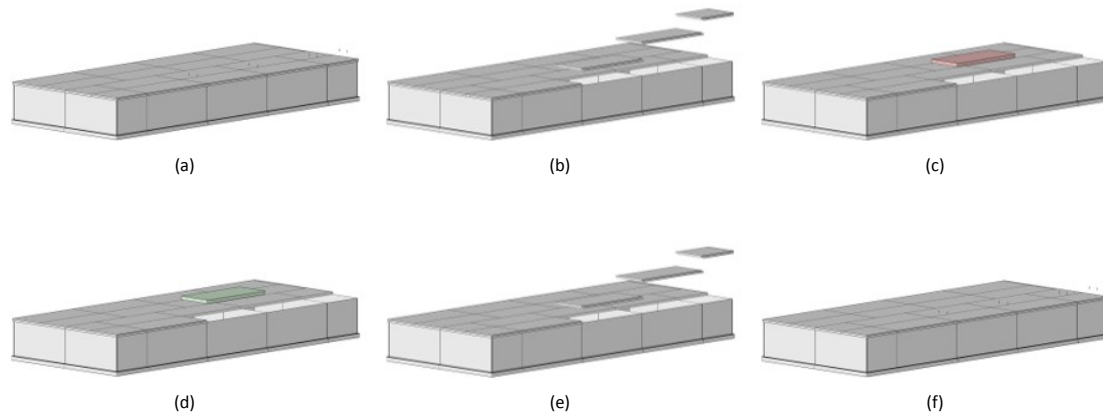

(a)	(b)	(c)
(d)	(e)	(f)

Figure 10.8: Replacement strategy of a floor panel

Although the floor slabs are fully enclosed by other building elements, replacement of the element is rather uncomplicated. First, screws and seals need to be extracted from the roof plates that need to be removed (Figure 10.8a), after which the roof slabs are removed (Figure 10.8b). Subsequently the designated floor slab can be lifted out of the pavilion (Figure 10.8c) and be replaced by a new one (Figure 10.8d). Finally, likewise the roof panel replacement, the roof slabs are placed into position (Figure 10.8e) and lastly, the seals and bolts are inserted (Figure 10.8f).

10.4. Conclusion structural redundancy

After this chapter, answer can be given to the sub-question *'How is taken care of redundancy if one building element fails?'*. This question is applied to four parts: a roof element, an inner- and outer wall panel and a floor slab.

Element	Risk (RS)	Damage to structural element
Inner wall	42	Lateral breakage on one side
Outer wall	210	Lateral breakage on two sides

Table 10.2: Building elements and their risk of failure

Secondary load bearing paths are present in case of failure of a roof slab. The particular building component is subsequently easy replaceable by removing the consecutive mounted roof slabs.

The inner wall panel is subject to breakage on one side (Table 10.2). The remaining two glass panes are sufficient to keep the interior wall from buckling. Replacement of the element is rather extensive since the IGU's on one side additionally need to be removed. This may be a reason to reconsidering the detailing (the 'coffee-cup-hand' system).

Outer wall panels on the other hand are more subject to breakage (Table 10.2), but less complex in words of the replacement procedure.

It is very unlikely for a floor panel to fail because of its thickness. Also, replacement of this component is relatively easy since the element is freely supported on the base profiles.

11

Transportation and assembly procedure

A building can be designed as well as architecturally and structurally possible, it is also very important that the manufacturability is sufficient to realise the structure. This chapter looks at the feasibility of transport and the assembly method of the pavilion.
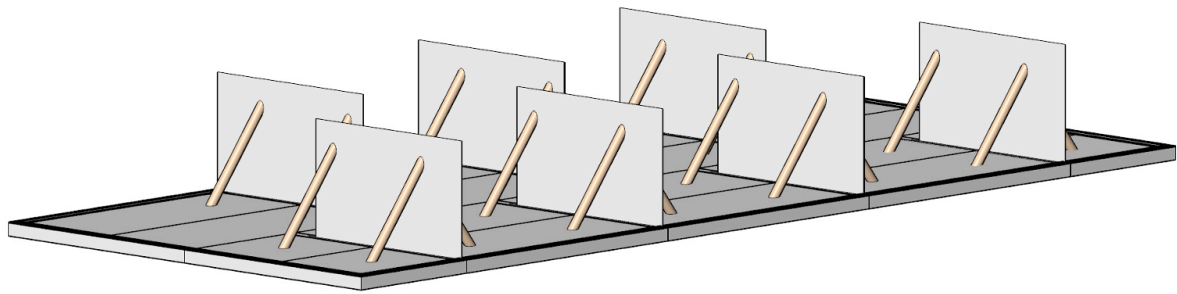

Figure 11.1: Assembly of the inner walls: temporary struts are needed

11.1. Transportation

The construction elements are transported by road. This requires a maximum of accurate container analysis and possible solutions to capacity problems.

11.1.1. Container fit

One of the requirements from the List of Requirements describes that the building elements will fit into a standard container in order to avoid exceptional transport. A standard container has external and internal dimensions as defined in Table 11.1.

	Dimensions [mm]	
	External	*Internal*
Length	6100	5898
Width	2440	2352
Height	2590	2393

Table 11.1: Dimensions of a standard container [65]

The largest building elements per size are shown in Table 11.2. It is noticeable that the dimensions are different from the grid dimensions. The deviation from the grid sizes is partly due to the joints that are attached to the components en and overlapping of elements for structural or building physical reasons.

From the table it can be seen that the largest building components do not fit in the standard container; their sizes in a particular direction exceed the maximum internal sizes (Table 11.1) of a container.

	Dimension [mm]	Building element	Container fit	Deviation
Length	6225	Base profile	No	+5.5%
Width	450	Floor slab	Yes	-80.9%
Height	2550	Roof slab	No	6.6%

Table 11.2: Maximum dimensions in length, width and height as they are positioned in a container. The values do not include necessary protection material.

All building elements are transported in standard containers, even though glass transport is normally done by special glass trucks. As a result, transportation may be as universal and simple as possible.

As a protective precaution, packing material is wrapped around the building elements. The glass subsequently is less fragile during transit, the second transport criterion of list of requirements will be in this manner be fulfilled.

11.1.2. Revised grid-size

Figure 11.2 shows all building elements in a standard container. The left container shows the four different basic profiles. With a scaffold in the container, several rows of basic profiles can be transported (maximum of four rows). The container on the right contains the three different glass walls, the two different roof and floor labs.

For visualisation purposes, the containers in the image have been enlarged by 8% to allow the building elements to fit inside. Packaging and protective materials are not shown.
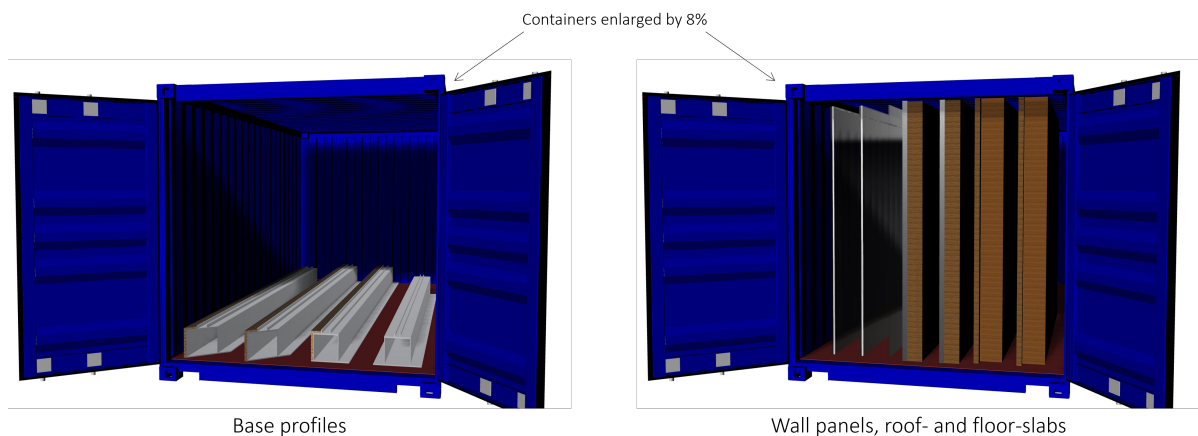

Containers enlarged by 8%

| Base profiles | Wall panels, roof- and floor-slabs |

Figure 11.2: Building components in an 8% enlarged standard container

Therefore, in order for the building elements to fit into standard containers, they will have to be reduced by 8%. This implies that the grid-size of the pavilion should also be reduced by 8%. Table 11.3 shows the revised grid size. It was decided not to take it into account in the structural calculation, due to the simplicity of the old grid size. Structural spoken, this generally means that the building elements in the pavilion are designed more conservatively than in the old grid, i.e. that the unity checks should be lower than calculated. The decreased grid size and height, however, lower the internal height of the pavilion. As a result, the comfort of the visitor decreases.

	Old grid	Revised grid
x-directional grid distance	6000	5520
y-directional grid distance	2500	2300
height	2500	2300

Table 11.3: Revised grid-size by 8%

11.2. Assembly procedure

Section 11.2 deals with the installation of the pavilion, focusing on the sequence of construction. First, this sequence is described, after which important points are emphasised separately.

11.2.1. Sequence

In Appendix B.6, the sequence can be seen with the particular building steps. Here, in Figure 11.3, a short version is shown.
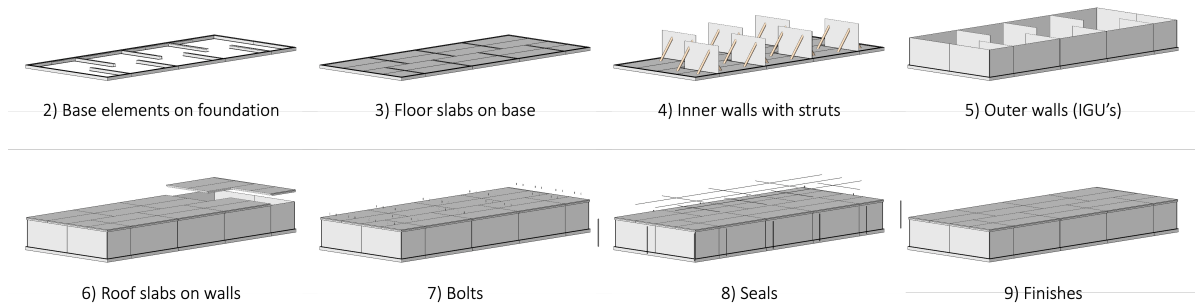

| 2) Base elements on foundation | 3) Floor slabs on base | 4) Inner walls with struts | 5) Outer walls (IGU's) |

| 6) Roof slabs on walls | 7) Bolts | 8) Seals | 9) Finishes |

Figure 11.3: Building sequence of the pavilion, step 1 (foundation) is not incorporated. Larger version is showcased in Appendix B.

1. Placing the foundation (not on image)

Technical aspects of the foundation are not included in this study. However, it is important that the foundation is laid first at the building site. As described in Chapter 7 of this part, the foundation will consist of plates that can easily be lifted on location.

2. Putting base elements on foundation

Next, the steel base profiles will be laid on the foundation. In this phase, it's essential that the measurements are correct: the profiles form the base for the structural grid.

The hat profiles (THQ265) are internal and the cap profiles (RHFSB265) form the end of the whole. The angled cap profiles have to be connected closely in the corners.

3. Laying floor slabs on base elements

The floor plates can be hoisted on the steel profiles' 'feet' afterwards. The plates are placed on the bearing blocks on the steel. Possible installation and services in the floor slabs are subsequently connected.

4. Placing inner walls

In step 4, the glass inner walls are installed. This is done by removing the panels from the container and then using glass lifters to lift the laminated panes to their destination. The pieces are then precisely positioned into the steel 'hat' profiles. The inner walls should be placed with the laminated titanium elements pointing to the outside of the pavilion.

Struts provide the temporary lateral stability of the walls. The struts are placed on the floor elements and hold the glass with a soft intermediate layer. After placement of the outer walls (IGU's, step 5), these temporary facilities can be lifted out of the pavilion from above.

5. Placing outer walls

After that, the insulated glass units (outer walls) can be installed. The order in which they are arranged is key. Installation can commence on two sides: at the location of the pavilion doors. The pavilion's design does not include doors, but it is assumed that there is a chance of an irregularity in the glass walls, resulting in an opening.

From the two possible openings, the outer glass walls are placed in a clockwise direction. On one side of an IGU, the 'cup' element is placed in the 'hand' element of the inner wall; on the other side, the 'coffee' element, together with the already assembled 'cup' and 'hand' elements, completes connection D. Possible installations and services can be implemented in the gap between the glass walls, the seals are later inserted (step 8).

6. Installing roof slabs

Now that the walls are in place, the roof can be assembled. The short ends of individual roof panels are installed on the walls, as depicted in the structural grid. This should be done in a specific order due to the configuration of connection type B.

The four rows of slabs are laid lengthwise, starting on one of the short sides. At the ends, the plates are laid over the the glass panels.

Step 6 is parallel to step 7: inserting the bolts. The recess in the CLT roof slabs with the rubber will guarantee the temporary horizontal and vertical stability, for the time between placement of the slabs and insertion of the bolts. Possible installations and services can be interconnected from this moment.

7. Inserting bolts into roof

The moment a roof slab is laid on top of the glass walls, bolts are inserted at both ends to fasten the construction element. As connection types A and B are designed (Chapter 8), $120\ mm$ steel bolts are placed from the top of the timber roof-slabs, in a recess. The bolts end in steel blocks which are glued on top of the walls. Due to tolerance phenomena, the bolts must be positioned accurately. Any tolerances are taken care of by the oversized diameter of the hole in the CLT.

8. Inserting seals

The structural elements are now assembled and any services and installations are connected. This is the moment when the seals can be attached to the pavilion. With simple, oblong pushing gaskets made out of rubber, these can be fixed without the use of heavy equipment. From that moment on, the pavilion can be considered weather tight.

9. Finishes

Finally, the pavilion is finished to the satisfaction of the client. The building is decorated and the art is placed. It is now ready for use.

11.2.2. Points of attention

During assembly and disassembly, certain points of attention arise:

- Due to the developed 'coffee-cup-hand system', it is important that the outer walls are put together in a certain order. It is assumed that a start can be made at the location of the panels with doors. In this way, the outer walls can be installed from two sides in a clockwise direction.
- Care must be taken during the removal of the temporary struts. The robustness of the steel elements bring the danger of dangling and hitting a fragile glass wall.
- The configuration of the roof details require the roof-slabs to be positioned in a certain order; from one end to the other in y-direction.
- Disassembling the pavilion is done in reverse order to assembly. When disassembling, the status of the various elements must be checked. If a building element no longer meets the requirements, or if there is visible damage, it should be replaced before the building system is assembled at another location. It is expected that the seals will deteriorate over time and therefore need to be replaced from time to time. This is because they are subject to weather conditions and frequent abrasion during (dis)assembly.

11.3. Conclusion of the transportation and assembly procedure

The answer to the question *'How is the building system being transported and (dis)assembled?'* is divided into two parts: transportation and (dis)assembly.

11.3.1. Transportation

The building elements designed in Chapter 7 do not appear to fit in a standard shipping container. This means that one of the transport requirements in the List of Requirements has not been met. Internal dimensions, as well as protruding connecting features of the construction components, cause the transportation issue.

If the building components were reduced by 8%, they would fit into a standard container. This adjustment would make the grid dimensions of the pavilion irregular and less practical for design and construction.

11.3.2. (Dis)assembly

The pavilion can be easily assembled in eight steps with the building system:

1. Laying the foundation
2. Putting base elements on foundation
3. Laying floor slabs on top of base elements
4. Placing the inner wall panels with temporary struts
5. Placing outer wall panels in a specific order
6. Laying roof slabs on top in specific order
7. Inserting bolts to connect roof to walls
8. Inserting the seals

Due to the developed coffee-cup-hand system, it is important that the outer walls are put together in a certain sequence. Even so, the roof slabs require a particular assembly order.

The pavilion is demounted in the opposite sequence as listed above.

Part V

Conclusions

12

Discussion

For this research, a design was made for a demountable pavilion using structural glass. Due to the modular design of this pavilion, a building system has been developed that standardises the reuse of glass as a structural material. A strategy in case of failure of a building element and a description of the transport and assembly procedure in detail has been presented. Throughout this research, assumptions and simplifications have been made that could affect the outcome of the project. This chapter describes what that could imply.

12.1. Validity

The design of the building system has been validated by building physics simulations and structural calculations evolved from the design of the pavilion. Structural calculations are based on the Eurocodes and complex computations are validated in computer models.

Based on the holistic design approach of this research, the final results would not be the same if this study were to be repeated. This, however, does not mean that the result of this thesis is invalid. Design freedom and the creativity that comes with that bring other students or structural designers to different final designs for this assignment.

12.2. Results

Unity checks performed on the strength and stiffness of the building elements show that the glass components are structurally safe. Due to aesthetic preferences, design of certain connections and the need for standardisation the building components become more robust. Therefore, most unity checks are well below 0.99, implying that the glass walls are over-dimensioned.

A check for compressive stress perpendicular to the grain in the cross-laminated timber (CLT) of the roofing slabs resulted in a unity check of 2.61. The roof structure is therefore theoretically regarded as not safe. Reconsideration of the roof details is necessary to lower the stress perpendicular to the grain. A larger support area could be the solution to this problem.

The results from the finite element analysis do not completely match the expectations. From a structural point of view, the boundary conditions of the modelled outer walls are challenging to approximate by hand. The out-of-plane deflection and tensile stresses in the glass were estimated using numerous simplifications for the four-sided laterally supported insulated glass unit (IGU). However, the approximation neglects the fact that the glass is supported horizontally by rubber at the top and bottom.

In addition, the 'coffee-cup-hand' connection, of which there are two on each side across the height of the IGU's, have been simplified into a linear hinged connection in the outer wall analysis. The expectations of the deflection, tensile stress and support reactions turned out to be smaller than the results from the finite element model. Nevertheless, the qualitative results of the outer wall computational analyses can be considered reasonable. The models show the maximum deflection at the expected locations and the maximum principal tensile stress in the glass at the positions of the laminated titanium elements. The order of magnitude of the quantitative results are also plausible, although real-life testing should prove the reliability.

The method of dimensioning and analysing the 'coffee-cup-hand' detail needs further elaboration. The prediction of the maximum stress in the glass and the finite element computer model are based on a two-dimensional scenario. In addition, both models are cut to a certain length, which means that the entire glass plate has no influence on the mechanical behaviour.

In reality, the glass panel as a whole does cooperate with the local mechanical behaviour. It is expected that the stresses around the titanium element will therefore be lower in reality than computed in the models.

The findings of the 'coffee-cup-hand' connection type are less reliable as a result of these simplifications. For instance, there is a significant difference between the FEM results and the manual calculations' expectations. The unity check for the tensile stress in the glass is 0.99 since the dimensions of the laminated element were optimised throughout the design phase. The same check is 0.27 according to the computer analysis. Both are on the safe side, but due to the significant variance and degree of simplification, it is not legit to make a well-founded comment regarding the checks' safety.

The pavilion cannot be considered as a sustainable building system in terms of volume material needed, because it is reasonably over-dimensioned. This statement may however be challenged by the fact that the building system is reusable in a variety of configurations. The created system is multi-applicable and therefore a long-term sustainable solution for temporary construction.

Remarks that the designed building system is relatively unsustainable may also be based on the fact that glass is, in principle, not a sustainable solution as a construction material. The dilemma for an engineer is considering whether to use glass in projects or to use a material with a significantly lower CO_2 footprint, such as bio-based products. As shown in the literature, the first option will create remarkable structures with a focus on transparency. The latter generally leads to less transparent structures.

There are several methods for applying a sustainability label to a building. Glass has a significant negative impact on this score due to its carbon dioxide emissions during manufacturing. The engineer's decision to choose sustainable building materials is then self-evident.

12.3. Limitations

It should be noted that this study was limited to the mindset and skills of a building engineer. The final result may be different if an architect, structural engineer, building physicist, and others had contributed their expertise. Therefore, no general statement can be made about the ultimate feasibility of the developed building system that is needed to realise the pavilion. More investigation is necessary and possible topics are presented by 'Recommendations' (Chapter 14). Below, the general limitations of this research are the following:

- It is assumed that the roof mechanically behaves as a diaphragm in the lateral stability calculations. However, the roof details are not designed as moment resistant joints. Also, no design is made for the roof to roof details on the longitudinal side of the roof slabs (in the x-direction).
- It should be noted that the check on the stress perpendicular to the grain in the roof details do not satisfy the building regulations. The roof connections should therefore be reconsidered.
- Another challenge regarding the timber roof are the notches made at the locations of the roof connections. The CLT loses $56\,mm$ of thickness at this point, as shown in Figure 12.1. The locations of the support are the places in which the highest shear forces are situated. A smaller thickness of the roof slab at the support locations means that the stresses become undesirably larger.
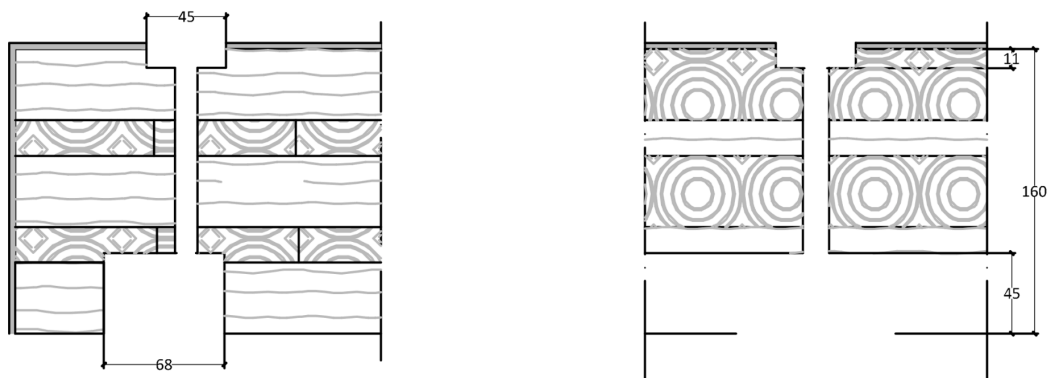

Figure 12.1: Gaps in the CLT roof slabs

- The glass strength and equivalent thickness is calculated according to NEN2608 (see Appendix D). As a starting point, it is given that the glass is loaded in pane (by the vertical loading of the roof). This is only the situation of the $5\,m$ IGU's and the inner walls. The calculation gives e.g. a value of $f_{\mathrm{mt;u;d}} = 36.7\,N/mm^2$ (for a load of 5 seconds: critical wind load). However, the outer wall panels on the longitudonal side, the IGU's of $6\,m$ are not loaded in-pane; the result for the strength of the glass is subsequently $45.8\,N/mm^2$. As a result, the unity checks for the $6\,m$ IGU will in fact be smaller than calculated.

- The detailing of the seals is not considered, these seals are assumed to be pushing gaskets which can easily seal the pavilion. However, detailed designs of the seals are necessary in order to ensure the pavilion's weather-tightness.
- The simplification of 'coffee-cup-hand' detail in 2D creates a distorted view of reality. The difference in unity checks between the expectations and the results indicates a significant margin of error. The simplification from 3D reality to 2D model and other simplifications are the cause of this. See 'Recommendations' for more elaboration.
- Checks on delamination of the SentryGlas® around the location of the laminated titanium element of the 'coffee-cup-hand' detail are based on an assumed tensile strength of $5 \ N/mm^2$. Research in delamination of SentryGlas® is, however, in its infancy. Several papers of Louter and Santarsiero describe tensile stresses in SentryGlas® [66] [67], but no designated value for the strength is given in codes and manufacturer's brochures. The value of $5 \ N/mm^2$ is based on contact with experienced engineers.

12.4. Implications

This research can inspire engineers and architects to think about reusing structural glass as a building product. The present study complements existing design strategies for structural glass since previous studies and designs of structural glass buildings, that are weather- and windproof, have not focused on demountability. The wall connections (the 'coffee-cup-hand' system) can be seen as a novel connection type, which emphasises the transparency of a building, but also satisfies demountability.

On the basis of this study, engineers could in the future present a solution for the use of structural glass in temporary buildings. Using this report as a basis, engineers will be able to make the world of structural glass a tiny bit more sustainable.

It is difficult to draw up a vision of the future for the world of structural glass. Much research and work is currently being done to ensure a sustainable future for glass. Among other things, companies and research institutions are looking at high-quality recycling options, hydrogen-powered glass furnaces, improving glass standards and so on. There is a lot of interest in these kinds of sustainable solutions and therefore it is safe to say that there is a significant future for structural glass in the built environment.

Although this research is a starting point for the reuse of structural glass as a building component, many follow-up initiatives are necessary. Some ideas are presented in the 'Recommendations' chapter later in this report.

13

Conclusion

This research has searched for an answer to the question: 'How can glass be applied as load-bearing material in temporary modular building units to realise easy-to-(dis)assemble, transparent and transportable structure?'. A holistic approach for a temporary pavilion design is used to find an answer. All sub-questions are successfully answered in the conclusion of each individual chapter and lead to the answer of the research question.

The answer to the research question is the developed building system with four different types of components: roof, wall, floor and base. Due to the physical characteristics of the case study and building practice, this ends up in nine different elements. The elements combined in multiples create a complete building by their connection typology.

13.1. Pavilion Design and building components

The imaginary pavilion is $24\ m$ in length (x-direction), $10\ m$ in width (y-direction) and $2.50\ m$ in height (z-direction), all measurements are grid dimensions. The stability in both x- and y-direction is ensured by the diaphragm action in the wall panels. Table 13.1 summarises the most important structural checks of the building elements.

Component	Check	Method	Design value	Allowable	u.c.	Result
Roof	Compression $\perp$ to grain	Hand calc	$\sigma_{c;\perp;d} = 6.76\ N/mm^2$	2.59	2.61	*NOT OK*
Inner wall	Bucking	Hand calc	$f_d = 13.54\ N/mm^1$	408.65	0.03	*OK*
IGU 5 m	Deflection	FEA	$w_{max} = 12.46\ mm$	25.00	0.50	*OK*
	Tensile stress	FEA	$\sigma_1 = 26.69\ N/mm^2$	36.70	0.73	*OK*
IGU 6 m	Deflection	FEA	$w_{max} = 14.28\ mm$	50.00	0.29	*OK*
	Tensile stress	FEA	$\sigma_1 = 14.16\ N/mm^2$	36.70	0.39	*OK*
Base	Vertical uplift of wall	Hand calc	$F = 6.92\ kN$	9.08	0.76	*OK*
'Coffee-cup-hand' detail	Tensile stress glass	FEA	$\sigma_1 = 9.79\ N/mm^2$	36.70	0.27	*OK*
	Tensile stress SentryGlas®	FEA	$\sigma_1 = 2.70\ N/mm^2$	5.00	0.54	*OK*

Table 13.1: Performed unity checks

Roof and floor

The roof consists out of roof slabs of two different geometries: slabs of 6.00x2.50 m and slabs of 3x2.5 m. The floor is composed with floor slabs of 6.00x2.50 m and 3.00x2.50 m as well. Both roof and floor slabs are cross-laminated timber (CLT) plates of $160\ mm$ and $210\ mm$ thick respectively.

Walls

The walls are of a glass lamination of 5.10.5 heat-strengthened panels, laminated with a $1.52\ mm$ SentryGlas® layer. The inner walls are $4.25x2.50\ m$. The outer walls are 6.00x2.50 m in y-direction and 5.00x2.50 m in x-direction. All outer walls are insulated glass units (IGU). They are consisting out of the prescribed laminated composition with a cavity of $15\ mm$ and a $10\ mm$ fully tempered panel on the outside.

Vertical load transfer is guaranteed by the walls in the x-direction (inner walls as well as the 5 m IGU's). Lateral stability is provided by all walls via diaphragm action.

Finite element analysis is performed to check the critical panels on out-of-plane deflection and tensile stresses due to bending of the panel. Both the $5\ m$ and $6\ m$ IGU's are modelled because they have different boundary conditions and different allowable deflection limits. The maximum deflection appears in the $6\ m$ IGU and is $14.28\ mm$, the maximum tensile stress is located in the $5\ m$ long wall panel and is $26.69\ N/mm^2$ (Table 13.1).

Base
Steel 'hat' (THQ) and 'cap' (RHSFB) profiles carry the glass panels. Building physics analysis shows that the outer base ('cap') profiles need insulation in order to prevent condensation in the steel. A layer of $20\ mm$ insulation with a $20\ mm$ wood cover is added on the outside of the profile.

13.2. Connections
Two type of roof connections, three type of wall connections and two type of base connections were established. Specific novelty can be found in the design of connections inner wall to outer wall and outer wall to outer wall.

Roof connections
Two roof connections are established, one at the location of the outer wall panels, the other one at the location of the inner walls. The design however, did not to satisfy the CLT strength requirements for compression perpendicular to the grain, as can be seen in Table 13.1.

Wall connections
The joint between two $5\ m$ IGU's (the outer wall panels on the short side of the pavilion) do not need to transfer forces. Therefore, this connection only exists out of a $2.5\ m$ long rubber pushing gasket.

For the other wall joints a so-called 'coffee-cup-hand' system is invented. At two locations along the height of glass panels, titanium elements of $45\ mm$ in height are laminated $30\ mm$ in the glass. These elements together can be placed into each other and form a hinged connection between wall panels.

During the design phase of the 'coffee-cup-hand' details, a rough assumption was made for distance 'a'. Parameter 'a' defines the distance from the bending point of the outer laminated glass pane to the location in that pane where the beginning of the titanium element can perpendicularly be found. Subsequently, the finite elements analysis demonstrated that distance 'a' is in line with the assumption.

Consecutive finite element analysis shows that the maximum tensile stress in the glass near the 'coffee-cup-hand' connections is $9.79\ N/mm^2$. The maximum tensile stress in the SentryGlas interlayer is $2.70\ N/mm^2$. These values are within the maximum permissible stresses.

Base connections
Floor slabs are put on a rubber bearing block, which is placed on the 'feet' of the base profiles (the steel 'hat' and 'cap' beams). Glass is put on top of the steel profiles, at two particular locations supported by HDPE blocks ($500\ mm$ from the glass edges). Along the length of the glass walls on the sides the panels are lateral supported by rubbers and steel plates.

13.3. Failure strategy, transportation and (dis)assembly
In failure analysis, it is incorporated that the glass walls are subject to possible breakage from both sides. Secondary load bearing paths are guaranteed in case of complete collapse of a building element. Additionally, a replacement strategy for each different type of building component is presented.

The building elements described do not fit into a standard container due to protrusions and outer dimensions. If the grid dimension were reduced by 8%, all building elements including fixing and protection could be transported in standard containers.

The pavilion is assembled in nine clear steps, from foundation to finish. Temporary stability of the walls is provided by struts. The order of assembly of the roof and walls has to be taken into account because of the designed connections. Disassembling the pavilion goes in the reverse order.

This design research showed that the proposed building system, together with minor enhancements, is able to apply glass as a structural material in easy-to-(dis)assemble and transportable structures.

14

Recommendations

Two types of recommendations are distinguished and elaborated on: recommendations for practice and recommendations for further research.

14.1. Recommendations for practice

Recommendations for practice are:

- **Initial sustainability issues with glass**
  As written in the discussion, environmental building labels do not explicitly look at the re-use potential of a building and its building components. The Dutch *'MPG' (environmental performance of buildings)* scoring is intentionally not meant for temporary structures. Scoring would therefore, for the case of the temporary pavilion of this research, not be done by environmental determination methods, but with common sense. It is advised to use this common sense and emphasise on the reuse potential of demountable glass structures, rather than focus on the initial environmental scoring.

- **Building system in a different composition**
  The building system developed in this study was only designed and calculated for the case study; the temporary art pavilion. It would be interesting to investigate the building system's limits: what kinds of alternatives necessitate changes in the building system's design? Alternatives include larger floor space, different building function or another location for the pavilion.

- **Optimise glass**
  From the unity checks of the previous chapter it can be concluded that all building elements, except for the roof, are under-dimensioned. Optimisation of the building elements to a unity check of approximately 0.95 would mean that the building is efficiently designed in terms of material volume. As a result, the structure will be lighter which introduces some benefits. Firstly, the foundation can be designed lighter; less material is needed and therefore positively influences the sustainability of the pavilion. Second, the structure will be easier to assemble and disassemble, less heavy installation machines will be required. Lastly, transportation is lighter which has another positive effect on the sustainability.

- **Non-glass element verification**
  No extensive verification has been performed on the non-glass elements of the building system. The check on the compression perpendicular to the grain in the CLT roof slab at the position of connections A and B showed that the building codes are not satisfied. Danger arises of collapse of the roof, meaning the roof slabs should be reconsidered. Besides, the steel base profiles are not checked on a structural level. Due to the fact that no focus was put on the foundation, the building envelope is designed until ground surface. The insulation below the pavilion should be investigated. It is recommended to look into insulation challenges below the steel profiles; hypothetically condensation will now occur from the bottom.

- **Connection design**
  The connection design presented in this study can be considered as an initial design. The joints laminated onto the glass (connections A and B) and the joints laminated into the glass ('coffee-cup-hand' systems) are made of titanium. This choice was made because of the behaviour of the material under temperature differences. Titanium is much less subject to compaction and expansion than steel although, in general, steel is easier to manufacture and cheaper. However, this has not been researched in detail and it is recommended to look into the difference of implementing steel instead of titanium in the joints.

- **Tolerances**
  Tolerances are described in general, but not technically. All kinds of tolerances occur during the realisation of the pavilion. In the first place, there are production tolerances: laminated glass panels of a format 2.5x6 can deviate from

each other by up to $6\ mm$. Besides production tolerances, there are also tolerances at the building site during the assembly of the pavilion. It would be worthwhile to look in detail at the tolerances in the assembly of the 'coffee-cup-hand' system, since the elements are each laminated into a large glass panel.

- **Implementation of services and installations**
  In this study, locations have been indicated where the services and pipelines may be included. However, for a integral building design, the facilities should be described in detail. Facilities include the security of the pavilion, climate installations, electrical cables, sun-shading and so on. It is therefore interesting to look at how the services and installations can be implemented in the building system, without adversely affecting the demountability of a pavilion.
- **Feasibility of a demountable structural glass pavilion**
  The reuse of structural glass as a building element is considered in this report and it seems feasible, with some minor modifications, to implement the material in a demountable building system. However, it is interesting and valuable to look at the comparison with a standard system such as tent structures. What are the advantages and disadvantages in terms of aesthetics, transport, (dis)assembly and costs? In this manner, the feasibility of a temporary pavilion in structural glass can be examined.

14.2. Recommendations for further research

Recommendations for further research are:

- **Sustainable glass production potential**
  In the terminology of the circular economy, the reuse of glass is the focus of this report. As described in the introduction, it is also important to recycle and reduce the building material. But, what if the production process can be made such that flat glass can be produced in a climate-neutral way? During the course of this research, a press release was issued by NSG (Sep 2021) who managed to successfully manufacture architectural glass using a hydrogen-powered furnace. Further research into this production method could positively change the world of (structural) glass.
- **Reversible seals for glass**
  The joints in the pavilion's design are filled with elongated pushing gaskets. These rubbers ensure the weather tightness of the pavilion. However, there will be challenges in applying these seals in the corners of the pavilion (connection E). Also, it is now unclear how the pushing gaskets will be kept in place at the places of connections C and D during small displacements of the IGU's due to loading. It is advised to design a specific kind of seal which might be incorporated in the detailing of the joints. Important factors to keep in mind are the demountability and the weather tightness.
- **Rubber deterioration**
  The roof and base connections use a glued rubber profile. The rubber serves to transfer horizontal loads from the walls to the non-glass building components and satisfies the weather tightness of the pavilion. Frequent assembly and disassembly of the building system inevitably wears out the rubber. Future research should check the durability of the rubber and investigate whether a rubber is the most suitable option for the connections designed in this thesis.
- **'Coffee-cup-hand' detail modelling and testing**
  The innovative designed connection type for the wall joints is simplified and modelled in 2D, which criticises the reliability of the results (see 'Discussion'). Improvement of the model, for example in a 3D FEA model, is necessary in order to draw a well-founded conclusion about the stress distribution in the glass and in the bond. It is also advisable to do tests in the laboratory to see how the titanium 'cup', 'coffee' and 'hand' assembly transfer lateral forces from glass panel to glass panel.

References

[1] Chiara Bedon, Xihong Zhang, Filipe Santos, et al. "Performance of structural glass facades under extreme loads – Design methods, existing research, current issues and trends". In: *Construction and Building Materials* 163 (2018), pp. 921–937. ISSN: 09500618. DOI: 10.1016/j.conbuildmat.2017.12.153. URL: https://doi.org/10.1016/j.conbuildmat.2017.12.153.

[2] Yvonne van Wilderen. *Verslag Glas Eindejaarsbijeenkomst bij Abt Velp*. 1996. URL: https://booosting.nl/news/show/id/760.

[3] J. Wurm. *Glass Structures - Design and Construction of Self-Supporting Skins*. 2007. ISBN: 9783764376086.

[4] FA Veer, Diana de Krom, and R Nijsse. "Demonstration of the Structural Resiliency of Damaged Sentryglas Laminated Heat Strengthened Glass Fins in Full Scale Testing". In: *International Journal of Structural Glass and Advanced Materials Research* 5.1 (2021), pp. 29–37.

[5] Toshihiko Ono and R.A. Allaire. "Fracture Analysis, a Basic Tool to Solve Breakage Issues". In: *Corning - Display Technologies* (2004). URL: https://www.corning.com/media/worldwide/cdt/documents/2_TIP_201.pdf.

[6] Paris IEA International Energy Agency. *Global status report for building and construction*. 2019.

[7] Julian Kirchherr, Denise Reike, and Marko Hekkert. "Conceptualizing the circular economy: An analysis of 114 definitions". In: *Resources, conservation and recycling* 127 (2017), pp. 221–232.

[8] Telesilla Bristogianni, Faidra Oikonomopoulou, Clarissa Justino De Lima, et al. "Structural cast glass components manufactured from waste glass: Diverting everyday discarded glass from the landfill to the building industry". In: *Heron* 63.1-2 (2018), pp. 57–102. ISSN: 15744078.

[9] Glass for Europe. "Recycling of end-of-life building glass. 2013". In: (). URL: https://glassforeurope.com/recycling-of-end-of-life-building-glass/.

[10] Aanbestedings Nieuws. "Herstel vliesgevel Koningskade 4, Den Haag aanbesteed door RWS". In: *Aanbestedings Nieuws* (2019). URL: http://www.aanbestedingsnieuws.nl/herstel-vliesgevel-koningskade-4-den-haag-aanbesteed-door-rws/.

[11] Nick Bertram, Steffen Fuchs, Jan Mischke, et al. In: *Modular construction: From projects to products* (2019). URL: https://www.mckinsey.com/business-functions/operations/our-insights/modular-construction-from-projects-to-products.

[12] Andrew William Lacey, Wensu Chen, Hong Hao, et al. "Structural response of modular buildings – An overview". In: *Journal of Building Engineering* 16 (2018), pp. 45–56. ISSN: 2352-7102. DOI: https://doi.org/10.1016/j.jobe.2017.12.008.

[13] Giovanni Valle. "Modular Construction: 16 Pros and Cons". In: *BuilderSpace.com* (). URL: https://www.builderspace.com/modular-construction-16-pros-and-cons.

[14] National Operational Guidance. "Demountable structures". In: *NFCC - National Fire Chiefs Council* (). URL: https://www.ukfrs.com/promos/16917.

[15] G DeBrincat and E. Arup. Glasgow Babic. "Re-Thinking the Life-Cycle of Architectural Glass". In: (2018).

[16] G B Hoogerwaard. "The road to sustainable load bearing glass designs: possibilities and limitations of current glass design with focus on the connections". In: *TU Delft repository* (2020).

[17] Rotterdam Architectuurprijs. 2019. URL: https://www.rotterdamarchitectuurprijs.nl/vorige-edities/2019/penthouse-west399.html.

[18] Mark Breach. *Dissertation Writing for Engineers and Scientists*. Pearson Education, 2009.

[19] Cepezed. *Bouwdeel d(emontabel): een project van cepezed*. URL: https://www.cepezed.nl/nl/project/bouwdeel-demontabel/28429/.

[20] LocHal. *De Glazen zaal*. 2018. URL: https://lochal.nl/werken-ontmoeten/ruimtes/de-glazen-zaal.

[21] Octatube. *Beurs van Berlage*. 2018. URL: `https://www.octatube.nl/nl_NL/project-item/projectitem/27-beurs-van-berlage.html`.

[22] Octatube. *Heropbouw Glazen Zaal*. 2018. URL: `https://www.octatube.nl/nl_NL/project-item/projectitem/210-heropbouw-glazen-zaal.html`.

[23] *Glaspavilon*. 2013. URL: `https://facadeworld.com/2013/09/19/glaspavilon/`.

[24] F. Oikonomopoulou. 2021.

[25] Christian Schittich, Gerald Staib, Dieter Balkow, et al. *Glass construction manual*. Walter de Gruyter, 2012.

[26] Institution of Structural Engineers. Institution of Structural Engineers, 2014. ISBN: 978-1-906335-25-0. URL: `https://app.knovel.com/hotlink/toc/id:kpSUGBE002/structural-use-glass/structural-use-glass`.

[27] Ministerie van Binnenlandse Zaken en Koninkrijksrelaties. 2011.

[28] *Kabelnetgevels Markthal Rotterdam*. 2014. URL: `https://www.octatube.nl/nl_NL/project-item.html/projectitem/6`.

[29] Xavier Centelles, J. Ramon Castro, and Luisa F. Cabeza. "Experimental results of mechanical, adhesive, and laminated connections for laminated glass elements – A review". In: *Engineering Structures* 180 (2019), pp. 192–204. ISSN: 0141-0296. DOI: `https://doi.org/10.1016/j.engstruct.2018.11.029`. URL: `https://www.sciencedirect.com/science/article/pii/S0141029618311313`.

[30] C. Noteboom. "CIE4285 Structural Glass Reader - Appendix Calculations. 2020, Delft University of Technology". In: ().

[31] Jan Belis, Christian Louter, Jens H. Nielsen, et al. "Architectural Glass". In: *Springer Handbook of Glass*. Ed. by J. David Musgraves, Juejun Hu, and Laurent Calvez. Cham: Springer International Publishing, 2019, pp. 1781–1819. ISBN: 978-3-319-93728-1. DOI: `10.1007/978-3-319-93728-1_52`. URL: `https://doi.org/10.1007/978-3-319-93728-1_52`.

[32] Fred Veer, Telesilla Bristogianni, and Clarissa Justino De Lima. "An overview of some recent developments in glass science and their relevance to quality control in the glass industry". In: *Heron* 63.1-2 (2018), pp. 15–30. ISSN: 15744078. DOI: `10.7480/cgc.6.2197`.

[33] Rebecca Hartwell. *Unlocking the Re-use Potential of Glass Façade Systems*. 2020. URL: `https://www.glassonweb.com/article/unlocking-re-use-potential-glass-facade-systems`.

[34] Rob Nijsse. "Editorial". English. In: *Heron* 63.1/2 (Oct. 2018), pp. 3–13. ISSN: 0046-7316.

[35] *SOLOS Glass - How Float Glass is Made*. 2017. URL: `https://www.youtube.com/watch?v=JMGkbrETU8M`.

[36] F. Oikonomopoulou, T. Bristogianni, L. Barou, et al. "The potential of cast glass in structural applications. Lessons learned from large-scale castings and state-of-the art load-bearing cast glass in architecture". In: *Journal of Building Engineering* 20 (2018), pp. 213–234. ISSN: 2352-7102. DOI: `https://doi.org/10.1016/j.jobe.2018.07.014`. URL: `https://www.sciencedirect.com/science/article/pii/S2352710218303231`.

[37] *What is the Extrusion Process: Ceramic Extrusion Technology*. URL: `https://www.corning.com/worldwide/en/innovation/materials-science/ceramics/how-it-works--extrusion.html?utm_source=youtube&utm_campaign=howitworks&utm_medium=social&utm_content=extrusion`.

[38] Ate Snijder, R. Nijsse, and C. Louter. 2018. "Building and Testing Lenticular Truss Bridge with Glass-Bundle Diagonals and Cast Glass Connections". In.

[39] A H Snijder, L P L van der Linden, C Goulas, et al. "The glass swing: a vector active structure made of glass struts and 3D-printed steel nodes". In: *Glass Structures & Engineering* 5.1 (2020), pp. 99–116. ISSN: 2363-5150. DOI: `10.1007/s40940-019-00110-9`. URL: `https://doi.org/10.1007/s40940-019-00110-9`.

[40] *SECURIT*. URL: `https://glassolutions.nl/nl/producten/securit`.

[41] X. Li, Z. P. Fang, F. L. Ng, et al. "Inspection and Image Analysis of Nickel Sulphide Inclusions in Toughened Glass Panels". In: *2006 9th International Conference on Control, Automation, Robotics and Vision*. 2006, pp. 1–6. DOI: `10.1109/ICARCV.2006.345068`.

[42] *Heat-Soaking*. URL: `https://www.guardianglass.com/eu/en/tools-and-resources/resources/glass-glossary/heat-soaking`.

[43] Andreas Kasper. "Spontaneous cracking of thermally toughened safety glass part three: statistic evaluation of field breakage records and consequences for residual breakage probability". In: *Glass Structures & Engineering* 4.3 (2019), pp. 345–376.

[44] Pavel Stratiy. "Numerical-and-Analytical Method of Estimation Insulated Glass Unit Deformations Caused by Climate Loads". In: *International Scientific Conference Energy Management of Municipal Transportation Facilities and Transport EMMFT 2017*. Ed. by Vera Murgul and Zdenka Popovic. Cham: Springer International Publishing, 2018, pp. 970–979. ISBN: 978-3-319-70987-1.

[45] M. Spijker. *Online interview with Mark Spijker from AGC Glass*. 2021.

[46] Stephan Morse. "Glass Performance Days". In: *Load Sharing of Insulating Glass Unit with Laminated Glass*. 2019. URL: `https://gpd.fi/events/gpd-finland-2019/presentation/load-sharing-of-insulating-glass-unit-with-laminated-glass/`.

[47] *Apple Westlake*. URL: `https://www.eocengineers.com/en/projects/apple-westlake-226`.

[48] Foster + Partners. *Foster + Partners, Nigel Young · Westlake Apple Store*. URL: `https://divisare.com/projects/286931-foster-partners-nigel-young-westlake-apple-store`.

[49] Manuel Santarsiero, Christian Louter, and Alain Nussbaumer. "Laminated connections for structural glass components: a full-scale experimental study". In: *Glass Structures & Engineering* 2.1 (2017), pp. 79–101.

[50] Steve Jobs, Karl Backus, Rosa Sheng, et al. *Glass support member*. 2004.

[51] Chiara Bedon and Manuel Santarsiero. "Laminated glass beams with thick embedded connections – Numerical analysis of full-scale specimens during cracking regime". In: *Composite Structures* 195 (2018), pp. 308–324. ISSN: 0263-8223. DOI: `https://doi.org/10.1016/j.compstruct.2018.04.083`. URL: `https://www.sciencedirect.com/science/article/pii/S0263822318307803`.

[52] Reinier De Graaf. *Four Walls and a Roof*. Harvard University Press, 2018.

[53] Kemal Hür. *Berlin-Marzahn - die einst Größte Plattenbausiedlung Europas wird 40*. 2017. URL: `https://www.deutschlandfunkkultur.de/berlin-marzahn-die-einst-groesste-plattenbausiedlung.1001.de.html?dram:article_id=397021`.

[54] Reinier de Graaf. *Reinier de Graaf: "Can a house be beautiful because of what we know, not what we see?"*. 2017. URL: `https://www.dezeen.com/2017/11/10/reinier-de-graaf-opinion-four-walls-roof-book-house-east-germany/`.

[55] Andrew William Lacey, Wensu Chen, Hong Hao, et al. "Review of bolted inter-module connections in modular steel buildings". In: *Journal of Building Engineering* 23 (2019), pp. 207–219.

[56] *Webshop JLM Glas, de online specialist voor HR dubbelglas en meer*. URL: `https://www.jlmglas.nl/`.

[57] Diana de Krom, Fred Veer, Kris Riemens, et al. "Façade becomes structure". In: *Challenging Glass Conference Proceedings*. Vol. 7. 2020.

[58] M. Meurs. *Interview with Michiel Meurs from 'FromAtoB Public Design'*. 2021.

[59] R-net. *Handboek R-net Bushaltes*. 2014. URL: `https://www.zuid-holland.nl/publish/pages/15739/a1_bijlage_4_141210_haltehandboek2014_def_lr.pdf`.

[60] Markus Feldmann. "Glass as a structural material in construction - towards a Eurocode on Structural Glass". In: *Construction standards - A driver for innovation and industry*. Eurocodes, 2015. URL: `https://ec.europa.eu/jrc/sites/jrcsh/files/20150603-riga-constructions-standards-feldmann.pdf`.

[61] *CLT by StoraEnso - Technical Brochure*. StoraEnso. URL: `https://www.storaenso.com/-/media/documents/download-center/documents/product-brochures/wood-products/clt-by-stora-enso-technical-brochure-en.pdf`.

[62] Curbell Plastics. *SentryGlas® Interlayer*. URL: `https://www.curbellplastics.com/Research-Solutions/Materials/SentryGlas-Interlayer`.

[63] Kenniscentrum Glas, OnderhoudNL Glas, Bouwend Nederland, et al. "Infosheet NEN 2608: Betrouwbare glassamenstellingen". In: (2017). URL: `https://www.kenniscentrumglas.nl/wp-content/uploads/Infosheet-NEN-2608.pdf`.

[64] Dannia Yang. "The Interplay between the Structural and Sustainability Performance of Laminated Glass". PhD thesis. 2021.

[65] iContainers. *20-foot container - dimensions, measurements and weight*. 2013. URL: `https://www.icont ainers.com/help/20-foot-container/#:~:text=The%5C%20dimensions%5C%20of%5C%20a% 5C%2020,wide%5C%20x%5C%207'%5C%2010%5C%E2%5C%80%5C%9D%5C%20high`.

[66] Manuel Santarsiero, Christian Louter, and Alain Nussbaumer. "Laminated connections under tensile load at different temperatures and strain rates". In: *International Journal of Adhesion and Adhesives* 79 (2017), pp. 23–49. ISSN: 0143-7496. DOI: `https://doi.org/10.1016/j.ijadhadh.2017.09.002`. URL: `https://www.sciencedirect.com/science/article/pii/S0143749617301598`.

[67] Manuel Santarsiero, Christian Louter, and Alain Nussbaumer. "Laminated connections for structural glass components: a full-scale experimental study". In: *Glass Structures & Engineering* 2.1 (2017), pp. 79–101. ISSN: 2363-5150. DOI: `10.1007/s40940-016-0033-2`. URL: `https://doi.org/10.1007/s40940-016-0033-2`.

[68] *Chatsworth Great Conservatory*. 2016. URL: `https://www.unicornwindows.co.uk/britains-finest-conservatory/`.

[69] Fred Veer. "Editorial". English. In: *Heron* 63.1/2 (Oct. 2018), pp. 1–2. ISSN: 0046-7316.

[70] 2019. URL: `https://www.youtube.com/watch?v=1ucfFFxLKNw`.

[71] James Watson, Jens Nielsen, and Mauro Overend. "A critical flaw size approach for predicting the strength of bolted glass connections". In: *Engineering Structures* 57 (2013), pp. 87–99. ISSN: 0141-0296. DOI: `https://doi.org/10.1016/j.engstruct.2013.07.026`. URL: `https://www.sciencedirect.com/science/article/pii/S0141029613003507`.

[72] Arcady V Dyskin, Elena Pasternak, and Yuri Estrin. "Mortarless structures based on topological interlocking". In: *Frontiers of Structural and Civil Engineering* 6.2 (2012), pp. 188–197.

[73] Faidra Oikonomopoulou, Telesilla Bristogianni, Lida Barou, et al. "Interlocking cast glass components, Exploring a demountable dry-assembly structural glass system". In: *Heron* 63.1/2 (2018), pp. 103–138.

[74] Pezhman Sharafi, Mina Mortazavi, Bijan Samali, et al. "Interlocking system for enhancing the integrity of multi-storey modular buildings". In: *Automation in Construction* 85 (2018), pp. 263–272. ISSN: 0926-5805. DOI: `https://doi.org/10.1016/j.autcon.2017.10.023`. URL: `https://www.sciencedirect.com/science/article/pii/S092658051730256X`.

[75] AC van der Linden, P Erdtsieck, IM Kuijpers-van Gaalen, et al. *Building Physics*. ThiemeMeulenhoff, 2013.

[76] Keira Proctor and Chris Sanders. *Webinar: Introduction To Building Physics; A Proctor Group*. 2020. URL: `https://www.proctorgroup.com/intro-to-building-physics-heat-air-moisture-movement`.

[77] Pascal van Dort. "Webinar video series: Architectural acoustics for interior and design". In: *Rockfon*. 2020. URL: `https://www.rockfon.co.uk/knowledge-centre/learning/online-training-courses/acoustics-general-acoustics/`.

[78] Paul Andersen. *Light Absorption, Reflection & Transmission*. 2015. URL: `http://www.bozemanscience.com/ap-phys-118-light-switching-mediums`.

[79] Paressa Loussos. *Interview about Building Physics with specialist Paressa from ABT (04-May-2021)*.

[80] J. Breunese A.J.; Maljaars. TU Delft, 2015. ISBN: 9789059728868.

[81] Kingspan Group. *Kingspan and Fire Safety*. URL: `https://www.kingspan.com/gb/en-gb/fire-safety-en`.

[82] Z Nodehi. *Behaviour of structural glass at high temperatures*. 2016.

[83] Andrew Watts. *Modern construction envelopes*. Birkhäuser, 2014.

[84] Centre for the Protection of National Infrastructure. *Introduction to Glass Curtain Wall Systems*. 2019. URL: `https://www.cpni.gov.uk/glazed-facades`.

[85] Keith Boswell. *Exterior building enclosures: design process and composition for innovative façades*. John Wiley & Sons, 2013.

[86] Sedak. *Glass lamination: the perfect combination of aspirations and quality*. 2021. URL: `https://www.sedak.com/en/skills/laminating/`.

List of Figures

List of Tables

A

Appendix table of content

The structure of the appendices is as follows:

- A: Table of contents
- B: Figures

    - Introduction images
    - Literature review images
    - List of requirements
    - Details
    - Building physical analysis of the connections
    - Assembly sequence

- C: Literature review in depth

    - Glass as building material
    - Connections
    - Building physics
    - Reference projects

- D: Structural verification

    - Vertical load transfer
    - Horizontal load transfer
    - Glass parameters
    - Building element verification
    - Dimensioning of the 'coffee-cup-hand' system
    - Check friction performance rubber

- E: Connection methods study (pre-designs)

    - Type A: Interlocking
    - Type B: Friction
    - Type C: Embedded

- F: DIANA FEA reports

    - IGU $5\,m$ - ULS report
    - IGU $5\,m$ - SLS report
    - IGU $6\,m$ - ULS report
    - IGU $6\,m$ - SLS report
    - 'Coffee-cup-hand' system

B

Figures

B.1. Introduction images

B.1.1. Modularity scales and complexity
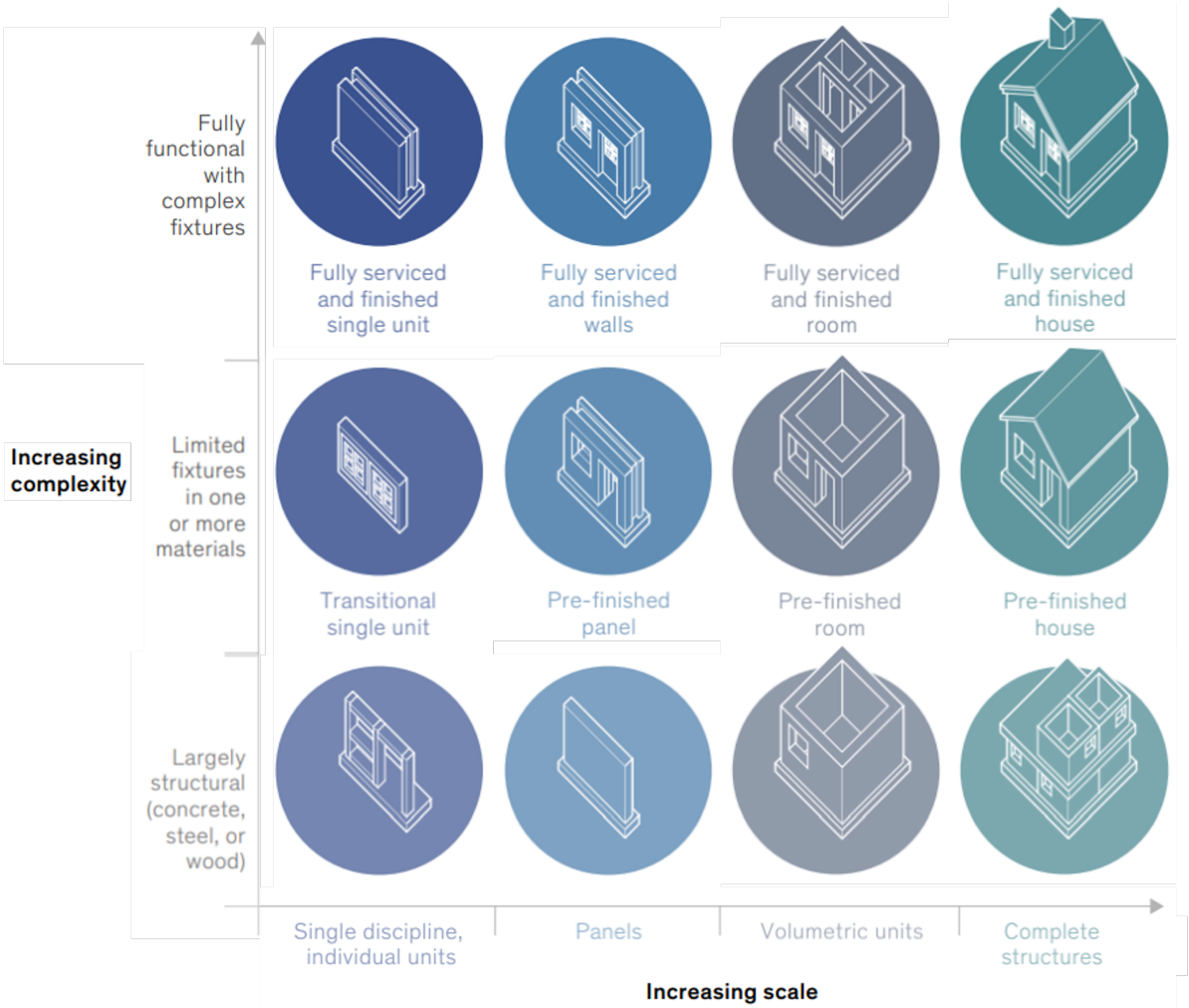
Figure B.1: Modular construction levels of [11]

B.1.2. Walking routes

Route - 1
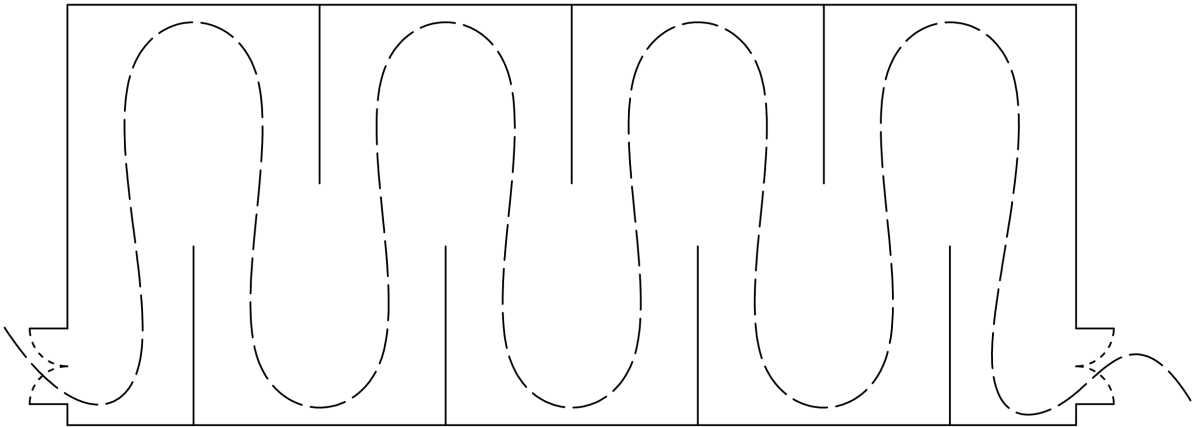
Figure B.2: Route possibility 1

Route 2
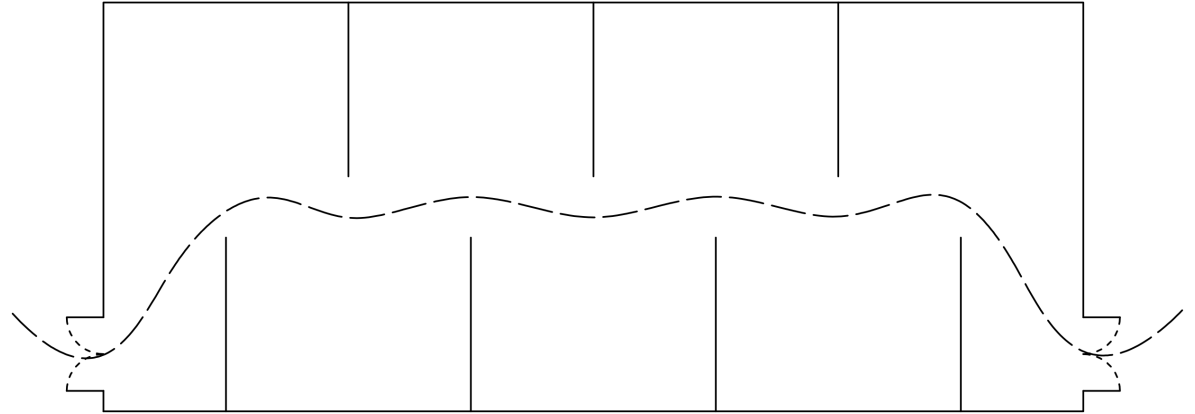
Figure B.3: Route possibility 2

B.2. Literature review images

Evolution of Glass

Timeline locations: Mesopotamia · Egypt · Syria · Roman Empire · Middle Ages · Venice

Timeline scale: 500 BC · 0 · 500 AD · 1500 AD · 1700 AD · 2000 AD

Production method
- Hollow rod
- Cylinder sheet glass
- Cast and drawn plates
- Flat glass by blowing iron
- Brown cylinder sheet
- Crown glass
- Cast glass
- Cast & Roll

Use
- Building envelope
- Building envelope (Churches & Monasteries)
- Tableware
- Building envelope
- Mirrors
- Structural glass

Image labels:
- Claw breaker
- Moreton Hall
- Leadlight
- Chartes Cathedral
- Murano Glass
- Bicheroux process

(R)evolution of Structural Glass in Buildings

Float
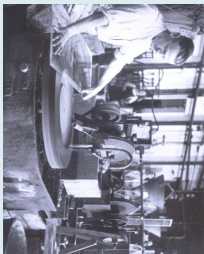
Pilkington Float Glass

Willes Faber & Dumas Building

Salisbury Centre

Sonsbeek Pavilion

Temple d'Amour

Apple Cube 1
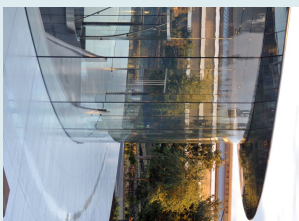
Steve Jobs Theatre

Cast
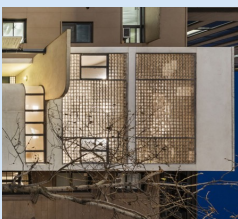
William Lescaze House & Office

Crown Fountain
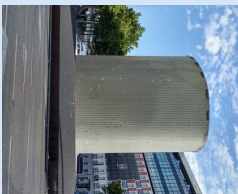
Atocha Memorial

Crystal House

Extruded
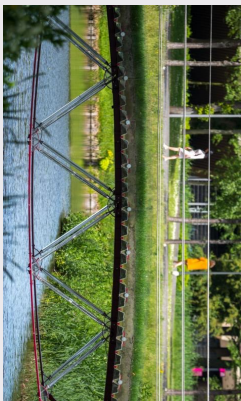
Glass truss bridge (2017)

Glass swing (2019)

1934
1960
1970
1980
1990
2000
2010
2020
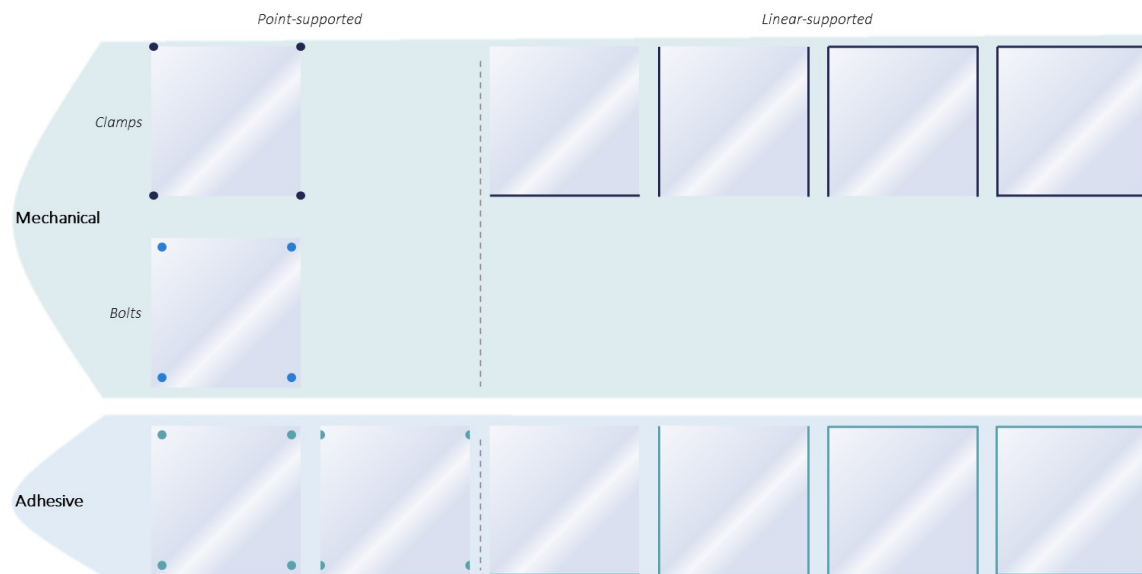
B.2.1. Connections

Figure B.4: Connection overview - support conditions
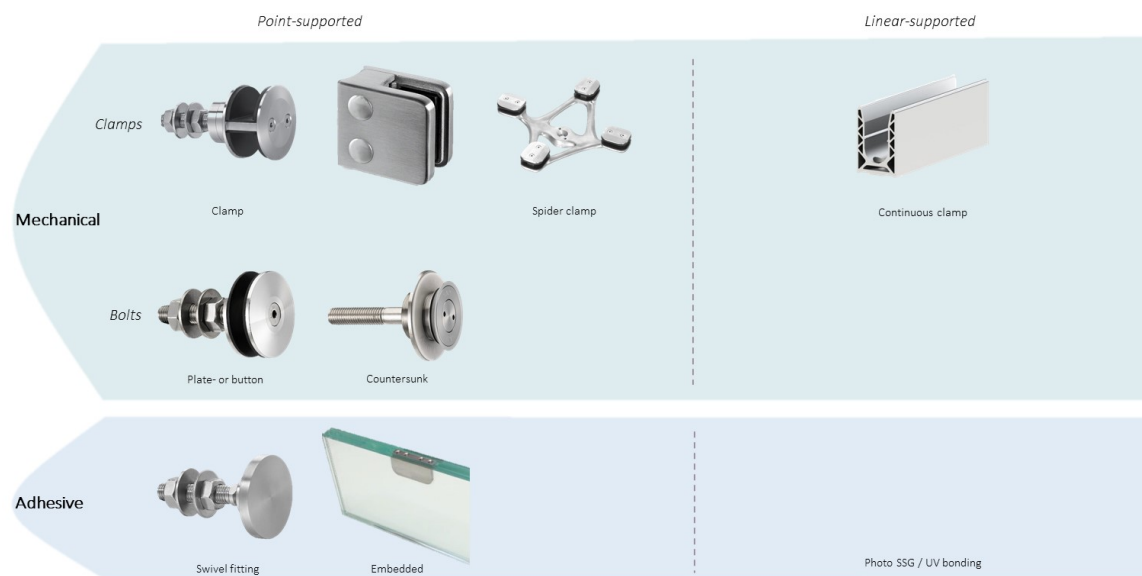
Figure B.5: Connection overview - examples of connections
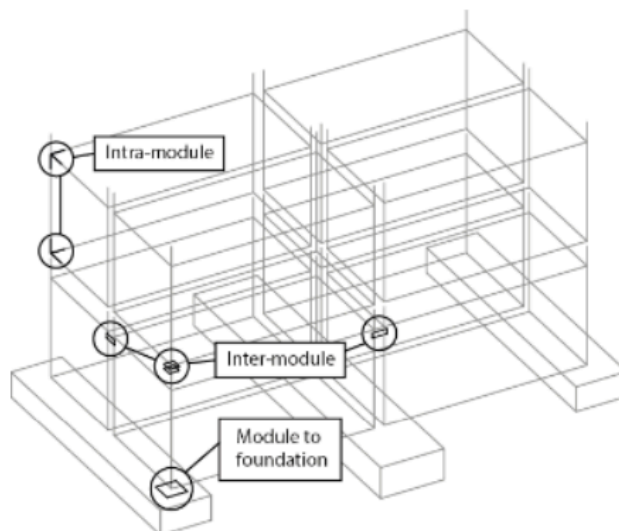
Fig. 4. Illustration of connection types

Table 3. Summary of connection types

Type	Sub-Type	Advantage	Disadvantage
Inter-module	Bolted	Reduced site work; demountable	Access, slotted holes, slip, bolt tensioning
	Welded	No slip, compact, accommodate misalignment	Site work, corrosion, not demountable
	Composite (concrete-steel)	Strength, no slip, compact	Site work, not demountable
Intra-module	Bolted	Tolerance for shop assembly, deconstructable	Relatively low moment capacity, ductility and rotation capacity
	Welded	Suited to factory based construction using jig to ensure module uniformity	Does not permit rotation, steel members should be designed for hogging moments and axial forces
Module to foundation	Chain/cable/keeper plate	Low cost	Limited to low rise construction; tensioning requirements
	Site weld to base plate	Rigid connection	Additional trade on site, hot work, damage to steel corrosion protection system
	Base plate – cast in anchor bolts	Ductility	Positioning of cast in anchor bolts, tolerance in steel base plate, corrosion
	Base plate embedded in concrete	Full column strength and good ductility	Positioning of column during concrete curing, site welding

Figure B.6: Different modular building connections, according to [12]

B.3. List of Requirements

The List of Requirements is shown on the next page.

List of Requirements

	Higher-level	Lower-level
Fabrication	• The modules must be of **high quality** to withstand a lifetime of at least 50 years.	• It would be ideal if the glass composition **is as clear as possible** in order to demonstrate the strength of structural glass.
Reversibility	• The system should be as **basic** as possible, with an emphasis on a small number of unique parts. • **Easy to (dis)assemble**, so no special machinery required. The instruction must be understandable for every craftsman.	• Only **dry** solutions, i.e. no 'wet' injection mortar.
Structural	• **Vertical** balance: Glass panels support the roof, which subsequently is carried by a steel beam foundation. • **Horizontal** balance: The roof and side panels offer stability. • **Non glass-penetrating** connections should be applied to avoid peak-stresses. • The structure should not collapse after a single **vandalism** assault (Fine & Kinney method).	• The components' relative **displacements** will have to be accommodated by the joints. In such a way that weather tightness is maintained and the coupling system functions as a constrain
Usage	• According to the building physics literature research, the U-value must be **below 4.1 W/m²K**. • The **height** must be greater than **2.1 meters**. [Bouwbesluit] • The pavilion should contain at least **two exits** for the visitor's safety.	• It is preferred that **no light at the roof** enters the building to make the visitor's experience as pleasant as possible. • The structure should be **aesthetically** pleasing, emphasising the power of glass regarding its transparency. • It is preferable for fire safety reasons if the pavilion just has **one level**.
Transportation	• All parts must fit inside a common **container** (600x2440x2600mm) to facilitate the ease of transport. • Because the elements will be relocated often, they must be **fall-proof**.	• The **most efficient use of container space** boosts transportation productivity. 2D components, for example, make optimal use of available space.
End of life	• The various elements should all be **easily recyclable or replaceable**.	
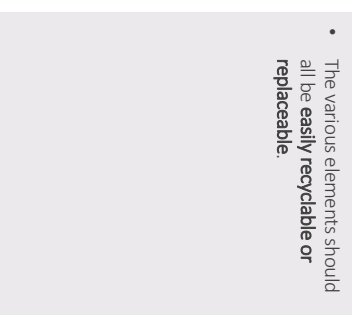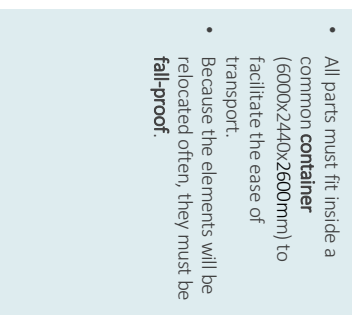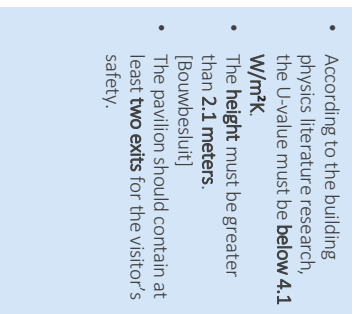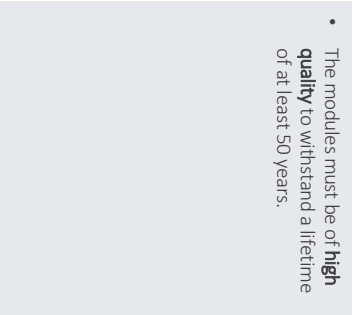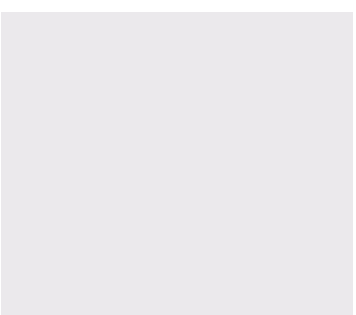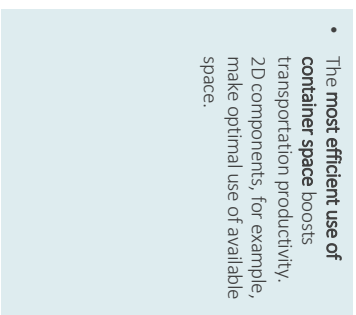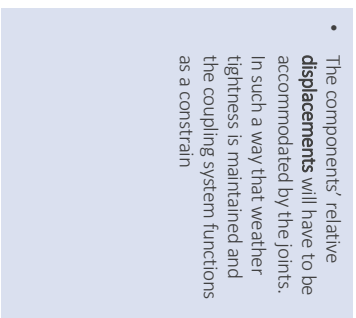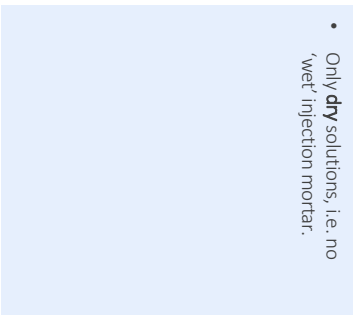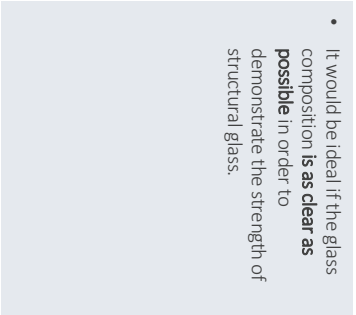
B.4. Details
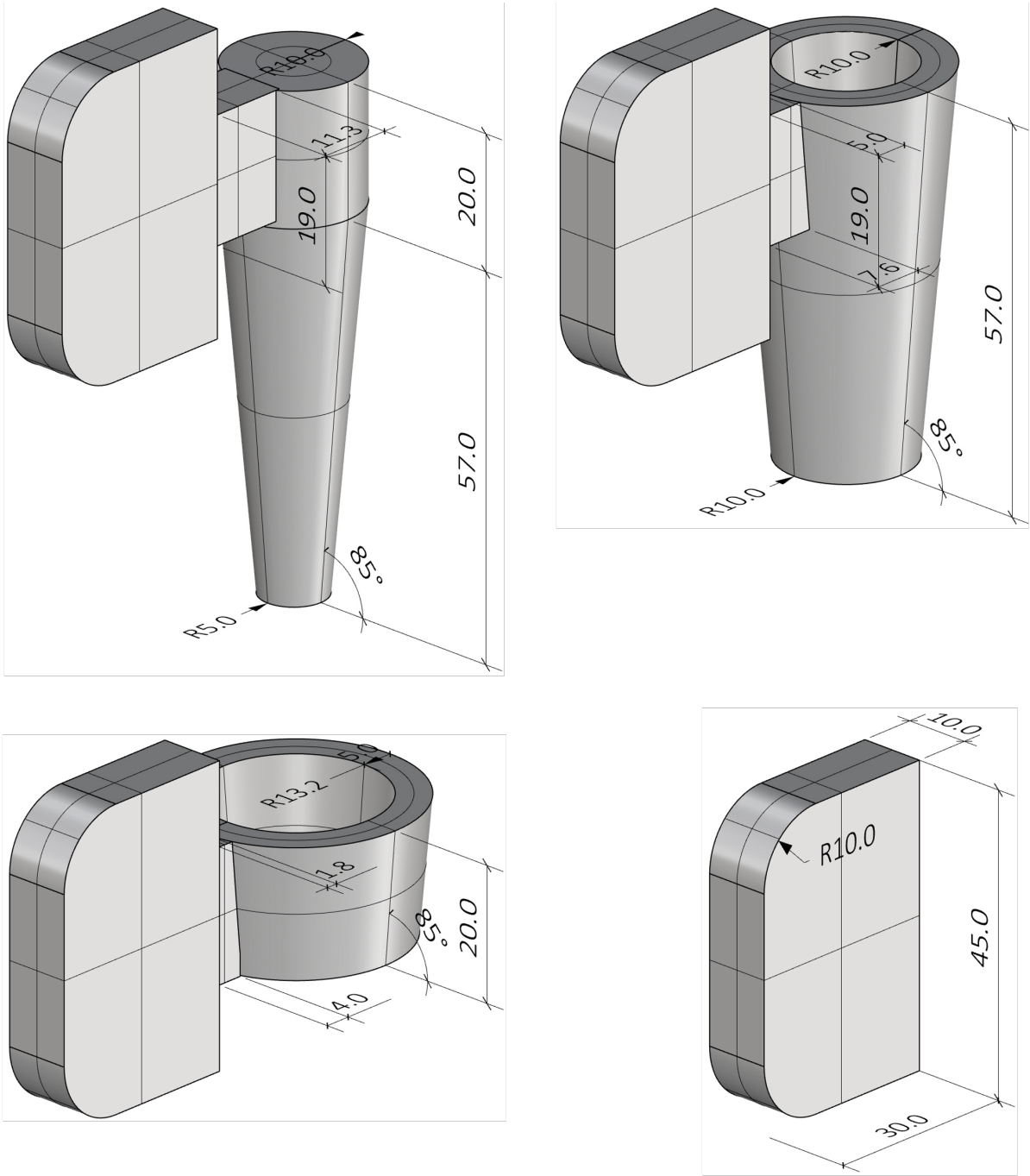
Figure B.7: Dimensions of the 'coffee-cup-hand' system

B.5. Building physical analysis of the connections

The following figures represent the building physical analysis at the position of the connections, to investigate whether the connections need insulation material to satisfy the norms. Connection G is not taken into account since this inner wall to base profile is situated inside of the pavilion, therefore no insulation measures need to be implemented there.

Three sub-figures are presented per connection:

- The model input for the analysis (geometry and materials)
- The temperature analysis
- The heat transfer analysis
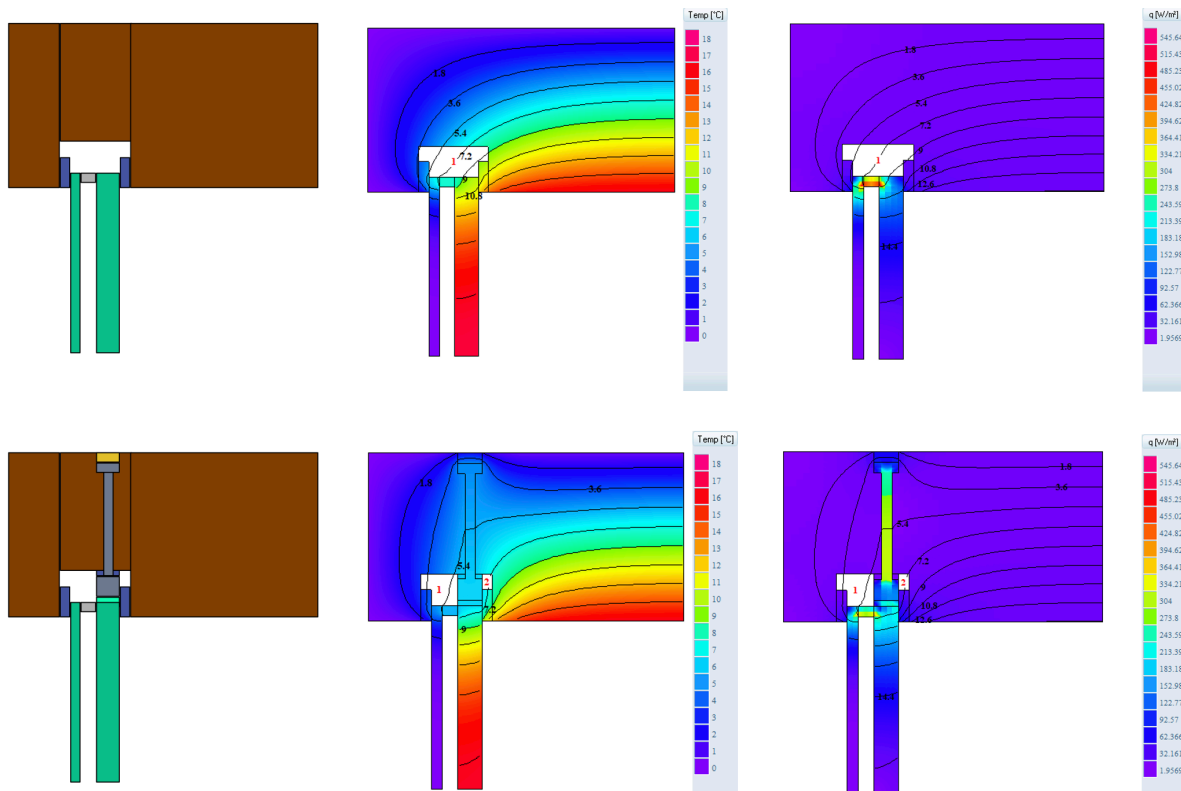
Figure B.8: Heat analysis of the roof to outer wall connection. The top row represents the joint outside connection A, the bottom row at the position of connection A. Heat transfer is observed in the steel bolt, which is expected. No insulation measures were taken.
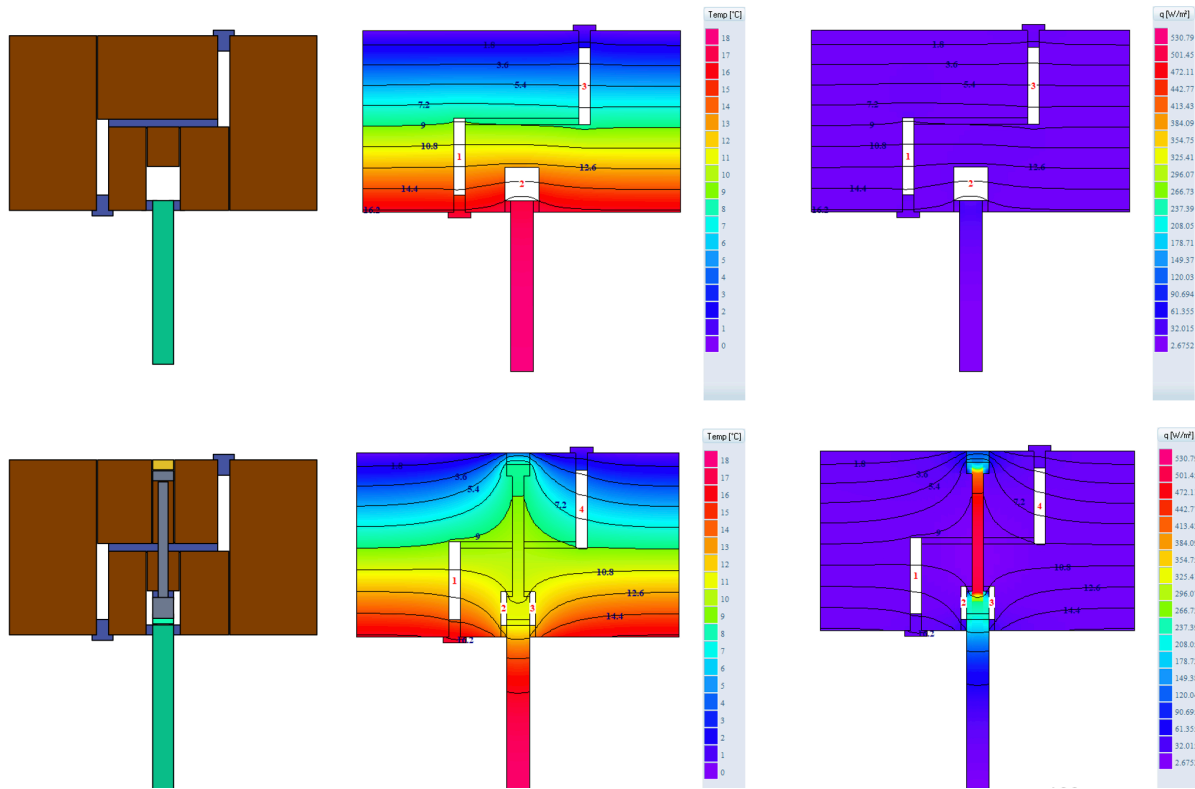
Figure B.9: Heat analysis of the roof to inner wall connection. The top row represents the joint outside connection B, the bottom row at the position of connection B. Heat transfer is observed in the steel bolt, which is expected. No insulation measures were taken.
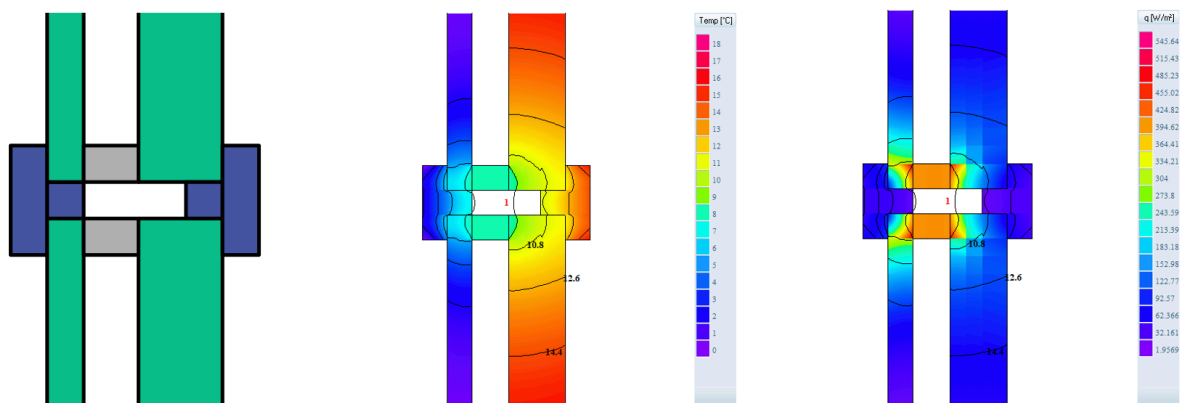
Figure B.10: Heat analysis of the joint between the IGU's on the short side of the pavilion. No structural connection is present here, only rubber pushing gaskets which, according to this analysis, satisfy the building physical regulations.
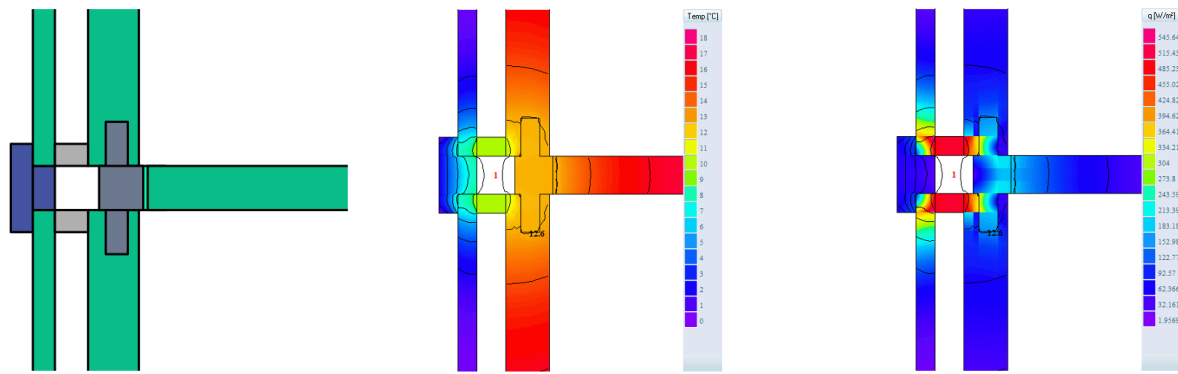
Figure B.11: Heat analysis of the outer wall to outer wall to inner wall connection ('coffee-cup-hand' system). Also here, no extra insulation measures are needed.
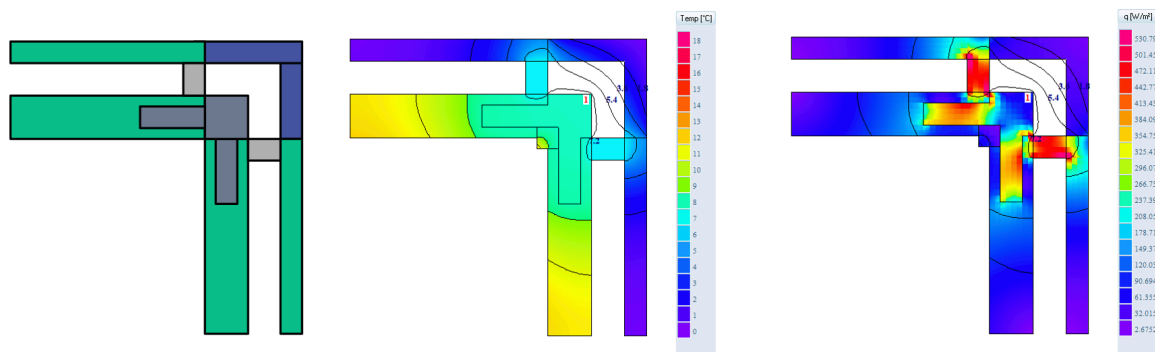
Figure B.12: Heat analysis of the outer wall to outer wall connection in the corners of the pavilion ('coffee-cup(-hand)' system). No insulation measures are needed
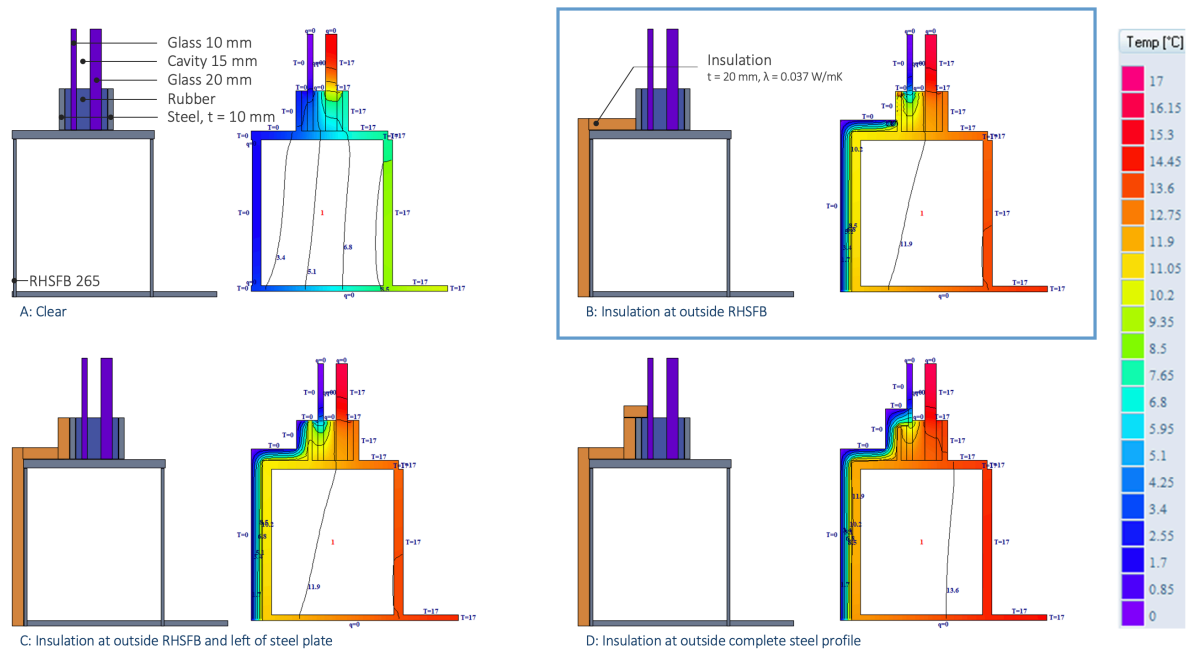
Figure B.13: Heat analysis of the outer wall to base profile joint. The initial analysis (upper-left) showed that condensation could occur in the steel profile due to large temperature differences and large heat transfer, so measures needed to be taken. Insulation of $20\ mm$ thick was added on the outside of the profile (upper-right) image, now satisfying the norms. Bottom left image shows the connection with $20\ mm$ of insulating material on the side of the welded steel plate. Bottom-right image is a version of the connection with complete insulation, also on top of the steel plate and rubber, sealing the entire base profile.

B.6. Assembly sequence

2) Putting base elements on foundation

3) Laying floor slabs on top of base elements

4) Placing inner wall panels with temporary struts

5) Placing outer wall panels in specific order

6) Laying roof slabs on top in specific order

7) Inserting bolts to connect roof to walls

8) Inserting the seals

9) Finished pavilion
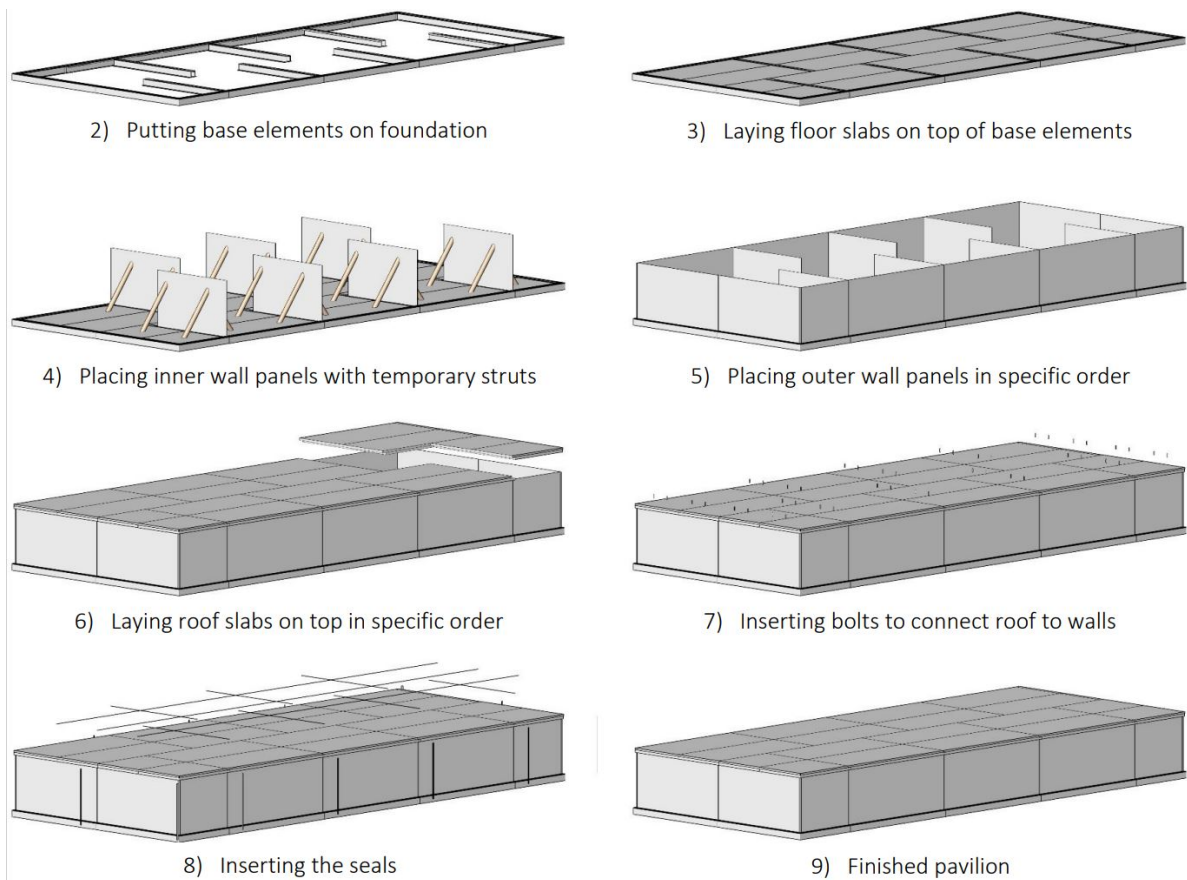
Figure B.14: Assembly sequence of the pavilion. Activity 1) is not shown: the laying of the foundation.

C
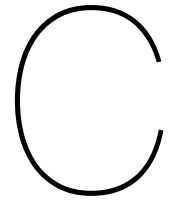
Literature review in depth

C.1. Glass as building material

Relevant topics are elaborated on in the main report. Background glass knowledge is shared in this section.

Historic overview

It is not known exactly when and where glass originated, but writers claim that the first materials resembling glass were discovered in Mesopotamia and Egypt. Examples include the melting of copper, which created an ash, or when clay was baked to glaze pottery. In the library of Assurbanipal in Nineveh, the oldest known recipe for glass was found, dating from around 650 BC. [3]

In the times of the Roman, flat glass was first introduced in the built environment as windows, as was found during the excavations of Pompeii and Herculaneum. By the expansion of the Roman Empire, the glass making technique was also introduced in the northern Alpine areas of the continent. During the beginning of the Middle Ages, glass was predominately used for the production of drinking horns and i.e. claw breakers. Contrary to the late Middle Ages, the period in which glass mainly functioned as windows for monasteries and churches. Figures in Appendix B shows a brief overview of the history of glass.

Production technologies

Brown cylindrical flat glass (1st century AD) and crown glass (4th century AD) remained the basis for glass production until the beginning of the 20th century. During the Italian Renaissance, Venetian glass makers entered the world of glassware. It became famous for the purity of the glass and the absence of any colour. This period can also be considered the revolution of glass (see Appendix B, section B.2). New production methods were invented, such as cast glass, and later the "pour and roll" method was one of the new glass-making inventions by Bicheroux in 1919. Glass was very expensive at the time, mainly because both sides of the panes had to be polished. [3]
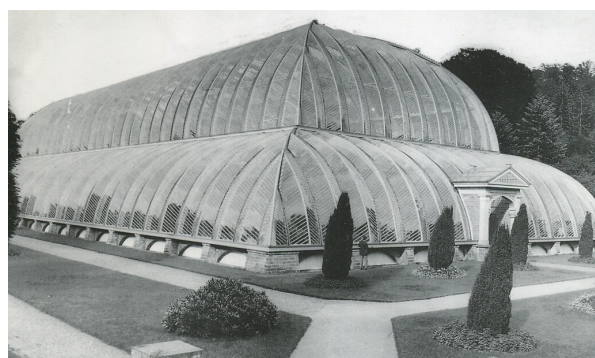
Figure C.1: Ridge-and-furrow system at greenhouse Chatsworth, 1840 [68]

Industrialisation advanced the process of glass manufacture and laid the foundations for glass in the construction world through the use of wrought and cast iron elements as load-bearing structures [69]. Brown cylindrical flat glass could now be produced in large quantities by new processes invented by the Chance brothers. Along with the use of the ridge-and-furrow system, the Chance brothers' invention paved the way for new types of greenhouse structures, such as the Chatsworth glasshouse (Figure C.1). Another example of such Victorian conservatory architecture is the Crystal Palace, built for the Great

Exhibition of London. This building was a structure of iron and glass with dimensions that had never been built before. From the mid-19th century, engineers focused more on reducing the supporting structure that supported the glass panels and was crucial in the design and engineering of large railway stations, department stores, arcades and domes [3].

As time passed by, architecture kept developing and the need arose for a smooth transition between inside and outside. The renowned architect Frank Lloyd Wright called the abolition of the conventional solid building envelope "the destruction of the box". Aiming at a new connection between man and nature, the seamless transition between inside and outside was made possible by the introduction of a lot of glass on the facades. Light, air and sunshine were then seen as important factors for the well-being of people in buildings. The first writings on 'glass facades' date from around the 1950s, this period can be regarded as the advent of curtain walling [25].

The literature describes various periods in which glass made its appearance as a building material. Wurm mentions the 1990's when technical developments were documented by several important publications. In contrast, Lenk and Dodd mention an earlier introduction of structural glass in the Willis Faber and Dumas building, in 1975. In this building, the glass fins act as a secondary load-bearing material: they transfer the force of the wind onto the façade panels [70].

utilitas
function

decent architecture

firmitas
structure

venustas
aesthetics
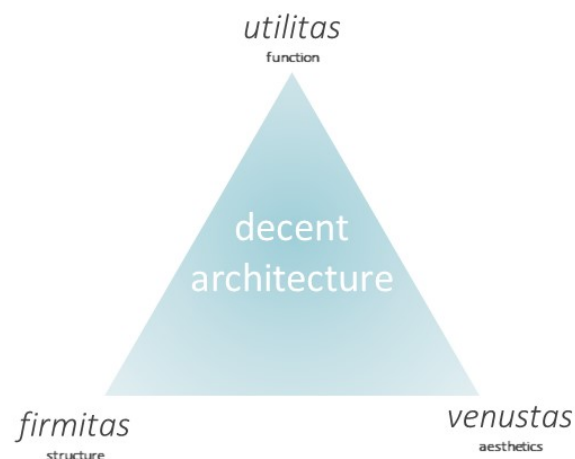
Figure C.2: Vitruvius' principles of good architecture *[own image]*

Speaking of contemporary glass architecture, Wurm finds that it stems from a mixture of two tendencies; first the beauty of the material itself and the new emphasis on mechanical forms [3]. Later, he states that with the Roman Vitruvius' principles of good architecture; *function, structure and beauty*, structural shapes are the result of a creative process on behalf of the architect and/or engineer, these principles can also be seen in Figure C.2. Today, we can argue whether sustainability, durability and other -ity's should also be implemented in Vitruvius' principles for a modern successful design.

C.2. Connections

This part of the background research describes different types of connections. As shown below, the relevant sub-topics can be found in the main report, the rest is shown here:

- Glass connections

    - Embedded laminated connections (shown in appendix Section C.2)
    - Continuous linear support connections
    - Clamp connections
    - Friction connections
    - Bolted connections
    - Adhesive connections

- Interlocking connections
- Glass interlocking systems
- Modular connections
- General (shown in appendix Section C.2)
- Modular interlocking connections

Glass connections

Different distinctions in glass connections are made by Bedon, IStructE and Wurm, of which the latter one is presented in the main report. The distinctions of Bedon and IStructE are shown here in Tables C.1 and C.2.

Connection type	Category
Clamped	Clamped
Bolted	
Countersunk	Bolted
Hybrid countersunk	
Adhesive	
Embedded	Adhesive
Embedded with insert	

Table C.1: Connection typology of Bedon [1], based on their mechanisms of load transfer

Connection type	Category
Continuous linear support	
Clamp	
Friction	Mechanical based
Bolted	
Adhesive	Adhesive based
Interlocking	*Dry stacked*

Table C.2: Connection typology of IStructE [26]

Continuous linear support connections

An example of a continuous linear support is framed glazing. Continuous linear joints are usually made of wood, aluminum, steel, plastic or EPDM profiles [25]. Setting blocks carry the vertical load of the glass panels and transfer the stresses to the underlying structure. Loads on floor slabs, for example, are distributed over continuous support connections. Continuous support connections differ in way of clamping because they are structurally based on gravity. Listed below are several types of support connections that can be used for continuous linear support of glass elements.

- Glazing bead
- Glazing bar
- Structural sealant glazing
- Clamping plate

Clamp connections

Clamped connections can typically be found in balustrades and facades (glass components with an insignificant role in the structural behaviour of a building). The visual distortion is minimum in clamped connections, meaning wide transparent elements can be created. The glass is being clamped by metal parts with an EPDM interlayer in between, a soft interlayer that is able to transfer the stresses over a larger area. By this layer peak stresses are avoided in the glass. Cap systems in curtain walls are an example of clamp connections, like in the Markthal Rotterdam (see Figure 5.1 at the beginning of this chapter) [1].

Friction connections

When preloaded bolts cause friction-grip in connections, the detail can be considered as a friction connections. Consequently, peak stresses are avoided by the area on which the connection is fastened. Local aluminium interlayers in friction connections of laminated glass avoid possible problems with interlayers that are subject to temperature and creep differences [1]. The local aluminium interlayers guaranty the resistance and stiffness against the pretensioned stresses.

An advantage of friction connection over bolted connections is their relative larger contact area with the glass panes. In the event of out-of-plane deformations, these connections offer greater resistance since local peak stresses near the bolts are avoided [1]. A disadvantage of prestressed friction joints is that they may be subject to stress relaxation on the long-term [29].

Bolted connections

Conventional glass connections are since the 1960's dominated by bolts. They can function as glass-to-glass connections (like fins to beams) and as a connection in the fixing of glass facade panels. The forces in bolted connections are transferred through the bolts themselves [1]. Bolted connections can be realised with normal shape bolts (Figure C.5 b) or with countersunk bolts (Figure C.5 c and d).

Tempered glass is in most cases required due to the high stresses that occur nearby the bolt-holes (peak stresses). Experienced workers are needed on-site when bolted connections are assembled, as the precision in tolerances and thermal movement is crucial. The gaps between bolts and the glass are most of the times filled with injection mortar or polymeric bushings, which allows the forces in the glass to be transferred to the bolts [1]. Injection mortar is generally the better solution when applying laminated glass; the mortar intercept the differences in lamination, see Figure C.3.
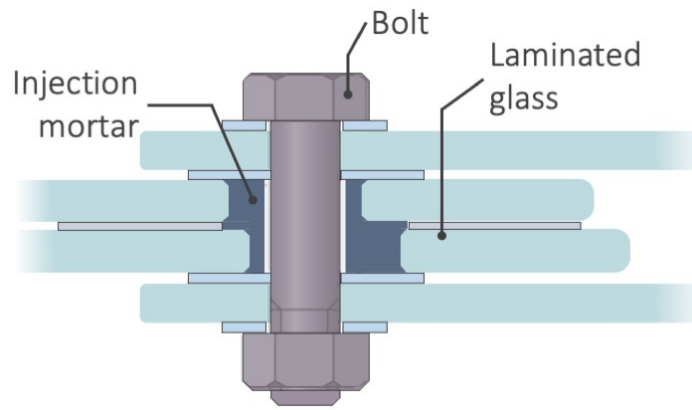
Figure C.3: Injection mortar in bolted connections takes care of lamination misalignment *[own figure, adapted from [31]]*

Watson, Nielson and Overend [71] claim that it is challenging to predict the occurring stresses that arise in the glass around holes. This complexity is mainly due to the stress state, the strength of glass and the presence of large residual thermal stresses. Maximum stresses in glass near bolt-holes can indeed be computed by extensive finite element modeling, but in literature simplified formulas can be found like given in equation C.1 [1].

$$\sigma_{max} = \frac{P * K_t}{t * (2 * c - d)}, with : \tag{C.1a}$$

$$K_t = 12.882 - 52.714 * \frac{d}{2 * c} + 89.762 * (\frac{d}{2 * c})^2 - 51.667 * (\frac{d}{2 * x})^3 \tag{C.1b}$$

Adhesive connections
Gluing glass to connecting elements is an adhesive way of detailing glass structures. Adhesive polymeric materials are used to connect construction elements by point, linear or a surface support. Figure C.5 e), f) and g), show adhesive point fittings.

Many types of adhesive materials exist and so on, a wide application that differ in resistance, appearance and more. The mechanical performance of adhesive connections are dependent on many variables such as climate, surface area, surface preparation, loading condition, chemical properties and many other aspects. Three different failure modes define the mechanical behaviour of an adhesive, these can be found in table C.3 [1].

Adhesive type connections are labour-intensive and require attention during the installation, but have several advantages above mechanical connections [1]:

- Larger contact area, i.e.:
  - less chance for peak stresses
- No drilling needed, i.e.:
  - easier production
  - residual stress field is unchanged
- Connectors do not penetrate the glass i.e.:
  - better architectural appearance
  - thermal bridges are avoided
  - in IGU's gass loss is prevented

Failure mode	Description
Adherent failure	Failure of the connected materials
Cohesive failure	Failure of the glue itself
Adhesive failure	Failure of the glued interface

Table C.3: Failure modes in adhesive connections [1]

Interlocking connections

To prevent structural parts (or bricks) from sliding relative from each other, bonding agents (mortar) or mechanical connections are typically applied. These assistance strategies can be avoided by using structural components with interlocking shapes. Friction subsequently keeps the structure balanced due to the (self)weight and form of interlocking structural components. Technically, the interconnecting geometry of the constituent components ensures the global structure's kinematic restriction in one or two directions, and so on, the structure's stability [72]. Promising interlocking glass solutions and modular interlocking connections are discussed in this section.

Glass interlocking systems

Maximum transparency is accomplished by employing a glass interlocking system, which cannot be obtained by utilising mechanical connections in most cases. The interlocking mechanism ensures the structural safety of a desired building without having the need to be assembled by mechanical or adhesive connection types [73]. In the structural glass domain, a lot of research is being put in the potential of interlocking cast glass bricks.

A variety of brick shapes were produced by kiln-casting glass. The interlocking mechanical capacity, residual stresses, manufacturability, and mass distribution of these were then examined in a comparative manner. Furthermore, an inquiry into the most appropriate dry transparent interlayer was carried out. To analyse the effects of the most critical geometrical characteristics of the interlocking mechanism on the structural behaviour of the system, a numerical model is created for the most favourable geometries. [73]

In Oikonomopoulou's study [73], five distinct kinds of interconnecting blocks have been created, as illustrated in Figure C.7. Prototypes were created as on a 1:2 scale and evaluated based on their scoring on the design criteria, as shown in the figure. Because the osteomorphic shape (type A, which is was shown to be the most optimum design of the five variations, it was also numerically evaluated. The dry intermediate layer that was applied in between the blocks was a $3\ mm$ thick PU70 interlayer.

The shape of the blocks was discovered to have a logical affect on the overall structural performance in shear force; a smaller amplitude in the shape of the block (Type A of Figure C.7) leads in a much lower capacity in shear. Furthermore, there is a greater risk of bending and, as a result, the failure mechanism of the system in such situations. In contrast, blocks with a larger amplitude ('higher' blocks) show a greater probability of shear lock failure, but are less susceptible to bending. The production of these higher blocks seemed to require a higher level of accuracy. [73]

Modular connections

Modular interlocking connections

Mechanical and adhesive connections have the drawback of requiring effort and accuracy in assembly and removal. Furthermore, under extreme stresses, the mechanical connections may loosen or the adhesive connection may fail.

Smart interlocking mechanisms are an innovative method to minimize these issues, used in combination with the necessary mechanical fasteners. With this sort of mechanism, researchers from Western Sydney University [74] have discovered a means to improve the integrity of multi-story modular buildings. The researchers have designed an *'easy to install, self-fit and self-locking mechanism'* [74] that is shown in Figure C.8. The so-called 'Modular Integrating System'(MIS) consists out of only two different type of connectors, that interlock with each other. The 'tongues' of connector strip A fit in the 'grooves' of connector type B and vice versa, see Figure C.8. Subsequently, the forces can be transferred via the contact area that exist by the MIS, between the modules in the connecting strips. The major objective of improving the overall integrity of a multi-layer modular construction was shown to be considerably achieved by simulations in finite element software. Similarly, they discovered that their approach aided in the assembly process and that the tolerances in the construction appeared to be better managed.
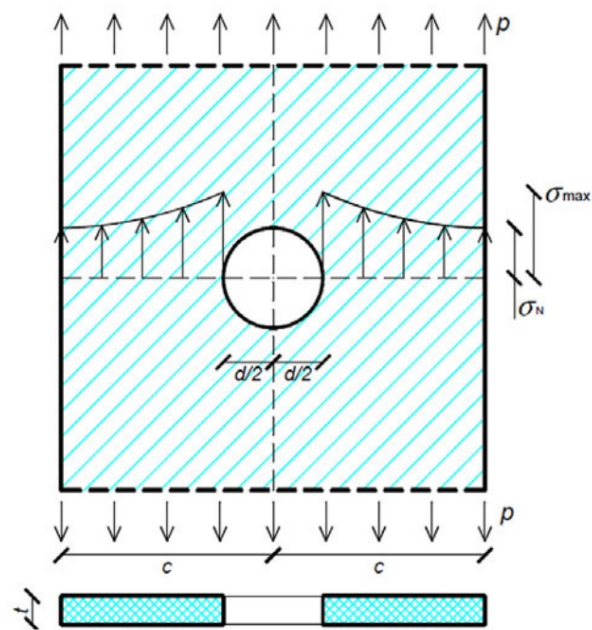
Figure C.4: Stresses near a hole occurring by a tensile force, see Equation C.1, figure from [1]
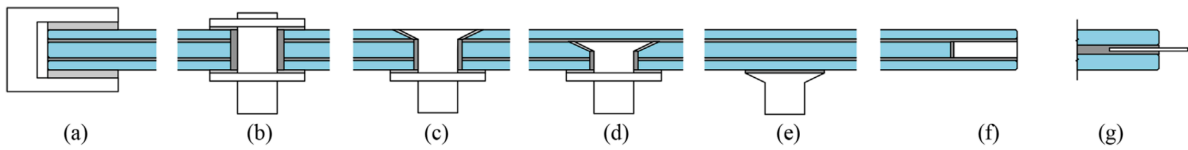
Figure C.5: Glass connection typologies. a) Clamped; b) Bolted; c) Countersunk; d) Hybrid countersunk; e) Adhesive; f) Embedded; g) Embedded with structural silicone [1]
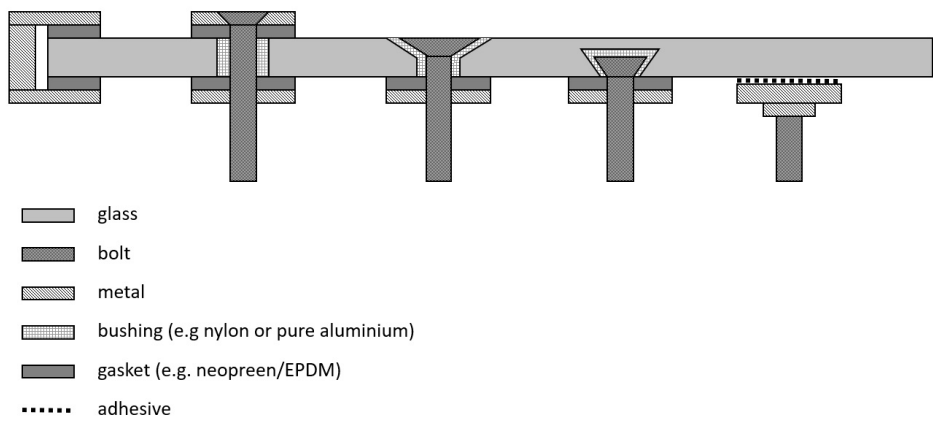
Figure C.6: Various types of point fitting

Block type	A	B	C	D	E
Interlocking mechanism	smooth curves	smooth curves	male and female blocks	sliding blocks – intense curves	semi-sphere keys for vertical stacking – ability to rotate
Shear capacity	high	high	moderate	moderate	moderate to high
Self-alignment	high	high	high	low	high
Multi functionality	high	high	moderate	moderate	high
Equal mass distribution / homogeneous annealing	effective	effective	risk of internal residual stresses	risk of internal residual stresses	effective
Lim. number of dif. units / ease of assembly	high	high	moderate	moderate	high

Figure C.7: The designs of Oikonomopoulou et al. [73] of different interlocking block types and their comparative assessment
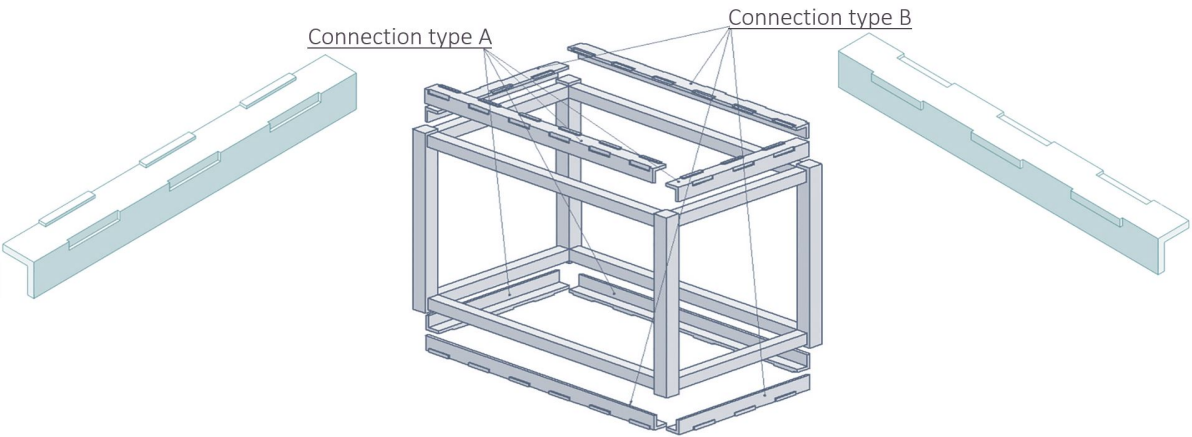
Figure C.8: The integrated interlocking strip connection of Shafari et al. [74]

C.3. Building physics

This appendix shows detailed building physic research from which the statements in Chapter 5 Section 5.3 are made. Six topics are elaborated on:

- Heat
- Air
- Moisture
- Acoustics
- Light
- Fire safety

Heat

General remarks

Managing heat transfer is a key characteristic in the consideration of building design processes regarding energy performance. Three main mechanism transfers are present in heat management: conduction, convection and radiation. Conduction is present when two objects are in contact with each other. The direct contact let heat flow from one material to the other. Convection, secondly, describes the heat transfer through fluid materials, which in buildings is in most cases air. Warmer air, for instance, is transferred in upward direction and cooler air is descending in building's cavities. A circular movement of air is now formed which is known as a convection current. Convective heat transfer is desired to be avoided in structures by making the building envelope as airtight as possible. Finally, radiation is formed by electromagnetic waves that transfer heat from material A to material B. This phenomenon, unlike conduction and convection, does not need material- or fluid contact. Infrared radiation can transfer in a vacuum and so on, can cause heat transfer. In the building industry, engineers try to minimise the radiation by implementing particular foil-type insulation. The heat transfer due to radiation can be calculated with Equation C.2 [75]. [76]

$$q_s = \frac{\epsilon_1 * \epsilon_2}{\epsilon_1 - \epsilon_1 * \epsilon_2 + \epsilon_2} * 56.7 * 10^{-9} * (T_1{}^4 - T_2{}^4)[W/m^2]$$

with: q_s = Net radiation transfer

ϵ_i = Emission coefficient of surface i

T_i = Temperature of surface i [K]

(C.2)

Source: [75]

Regarding material properties, the most important characteristics are thermal conductivity, thermal resistance, thermal mass and thermal transmittance. At first, the lower the thermal conductivity (lower λ value), the higher resistance again heat losses of the specific material. Steel for example has a relative high thermal conductivity (high λ value) because it transfers heat easily through the material itself. The second characteristic, thermal resistance (R), takes into account the thickness of the material, making it more valuable in building physic calculations. The R value can easily be calculated by dividing the thickness of the applied material by its thermal conductivity. Logically, the thicker the material, the higher the R-value, the higher the thermal insulation. Thirdly, thermal mass is the characteristic that deals with the preservation of heat. Steel has, compared to i.e. concrete, a low thermal mass, implying that a steel beam will cool down quicker than the concrete alternative. In the building sector it is important to maintain a stabilised temperature rather than a cycle of warm- and cold differences. Finally thermal transmittance (also the U-value) is the inverse of all R-values in an construction. It gives an impression of the total heat transfer through a wall for example, taking all used materials and thicknesses into account. The total heat resistance of a construction can be found by summing up the heat resistances of every particular material that is used. The single heat resistance of the materials is calculated by dividing the the thickness by the material's heat conduction coefficient (thermal conductivity), see Formula C.3 [75] [76]

Thermal conductivity	λ	1	[W/mK]
Thermal resistance	R	1	[m²K/W]
Thermal mass	C_{th}	1	[J/K]
Thermal transmittance	U	1	[W/(m²K)]

Table C.4: Relevant heat characteristics of glass [76]

$$R_{\text{construction}} = \sum R_{\text{m;i}} = \sum \frac{d_i}{\lambda_i}[m^2 * K/W]$$

d_i = Thickness of material i$[m]$

λ_i = Heat conduction coefficient of material i$[W/mK]$

(C.3)

Source: [75]

Thermal bridges in building envelopes are regions in which the thermal transmittance is high, so the heat transfers quicker from A to B. This is mostly the case in which structural elements intersect with the insulating materials. One can imagine that these thermal bridges have a significant effect on the thermal performance of a structure, reducing its U-value. In the European standards, methods for the U-value reduction by thermal bridges, as well as for the floor-, roof- and corner-junctions, are given by so-called ψ values. Not well designed building envelopes can contain thermal bridges with lower temperatures causing condensation. Condensation in a building envelope can be predicted by plotting a temperature gradient graph together with a dew-point graph. If these two graphs intersect, condensation will theoretically occur in your building structure.

An example of a method that predicts if condensation will occur is the Glaser method. First the designer should determine the temperature profile in the construction. Secondly, the maximum vapour pressure, p_{max} can be calculated for the known temperature and relative humidity. Hereafter, the p_{calc} must be calculated. Condensation, as stated above, will occur of $p_{calc} > p_{max}$.

Glass and thermal movement

The thermal conductivity of glass is relatively high, meaning that the thickness of glass seem to have only little influence on the heat proofing. What does make a significant difference, is using a cavity (insulated glass / IGU) or applying a coating (high-efficiency glass), see Figure C.9.
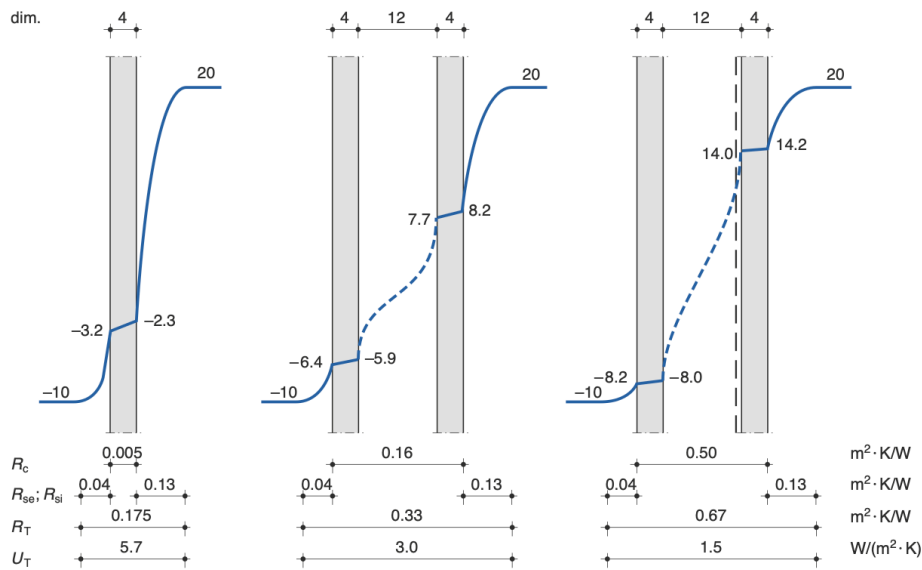
Figure C.9: Temperature differences in different glass constructions, from [75]

To prevent large radiant heat exchange through glass, a Low-E (low-emissioning insulating glass) coating can be applied on the glass. Radiative heat transfer can be calculated with Formula C.2, but in practice often simplified by Equation C.4. [75]

$$q_s = \alpha_s * \Delta T [W/m^2]$$

$$\text{with: } q_s = \text{Heat transfer by means of radiation} [W/m^2]$$

$$\alpha_s = \text{Heat transfer coefficient} [W/(m^2 K)] \tag{C.4}$$

$$\Delta T = T_1 - T_2 = \text{Temperature difference between both surfaces [K or C°]}$$

Source: [75]

Air

Air movement should be present in every building as ventilation, also 'planned air movement' to guarantee proper indoor air quality; unplanned air movement should be avoided in any case. Building should subsequently be air-tight, meaning no random gaps occur in a building envelope, windows that can be opened are not considered as these gaps. Infiltration describes the penetration of cold air into a building, exfiltration on the other hand showcases the movement of warm air leaking out of a building. [76]

Three different pressure phenomena influence the air tightness of a building. Firstly there is stack pressure which is present in taller buildings. Cooler air flows in the bottom and warmer air leaves the building at the top. Secondly wind pressure is present due to a difference in pressure on the building between the upwind (windward) and the downwind (leeward) directed facades. [76]

Moisture

Next to heat and air movement, moisture flow in a building is fundamental for the design of buildings. Good engineered moisture management is not only important for the well-being of occupants, it also improves the durability of the building's envelope. Several moisture sources affect the building's facade system. The outdoor climate is obviously one of them appearing in weather and rain. Indoor moisture production is partly defined by its occupants and function of the building. Densely populated areas like hotel lobbies or conference halls for example demand a more intense moisture management strategy than a single-family house. Also, 'wet' materials like concrete are responsible for a significant moisture production to the building's envelope, especially short after the building's completion. A problem that could arise is condensation in the building envelope due to high vapour pressures. [76]

Differences in vapour pressures cause the movement of moisture, known as vapour diffusion. These differences occur in case of temperature and relative humidity differences on both sides of a permeable materials. Vapour barriers are low permeable layers that slow down the movement of vapour in building envelopes. Another moisture movement phenomenon is capillary action. This is the movement of liquid in the non-gravitational direction, like water getting sucked up by a sponge. In buildings, the small pores in brickwork and concrete are an excellent environment for capillary action. No substantiating is needed that moisture in building envelopes are the cause of mold growth, damaging the building envelope's components. [76]

To asses and therefore prevent moisture movement in building envelope's, the engineer should first make a prediction of the possible moisture production and so, on the internal vapour pressure compared to the external climate. Secondly, the physical characteristic of the entire facade construction should be assessed and how this interacts with the possible available moisture sources. The effect of the outdoor climate should lastly be incorporated in the considerations. [76]

Acoustics

General remarks

As sound is the base for acoustics, it influences not only our psychological and physiological sense, but also our behaviour and cognition. Sound waves hitting a structure can be diffused, absorbed, reflected or transmitted through the material. High absorbingly sound materials are most of the times spongy, fluffy and soft. Smooth materials that are also hard are capable of diffusing sound waves, the sound waves will be reflected in different routes. Transmitted sound passes through a material. [77]

Glass and acoustics

Sound waves are similar to light waves. However, increased sound absorption can be achieved with thicker layers of glass and lamination, whereas light absorption is more dependent on the amount of layers of glass only. Laminated glass shows the same phenomena as mass-spring-mass systems regarding the damping of sound waves. Special PVB interlayers are developed that contain a soft core and function as an optimum sound barrier for the glass element. [3]

Specific sound insulation that has to comply with strict norms can be achieved with special acoustic PVB interlayers. [26]

Light

General remarks

There are three sorts of events that can occur as light travels from one medium to another, for example from air to a solid: absorption, reflection and transmission. Different wavelengths of light interact with the medium in different ways; some may be reflected, some may be absorbed, and some may be transmitted. Different wavelengths represent various colors.[78]

Reflection occurs when light bounces back off the surface it reaches. When light gets reflected on a surface, its angle of incidence is equal to its angle of reflection, measured from the normal line perpendicular to the surface. Absorption happens when light is turned into another kind of energy which in most cases is heat. A pure red object absorbs all colors except red on the wavelength spectrum. Transmission occurs when light can pass through a medium. [78]

Glass and light

Windows are openings in building skins which allow daylight to enter a structure. Glass in the windows cause not all daylight to enter the building. Although glass can be regarded as a high-transparency material, part of the incoming (solar) light is reflected and absorbed. Figure C.10 describes the approximate parts of the incoming light that are transmitted, absorbed and reflected for a single glass pane. The Light Entry Factor (LTA) describes how much light surpasses the glazing (transmitted part), expressed in a factor (see table C.5) [75]. The lower the total solar energy transmission, the lower the LTA-value.

The iron oxide content in glass is what gives the green colour to the material by absorbing the red light. Glass with a low-iron content is more transparent, hence absorbing less red light. This type of glass uses silicon dioxide of large purity in the production process and in practice transmittance is almost not dependent on the thickness of the glass pane. Using multiple layers of glass like in IGU's (insulated glass units), the light absorbance is the product of the absorbance of every individual pane. [3]
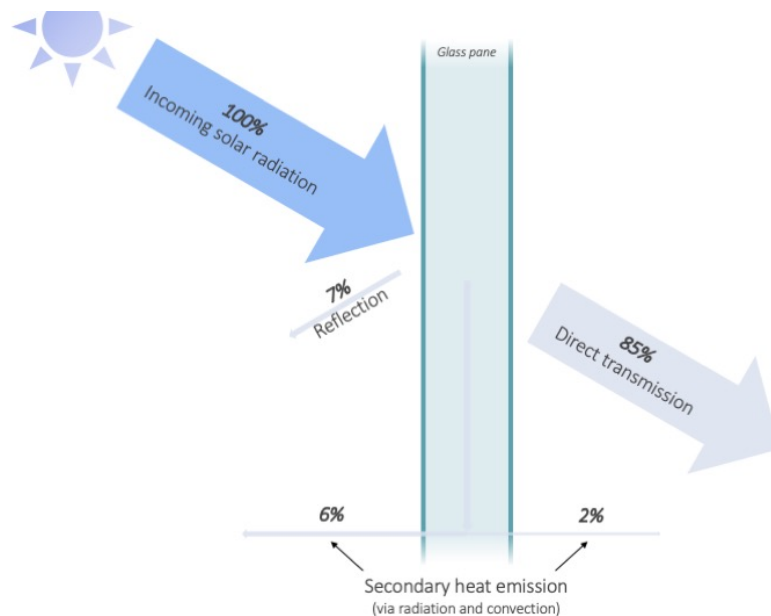
Figure C.10: Division of incoming solar light in transmittance, reflection and absorption for single glazing

Comparing the LTA with the heat gain, the g-value, it can be said that the relation between those two is approximately $LTA \leq 2 * g$ [79]. In other words: in cases of windows with a poor heat gain (low g-value), the light transmittance of the windows is expected to be also low.

Glass type	LTA value
Single glazing	$0.85 \sim 0.90$
Double glazing	$0.70 \sim 0.80$
HR^{++} insulation glazing	$0.70 \sim 0.80$
Solar control glass	< 0.70

Table C.5: Light transmittance values for different glass compositions [75]

Fire safety

General remarks

A material's fire resistance is a characteristic that specifies its resistance to fire, its capacity to contain its performance to the object's function for a defined duration. Building elements must be able to withstand fire for a set amount of time as stated in the standards, as well as prevent the fire from spreading.

The moment at which all exposed components reach ignition temperatures at the same time is known as the flashover. The fire begins to spread quickly from this point forward [80]. During the period prior to a fire's flashover, the reaction of the building elements is crucial. The combustibility and ignitability of a material determine its reaction (and contribution) to a fire.[81]

The fire resistance of an element is defined by three concepts. Load-bearing (R) means that the constructive element must preserve its mechanical resistance for a certain amount of time. Integrity (E) is the capacity to stop fire propagation to an element's unexposed side, for a certain amount of time. Lastly, thermal insulation (I) is the capacity to prevent heat from passing through an element for a predetermined amount of time. A structure can for example have the marking REI60, with means it should comply to above mentioned phenomena for at least a period of 60 minutes.

Glass and fire

Glass is a non-combustible material and therefor can not function as a fire proofing barrier in structures [3]. Additionally, according to the M.Sc. thesis research of Z. Nodehi at the TU Delft, annealed glass is not suitable to be used in fire situations because of the thermal breakage phenomenon. Meanwhile, heat strengthened and fully tempered glass could be used as structural elements during a fire, with some improvements [82]. Using borosilicate in stead of sodalime glass, for instance, enhances the the fire-rating due to its lower thermal expansion coefficient [3]. Nodehi also claims that attention should be

put on the tolerances of glass-to-steel connections. Increased temperature has an effect on the difference in expansion of those materials namely. [82]

Single layer glazing showcased no significant performance during fire tests, meaning that extra layers as outer panes should be applied as lamination, so that the middle glass layer is isolated and functions as the load bearing element, claims Nodehi. [82]

The wall system structures of Interior Glassolutions satisfy the 30- or 60-minute EW and EI-regulations of the Dutch Bouwbesluit and the European norms. The transparent sealant joint between two glass panels in these systems expands drastically in the event of a fire. The composed layer of foam is besides fire resistant also radiation proof in both directions.

Light		
Light transmittance	τ_v	[%]
External light reflection	ρ_v	[%]
Internal light reflection	ρ_{vi}	[%]
Colour rendering index	R_a	[%]
Energy		
Total solar energy transmittance	g	[%]
External energy reflection	ρ_e	[%]
Internal energy reflection	ρ_{ei}	[%]
Direct energy transmission	τ_e	[%]
Energy absorption glass i	α_e	[%]
Total energy absorption	α_e	[%]
Shading coefficient	SC	[-]
UV transmission	τ_{UV}	[%]
Selectivity		[-]
Thermal		
Thermal transmittance	U	W/(m^2∗K)
Acoustic		
Direct airborne sound reduction	Rw	[dB]

Table C.6: Output of the AGC configurator, with relevant building physic parameters in **bold**

C.4. Reference projects

The following reference projects are being discussed in this section. The most relevant projects are elaborated on in the main report, as stated.

CoCreation Centre Delft, 2020 - Has a façade that also functions as a stability element (shown in main report, Section 5.4)
Glass busstops - Ordinary structures that rely on a clear (diss)assembly procedure (shown in main report, Section 5.4)
Glaspavilon Aachen, 1995 - A reversible pavilion out of structural glass elements
Interlocking connectors and toggles - Topic related, completed research

Glaspavilon Aachen (1995)

The glass pavilion from 1995 by Ulrich Knaack and Thomas Link was built for the 125th anniversary of the Rheinisch-Westfälische Technische Hochschule Aachen. The pavilion is composed of a demountable glass construction supported by a steel substructure. Figure C.11 showcases an impression of the pavilion and a detail in which the simplicity and demountability of the upper en lower connections can be seen. [23]

The glass fins are supported by two steel-profiles that are bolted together. The horizontal stability of the pavilion is guaranteed by the beams and fins, but also by the wall panels in both directions. The dimensions of the building were 2.5x2.5x6.25 metres, and consisted of roof and wall panels (12 mm thick FT), roof beams (6.6HS) and fins (12.12.12 FT).

Toggles for glass projects

A curtain wall system is generally applied as a non load-bearing facade on buildings and can be designed with different systems: stick, unitised. clamped or bolt fixed. The stick system is mostly applied in ground-floor facades of tall buildings, shopping centres and on low-rise office buildings. In this system, vertical (mullions) and horizontal (transoms) components are interconnected and fastened on several places on the floor slabs. They mostly concise of metal (aluminium) profiles and have a large variety in appearance. Mullions and transoms are intended to carry the panels of the façade, which can be glass panels (functioning as windows) and spandrels to hide the internal structural elements. [83] [84]
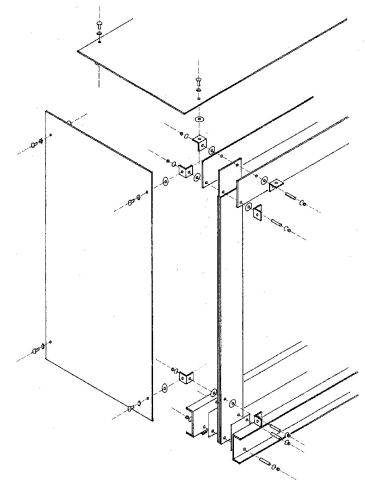
Figure C.11: Glaspavilon Aachen, from [23]

In Figure C.12 a stick system with toggle connection can be seen. From the drawing on the right it is clear that the toggle is an element that is implemented in the cavity of the insulated glass, along the entire length of the mullions and transoms. This forces the spacer to be placed deeper into the double glazing unit. [85] [83]

An compelling design by F. Oikonomopoulou (see Figure C.13a) was part of a small study from 2013 into reversible interlocking connection systems for glass structures. According to the designer the technology is *'quite outdated nowadays'*, although interesting for investigation in demountable connections for glass structures[1]. [24]

The connection was inspired by a simple modular children's table system. Two different kinds of components (a table leg and top) can be combined to form a table of any size. The top of the leg interlocks with the table top to form a stable table (Figure C.13b).

The main advantage of this type of connection is that no drilling is required, which is very desirable in glass in order to avoid possible peak voltages. However, according to the designers, it seemed that in glass it is very challenging to realise these type of linear interlocking connections in glass. The manufacturing process for these type of connections should be very precise and, additionally, the assembly procedure could turn out to be very complex.

---

[1] Based on personal communication with Dr. F.Oikonomopoulou from the Faculty of Architecture and the Built Environment, TU Delft.
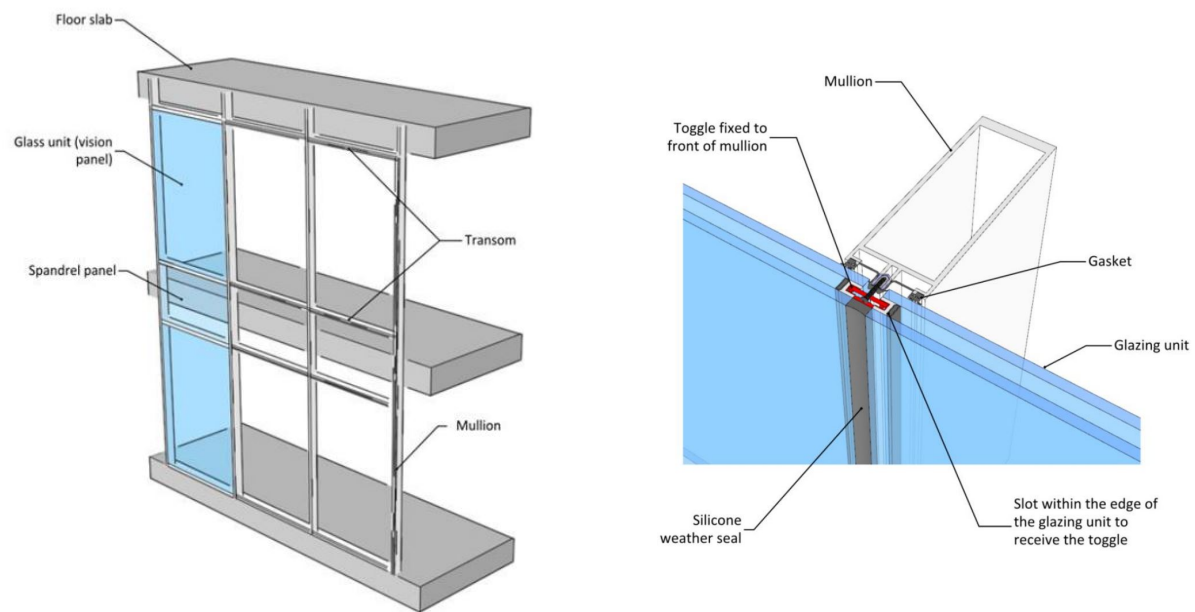
Figure C.12: Stick-system of a curtain wall facade which uses a toggle connection [84]

(a) Design by Faidra Oikonomopoulou

(b) The Connect 2 Play modulair children's table
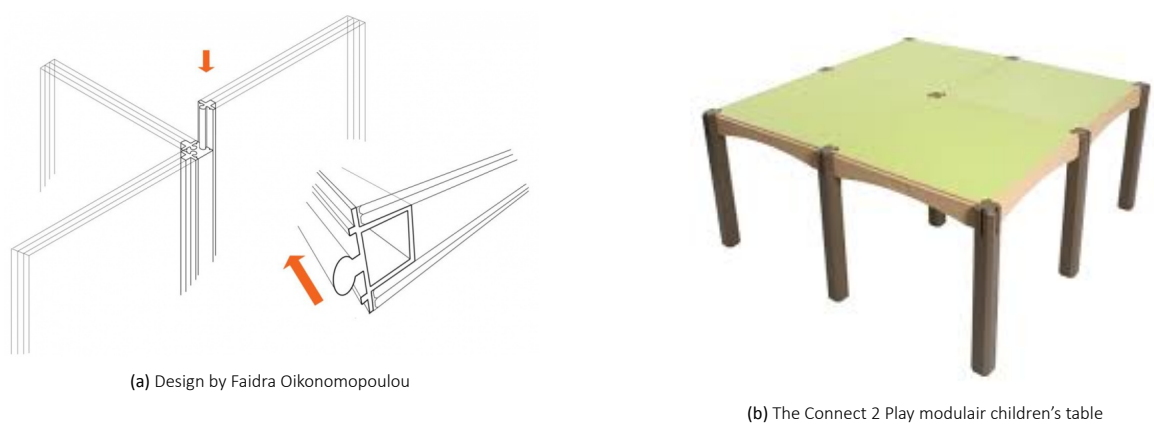
Figure C.13: Oikonomopoulou's connection and its inspiration

Structural verification

This section describes the calculation procedure for the verification of the structure. All calculations are made on the most critical force transfer. Using this particular approach, the force is determined with which the (dimensions of the) building elements and connections should be designed.

At first, the load transfer is explained in the first section, both in vertical and horizontal direction. The building elements are structurally verified next. Finally, the connections are calculated to check whether they are strong enough.
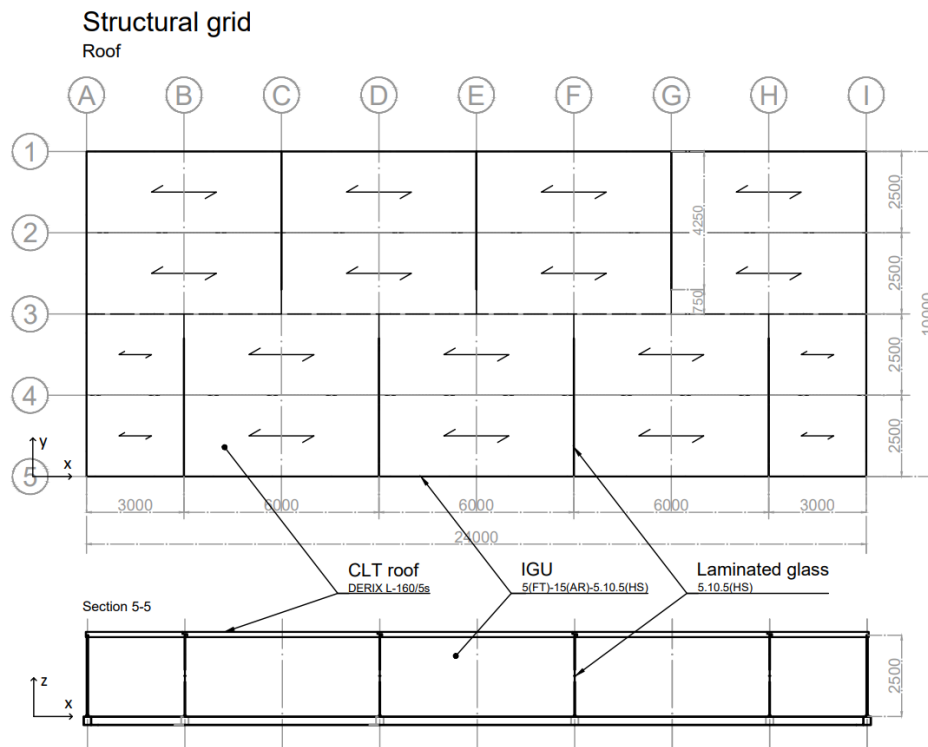
Figure D.1: Structural grid of the pavilion

The location of the critical building elements and connections are pointed out by grid letters and numbers, see Figure D.1

D.1. Vertical load transfer

Various forces act on the roof of the building in the vertical direction (Figure D.2).

Load bearing path

The vertical force acting on the roof will be transferred via the CLT roof panels to the internal walls and to the $5\ m$ long outer wall panels on the short side of the pavilion. The vertical force of the IGU's and the internal walls is transferred to the steel profiles of the basic structure, which then transfer it to the ground.

Loads

By distinguishing these consistently, a design load can be established for the building elements and their connections. Two type of loads are present:

- Permanent load (dead load)
- Variable loads (snow-, live- and windload)
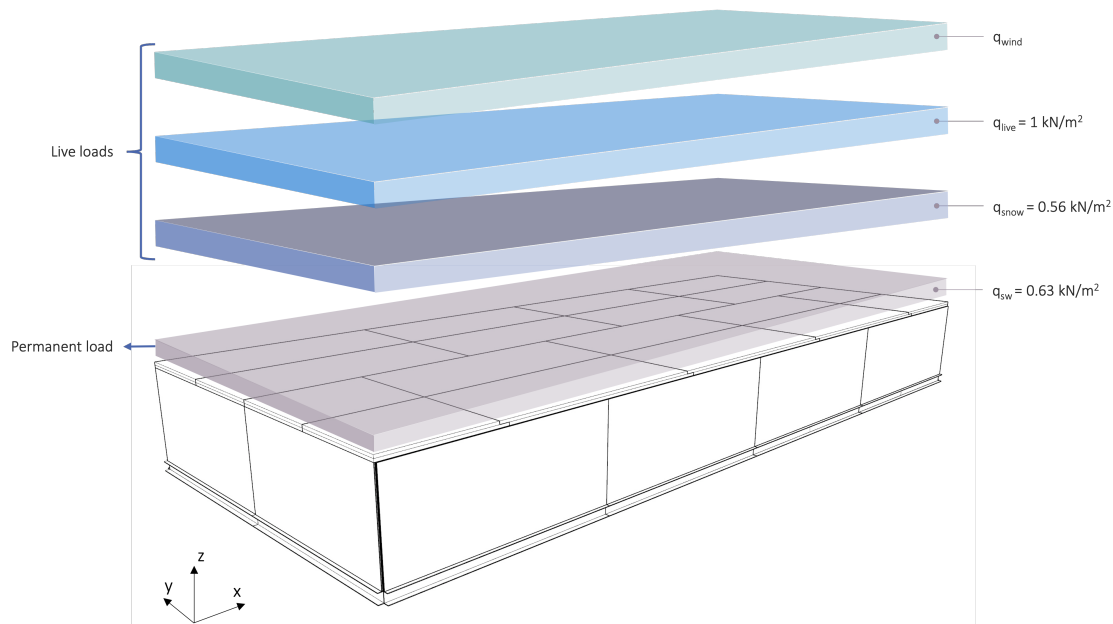
Figure D.2: Vertical loads acting on the building

Dead load

First the permanent load consist out of the dead weight of the roof itself. This is depicted by Derix to be $0.72\ kN/m^2$ with the chosen roofslab L-160/5s. The liveload consists of 3 different individual loads.

Snow load

To determine the snow load on the roof, Formula D.1 is used. s is the characteristic value of the snow load, which is $0.7\ kN/m^2$ for the Netherlands. μ_i is the shape coefficient picked from a designated table in Eurocode 1. In the case of the pavilion, μ is 0.8 since the roof contains an angle of 0 degrees. C_e is the exposure coefficient of 1.0, and C_t the thermal coefficient of also 1.0. This makes the snowload $0.56\ kN/m^2$.

$$s = \mu_i * C_e * C_t * s_k = 0.8 * 1.0 * 1.0 * 0.70 = 0.56\ kN/m^2 \tag{D.1}$$

Live load

Vertical variable loads on the roof of buildings have a distributed magnitude of $1.0\ kN/m^2$. This force includes the loading coming from i.e. workers on the roof who install the structure, or execute maintenance works.

Wind load

According to the Eurocode 1, a vertical uplift force from the wind could occur on the roof of buildings. To determine the magnitude of this force, the properties of the area in which the building is located, plus the properties of the building, are needed. These properties are based on the information given in the Scope (Part I, Section 2.3), the Design principles (Part II

Chapter 6) and the pavilion design (Part III, Chapter 7). After this the occurring wind force per surface can be determined by means of Equation D.2.

$$q_{\text{wind}} = c_s * c_d * c_{\text{pe}} * q_p(z_e)$$ (D.2)

Starting points wind load
- Windzone: 1 (Province of Noord-Holland, the Netherlands)
- Area: Urban (City)
- Low-rise building (Structural factor $c_s c_d = 1$)
- Closed building, internal pressure $+0.3$ or $-0.2\ kN/m^2$
- Flat roof

This means that the Peak velocity pressure, q_p for the pavilion's height of $2.5\ m$ is $0.69\ kN/m^2$. This pressure coefficient is equal for buildings with a height between 1 and 7 meters for urban areas in wind zone 1.

Wind direction	x	y
Height h	2.5	
Depth d	24	10
Width b	10	24
$e = 2 * h < b$	5 (e<d)	5 (e<d)
h/d	0.10<1.0	0.25<1.0

Table D.1: Dimensions for wind calculations

Wind calculation procedure
The values in Table D.1 are taken to define the different wind areas with the procedure from the Eurocode (Figure D.4). It can be seen that the wind zones change per wind direction (x or y), not only per plane, but also in size (Figures D.8 and D.9). The amount of square meter per area is subsequently calculated per wind direction. The factor c_{pe} of the wind equation D.2 is based on the area at which the wind is acting. The Eurocode provides key figures for c_{pe} for areas of $1\ m^2$ or smaller and for areas of $10\ m^2$ or larger (Figure D.3). If a wind zone has an area of $1 < A < 10\ m^2$, Formula D.3 must be used to determine the value for c_{pe}. With the c_s, c_d, c_{pe} and $q_p(z_e)$ now known, the wind pressure coefficient can be calculated for each wind area.

All above explained numbers are presented in Table D.2, in which every wind zone (A-I) is determined with its wind calculation values. A negative force means that wind suction is acting on the building in that particular area, a positive force means that the wind is acting as pressure.

$$c_{\text{pe}} = c_{\text{pe},1} - (c_{\text{pe},1} - c_{\text{pe},10}) * log_{10} A$$ (D.3)
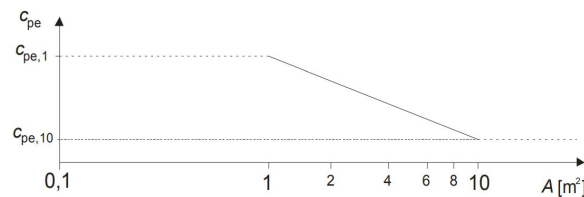
Figure D.3: The factor c_{pe} for area's between 1 and $10\ m^2$ need to be interpolated according to Equation D.3

Critical vertical loading
The critical load combination can now be established since all of the loads acting on the roof have been identified. If this load combination is taken into account, together with the load distribution of the roof, the most critical load-bearing building element can also be determined. With this data, a design load for the detailing can be given.

The above mentioned roof's load distribution is according to the scheme in Figure D.5, with the square meter per area calculated in Table D.3. The force distribution follows from the fact that the roof panels span in one direction: the longitudinal direction (direction x) of the pavilion. On the sides, the CLT panels are therefore not connected to the outer walls in a vertical direction. Since the inner walls of the pavilion are not constructed completely to the centerline of the pavilion, the force distribution of the roof slabs is not 100% one way. The surface, however, that a certain wall has to carry does not change because of this, as shown in the figure below.

(a) Zone A,B and C for e < d

(b) Zone D and E

(c) Zone F, G, H and I
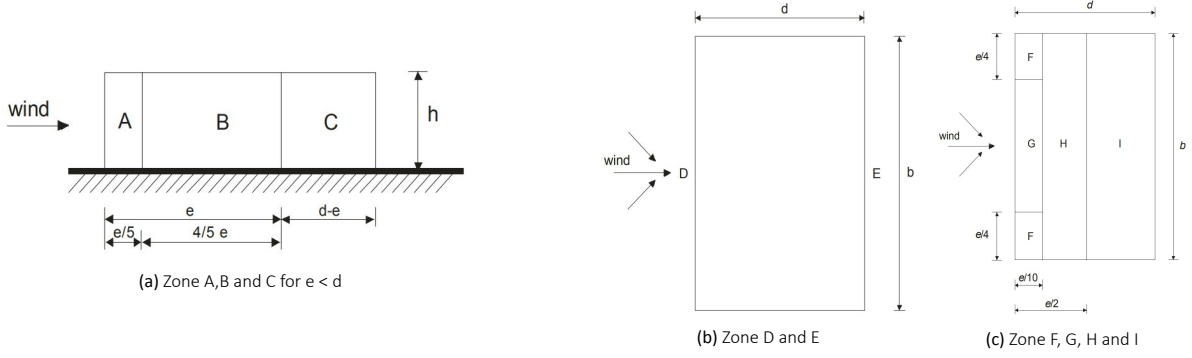
Figure D.4: Wind zone determination [84]

Zone	façade					roof			
	A	B	C	D	E	F (2x)	G	H	I
$c_{pe,10}$	-1.2	-0.8	-0.5	+0.7	-0.3	-1.8	-1.2	-0.7	±0.2
$c_{pe,1}$	-1.4	-1.1		+1.0		-2.5	-2.0	-1.2	-0.5
$Area_x$	2.5	10	47.5	25	25	0.6	3.8	20	215
$c_{pe;x}$	-1.32	-0.8	-0.5	+0.7	-0.3	-2.5	-1.54	-0.7	±0.2
$q_{w;x}$	-0.91	-0.56	-0.35	+0.48	-0.21	-1.73	-1.06	-0.48	±0.14
$F_{w;x}$	-2.28	-5.60	-16.63	+12.00	-5.18	-1.04	-4.04	-9.66	±30.10
$Area_y$	2.5	10	12.5	60	60	0.6	10.8	48	180
$c_{pe;y}$	-1.32	-0.8	-0.5	+0.7	-0.3	-2.5	-1.2	-0.7	±0.2
$q_{w;y}$	-0.91	-0.55	-0.35	+0.48	-0.21	-1.73	-0.83	-0.48	±0.14
$F_{w;y}$	-2.28	-5.50	-4.38	+28.98	-12.60	-1.04	-8.96	-23.04	±25.20

Table D.2: The pavilion's wind zones with pressure coefficients and equivalent forces

Downward critical load and element

The critical downward load appears to be a combination of the dead weight and the live load. This combination is the same over the entire surface of the roof.

$$f_d = 1.2 * q_{sw} + 1.5 * q_{live} \tag{D.4}$$

The structural element that carries the most roof area is therefore the most critical. This is an internal wall that carries a roof area of 5x6 metres. Figure D.3 showcases that 5 inner walls meet the normative conditions, the ones that carry the equivalent area of $30\ m^2$ (Area A 4).

Upward critical load and element

The only upward force on the roof that can occur is wind suction. Since this force is opposite to the direction of the roof's own weight, the latter must be multiplied by 0.9 instead of 1.2 in the load combination. In addition to the upward wind suction, a possible internal over-pressure of $0.2\ kn/m^2$ must also be taken into account. This additional load is incorporated in the q_{wind} of Formula D.5.

$$f_d = 0.9 * q_{sw} + 1.5 * q_{wind} \tag{D.5}$$

The subsequent normative building element carrying this upward load should be picked since the load is not equal on the entire roof. On the one hand, there are the wind zones in the corner that define the strongest wind suction, although this acts on a roof panel that is ultimately divided into smaller equivalent areas. On the other hand, further from the edge, there are the larger equivalent areas situated, but these ones carry a significantly lower uplift wind force.

By calculations, it seemed that the outer wall (the IGU of $5\ m$ depicted on Figure D.7) is transferring the highest force in the load combination. Two out of four of these IGU's carry the equivalent area of A_2, which is $15\ m^2$ (Figure D.3).
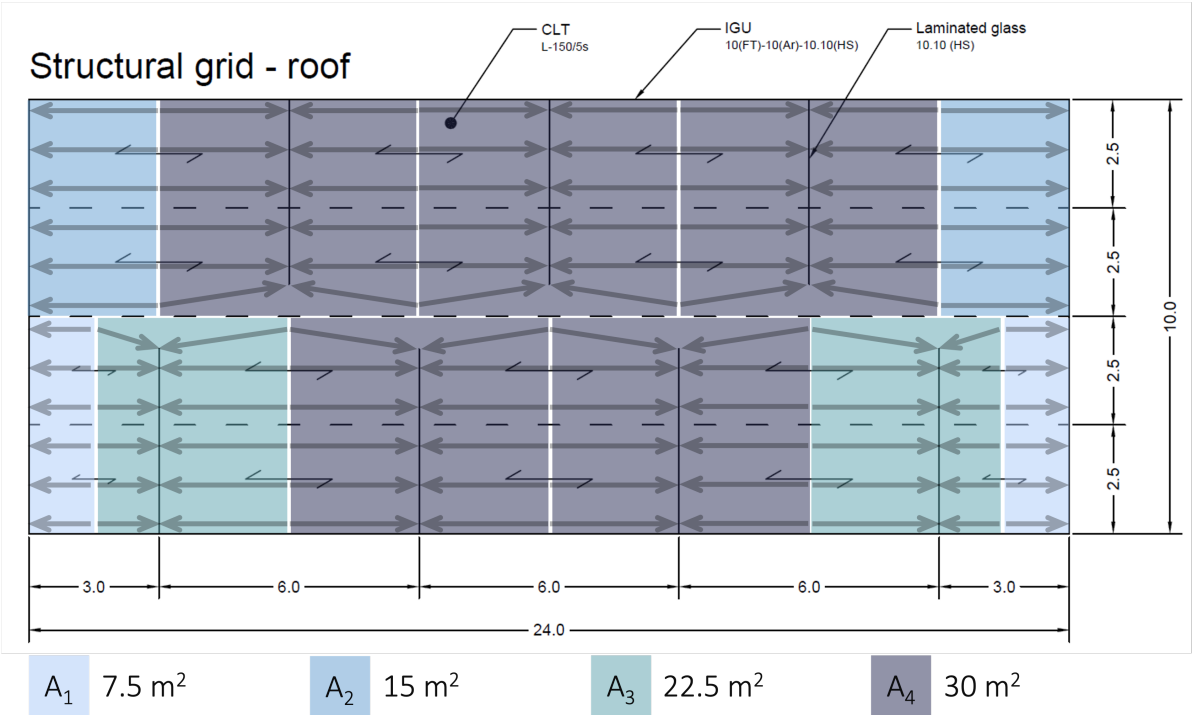
Figure D.5: Load transfer on the roof in case of vertical loads

	Area	Calculation	m^2
	A_1	$3.00 * 5.00$	7.50
	A_2	$3.00 * 5.00$	15.00
roof	A_3	$4.50 * 5.00$	22.50
	A_4	$6.00 * 5.00$	30.00
	A_5	$0.50 * 1.25 * 2.50$	1.56
	A_6	$[5.00 * 2.50 - (2 * A5)]/2$	5.47
facade	A_7	$[3.00 * 2.50 - (2 * A5)]2$	2.19
	A_8	$[6.00 * 2.50 - (2 * A5)]/2$	5.94

Table D.3: Division of force transfer on the IGU's, for a visual representation, see Figures D.5 and D.10
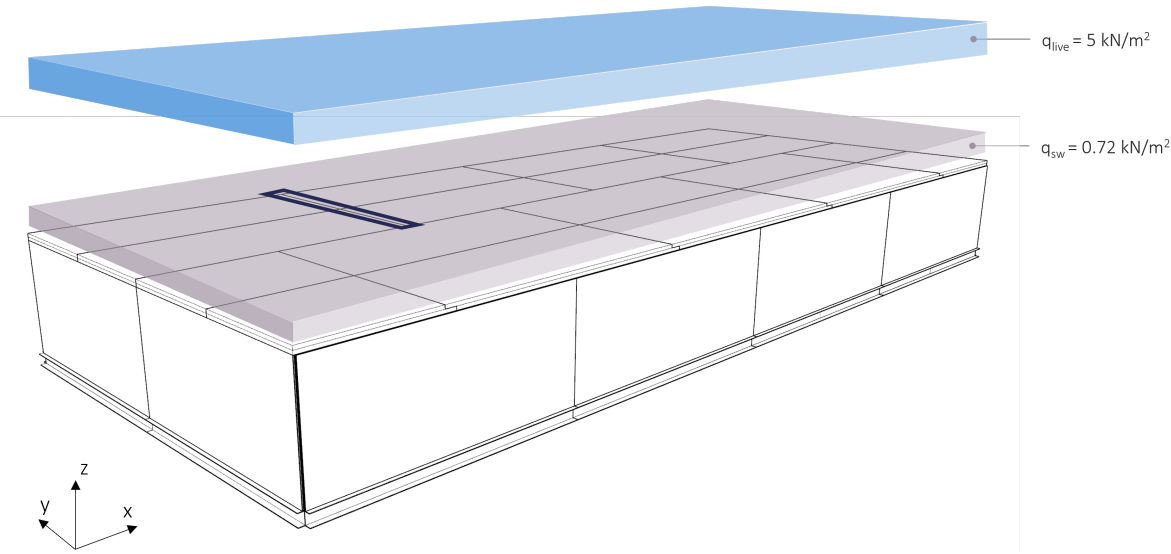
Figure D.6: Critical vertical loading in downward direction, with the governing load bearing element depicted. For the buckling check on this element, check section D.4.3 of this appendix.
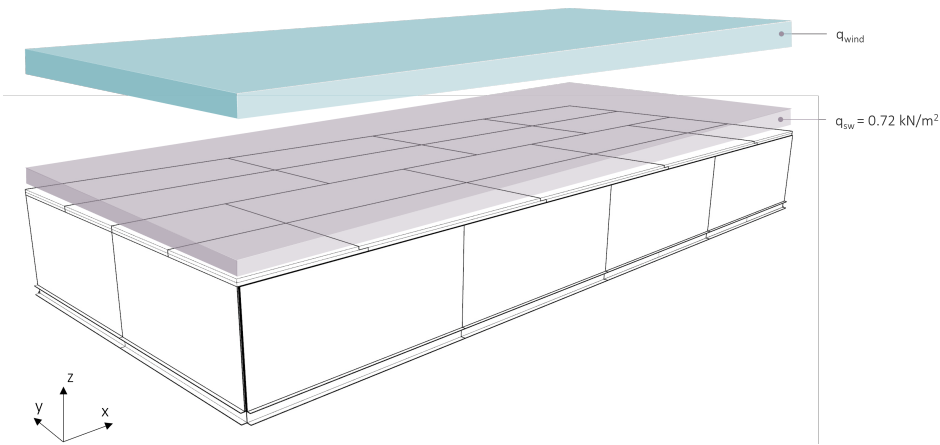
Figure D.7: Critical vertical loading in upward direction.

D.2. Horizontal load transfer

The horizontal force acting on the pavilion is the wind force. This load is determined in this section in the same way as the vertical wind force: by means of wind areas prescribed by the Eurocode. Having the critical horizontal load, the stress and deflection of the insulated glass units can be checked, as well as the design load for the connections.

Wind load

The wind on the pavilion has been simplified to two directions. When the wind comes from direction x, it falls on the short side of the pavilion. When the wind comes from direction y, it hits the long side of the pavilion.
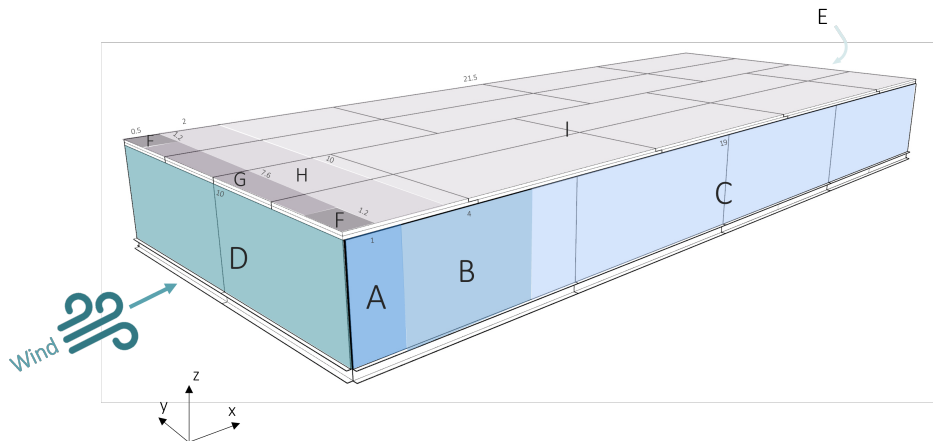
Figure D.8: Factor zones highlighted with wind from x-direction

Similar to the calculation of the vertical wind in the previous section, the wind force is divided into zones. These are also different for each side. Figure D.8 shows the wind zones on the pavilion in the case of an x-directed wind, Figure D.9 shows the wind zones in the case of a y-directed wind. Table D.2 shows the calculation values for wind loads in these two directions for the highlighted zones.
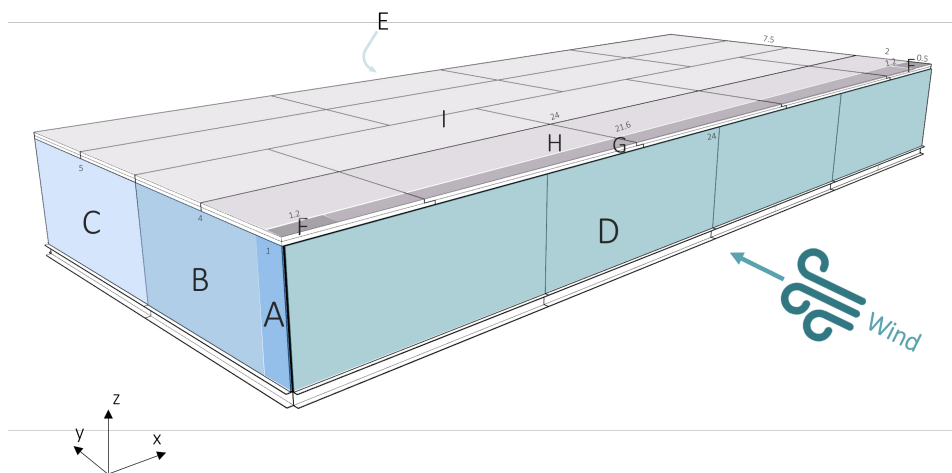
Figure D.9: Factor zones highlighted with wind from y-direction

Critical horizontal load

As the wind force is the only load in the horizontal direction, it is defining the normative horizontal load combination. Internal overpressure $(+0.2)$ and underpressure (-0.3) must be included in the calculation of the final design load. Overpressure is included in the case of normative wind suction on an IGU, underpressure in the case of normative wind pressure on a panel. This over- or underpressure is taken into account in equation D.6.

$$f_d = 1.5 * q_{\text{wind}} \qquad \text{(D.6)}$$

The force distribution of the IGU's is according to Figure D.10. As shown there, the load transfer of the panels on the short sides works slightly differently from that on the long sides.

The panels on the short side (see 'Elevation X' in the figure) are horizontally supported on three sides. At the top is the roof, at the bottom the basic structure. On one side of the panel is an IGU of the long side, which is able to absorb a part of the wind force, on the other side is the other 5 metres long panel. These are not structurally connected, so there will be no horizontal force transfer here either.

The panels on the long side ('Elevation Y1 / Y2' in Figure D.10) are supported horizontally on all four sides. At the upper edge of these panels, they are connected to the roof and at the bottom to the base, similar as the panels seen on 'Elevation X'. However, the six-metre-long panels from the long side are also supported horizontally on both left- and right-side by the adjacent panels, regardless of whether the adjacent IGU is parallel or perpendicular placed relative to it. In the case of a parallel placed IGU, the horizontal force is transferred to the side not by the neighbouring panel, but by an inner wall panel. This can be seen on the overall structural grid.
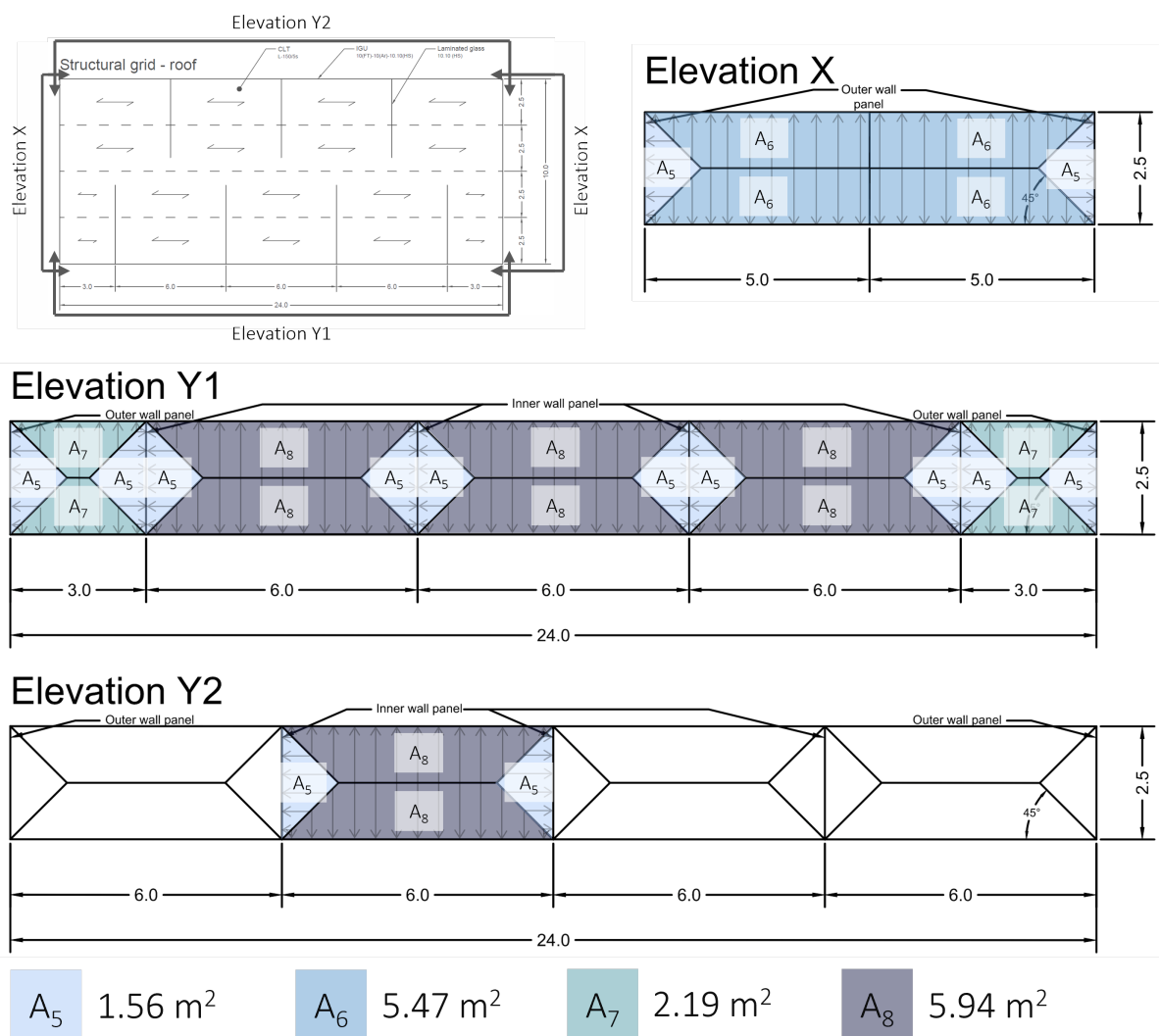
Figure D.10: Horizontal load transfer of the IGU panels. On the Y2 elevation, only one panel is highlighted, the other panels have an equal distribution.
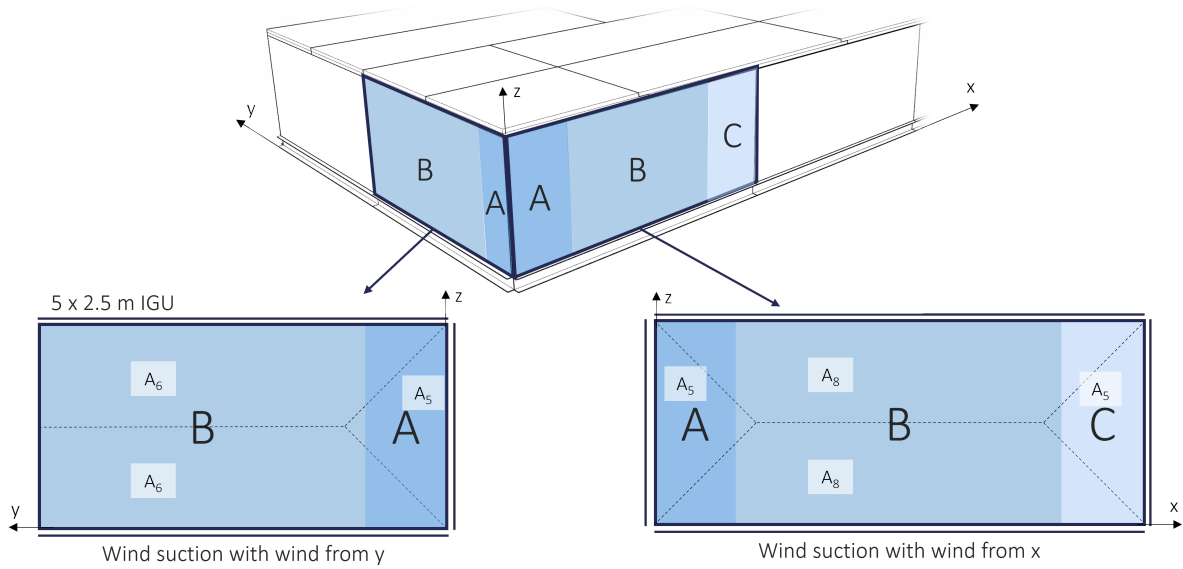
Figure D.11: Most critical panels caused by horizontal loading (wind)

D.3. Glass parameters

Calculation parameters of glass are calculated according to the method in NEN2608, using available Excel sheets from ABT bv. Here a clarification for the determination of the glass strength and the equivalent thickness. Isochoric pressure is not included, as all insulated glass units are larger than $1\ m^2$.

D.3.1. Glass strength

The glass strength is based on its tensile strength and calculated with Equation D.7. The parameters are explained in NEN2608. Starting points for the calculation are as follows:

- Float glass
- Heat-strengthened
- No free edges
- Zone: 1 (see Figure D.12)
- Glass is loaded in pane (see discussion for commentary)
- Load duration: $5\ sec$ (critical wind load)

The glass strength appears to be $36.7/mm^2$

$$f_{\text{mt;u;d}} = \frac{k_a * k_e * k_{\text{mod}} * k_{\text{sp}} * f_{\text{g;k}}}{\gamma_{\text{m;A}}} * \frac{k_e * k_z * (f_{\text{b;}} - k_{\text{sp}} * f_{\text{g;k}})}{\gamma_{\text{m;V}}} \tag{D.7}$$
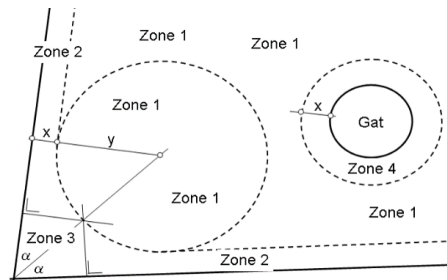
Figure D.12: Determination of glass zones according to NEN2608

D.3.2. Glass equivalent thickness

The equivalent thickness computation is based on available Excel sheets which is able to calculate the equivalent thickness for a double-layered laminated panel. It was decided to set the two pane thicknesses to be set at $9.7\ mm$ (the equivalent thickness of a $10\ mm$ sheet. This should give a reasonably reliable value for a triple-laminated panel of $20\ mm$ thickness. The parameters of the equivalent thickness calculations (Equation D.8 and D.9) are explained in NEN2608. Starting points for the determination of the equivalent thickness are:

- Plate width: $6000\ mm$, $5000\ mm$ and $4250\ mm$ (give the same result)
- Plate height: $2500\ mm$
- Thickness plate 1: $9.7\ mm$
- Thickness plate 2: $9.7\ mm$
- Temperature: $17\,^\circ C$
- Interlayer thickness: $1.52\ mm$
- Length edge: $6000\ mm$
- Load duration: $5\ sec$ (critical wind load)

The equivalent thickness for ULS calculations appears to be $19.3\ mm$ and for SLS $19.2\ mm$.

$$t_{\text{gg;u}} = MIN(\sqrt{\frac{(1 - \omega_\sigma) * \sum_{j=1}^{n}(t_{pl;j}^3) + \omega_\sigma * (\sum_{j=1}^{n}(t_{pl;j}))^3}{t_{pl;i} + 2 * \omega_\sigma * t_{m;i}}}) \tag{D.8}$$

$$t_{\text{gg;ser}} = \sqrt[3]{(1 - \omega_w) * \sum_{i=1}^{n}(t_{pl;i}^3) + \omega_w * (\sum_{i=1}^{n}(t_{pl;i}))^3} \tag{D.9}$$

D.4. Building element verification

This chapter shows the verification of the building elements by the following structure:

- Performed checks
- Checks

D.4.1. Roof
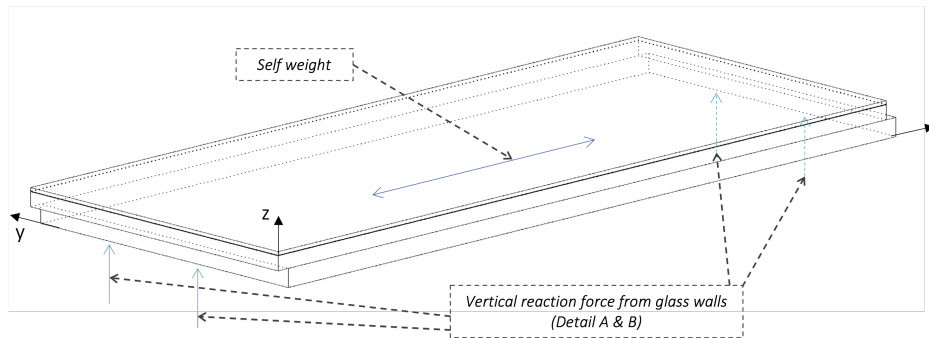
Roof slab – vertical load transfer

Figure D.13: Vertical load transfer in a roof slab
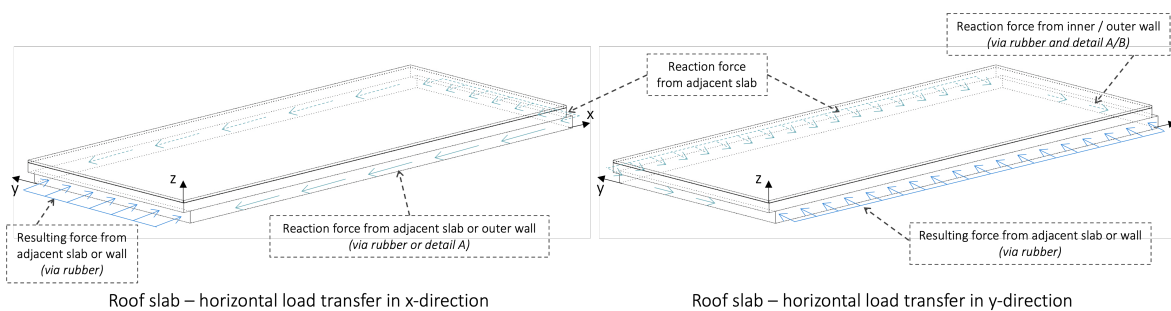
Roof slab – horizontal load transfer in x-direction   Roof slab – horizontal load transfer in y-direction

Figure D.14: Horizontal load transfer in a roof slab in x- and in y-direction

Performed checks

Owing to the fact that the CLT slab is chosen from a renowned CLT manufacturer (DERIX) product table, no global checks are performed for strength and stiffness.

On local level, a check is performed on the strength perpendicular to the grain at the location of the supports (Details A and B).

Stress perpendicular to the grain

The stress perpendicular to the grain is calculated according to Eurocode 5 (NEN-EN 1995-1-1, art.6.1.5). The starting points are as follows:

- Climate class 1
- Load duration: short (live load by maintenance work)
- Wood type: C24 (standard for CLT)
- Modification factor: $k_{mod} = 0.90$
- Material factor: $\gamma_M = 1.30$
- Compression strength perpendicular to grain: $f_{c;90;k} = 2.50 \ N/mm^2$
- Support width: $b = 20 \ mm$ (Connection types A and B)
- Support length: $l = 65 \ mm$
- C.t.c distance: $800 \ mm$ (shortest center-to-center distance)
- Design load: $8.46 \ kN$ (connection A), $16.92 \ kN$ (connection B)

The maximum compressive stress perpendicular to the grain at the support appears to be $3.38/mm^2$ for connection type A and $6.76\ N/mm^2$ for connection type B. As shown in the unity checks (Equation D.10 and D.11), both roof connections (CLT to glass) is not designed according to the norms. Redesign recommendations are given in Part IV.

$$A : u.c. = \frac{\sigma_{c;90;d}}{k_{c;90} * f_{c;90;d}} = \frac{3.38}{1.5 * 1.73} = 1.30 \tag{D.10}$$

$$B : u.c. = \frac{\sigma_{c;90;d}}{k_{c;90} * f_{c;90;d}} = \frac{6.76}{1.5 * 1.73} = 2.61 \tag{D.11}$$

D.4.2. Outer wall
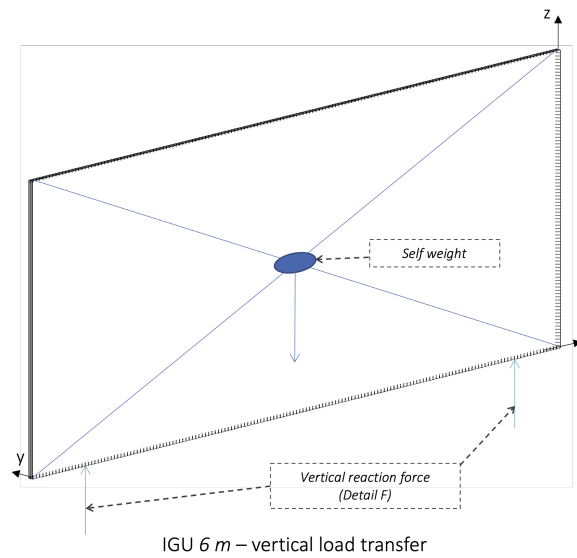
Figure D.15: Vertical load transfer in an IGU on the long side
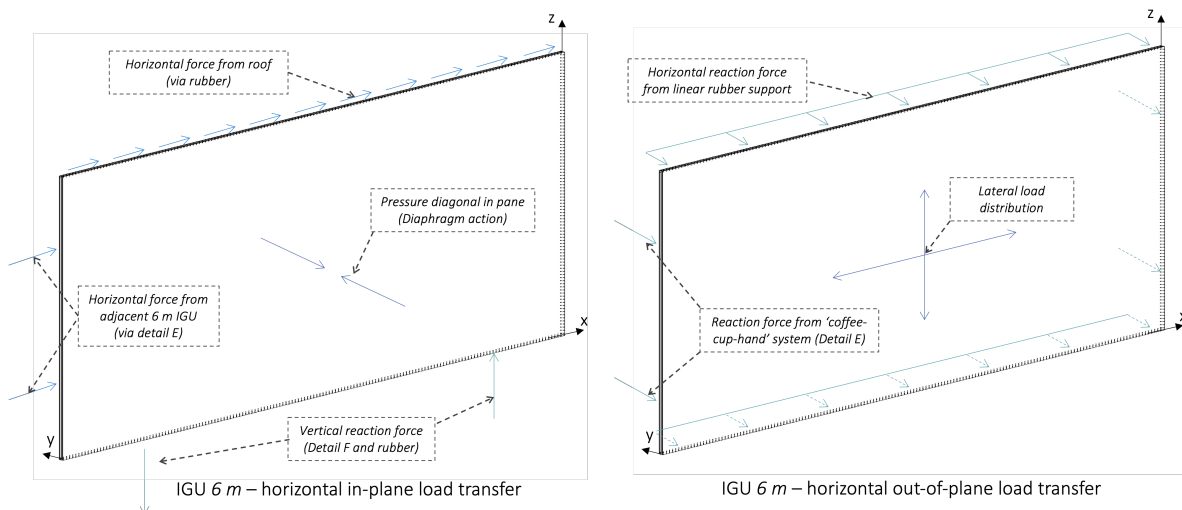
Figure D.16: Horizontal load transfer in an IGU on the long side

Performed checks

Tensile stresses in the glass, out-of-pane deflection are checked with finite element software in Chapter 9 of Part III. Two critical IGU's are checked: one $5\,m$ in length and one $6\,m$ in length with wind suction acting on the panel.

Checks

As described in the detailed analysis chapter of the main report, the results are shown in Table D.4.
Unity checks result in 0.50 for the deflection (SLS, $5\,m$ IGU) and 0.69 for the tensile stress (ULS, $6\,m$ IGU).

IGU $5\,m$ − vertical load transfer
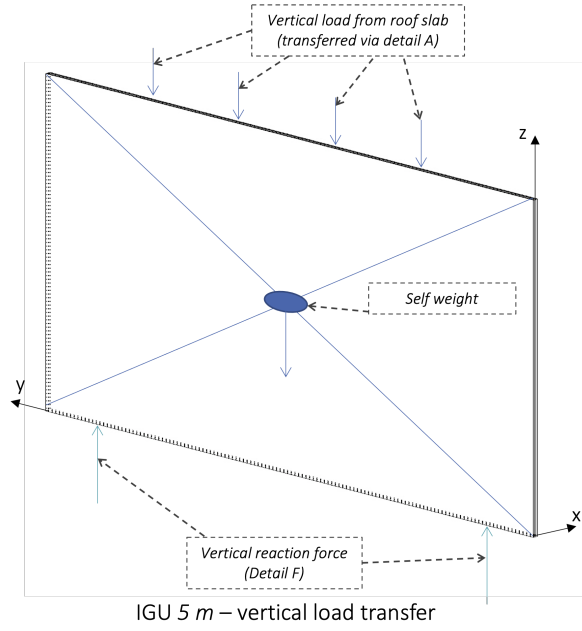
Figure D.17: Vertical load transfer in an IGU on the short side

Symbol	$5\,m$ **IGU**	$6\,m$ **IGU**	Unit
w_{max}	12.50	14.28	mm
$\sigma_{t_p;\,max}$	25.24	14.16	N/mm^2

Table D.4: Results of the IGU finite element modelling (Part III, Chapter 9)

D.4.3. Inner wall

Performed checks

Since the largest downward force in the pavilion is acting on inner walls, these are checked for buckling.

Bucking check

The most critical inner wall panel is checked on possible buckling. Check Figure D.20 for the buckling mechanism in this element.

Parameter	Value	Explanation
E	$70000\ N/mm^2$	Young's modulus glass
I	$3696.82\ mm^3$	$I_{tot} = 8/12 * t_{pl}{}^3$
n	1	Buckling mode, check figure
t_{pl}	$17.7\ mm$	ULS equivalent thickness glass
Design period	1 month	1-3 months as travelling pavilion
f_{roof}	$13.52\ N/mm^1$	Per unit length
$q_{sw;roof}$	$0.72\ kN/m^2$	Self weight Derix L-160/5s
q_{live}	$1\ kN/m^2$	Live load on roof

Table D.5: Parameters for the buckling check

$$F_{cr} = \frac{\pi^2 EI}{(nL)^2} = \frac{\pi^2 * 70000 * 3697}{(1 * 2500)^2} = 408.65\ N/mm^1 \tag{D.12}$$

The unity check for buckling results in 0.03, see Equation D.13.

$$u.c. = \frac{f_{roof}}{F_{cr}} = \frac{13.54}{408.65} = 0.03 \tag{D.13}$$
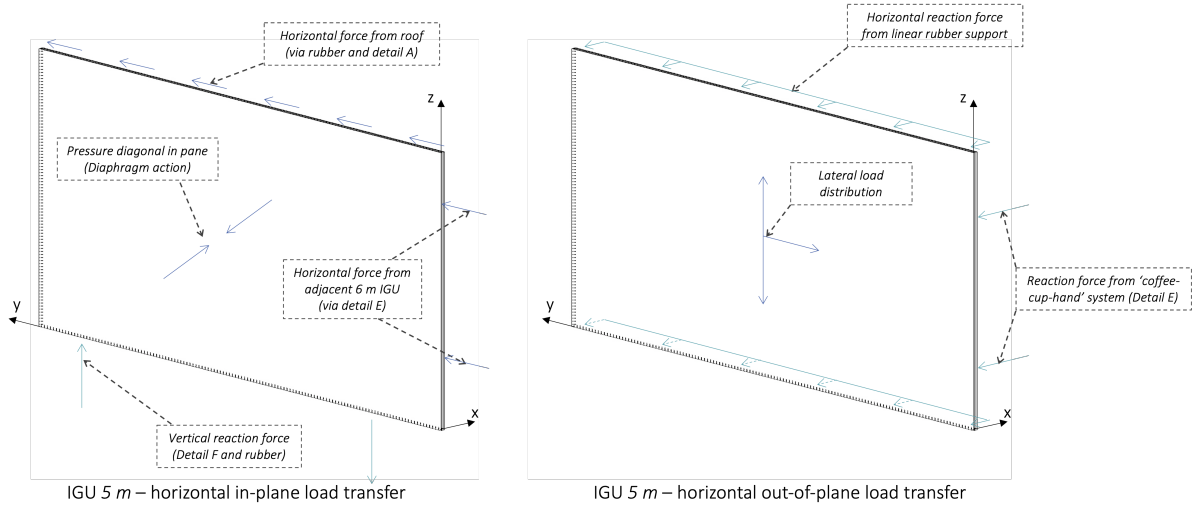
Figure D.18: Horizontal load transfer in an IGU on the short side

D.4.4. Floor

Performed checks
Likewise the roof slab, no global strength and stiffness checks are performed because the CLT slab is chosen from a renowned CLT manufacturer (DERIX) product table.

D.4.5. Base

Performed checks
The glass walls are placed into the base elements, without fastening. Calculations should prove that the glass walls stay in place during uplift wind forces on the roof.

Uplift of walls
The check assumes that the most critical roof slab for uplift wind is . Shown in Figure XX, the most critical panal is a $6x2.5\ m$ slab in the corner of the pavilion on which wind zone F is applied.

Combination	Permanent factor	Variable factor
ULS-2	0.90	1.50

Table D.6: Load combination for uplift wind check

The check is performed with the load factors from ULS-2 (see Table D.6). Pre-calculated and given values are:

- Self-weight roof: $q_{g;DERIX\_160} = 0.72\ kN/m^2$
- Area roof slab: $A_{roof} = 15\ m^2$
- Internal overpressure: $q_{int\_overpressure} = 0.2\ kN/m^2$
- Critical uplift force (design value) $F_{d;wind} = 4.67\ kN$
- Self-weight glass: $\rho_{glass} = 25\ kN/m^3$
- Glass area (short IGU) = $A_{glass} = 12.5\ m^2$

$$F_{d;uplift\_wind} = 1.5 * (0.5 * A_{roof} * q_{int\_overpressure}) + F_{d;wind} = 6.92\ kN \tag{D.14}$$

$$F_{d;sw\_roof+glass} = 0.9 * (0.5 * A_{roof} * q_{g;DERIX\_160} + \rho_{glass} * (0.5 * A_{glass}) * t = 9.08\ kN \tag{D.15}$$

$$u.c. = \frac{F_{d;uplift\_wind}}{F_{d;sw\_roof+glass}} = \frac{6.92}{9.08} = 0.76 \tag{D.16}$$

Innerwall – vertical load transfer

Innerwall – horizontal load transfer
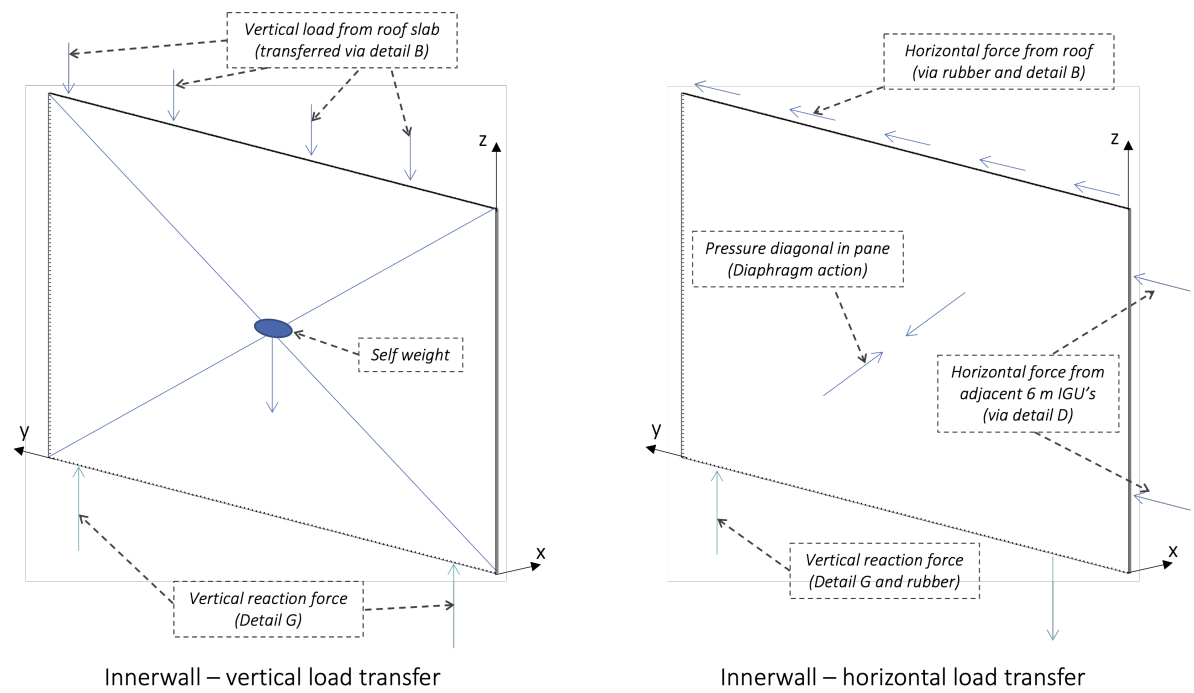
Figure D.19: Vertical and horizontal load transfer in an inner wall

Innerwall – vertical load transfer
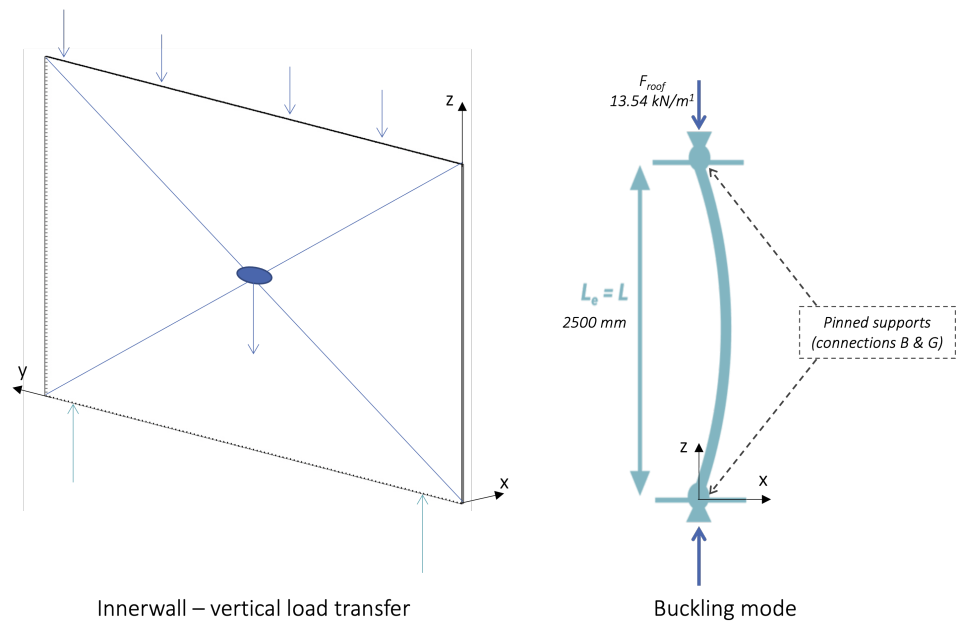
Buckling mode

Figure D.20: Forces on the inner wall panel and the buckling mode
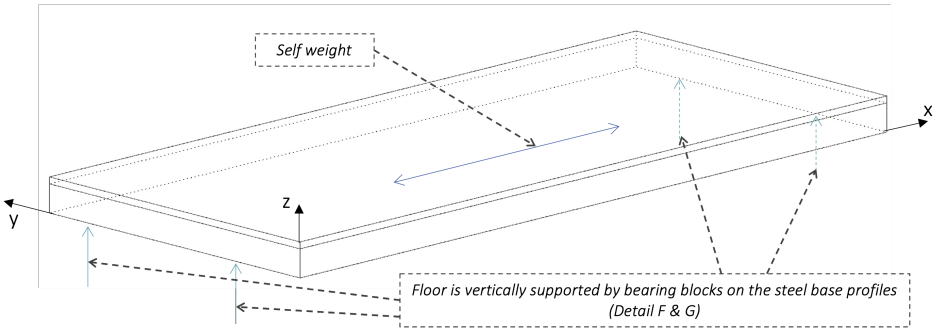
Floor slab – vertical load transfer

Figure D.21: Vertical load transfer in a floor slab
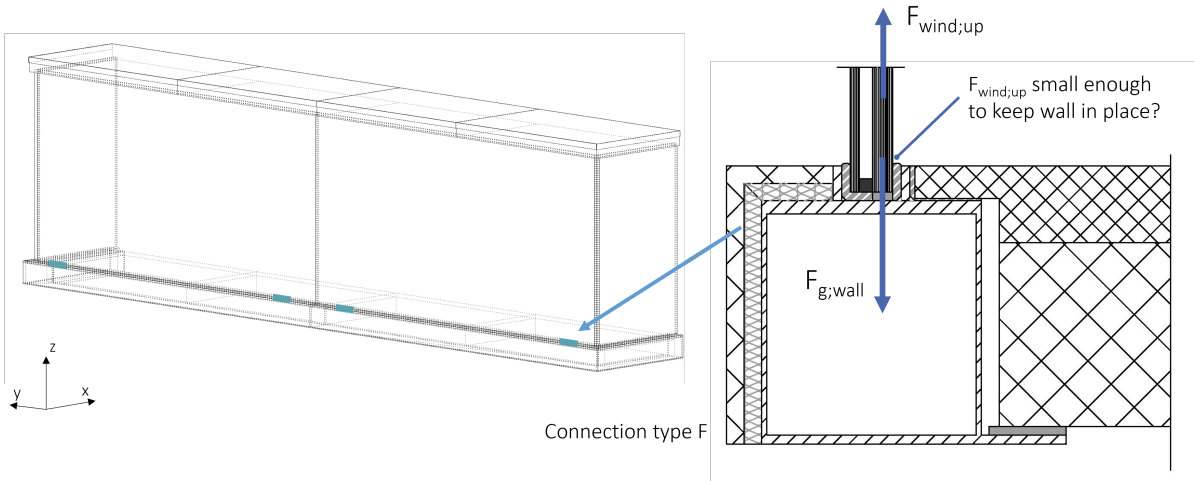
Figure D.22: Uplift wind forces at detail F
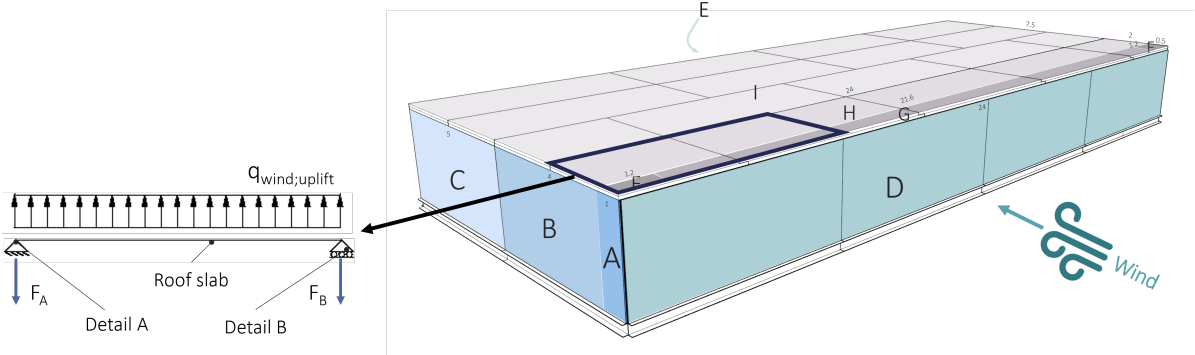
Figure D.23: Uplift wind transfer: from roof to detail A to detail F

D.5. Dimensioning of the 'coffee-cup-hand' system

The following procedure is performed to dimension the laminated titanium element and the glass pane thicknesses:

1. Starting point for the dimensioning is based on previous experiments and research of Santarsiero [49] on embedded elements in laminated glass, The conclusion there was that embedded elements seem an efficient means for load transfer. The elements Santarsiero used were $30\ mm$ embedded in the glass. This value is started with in the dimensioning of the 'coffee-cup-hand' system: depth 'd_e' in Figure D.24.
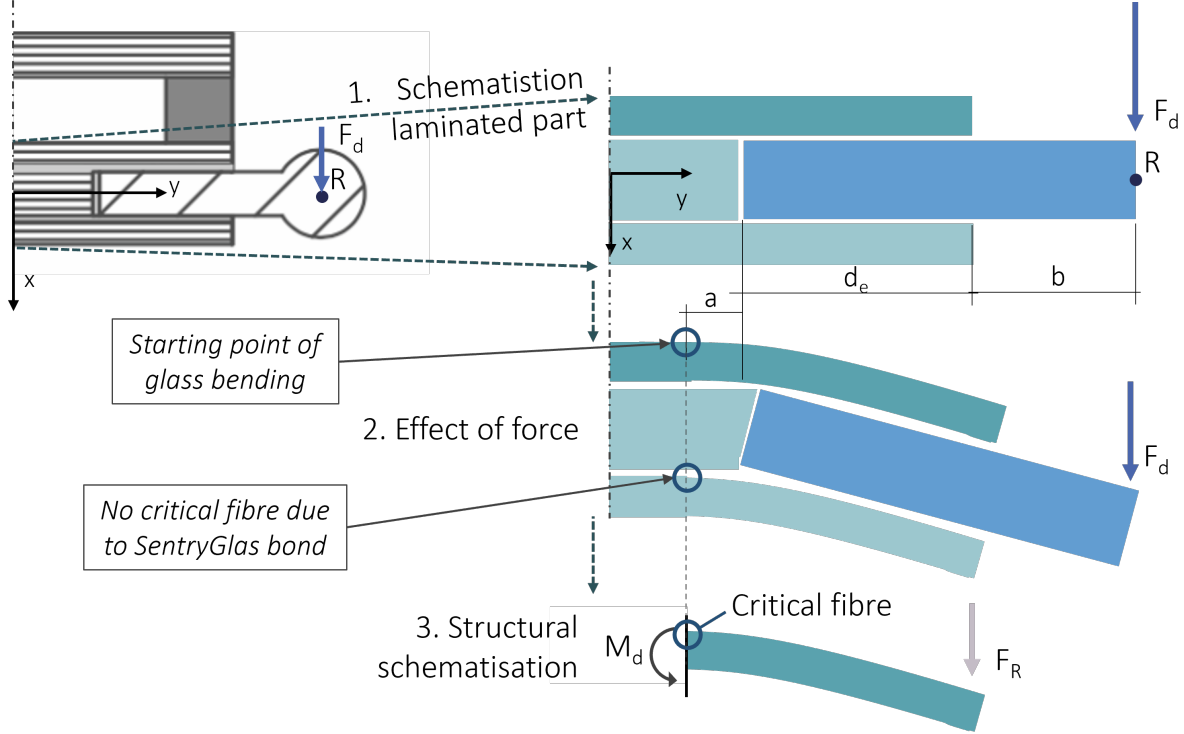
Figure D.24: Procedure for the determination of stresses in the glass for the dimensioning of the 'coffee-cup-hand' details

2. The IGU with the embedded titanium is schematised into a 2D composition, in which the insulating panel (and also the spacer) are left out, see Figure D.24.

3. The design force is $4.73\ kN$, acting as a support reaction from an inner wall to the critical IGU of $6\ m$ subjected to wind loading. Wind loading calculations can be found in this appendix. The load is put on the rotational center of the 'coffee-cup-hand' elements. This rotational centre is positioned at a distance 'b' away from the edge of the laminated glass (Figure D.24).

4. An analysis is made of what happens in the glass when the force of $4.73\ kN$ is applied at point 'R'. From this an assumption was made for the place from where the glass starts bending; at a distance 'a' parallel to the beginning of the titanium element. In the following steps, the distance 'a' is assumed to be two options: '$a = 5\ mm$' and '$a = 10\ mm$'.

5. Schematising the situation in a structural diagram for the critical glass pane is done by a cantilevering beam (Figure D.24). The position of the critical fibre can be depicted. The beam has a length of distance 'a' plus distance 'd_e' plus distance 'b'.

6. The maximum tensile stress occurring in the glass panel is in the top fibre at the position of the moment resisting joint. This stress is calculated by Equation D.17. The design moment is calculated by multiplying the design force by the distance, divided by the height of the laminated titanium element. The calculation for the section modulus 'W' includes the parameters 'b' (width) and 'h' (height). For the situation of this calculation, the width is the height of the laminated titanium element (h_e), the height is regarded as the equivalent glass thickness of the outer pane '$t_{eq;1}$'. Both values are variables.

$$\sigma_{t;d} = \frac{M_d}{W} = \frac{(F_d * (a + d_e + b))/h_e}{(1/6) * h_e * t_{eq;1}^2} \tag{D.17}$$

7. With set values, the maximum tensile stress in the glass can be calculated. The unity check, subsequently, shows if the stress in the glass is smaller or higher than the glass strength '$f'_{tm;u;d}$ of $36.7\ N/mm^2$. However, an optimisation

study is performed by software AutoStudy to find the perfect parameters for the dimensioning of the laminated titanium element and the thicknesses of the glass panes. The goal of the AutoStudy is to get the unity check value closest to 0.99.

8. Input of the AutoStudy optimisation are as following:

   - **Outer pane thickness**: $t_{t_p;\,1.3} = 3, 4, 5, 6$ or $8\,mm$. The numerical computer model incorporates the corresponding equivalent glass thicknesses.
   - **Inner pane thickness** $t_{t_p;\,1.3} = 6, 8, 10, 12$ or $15\,mm$. Also here, the numerical computer model incorporates the corresponding equivalent glass thicknesses.
   - **Height element** $30 \leq h_e \leq 100\,mm$, with steps of $5\,mm$.
   - Distance $'a'$ is either 5 or $10\,mm$, as described in step 4.
   - Distance $'b'$ is $20, 25$ or $30\,mm$.
   - Amount of elements n_e in between the IGU's is any number between 2 and 6.

9. Afterwards, the AutoStudy analysis is started, resulting in a matrix with 1700 different possibilities. The dimensions most optimum variant are showcased in Table D.7.

Description	Symbol	Value		Unit
Outer pane thickness	$t_{t_p;\,1.3}$	5		mm
Inner pane thickness	$t_{t_p;\,1.3}$	10		mm
Depth element	d_e	30		mm
Height element	h_e	45		mm
Distance a	a	10		mm
Distance b	b	20		mm
Amount of elements	n_e	2		-
Unity check	u.c.	0.24	0.99	-
Wind direction on glass pane	*push*	*suc*		

Table D.7: Final dimensions of the laminated part of the 'coffee-cup-hand' system. Visualisation in Figure B.7, Appendix B.

Results

ID	UNITY CHECK CONSTRAINT	OUTER PANE THICKNESS	INNER PANE THICKNESS	HIGHT ELEMENT	DISTANCE A	DISTANCE B	AMOUNT OF ELEMENTS	UNITY CHECK	SCORE
G20C9	0.99	5.00	10.00	45.00	10.00	20.00	2.00	● 0.99	● 0.87
G83C14	0.99	5.00	15.00	45.00	10.00	20.00	2.00	● 0.99	● 0.87
G93C15	0.98	5.00	8.00	40.00	10.00	30.00	3.00	● 0.98	● 0.88

Figure D.25: Autostudy results for the dimensioning of detail D. Parameters from left to right: *Unity check constraint; Outer pane thickness; Inner pane thickness; Height element; Distance A; Distance B; Amount of elements; Unity check; Score.*

D.6. Check friction performance rubber

The calculations in this section were performed for a connection that was never used in the final design. However, these calculations give an idea about the friction potential of the rubbers of the final roof and base connections.
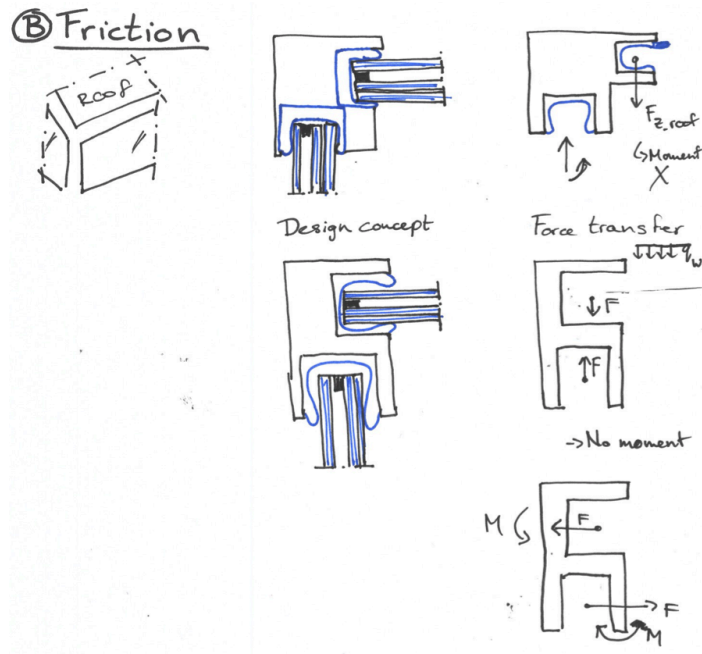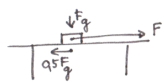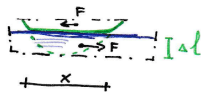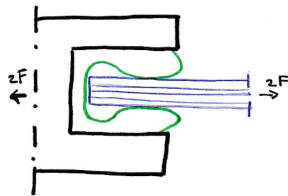
Wind vb.

What is the uplift force? Flat roof Closed building

Eg.: $A \approx 200 \ m^2$ Urban

$b = 10$ $l = 20$ $h = 3$ Sharp eaves

Self weight roof neglected
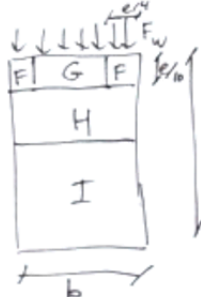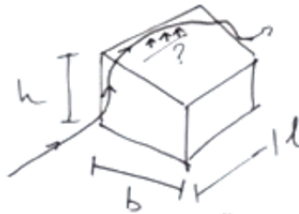
Local // Zone F

$e = b \leq 2h = 6 \ m$

$d = l \ \frac{e}{2}$

$A_{F} = \frac{e}{4} \cdot \frac{e}{10} = \frac{36}{40} = \frac{9}{10} \ m^2 = A_{ref}$

$C_{f_{F}} = -1,8$; $q_p (3) \overset{AMS}{=} 0,77 \ kN/m^2$

$F_{w_{F}} = -1,8 \cdot 0,77 \cdot \frac{9}{10} = 1,2474 \approx 1,25 \ kN = F_{d}$

$s = \frac{e}{4} + \frac{e}{10} = \frac{84}{40} = 2,1 \ m$

Calculation rubber: $f_R = 1 N/mm^2/rub. \Rightarrow 2 N/mm^2$

$2 \cdot 2,1m = 4 \ 200 \ N = 4,2 \ kN \gg 1,25 \ kN$ uplift
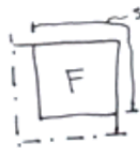
Global // Complete roof (without internal walls)

$\boxed{F}$: $F_d = 1,25 \ kN$

$\boxed{G}$: $A_{ref} = (10 - 2 \cdot \frac{e}{4}) \cdot \frac{e}{10} = \frac{42}{10} = 4,2 m^2$

$C_{f_{G}} = -1,2$

$F_{w_{G}} = -1,2 \cdot 0,77 \cdot 4,2 = 3,88 \ kN$

$\boxed{H}$ $A_{ref} = (\frac{e}{2} - \frac{e}{10}) \cdot b = (3 - 0,6) \cdot 10 = 24 m^2$

$C_{f_{H}} = -0,7$

$F_{w_{H}} = -0,7 \cdot 0,77 \cdot 24 = 12,94 \ kN$

$\boxed{I}$ $A_{ref} = (d (=l) - \frac{e}{2}) \cdot b = (20 - 3) \cdot 10 = 170 m^2$

$C_f = \pm 0,2 = -0,2$

$F_w = -0,2 \cdot 0,77 \cdot 170 = 26,18 \ kN$

$\Sigma F_w = -44,25 \ kN$

Check: Perimeter $= 2 \cdot b + 2 \cdot l = 60m$

$f_d = 60 \cdot 2 N/mm^2 = 120 \ kN \gg 44,25$ ✓

E

Connection methods study

This entire Appendix is outdated, but it contains a worthy prestudy for the design of the connections of 8.

The three types of connections are inspired by connection typologies and described below with the descriptions according to Google's dictionary.

| A. | B. | C. |
| Interlocking | Friction | Embedded |

Figure E.1: Three variants of connection typology

- **Interlocking** - *'(of two or more things) having parts that overlap or fit together.'*
- **Friction** - *'the resistance that one surface or object encounters when moving over another.'*
- **Friction** - *'(of an object) fixed firmly and deeply in a surrounding mass; implanted.'*

Above mentioned variants will be explored in this chapter, after which a choice on one of the types will be made and further details will be provided. There are two main questions arising in the design of all three coupler variants, namely:

- How is taken care of the tolerances and deflections?
- What material is the coupler made out of?

These questions will be answered in the detailed design of the chosen variant.

E.1. Type A: Interlocking

The connection system is inspired by the intra-modular connection showed earlier in the literature review, and here in Figure E.2. The primary difference is that, as indicated in the figure, connection types A and B are screwed to the module. A severe requirement in this glass project is that the connections do not penetrate the glass, therefore the designs of the coupler and glass composition for type *A* diverge from the steel design.
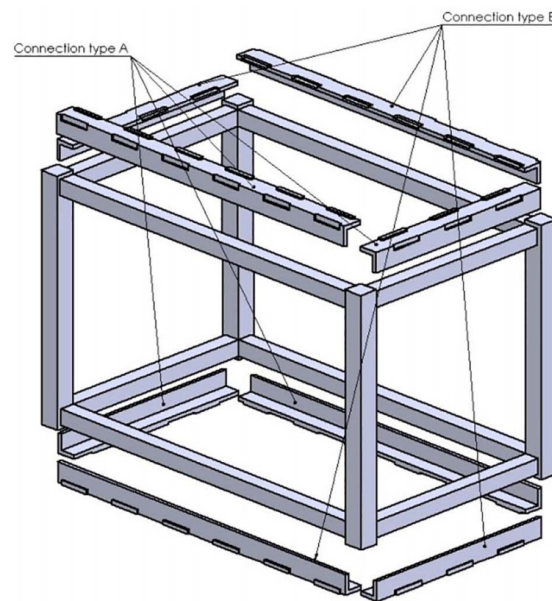
Figure E.2: Example of an intra-modular interlocking connection in steel [74]

The connection system variant is based on an interlocking mechanism. The two parts may be slid together like jigsaw pieces by creating notches in the glass panel and having these notches 'in negative' in the coupling piece. These cuts provide the components with a desirable contact surface for transferring forces. As can be seen from the drawings, bolts are needed to assemble coupling piece variant A together with the building elements. The bolts solely penetrate the coupler (and roof), and not the glass.
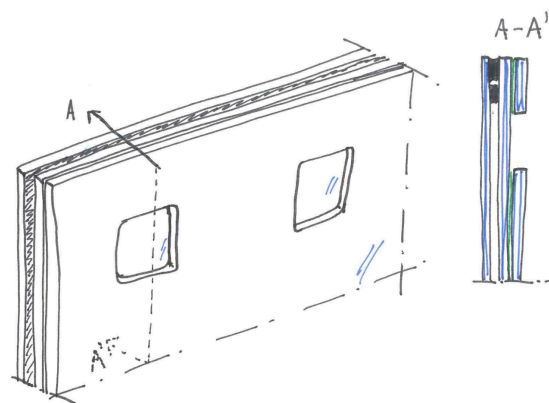
Figure E.3: Section of the glass panel with the interlocking design principle; here variant A.1 *(- CAD-drawings to come)*

Two shape typologies are distinguished in the interlocking solution for the coupling system, A.1 and A.2, only differing in shape of the interlocking mechanism.

A.1

Version A.1 is based on a hole that does not reach all the way to the edge of the IGU; nonetheless, the holes act as 'islands' on the IGU and coupling system. The vertical upward force generated by the wind can likewise be transmitted to the panel in

this way. The force is transferred and each direction is determined by the glass contact surface on the coupling system. For a visual elaboration, see Figure E.4 and E.6.
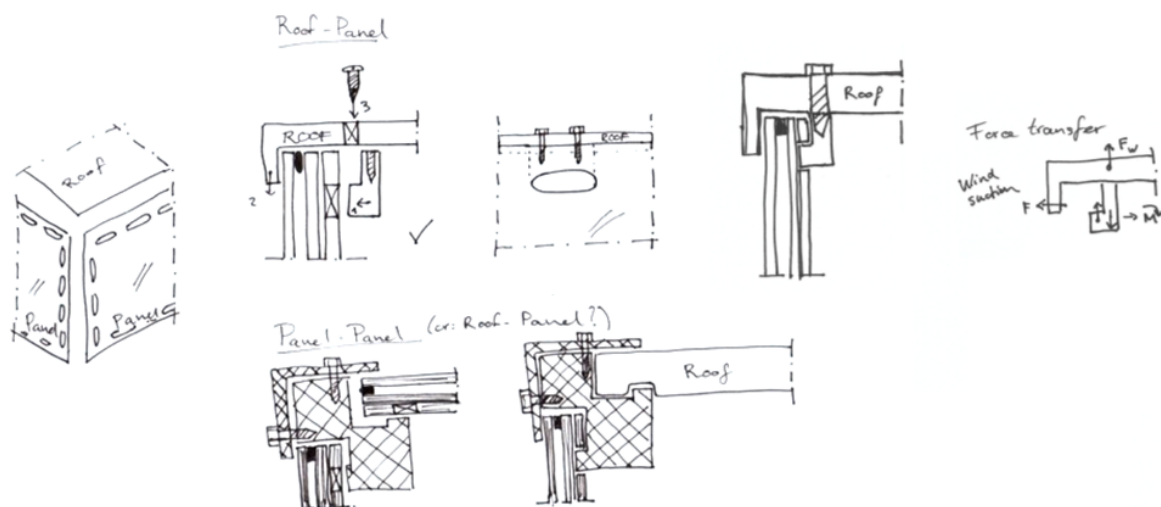
Figure E.4: Connection type A.1: Interlocking 1 with different shapes of the coupler *(- CAD-drawings to come)*

A.2

The second option for variant 1 is similar to A.1, but differs in shape. The interconnecting patterns in A.2 are no longer islands on the IGU, but instead reach all the way to the edge. A contact surface is formed by making the shape wider on the outside than on the edge, allowing the upward vertical forces to be transmitted as well. Sharp edges must be avoided in order to avoid high peak stresses and excessive manufacturing accuracy. For example, in Figure E.5, the form at the bottom would be preferable to the one at the upper left.
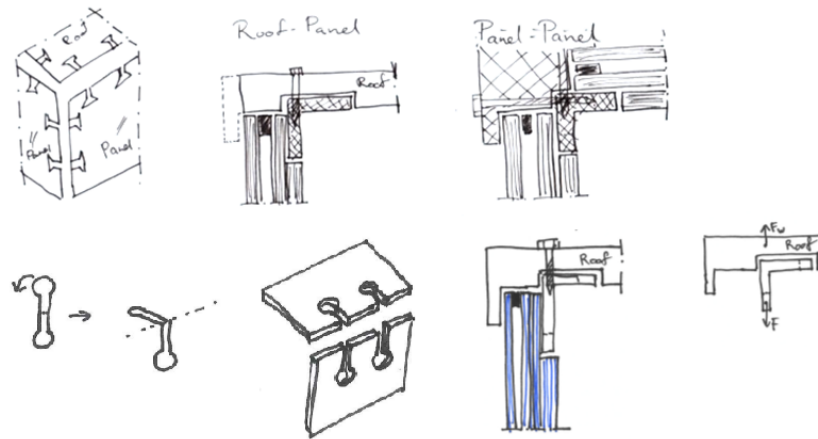
Figure E.5: Connection type A.2: Interlocking 2 *(- CAD-drawings to come)*

E.1.1. Chosen option for variant A

The shape of the interlocking element is the only change between the two version A choices. The A.1 system features a basic interlocking element, but the A.2 system has a somewhat more complex shape. Option A.1 is picked based on this assertion, as the production process will be easier. Furthermore, with this option, a larger contact area for the vertical upward wind force may be accomplished, resulting in increased resilience. This option is shown in Figure E.6
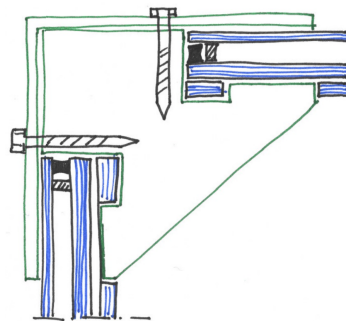
Figure E.6: Connection type A.1: final shape *(- CAD-drawings to come)*

E.1.2. Points of attention for variant A

The design of version A offers several challenges. To begin, it is important to consider how the force distribution in the coupling component is ensured. It will also be required to determine the size of the contact area between the outer L-shaped portion and the exterior of the IGU. On the interior, the size of the cutouts will have to be calculated in order to effectively transfer horizontal and vertical stresses. It is vital to double-check if the outer panel of the laminated side of the IGU is just 10 mm thick. Finally, the distance between two panels that are at perpendicularly to one other should be found out regarding the strength and stiffness of the coupling element.

One could argue that the production of the IGU could be problematic. However, a very clear production sequence is shown in Figure E.7. To make the IGU, three glass panels of the same size are necessary. Secondly, the cutouts in one of the panels is made by water-jet cutting. Later, that particular panel is being laminated on another pane, by applying a SentryGlass interlayer with the same cutouts. The spacers are applied and, lastly the outer panel is applied onto the laminated glass composition.

SentryGlass interlayers with cutouts have already shown to function in, for example (Figure E.8), glass stair stringers. Here, on the outer laminated glass panel, a titanium . Of course also the laminated connections from Eckersley O'Callaghan at the 2011 Apple Cube in New-York have shown to be functioning properly.
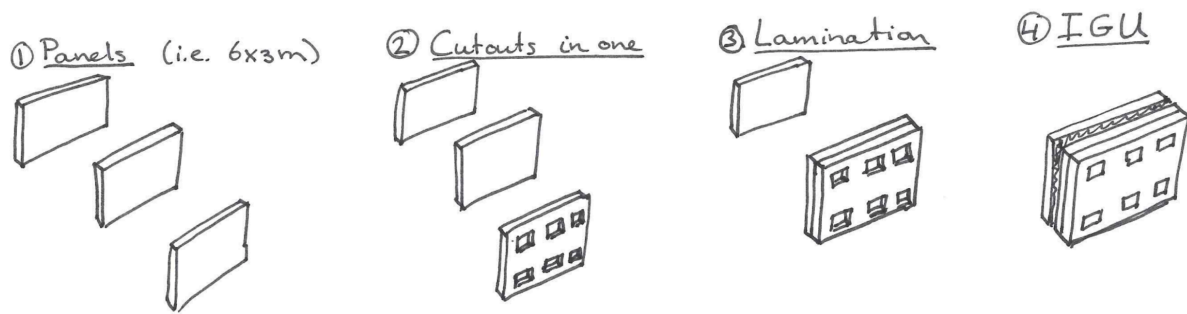
Figure E.7: Production sequence of variant A (here: A.1)

Figure E.8: Cutouts in laminated glass [86]

E.2. Type B: Friction

The forces are transferred from the roof to the side panels via friction in the second variant. This may be accomplished in a variety of ways, which is why this variation allows for another variety of possibilities (see Figure E.9).

To secure the connection, B.1 employs a unique click method. Due to the (limited) contact surface in the hooks, it could endure the upward wind force. The hook's composition (shown in green in Figure E.9) is yet unknown, but it will need to be a somewhat flexible material in order to be pushed in and out of each other.

Option B.2 is generated by fritting a part of the glass surface and producing a similar roughness in the connecting piece. The roughness generates a certain amount of friction, which allows the IGU to sit properly in the coupler. This alternative has the potential to be degraded after frequent disassembly, making it less dependable as a structural link.

The last alternative for Variant B is a rubber in the coupling piece, seen in Figure E.9 as the green component at B.3. The rubber compresses and produces resistance when the IGU is inserted into the coupling piece. This sort of connection, like B.2, might be damaged if it is often moved in and out of the hall.

E.2.1. Chosen option for variant B

In the case of options B.1 and B.2, horizontal force transfer is challenging, as indicated in Section 7.1. Although these connections are theoretically adequate for transmitting vertical upward force, they will exhibit their inadequacies in the longitudinal direction. Option B.3 would perform better in the event of longitudinal shear pressures due to the rubber's clamping ability. The amount of force that the rubber could transfer with a theoretical compression of 1 mm is indicated in Appendix B Section D.6.

E.2.2. Points of attention for variant B

Variation B, like variant A, has its own set of challenges. The rubber used in the coupling system must be handled with care. The building system's longevity is a wish, with a minimum life span of 50 years. Because of its long lifespan and ability to be disassembled, the rubber will eventually wear out and need to be replaced. Furthermore, it must be investigated further to see if this connection is capable of correctly transferring forces. It is assumed in Appendix D.6 that the rubber fits precisely everywhere and that the force is evenly distributed over the joint's length.
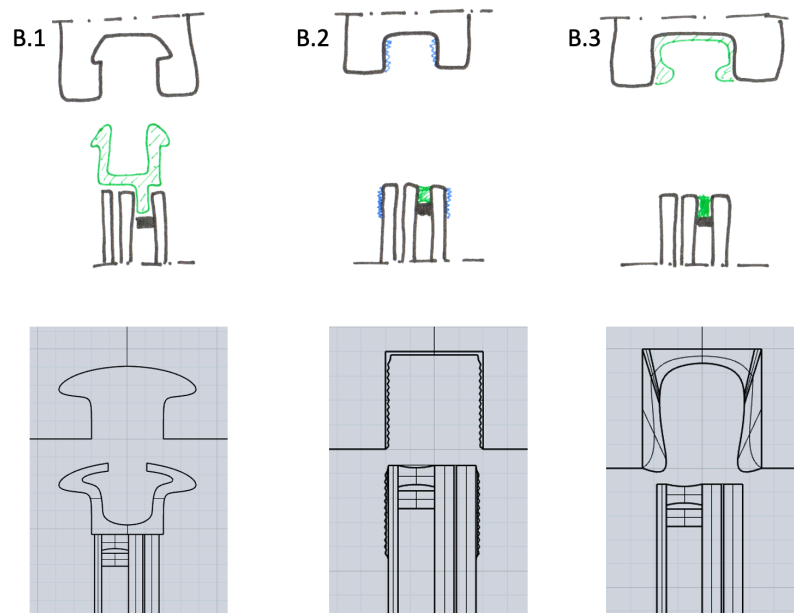
Figure E.9: Options for type B

E.3. Type C: Embedded

The coupling system's third and final design combines Eckersley O'Callaghan's laminated titanium connectors with the preexisting toggle concept in an IGU. An element will be placed in the spacer at various locations across the IGU and protrude on the sides with a ring. The upper ring is x distance from the top of the panel on one side, while the lower ring is x distance from the bottom on the other. A long slat may be placed from the top and the panels are now constructively connected by positioning two panels next to each other and having the rings above each other.
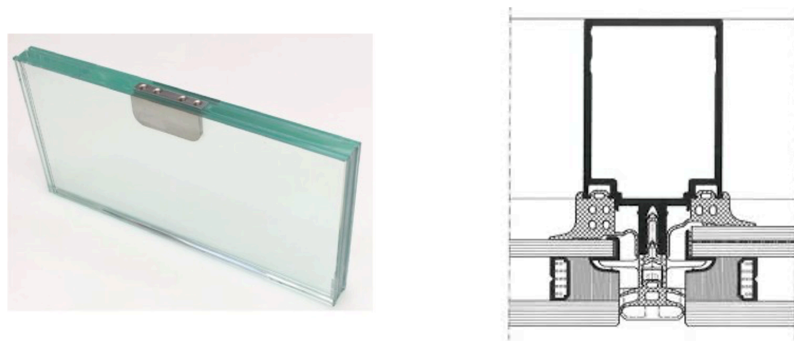
Figure E.10: Inspiration for variant C. Left: Laminated titanium connections *[EOC]*, right: Toggle-principle in an IGU

A structural silicone seal is frequently utilized to seal the joint in current solutions based on a similar idea. This is less ideal in the context of this study since it reduces the dismountability of the finished structure. As a result, if version C is chosen, the coupler will ensure that the connection is demountable and weatherproof. This is accomplished by placing two components on both sides of the link. These two components use the same ring topology as the IGU's integrated connection. The bar will then connect the IGUs to the connection in this manner. See Figure E.10 for an example.

E.3.1. Points of attention for variant C

The last variation demonstrates the challenge of assembling the system with high accuracy. F. Oikonomopoulou's design proved to have highly tight manufacturing requirements and a difficult assembly process, as stated in the reference projects (Section XX). Since variant C is similar to Oikonomopoulou's male-female model, similar problems are expected to occur.
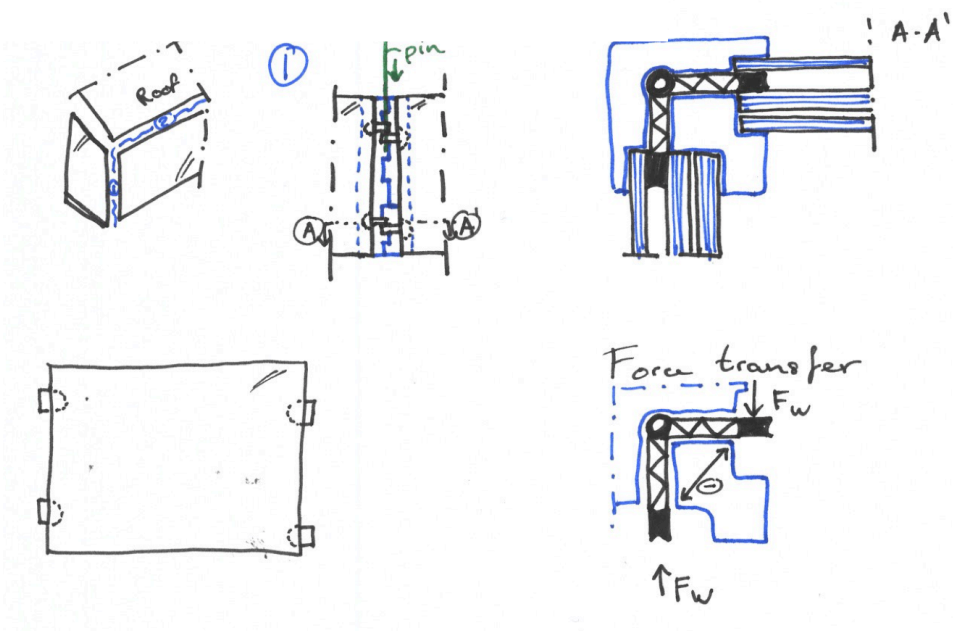
Figure E.11: Schematic design for variant C: Embedded

F
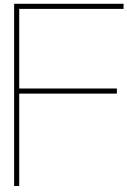
DIANA FEA reports

Two reports per IGU were made as the equivalent glass thickness differs in the ULS and the SLS situation. The content of this appendix:

- IGU $5\,m$ - ULS report
- IGU $5\,m$ - SLS report
- IGU $6\,m$ - ULS report
- IGU $6\,m$ - SLS report
- 'Coffee-cup-hand' system

IGU 5 - ULS

Part of M.Sc. thesis 'Design of a demountable structural glass pavilion'

Wouter Lasonder

15-03-2022

Introduction

Project information

Diana project name	Pro_IGU/Pro.dpf
Analysis aspects	['Structural', 'Groundwater flow', 'Design analysis']
Model dimension	['Three dimensional']
Default mesher type	HEXQUAD
Default mesher order	LINEAR
Diana version	Diana 10.5, Latest update: 2022-02-03 13:49:38
System	Windows NT 6.2 Build 9200
Model sizebox	10.0

Dimensions

Axes	Minimum coordinate [mm]	Maximum coordinate [mm]
X	-5.1e+02	-5.1e+02
Y	-2.5e+03	2.5e+03
Z	0	2.5e+03

Project details

Units

The following units are applied

Quantity	Unit	Symbol
Length	millimeter	mm
Mass	ton	T
Force	newton	N
Time	second	s
Temperature	kelvin	K
Angle	degree	°

Directions

The following directions are defined:

Name	X	Y	Z
X	1	0	0
Y	0	1	0
Z	0	0	1

Model characteristics

The model consists of the following shapes, reinforcements, piles and interfaces:

Shapes

Name	Set	Element Class	Material	Geometry	Seeding method	Element size [mm]	Division
Laminated glass A	Shapes	FLASHL	Glass	Element geometry 1	Divisions	0	5
Laminated glass B	Shapes	FLASHL	Glass	Element geometry 1	Divisions	0	5
Spring supports 1	Shapes	MASS	Springs - boundary		Divisions	0	5
Spring supports 2	Shapes	MASS	Springs - boundary		Divisions	0	5
Spring supports 3	Shapes	MASS	Springs - boundary		Divisions	0	5
Spring supports 4	Shapes	MASS	Springs - boundary		Divisions	0	5
Spring supports 5	Shapes	MASS	Springs - boundary		Divisions	0	5
Spring supports 6	Shapes	MASS	Springs - boundary		Divisions	0	5
Spring supports 7	Shapes	MASS	Springs - boundary		Divisions	0	5
Spring supports 8	Shapes	MASS	Springs - boundary		Divisions	0	5
Spring supports 9	Shapes	MASS	Springs - boundary		Divisions	0	5
Spring supports 10	Shapes	MASS	Springs - boundary		Divisions	0	5
Spring supports 11	Shapes	MASS	Springs - boundary		Divisions	0	5
Spring supports 16	Shapes	MASS	Springs - boundary		Divisions	0	5
Spring supports 17	Shapes	MASS	Springs - boundary		Divisions	0	5
Spring supports 18	Shapes	MASS	Springs - boundary		Divisions	0	5
Spring supports 19	Shapes	MASS	Springs - boundary		Divisions	0	5
Spring supports 20	Shapes	MASS	Springs - boundary		Divisions	0	5
Spring supports 21	Shapes	MASS	Springs - boundary		Divisions	0	5
Spring supports 22	Shapes	MASS	Springs - boundary		Divisions	0	5
Spring supports 23	Shapes	MASS	Springs - boundary		Divisions	0	5
Spring supports 24	Shapes	MASS	Springs - boundary		Divisions	0	5
Spring supports 25	Shapes	MASS	Springs - boundary		Divisions	0	5

Name	Set	Element Class	Material	Geometry	Seeding method	Element size [mm]	Division
Spring supports 26	Shapes	MASS	Springs - boundary		Divisions	0	5
Detail F1_line	Shapes	CLS3B3	Glass	Element geometry 5	Divisions	0	5
Detail F2_line	Shapes	CLS3B3	Glass	Element geometry 5	Divisions	0	5
Detail D1_new	Shapes	FLASHL	Titanium	Element geometry 2	Divisions	0	5
Detail D2_new	Shapes	FLASHL	Titanium	Element geometry 2	Divisions	0	5
Glass Detail D 1	Shapes	FLASHL	Glass	Element geometry 7	Divisions	0	1
Glass Detail D 2	Shapes	FLASHL	Glass	Element geometry 7	Divisions	0	1

Interfaces

Name	Interface Type	Element Class	Material
Spring supports 1	Boundary spring	SPRING	Springs
Spring supports 2	Boundary spring	SPRING	Springs
Spring supports 3	Boundary spring	SPRING	Springs
Spring supports 4	Boundary spring	SPRING	Springs
Spring supports 5	Boundary spring	SPRING	Springs
Spring supports 6	Boundary spring	SPRING	Springs
Spring supports 7	Boundary spring	SPRING	Springs
Spring supports 8	Boundary spring	SPRING	Springs
Spring supports 9	Boundary spring	SPRING	Springs
Spring supports 10	Boundary spring	SPRING	Springs
Spring supports 11	Boundary spring	SPRING	Springs
Spring supports 16	Boundary spring	SPRING	Springs
Spring supports 17	Boundary spring	SPRING	Springs
Spring supports 18	Boundary spring	SPRING	Springs
Spring supports 19	Boundary spring	SPRING	Springs
Spring supports 20	Boundary spring	SPRING	Springs
Spring supports 21	Boundary spring	SPRING	Springs
Spring supports 22	Boundary spring	SPRING	Springs
Spring supports 23	Boundary spring	SPRING	Springs
Spring supports 24	Boundary spring	SPRING	Springs
Spring supports 25	Boundary spring	SPRING	Springs
Spring supports 26	Boundary spring	SPRING	Springs

The Mesh consists of the following parts:

Mesh Sets

Name	# Elements	Material	geometry	Data
Laminated glass A	1110	Glass	Element geometry 1	
Laminated glass B	4003	Glass	Element geometry 1	
Spring supports 1	1	Springs - boundary		
Spring supports 2	1	Springs - boundary		
Spring supports 3	1	Springs - boundary		
Spring supports 4	1	Springs - boundary		
Spring supports 5	1	Springs - boundary		
Spring supports 6	1	Springs - boundary		
Spring supports 7	1	Springs - boundary		
Spring supports 8	1	Springs - boundary		
Spring supports 9	1	Springs - boundary		
Spring supports 10	1	Springs - boundary		
Spring supports 11	1	Springs - boundary		
Spring supports 16	1	Springs - boundary		
Spring supports 17	1	Springs - boundary		
Spring supports 18	1	Springs - boundary		
Spring supports 19	1	Springs - boundary		
Spring supports 20	1	Springs - boundary		
Spring supports 21	1	Springs - boundary		
Spring supports 22	1	Springs - boundary		
Spring supports 23	1	Springs - boundary		
Spring supports 24	1	Springs - boundary		
Spring supports 25	1	Springs - boundary		
Spring supports 26	1	Springs - boundary		
Detail F1_line	2	Glass	Element geometry 5	
Detail F2_line	2	Glass	Element geometry 5	
Detail D1_new	20	Titanium	Element geometry 2	
Detail D2_new	20	Titanium	Element geometry 2	
Glass Detail D 1	19	Glass	Element geometry 7	
Glass Detail D 2	19	Glass	Element geometry 7	
Detail A & F	22	Springs	Springs	

Materials

Material: Glass

Name	Value
Material class	Concrete and masonry
Material model	Linear elastic isotropic
Color	grey
Young's modulus	70000 N/mm^2
Poisson's ratio	0.23
Mass density	2.5e-09 T/mm^3

Material: Titanium

Name	Value
Material class	Steel
Material model	Linear elastic isotropic
Color	steelblue
Young's modulus	106000 N/mm^2
Poisson's ratio	0.34
Mass density	4.26e-09 T/mm^3

Material: Springs

Name	Value
Material class	Springs and dashpots
Material model	Translational spring/dashpot
Color	gold
Spring stiffness	0.5 N/mm
Spring behavior	Force-elongation diagram
Elongation-Force	-5.1 -10000 -5 -2.5 0 0 5 2.5 5.1 10000 mm

Elongation-Force

Material: Springs - boundary

Name	Value
Material class	Mass elements
Material model	Point mass
Color	darkred
Mass/damping behavior	Isotropic translational mass/damping
Concentrated mass	1e-06 T

Material: Detail F

Name	Value
Material class	Interface elements
Material model	Linear elasticity
Color	silver
Type	3D surface interface
Normal stiffness modulus-z	1e+10 N/mm^3
Shear stiffness modulus-x	1e+10 N/mm^3
Shear stiffness modulus-y	1e+10 N/mm^3

Material: Material 6

Name	Value
Material class	Interface elements

Name	Value
Material model	Nonlinear elasticity
Color	silver
Type	3D surface interface
Normal stiffness modulus-z	1e+06 N/mm^3
Shear stiffness modulus-x	1e+06 N/mm^3
Shear stiffness modulus-y	1e+06 N/mm^3
No-tension or diagram	No-tension with shear stiffness reduction
Tension reduction parameters	0 0 mm
Reduction parameters in first shear direction	0 0 mm
Reduction parameters in second shear direction	0 0 mm

Geometry

Geometry: Element geometry 1

Name	Value
Geometry class	Sheets
Geometry model	Regular flat shell elements
Thickness	19.3 mm
Orthotropic thickness	False
Shape factor	1.5

Geometry: Element geometry 2

Name	Value
Geometry class	Sheets
Geometry model	Regular flat shell elements
Thickness	10 mm
Orthotropic thickness	False
Shape factor	1.5

Geometry: Element geometry 3

Name	Value
Geometry class	Lines
Geometry model	Shell line interface elements
Thickness	19.3 mm
Shape definition type	Flat
Direction vector	Normal to shell plane

Name	Value
Direction vector normal to shell plane	0 1 0

Geometry: Element geometry 4

Name	Value
Geometry class	Lines
Geometry model	Regular truss element
Cross-section	1 mm^2

Geometry: Element geometry 5

Name	Value
Geometry class	Lines
Geometry model	3D Class-III beam elements
Shape	Rectangle
Dimensions of a filled rectangle	1 1 mm

Geometry: Element geometry 7

Name	Value
Geometry class	Sheets
Geometry model	Regular flat shell elements
Thickness	9.6 mm
Orthotropic thickness	False
Shape factor	1.5

Geometry: Springs

Name	Value
Geometry class	Points
Geometry model	Translation springs/dashpots
Working direction	1 0 0

Supports and loads

Geometry support sets

Detail D

Name	Target	Translation	Rotation
Detail D	LINE	X,Y	

Detail F_z

Name	Target	Translation	Rotation
Detail F_z	LINE	Z	

Geometry load cases

Permanent loads

Name	Target	Type	Direction	DOF	Value	Unit
Self weight	model	WEIGHT				

Wind

Name	Target	Type	Direction	DOF	Value	Unit
Wind A	SURFAC	FORCE	X		-0.0012	N/mm^2
Wind B	SURFAC	FORCE	X		-0.00086	N/mm^2

Analysis settings

Analysis: Analysis1

Definition

```
Structural nonlinear
  Structural nonlinear
    Evaluate model
      Evaluate elements
        Average nodal normals
          Tolerance angle  = 20
        Evaluate composed elements
      Assemble Elements
        Tolerance  = 1e-06
      Setup matrices
      Setup load vectors
    Nonlinear effects
      Physical nonlinear
        Plasticity
          MMC model
          Tangent stiffness  = First order
          Maximum number of iterations  = 25
          Sub-stepping in internal iteration  = 0.01
          Yield function tolerance  = 0.0001
        Creep
          Creep approximation  = Zero order
          Maximum number of iterations  = 1
          Stress accuracy tolerance  = 0.0001
        Corrosion influence
        Temperature influence
        Concentration influence
        Cracking
          Crack normal stiffness  = Secant
          Threshold angle between cracks  = 60
          Tension cut-off tolerance  = 0.001
        Total strain based cracking
          Crack normal stiffness  = Secant
        Nonlinear elastic material
        Viscoelastic material
        Viscoplastic material
        Maturity dependent material
        Degree of reaction dependent material
        Pressure influence
        Hyperelastic material
        Interface nonlinearity
          Tangent stiffness  = Consistent
          Maximum number of iterations  = 25
          Yield function tolerance  = 0.0001
        Contact
        Material shrinkage
        Material swelling
        Simple soil material
          Tangen  = Linear
        Simple stress dependent material
        Engineering masonry material
        Perfectly matched layer material
        Kotsovos concrete material
      Linear stress/strain determination for linear elements  = False
      Recompute total stress for modified elasticity  = False
    Execute steps
```

```
Execute steps
  Step type  = Load steps
  Load steps
   Load set  = 1
   Steps
     Step size  = Explicit
     Explicit
  Equilibrium iteration
   Maximum number of iterations  = 10
   Continuation method  = False
   Iteration method settings
     Iteration method  = Newton-Raphson
     Newton-Raphson
     Switch  = False
   Convergence criteria
     Simultaneously satisfied criteria  = False
     Force norm
     Displacement norm
  Logging information
   Logging report
     Verbosity  = Brief
     Logging sequence  = Step
   Plasticity information
   Crack information
   Reaction forces information
Execute steps
  Step type  = Load steps
  Load steps
   Load set  = 2
   Steps
     Step size  = Explicit
     Explicit
  Equilibrium iteration
   Maximum number of iterations  = 10
   Continuation method  = False
   Iteration method settings
     Iteration method  = Newton-Raphson
     Newton-Raphson
     Switch  = False
   Convergence criteria
     Simultaneously satisfied criteria  = False
     Force norm
     Displacement norm
  Logging information
   Logging report
     Verbosity  = Brief
     Logging sequence  = Step
   Plasticity information
   Crack information
   Reaction forces information
Solution method
 Method  = Parallel Direct Sparse
 Convergence tolerance  = 1e-08
 Parallel Direct Sparse
   Factorization
Output
```

```
  Output
   Device  = DIANA native
   Option  = Binary
   Seltyp  = PRIMAR
   Select
    Blknam  = OUTPUT
    Modsel  = Complete
    Casety  = STEPS
    Steps
     User selection  = ALL
   Primar
```

DCF Commands

```
*NONLIN LABEL="Structural nonlinear"
  BEGIN EXECUT
    TEXT "new execute block 3"
    BEGIN LOAD
      LOADNR 1
      STEPS EXPLIC
    END LOAD
    ITERAT METHOD NEWTON
  END EXECUT
  BEGIN EXECUT
    TEXT "new execute block 2"
    BEGIN LOAD
      LOADNR 2
      STEPS EXPLIC SIZES 0.05(20)
    END LOAD
    ITERAT METHOD NEWTON
  END EXECUT
  SOLVE PARDIS
  BEGIN OUTPUT
    TEXT "Output"
    BINARY
    SELECT STEPS ALL /
  END OUTPUT
 *END
```

Phases

Results

Analysis1
Load-step 21 , Load-factor 1.0000
Cauchy Total Stresses in-plane principal components layer 1
min: -19.00N/mm² max: 26.46N/mm²

S
(N/mm²)
26.46
20.78
15.09
9.41
3.73
-1.96
-7.64
-13.32
-19.00
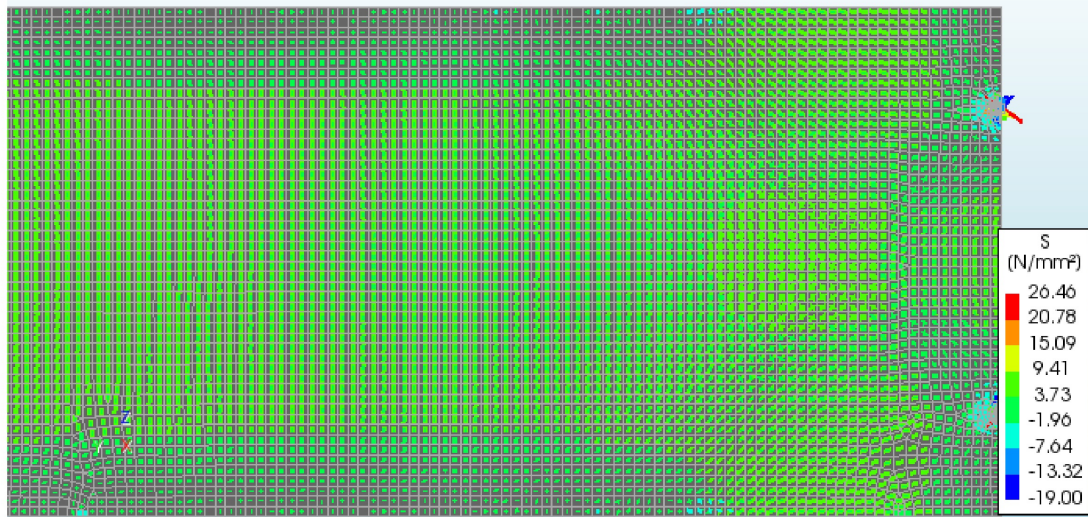
IGU 5 - SLS

Part of M.Sc. thesis 'Design of a structural glass pavilion'

Wouter Lasonder

15-03-2022

Introduction

Project information

Diana project name	Pro_IGU/Pro.dpf
Analysis aspects	['Structural', 'Groundwater flow', 'Design analysis']
Model dimension	['Three dimensional']
Default mesher type	HEXQUAD
Default mesher order	LINEAR
Diana version	Diana 10.5, Latest update: 2022-02-03 13:49:38
System	Windows NT 6.2 Build 9200
Model sizebox	10.0

Dimensions

Axes	Minimum coordinate [mm]	Maximum coordinate [mm]
X	-5.1e+02	-5.1e+02
Y	-2.5e+03	2.5e+03
Z	0	2.5e+03

Project details

Units

The following units are applied

Quantity	Unit	Symbol
Length	millimeter	mm
Mass	ton	T
Force	newton	N
Time	second	s
Temperature	kelvin	K
Angle	degree	°

Directions

The following directions are defined:

Name	X	Y	Z
X	1	0	0
Y	0	1	0
Z	0	0	1

Model characteristics

The model consists of the following shapes, reinforcements, piles and interfaces:

Shapes

Name	Set	Element Class	Material	Geometry	Seeding method	Element size [mm]	Division
Laminated glass A	Shapes	FLASHL	Glass	Element geometry 1	Divisions	0	5
Laminated glass B	Shapes	FLASHL	Glass	Element geometry 1	Divisions	0	5
Spring supports 1	Shapes	MASS	Springs - boundary		Divisions	0	5
Spring supports 2	Shapes	MASS	Springs - boundary		Divisions	0	5
Spring supports 3	Shapes	MASS	Springs - boundary		Divisions	0	5
Spring supports 4	Shapes	MASS	Springs - boundary		Divisions	0	5
Spring supports 5	Shapes	MASS	Springs - boundary		Divisions	0	5
Spring supports 6	Shapes	MASS	Springs - boundary		Divisions	0	5
Spring supports 7	Shapes	MASS	Springs - boundary		Divisions	0	5
Spring supports 8	Shapes	MASS	Springs - boundary		Divisions	0	5
Spring supports 9	Shapes	MASS	Springs - boundary		Divisions	0	5
Spring supports 10	Shapes	MASS	Springs - boundary		Divisions	0	5
Spring supports 11	Shapes	MASS	Springs - boundary		Divisions	0	5
Spring supports 16	Shapes	MASS	Springs - boundary		Divisions	0	5
Spring supports 17	Shapes	MASS	Springs - boundary		Divisions	0	5
Spring supports 18	Shapes	MASS	Springs - boundary		Divisions	0	5
Spring supports 19	Shapes	MASS	Springs - boundary		Divisions	0	5
Spring supports 20	Shapes	MASS	Springs - boundary		Divisions	0	5
Spring supports 21	Shapes	MASS	Springs - boundary		Divisions	0	5
Spring supports 22	Shapes	MASS	Springs - boundary		Divisions	0	5
Spring supports 23	Shapes	MASS	Springs - boundary		Divisions	0	5
Spring supports 24	Shapes	MASS	Springs - boundary		Divisions	0	5
Spring supports 25	Shapes	MASS	Springs - boundary		Divisions	0	5

Name	Set	Element Class	Material	Geometry	Seeding method	Element size [mm]	Division
Spring supports 26	Shapes	MASS	Springs - boundary		Divisions	0	5
Detail F1_line	Shapes	CLS3B3	Glass	Element geometry 5	Divisions	0	5
Detail F2_line	Shapes	CLS3B3	Glass	Element geometry 5	Divisions	0	5
Detail D1_new	Shapes	FLASHL	Titanium	Element geometry 2	Divisions	0	5
Detail D2_new	Shapes	FLASHL	Titanium	Element geometry 2	Divisions	0	5
Glass Detail D 1	Shapes	FLASHL	Glass	Element geometry 7	Divisions	0	1
Glass Detail D 2	Shapes	FLASHL	Glass	Element geometry 7	Divisions	0	1

Interfaces

Name	Interface Type	Element Class	Material
Spring supports 1	Boundary spring	SPRING	Springs
Spring supports 2	Boundary spring	SPRING	Springs
Spring supports 3	Boundary spring	SPRING	Springs
Spring supports 4	Boundary spring	SPRING	Springs
Spring supports 5	Boundary spring	SPRING	Springs
Spring supports 6	Boundary spring	SPRING	Springs
Spring supports 7	Boundary spring	SPRING	Springs
Spring supports 8	Boundary spring	SPRING	Springs
Spring supports 9	Boundary spring	SPRING	Springs
Spring supports 10	Boundary spring	SPRING	Springs
Spring supports 11	Boundary spring	SPRING	Springs
Spring supports 16	Boundary spring	SPRING	Springs
Spring supports 17	Boundary spring	SPRING	Springs
Spring supports 18	Boundary spring	SPRING	Springs
Spring supports 19	Boundary spring	SPRING	Springs
Spring supports 20	Boundary spring	SPRING	Springs
Spring supports 21	Boundary spring	SPRING	Springs
Spring supports 22	Boundary spring	SPRING	Springs
Spring supports 23	Boundary spring	SPRING	Springs
Spring supports 24	Boundary spring	SPRING	Springs
Spring supports 25	Boundary spring	SPRING	Springs
Spring supports 26	Boundary spring	SPRING	Springs

The Mesh consists of the following parts:

Mesh Sets

Name	# Elements	Material	geometry	Data
Laminated glass A	1110	Glass	Element geometry 1	
Laminated glass B	4003	Glass	Element geometry 1	
Spring supports 1	1	Springs - boundary		
Spring supports 2	1	Springs - boundary		
Spring supports 3	1	Springs - boundary		
Spring supports 4	1	Springs - boundary		
Spring supports 5	1	Springs - boundary		
Spring supports 6	1	Springs - boundary		
Spring supports 7	1	Springs - boundary		
Spring supports 8	1	Springs - boundary		
Spring supports 9	1	Springs - boundary		
Spring supports 10	1	Springs - boundary		
Spring supports 11	1	Springs - boundary		
Spring supports 16	1	Springs - boundary		
Spring supports 17	1	Springs - boundary		
Spring supports 18	1	Springs - boundary		
Spring supports 19	1	Springs - boundary		
Spring supports 20	1	Springs - boundary		
Spring supports 21	1	Springs - boundary		
Spring supports 22	1	Springs - boundary		
Spring supports 23	1	Springs - boundary		
Spring supports 24	1	Springs - boundary		
Spring supports 25	1	Springs - boundary		
Spring supports 26	1	Springs - boundary		
Detail F1_line	2	Glass	Element geometry 5	
Detail F2_line	2	Glass	Element geometry 5	
Detail D1_new	20	Titanium	Element geometry 2	
Detail D2_new	20	Titanium	Element geometry 2	
Glass Detail D 1	19	Glass	Element geometry 7	
Glass Detail D 2	19	Glass	Element geometry 7	
Detail A & F	22	Springs	Springs	

Materials

Material: Glass

Name	Value
Material class	Concrete and masonry
Material model	Linear elastic isotropic
Color	grey
Young's modulus	70000 N/mm^2
Poisson's ratio	0.23
Mass density	2.5e-09 T/mm^3

Material: Titanium

Name	Value
Material class	Steel
Material model	Linear elastic isotropic
Color	steelblue
Young's modulus	106000 N/mm^2
Poisson's ratio	0.34
Mass density	4.26e-09 T/mm^3

Material: Springs

Name	Value
Material class	Springs and dashpots
Material model	Translational spring/dashpot
Color	gold
Spring stiffness	0.5 N/mm
Spring behavior	Force-elongation diagram
Elongation-Force	-5.1 -10000 -5 -2.5 0 0 5 2.5 5.1 10000 mm

Elongation-Force

Material: Springs - boundary

Name	Value
Material class	Mass elements
Material model	Point mass
Color	darkred
Mass/damping behavior	Isotropic translational mass/damping
Concentrated mass	1e-06 T

Material: Detail F

Name	Value
Material class	Interface elements
Material model	Linear elasticity
Color	silver
Type	3D surface interface
Normal stiffness modulus-z	1e+10 N/mm^3
Shear stiffness modulus-x	1e+10 N/mm^3
Shear stiffness modulus-y	1e+10 N/mm^3

Material: Material 6

Name	Value
Material class	Interface elements

Name	Value
Material model	Nonlinear elasticity
Color	silver
Type	3D surface interface
Normal stiffness modulus-z	1e+06 N/mm^3
Shear stiffness modulus-x	1e+06 N/mm^3
Shear stiffness modulus-y	1e+06 N/mm^3
No-tension or diagram	No-tension with shear stiffness reduction
Tension reduction parameters	0 0 mm
Reduction parameters in first shear direction	0 0 mm
Reduction parameters in second shear direction	0 0 mm

Geometry

Geometry: Element geometry 1

Name	Value
Geometry class	Sheets
Geometry model	Regular flat shell elements
Thickness	19.2 mm
Orthotropic thickness	False
Shape factor	1.5

Geometry: Element geometry 2

Name	Value
Geometry class	Sheets
Geometry model	Regular flat shell elements
Thickness	10 mm
Orthotropic thickness	False
Shape factor	1.5

Geometry: Element geometry 3

Name	Value
Geometry class	Lines
Geometry model	Shell line interface elements
Thickness	19.2 mm
Shape definition type	Flat
Direction vector	Normal to shell plane

Name	Value
Direction vector normal to shell plane	0 1 0

Geometry: Element geometry 4

Name	Value
Geometry class	Lines
Geometry model	Regular truss element
Cross-section	1 mm^2

Geometry: Element geometry 5

Name	Value
Geometry class	Lines
Geometry model	3D Class-III beam elements
Shape	Rectangle
Dimensions of a filled rectangle	1 1 mm

Geometry: Element geometry 7

Name	Value
Geometry class	Sheets
Geometry model	Regular flat shell elements
Thickness	9.6 mm
Orthotropic thickness	False
Shape factor	1.5

Geometry: Springs

Name	Value
Geometry class	Points
Geometry model	Translation springs/dashpots
Working direction	1 0 0

Supports and loads

Geometry support sets

Detail D

Name	Target	Translation	Rotation
Detail D	LINE	X,Y	

Detail F_z

Name	Target	Translation	Rotation
Detail F_z	LINE	Z	

Geometry load cases

Permanent loads

Name	Target	Type	Direction	DOF	Value	Unit
Self weight	model	WEIGHT				

Wind

Name	Target	Type	Direction	DOF	Value	Unit
Wind A	SURFAC	FORCE	X		-0.0012	N/mm^2
Wind B	SURFAC	FORCE	X		-0.00086	N/mm^2

Analysis settings

Analysis: Analysis1

Definition

```
Structural nonlinear
 Structural nonlinear
  Evaluate model
   Evaluate elements
    Average nodal normals
     Tolerance angle  = 20
    Evaluate composed elements
   Assemble Elements
    Tolerance  = 1e-06
   Setup matrices
   Setup load vectors
  Nonlinear effects
   Physical nonlinear
    Plasticity
     MMC model
     Tangent stiffness  = First order
     Maximum number of iterations  = 25
     Sub-stepping in internal iteration  = 0.01
     Yield function tolerance  = 0.0001
    Creep
     Creep approximation  = Zero order
     Maximum number of iterations  = 1
     Stress accuracy tolerance  = 0.0001
    Corrosion influence
    Temperature influence
    Concentration influence
    Cracking
     Crack normal stiffness  = Secant
     Threshold angle between cracks  = 60
     Tension cut-off tolerance  = 0.001
    Total strain based cracking
     Crack normal stiffness  = Secant
    Nonlinear elastic material
    Viscoelastic material
    Viscoplastic material
    Maturity dependent material
    Degree of reaction dependent material
    Pressure influence
    Hyperelastic material
    Interface nonlinearity
     Tangent stiffness  = Consistent
     Maximum number of iterations  = 25
     Yield function tolerance  = 0.0001
    Contact
    Material shrinkage
    Material swelling
    Simple soil material
     Tangen  = Linear
    Simple stress dependent material
    Engineering masonry material
    Perfectly matched layer material
    Kotsovos concrete material
   Linear stress/strain determination for linear elements  = False
   Recompute total stress for modified elasticity  = False
  Execute steps
```

```
Execute steps
  Step type  = Load steps
  Load steps
    Load set  = 1
    Steps
      Step size  = Explicit
      Explicit
  Equilibrium iteration
    Maximum number of iterations  = 10
    Continuation method  = False
    Iteration method settings
      Iteration method  = Newton-Raphson
      Newton-Raphson
      Switch  = False
    Convergence criteria
      Simultaneously satisfied criteria  = False
      Force norm
      Displacement norm
  Logging information
    Logging report
      Verbosity  = Brief
      Logging sequence  = Step
    Plasticity information
    Crack information
    Reaction forces information
Execute steps
  Step type  = Load steps
  Load steps
    Load set  = 2
    Steps
      Step size  = Explicit
      Explicit
  Equilibrium iteration
    Maximum number of iterations  = 10
    Continuation method  = False
    Iteration method settings
      Iteration method  = Newton-Raphson
      Newton-Raphson
      Switch  = False
    Convergence criteria
      Simultaneously satisfied criteria  = False
      Force norm
      Displacement norm
  Logging information
    Logging report
      Verbosity  = Brief
      Logging sequence  = Step
    Plasticity information
    Crack information
    Reaction forces information
Solution method
 Method  = Parallel Direct Sparse
 Convergence tolerance  = 1e-08
 Parallel Direct Sparse
   Factorization
Output
```

```
   Output
     Device  = DIANA native
     Option  = Binary
     Seltyp  = PRIMAR
     Select
      Blknam  = OUTPUT
      Modsel  = Complete
      Casety  = STEPS
      Steps
       User selection  = ALL
     Primar
```

DCF Commands

```
*NONLIN LABEL="Structural nonlinear"
  BEGIN EXECUT
    TEXT "new execute block 3"
    BEGIN LOAD
      LOADNR 1
      STEPS EXPLIC
    END LOAD
    ITERAT METHOD NEWTON
  END EXECUT
  BEGIN EXECUT
    TEXT "new execute block 2"
    BEGIN LOAD
      LOADNR 2
      STEPS EXPLIC SIZES 0.05(20)
    END LOAD
    ITERAT METHOD NEWTON
  END EXECUT
  SOLVE PARDIS
  BEGIN OUTPUT
    TEXT "Output"
    BINARY
    SELECT STEPS ALL /
  END OUTPUT
 *END
```

Phases

Results

Analysis1
Load-step 20, Load-factor 1.0000
Displacements TDtX
min: -12.50mm max: 0.46mm

TDtX
(mm)

0.46
-1.16
-2.78
-4.40
-6.02
-7.64
-9.26
-10.88
-12.50
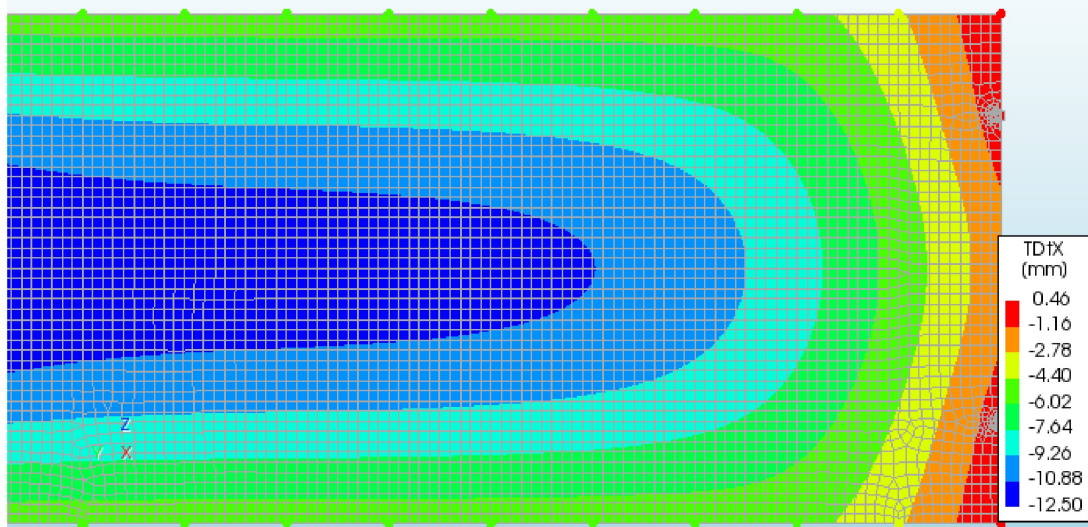
20220222_Pro_IGU_6_ULS_TEST

Part of M.Sc. thesis 'Design of a demountable structural glass pavilion

Wouter Lasonder

15-03-2022

Introduction

Project information

Diana project name	Pro_IGU/Pro.dpf
Analysis aspects	['Structural', 'Groundwater flow', 'Design analysis']
Model dimension	['Three dimensional']
Default mesher type	HEXQUAD
Default mesher order	LINEAR
Diana version	Diana 10.5, Latest update: 2022-02-03 13:49:38
System	Windows NT 6.2 Build 9200
Model sizebox	10.0

Dimensions

Axes	Minimum coordinate [mm]	Maximum coordinate [mm]
X	-3e+03	3e+03
Y	0	0
Z	0	2.5e+03

Project details

Units

The following units are applied

Quantity	Unit	Symbol
Length	millimeter	mm
Mass	ton	T
Force	newton	N
Time	second	s
Temperature	kelvin	K
Angle	radian	rad

Directions

The following directions are defined:

Name	X	Y	Z
X	1	0	0
Y	0	1	0
Z	0	0	1

Model characteristics

The model consists of the following shapes, reinforcements, piles and interfaces:

Shapes

Name	Set	Element Class	Material	Geometry	Seeding method	Element size [mm]	Division
Laminated glass A	Shapes	FLASHL	Glass	Element geometry 1	Divisions	0	5
Laminated glass B	Shapes	FLASHL	Glass	Element geometry 1	Divisions	0	5
Laminated glass C	Shapes	FLASHL	Glass	Element geometry 1	Divisions	0	5
Spring supports 1	Shapes	MASS	Springs - boundary		Divisions	0	5
Spring supports 2	Shapes	MASS	Springs - boundary		Divisions	0	5
Spring supports 3	Shapes	MASS	Springs - boundary		Divisions	0	5
Spring supports 4	Shapes	MASS	Springs - boundary		Divisions	0	5
Spring supports 5	Shapes	MASS	Springs - boundary		Divisions	0	5
Spring supports 6	Shapes	MASS	Springs - boundary		Divisions	0	5
Spring supports 7	Shapes	MASS	Springs - boundary		Divisions	0	5
Spring supports 8	Shapes	MASS	Springs - boundary		Divisions	0	5
Spring supports 9	Shapes	MASS	Springs - boundary		Divisions	0	5
Spring supports 10	Shapes	MASS	Springs - boundary		Divisions	0	5
Spring supports 11	Shapes	MASS	Springs - boundary		Divisions	0	5
Spring supports 12	Shapes	MASS	Springs - boundary		Divisions	0	5
Spring supports 13	Shapes	MASS	Springs - boundary		Divisions	0	5
Spring supports 14	Shapes	MASS	Springs - boundary		Divisions	0	5
Spring supports 15	Shapes	MASS	Springs - boundary		Divisions	0	5
Spring supports 16	Shapes	MASS	Springs - boundary		Divisions	0	5
Spring supports 17	Shapes	MASS	Springs - boundary		Divisions	0	5
Spring supports 18	Shapes	MASS	Springs - boundary		Divisions	0	5
Spring supports 19	Shapes	MASS	Springs - boundary		Divisions	0	5
Spring supports 20	Shapes	MASS	Springs - boundary		Divisions	0	5

Name	Set	Element Class	Material	Geometry	Seeding method	Element size [mm]	Division
Spring supports 21	Shapes	MASS	Springs - boundary		Divisions	0	5
Spring supports 22	Shapes	MASS	Springs - boundary		Divisions	0	5
Spring supports 23	Shapes	MASS	Springs - boundary		Divisions	0	5
Spring supports 24	Shapes	MASS	Springs - boundary		Divisions	0	5
Spring supports 25	Shapes	MASS	Springs - boundary		Divisions	0	5
Spring supports 26	Shapes	MASS	Springs - boundary		Divisions	0	5
Detail F1_line	Shapes	CLS3B3	Glass	Element geometry 5	Divisions	0	5
Detail F2_line	Shapes	CLS3B3	Glass	Element geometry 5	Divisions	0	5
Detail D1_new	Shapes	FLASHL	Titanium	Element geometry 2	Divisions	0	5
Detail D2_new	Shapes	FLASHL	Titanium	Element geometry 2	Divisions	0	5
Detail D3_new	Shapes	FLASHL	Titanium	Element geometry 2	Divisions	0	5
Detail D4_new	Shapes	FLASHL	Titanium	Element geometry 2	Divisions	0	5
Glass Detail D 1	Shapes	FLASHL	Glass	Element geometry 7	Divisions	0	1
Glass Detail D 2	Shapes	FLASHL	Glass	Element geometry 7	Divisions	0	1
Glass Detail D 3	Shapes	FLASHL	Glass	Element geometry 7	Divisions	0	1
Glass Detail D 4	Shapes	FLASHL	Glass	Element geometry 7	Divisions	0	1

Interfaces

Name	Interface Type	Element Class	Material
Spring supports 1	Boundary spring	SPRING	Springs
Spring supports 2	Boundary spring	SPRING	Springs
Spring supports 3	Boundary spring	SPRING	Springs
Spring supports 4	Boundary spring	SPRING	Springs
Spring supports 5	Boundary spring	SPRING	Springs
Spring supports 6	Boundary spring	SPRING	Springs
Spring supports 7	Boundary spring	SPRING	Springs
Spring supports 8	Boundary spring	SPRING	Springs

Name	Interface Type	Element Class	Material
Spring supports 9	Boundary spring	SPRING	Springs
Spring supports 10	Boundary spring	SPRING	Springs
Spring supports 11	Boundary spring	SPRING	Springs
Spring supports 12	Boundary spring	SPRING	Springs
Spring supports 13	Boundary spring	SPRING	Springs
Spring supports 14	Boundary spring	SPRING	Springs
Spring supports 15	Boundary spring	SPRING	Springs
Spring supports 16	Boundary spring	SPRING	Springs
Spring supports 17	Boundary spring	SPRING	Springs
Spring supports 18	Boundary spring	SPRING	Springs
Spring supports 19	Boundary spring	SPRING	Springs
Spring supports 20	Boundary spring	SPRING	Springs
Spring supports 21	Boundary spring	SPRING	Springs
Spring supports 22	Boundary spring	SPRING	Springs
Spring supports 23	Boundary spring	SPRING	Springs
Spring supports 24	Boundary spring	SPRING	Springs
Spring supports 25	Boundary spring	SPRING	Springs
Spring supports 26	Boundary spring	SPRING	Springs

The Mesh consists of the following parts:

Mesh Sets

Name	# Elements	Material	geometry	Data
Laminated glass A	1089	Glass	Element geometry 1	
Laminated glass B	4000	Glass	Element geometry 1	
Laminated glass C	1113	Glass	Element geometry 1	
Spring supports 1	1	Springs - boundary		
Spring supports 2	1	Springs - boundary		
Spring supports 3	1	Springs - boundary		
Spring supports 4	1	Springs - boundary		
Spring supports 5	1	Springs - boundary		
Spring supports 6	1	Springs - boundary		
Spring supports 7	1	Springs - boundary		
Spring supports 8	1	Springs - boundary		
Spring supports 9	1	Springs - boundary		
Spring supports 10	1	Springs - boundary		
Spring supports 11	1	Springs - boundary		
Spring supports 12	1	Springs - boundary		

Name	# Elements	Material	geometry	Data
Spring supports 13	1	Springs - boundary		
Spring supports 14	1	Springs - boundary		
Spring supports 15	1	Springs - boundary		
Spring supports 16	1	Springs - boundary		
Spring supports 17	1	Springs - boundary		
Spring supports 18	1	Springs - boundary		
Spring supports 19	1	Springs - boundary		
Spring supports 20	1	Springs - boundary		
Spring supports 21	1	Springs - boundary		
Spring supports 22	1	Springs - boundary		
Spring supports 23	1	Springs - boundary		
Spring supports 24	1	Springs - boundary		
Spring supports 25	1	Springs - boundary		
Spring supports 26	1	Springs - boundary		
Detail F1_line	2	Glass	Element geometry 5	
Detail F2_line	2	Glass	Element geometry 5	
Detail D1_new	20	Titanium	Element geometry 2	
Detail D2_new	20	Titanium	Element geometry 2	
Detail D3_new	20	Titanium	Element geometry 2	
Detail D4_new	20	Titanium	Element geometry 2	
Glass Detail D 1	19	Glass	Element geometry 7	
Glass Detail D 2	19	Glass	Element geometry 7	
Glass Detail D 3	19	Glass	Element geometry 7	
Glass Detail D 4	19	Glass	Element geometry 7	
Detail A & F	26	Springs	Springs	

Materials

Material: Glass

Name	Value
Material class	Concrete and masonry
Material model	Linear elastic isotropic
Color	grey
Young's modulus	70000 N/mm^2
Poisson's ratio	0.23
Mass density	2.5e-09 T/mm^3

Material: Titanium

Name	Value
Material class	Steel
Material model	Linear elastic isotropic
Color	steelblue
Young's modulus	106000 N/mm^2
Poisson's ratio	0.34
Mass density	4.26e-09 T/mm^3

Material: Detail F

Name	Value
Material class	Interface elements
Material model	Linear elasticity
Color	silver
Type	3D surface interface
Normal stiffness modulus-z	1e+10 N/mm^3
Shear stiffness modulus-x	1e+10 N/mm^3
Shear stiffness modulus-y	1e+10 N/mm^3

Material: Springs

Name	Value
Material class	Springs and dashpots
Material model	Translational spring/dashpot
Color	gold
Spring stiffness	0.5 N/mm
Spring behavior	Force-elongation diagram
Elongation-Force	-5.1 -10000 -5 -2.5 0 0 5 2.5 5.1 10000 mm

Elongation-Force

Material: Springs - boundary

Name	Value
Material class	Mass elements
Material model	Point mass
Color	darkred
Mass/damping behavior	Isotropic translational mass/damping
Concentrated mass	1 T

Material: Material 6

Name	Value
Material class	Interface elements
Material model	Nonlinear elasticity
Color	silver
Type	3D surface interface
Normal stiffness modulus-z	1e+06 N/mm^3
Shear stiffness modulus-x	1e+06 N/mm^3
Shear stiffness modulus-y	1e+06 N/mm^3
No-tension or diagram	No-tension with shear stiffness reduction
Tension reduction parameters	0 0 mm
Reduction parameters in first shear direction	0 0 mm
Reduction parameters in second shear direction	0 0 mm

Geometry

Geometry: Element geometry 1

Name	Value
Geometry class	Sheets
Geometry model	Regular flat shell elements
Thickness	19.3 mm
Orthotropic thickness	False
Shape factor	1.5

Geometry: Element geometry 2

Name	Value
Geometry class	Sheets
Geometry model	Regular flat shell elements
Thickness	10 mm
Orthotropic thickness	False
Shape factor	1.5

Geometry: Element geometry 3

Name	Value
Geometry class	Lines
Geometry model	Shell line interface elements
Thickness	19.3 mm
Shape definition type	Flat
Direction vector	Normal to shell plane
Direction vector normal to shell plane	0 1 0

Geometry: Element geometry 4

Name	Value
Geometry class	Lines
Geometry model	Regular truss element
Cross-section	1 mm^2

Geometry: Element geometry 5

Name	Value
Geometry class	Lines

Name	Value
Geometry model	3D Class-III beam elements
Shape	Rectangle
Dimensions of a filled rectangle	1 1 mm

Geometry: Element geometry 7

Name	Value
Geometry class	Sheets
Geometry model	Regular flat shell elements
Thickness	9.6 mm
Orthotropic thickness	False
Shape factor	1.5

Geometry: Springs

Name	Value
Geometry class	Points
Geometry model	Translation springs/dashpots
Working direction	0 1 0

Supports and loads

Geometry support sets

Detail D

Name	Target	Translation	Rotation
Detail D	LINE	X,Y	

Detail F_z

Name	Target	Translation	Rotation
Detail F_z	LINE	Z	

Geometry load cases

Permanent loads

Name	Target	Type	Direction	DOF	Value	Unit
Self weight	model	WEIGHT				

Wind

Name	Target	Type	Direction	DOF	Value	Unit
Wind A	SURFAC	FORCE	Y		-0.0012	N/mm^2
Wind B	SURFAC	FORCE	Y		-0.00086	N/mm^2
Wind C	SURFAC	FORCE	Y		-0.00065	N/mm^2

Analysis settings

Analysis: Analysis1

Definition

```
Structural nonlinear
 Structural nonlinear
  Evaluate model
   Evaluate elements
    Average nodal normals
     Tolerance angle  = 0.349066
    Evaluate composed elements
   Assemble Elements
    Tolerance  = 1e-06
   Setup matrices
   Setup load vectors
  Nonlinear effects
   Physical nonlinear
    Plasticity
     MMC model
     Tangent stiffness  = First order
     Maximum number of iterations  = 25
     Sub-stepping in internal iteration  = 0.01
     Yield function tolerance  = 0.0001
    Creep
     Creep approximation  = Zero order
     Maximum number of iterations  = 1
     Stress accuracy tolerance  = 0.0001
    Corrosion influence
    Temperature influence
    Concentration influence
    Cracking
     Crack normal stiffness  = Secant
     Threshold angle between cracks  = 60
     Tension cut-off tolerance  = 0.001
    Total strain based cracking
     Crack normal stiffness  = Secant
    Nonlinear elastic material
    Viscoelastic material
    Viscoplastic material
    Maturity dependent material
    Degree of reaction dependent material
    Pressure influence
    Hyperelastic material
    Interface nonlinearity
     Tangent stiffness  = Consistent
     Maximum number of iterations  = 25
     Yield function tolerance  = 0.0001
    Contact
    Material shrinkage
    Material swelling
    Simple soil material
     Tangen  = Linear
    Simple stress dependent material
    Engineering masonry material
    Perfectly matched layer material
    Kotsovos concrete material
   Linear stress/strain determination for linear elements  = False
   Recompute total stress for modified elasticity  = False
  Execute steps
```

```
   Execute steps
     Step type  = Load steps
     Load steps
       Load set  = 1
       Steps
         Step size  = Explicit
         Explicit
     Equilibrium iteration
       Maximum number of iterations  = 10
       Continuation method  = False
       Iteration method settings
         Iteration method  = Newton-Raphson
         Newton-Raphson
         Switch  = False
       Convergence criteria
         Simultaneously satisfied criteria  = False
         Force norm
         Displacement norm
     Logging information
       Logging report
         Verbosity  = Brief
         Logging sequence  = Step
       Plasticity information
       Crack information
       Reaction forces information
 Solution method
   Method  = Parallel Direct Sparse
   Convergence tolerance  = 1e-08
   Parallel Direct Sparse
     Factorization
 Output
   Output
     Device  = DIANA native
     Option  = Binary
     Seltyp  = PRIMAR
     Select
       Blknam  = OUTPUT
       Modsel  = Complete
       Casety  = STEPS
       Steps
         User selection  = ALL
     Primar
```

DCF Commands

```
*NONLIN LABEL="Structural nonlinear"
  BEGIN EXECUT
    TEXT "new execute block 2"
    BEGIN LOAD
      LOADNR 1
      STEPS EXPLIC SIZES 0.05(20)
    END LOAD
    ITERAT METHOD NEWTON
  END EXECUT
  SOLVE PARDIS
  BEGIN OUTPUT
    TEXT "Output"
    BINARY
    SELECT STEPS ALL /
  END OUTPUT
*END
```

Phases

Results

20220222_Pro_IGU_6_SLS_TEST

Part of M.Sc. thesis 'Design of a demountable structural glass pavilion

Wouter Lasonder

15-03-2022

Introduction

Project information

Diana project name	Pro_IGU/Pro.dpf
Analysis aspects	['Structural', 'Groundwater flow', 'Design analysis']
Model dimension	['Three dimensional']
Default mesher type	HEXQUAD
Default mesher order	LINEAR
Diana version	Diana 10.5, Latest update: 2022-02-03 13:49:38
System	Windows NT 6.2 Build 9200
Model sizebox	10.0

Dimensions

Axes	Minimum coordinate [mm]	Maximum coordinate [mm]
X	-3e+03	3e+03
Y	0	0
Z	0	2.5e+03

Project details

Units

The following units are applied

Quantity	Unit	Symbol
Length	millimeter	mm
Mass	ton	T
Force	newton	N
Time	second	s
Temperature	kelvin	K
Angle	radian	rad

Directions

The following directions are defined:

Name	X	Y	Z
X	1	0	0
Y	0	1	0
Z	0	0	1

Model characteristics

The model consists of the following shapes, reinforcements, piles and interfaces:

Shapes

Name	Set	Element Class	Material	Geometry	Seeding method	Element size [mm]	Division
Laminated glass A	Shapes	FLASHL	Glass	Element geometry 1	Divisions	0	5
Laminated glass B	Shapes	FLASHL	Glass	Element geometry 1	Divisions	0	5
Laminated glass C	Shapes	FLASHL	Glass	Element geometry 1	Divisions	0	5
Spring supports 1	Shapes	MASS	Springs - boundary		Divisions	0	5
Spring supports 2	Shapes	MASS	Springs - boundary		Divisions	0	5
Spring supports 3	Shapes	MASS	Springs - boundary		Divisions	0	5
Spring supports 4	Shapes	MASS	Springs - boundary		Divisions	0	5
Spring supports 5	Shapes	MASS	Springs - boundary		Divisions	0	5
Spring supports 6	Shapes	MASS	Springs - boundary		Divisions	0	5
Spring supports 7	Shapes	MASS	Springs - boundary		Divisions	0	5
Spring supports 8	Shapes	MASS	Springs - boundary		Divisions	0	5
Spring supports 9	Shapes	MASS	Springs - boundary		Divisions	0	5
Spring supports 10	Shapes	MASS	Springs - boundary		Divisions	0	5
Spring supports 11	Shapes	MASS	Springs - boundary		Divisions	0	5
Spring supports 12	Shapes	MASS	Springs - boundary		Divisions	0	5
Spring supports 13	Shapes	MASS	Springs - boundary		Divisions	0	5
Spring supports 14	Shapes	MASS	Springs - boundary		Divisions	0	5
Spring supports 15	Shapes	MASS	Springs - boundary		Divisions	0	5
Spring supports 16	Shapes	MASS	Springs - boundary		Divisions	0	5
Spring supports 17	Shapes	MASS	Springs - boundary		Divisions	0	5
Spring supports 18	Shapes	MASS	Springs - boundary		Divisions	0	5
Spring supports 19	Shapes	MASS	Springs - boundary		Divisions	0	5
Spring supports 20	Shapes	MASS	Springs - boundary		Divisions	0	5

Name	Set	Element Class	Material	Geometry	Seeding method	Element size [mm]	Division
Spring supports 21	Shapes	MASS	Springs - boundary		Divisions	0	5
Spring supports 22	Shapes	MASS	Springs - boundary		Divisions	0	5
Spring supports 23	Shapes	MASS	Springs - boundary		Divisions	0	5
Spring supports 24	Shapes	MASS	Springs - boundary		Divisions	0	5
Spring supports 25	Shapes	MASS	Springs - boundary		Divisions	0	5
Spring supports 26	Shapes	MASS	Springs - boundary		Divisions	0	5
Detail F1_line	Shapes	CLS3B3	Glass	Element geometry 5	Divisions	0	5
Detail F2_line	Shapes	CLS3B3	Glass	Element geometry 5	Divisions	0	5
Detail D1_new	Shapes	FLASHL	Titanium	Element geometry 2	Divisions	0	5
Detail D2_new	Shapes	FLASHL	Titanium	Element geometry 2	Divisions	0	5
Detail D3_new	Shapes	FLASHL	Titanium	Element geometry 2	Divisions	0	5
Detail D4_new	Shapes	FLASHL	Titanium	Element geometry 2	Divisions	0	5
Glass Detail D 1	Shapes	FLASHL	Glass	Element geometry 7	Divisions	0	1
Glass Detail D 2	Shapes	FLASHL	Glass	Element geometry 7	Divisions	0	1
Glass Detail D 3	Shapes	FLASHL	Glass	Element geometry 7	Divisions	0	1
Glass Detail D 4	Shapes	FLASHL	Glass	Element geometry 7	Divisions	0	1

Interfaces

Name	Interface Type	Element Class	Material
Spring supports 1	Boundary spring	SPRING	Springs
Spring supports 2	Boundary spring	SPRING	Springs
Spring supports 3	Boundary spring	SPRING	Springs
Spring supports 4	Boundary spring	SPRING	Springs
Spring supports 5	Boundary spring	SPRING	Springs
Spring supports 6	Boundary spring	SPRING	Springs
Spring supports 7	Boundary spring	SPRING	Springs
Spring supports 8	Boundary spring	SPRING	Springs

Name	Interface Type	Element Class	Material
Spring supports 9	Boundary spring	SPRING	Springs
Spring supports 10	Boundary spring	SPRING	Springs
Spring supports 11	Boundary spring	SPRING	Springs
Spring supports 12	Boundary spring	SPRING	Springs
Spring supports 13	Boundary spring	SPRING	Springs
Spring supports 14	Boundary spring	SPRING	Springs
Spring supports 15	Boundary spring	SPRING	Springs
Spring supports 16	Boundary spring	SPRING	Springs
Spring supports 17	Boundary spring	SPRING	Springs
Spring supports 18	Boundary spring	SPRING	Springs
Spring supports 19	Boundary spring	SPRING	Springs
Spring supports 20	Boundary spring	SPRING	Springs
Spring supports 21	Boundary spring	SPRING	Springs
Spring supports 22	Boundary spring	SPRING	Springs
Spring supports 23	Boundary spring	SPRING	Springs
Spring supports 24	Boundary spring	SPRING	Springs
Spring supports 25	Boundary spring	SPRING	Springs
Spring supports 26	Boundary spring	SPRING	Springs

The Mesh consists of the following parts:

Mesh Sets

Name	# Elements	Material	geometry	Data
Laminated glass A	1089	Glass	Element geometry 1	
Laminated glass B	4000	Glass	Element geometry 1	
Laminated glass C	1113	Glass	Element geometry 1	
Spring supports 1	1	Springs - boundary		
Spring supports 2	1	Springs - boundary		
Spring supports 3	1	Springs - boundary		
Spring supports 4	1	Springs - boundary		
Spring supports 5	1	Springs - boundary		
Spring supports 6	1	Springs - boundary		
Spring supports 7	1	Springs - boundary		
Spring supports 8	1	Springs - boundary		
Spring supports 9	1	Springs - boundary		
Spring supports 10	1	Springs - boundary		
Spring supports 11	1	Springs - boundary		
Spring supports 12	1	Springs - boundary		

Name	# Elements	Material	geometry	Data
Spring supports 13	1	Springs - boundary		
Spring supports 14	1	Springs - boundary		
Spring supports 15	1	Springs - boundary		
Spring supports 16	1	Springs - boundary		
Spring supports 17	1	Springs - boundary		
Spring supports 18	1	Springs - boundary		
Spring supports 19	1	Springs - boundary		
Spring supports 20	1	Springs - boundary		
Spring supports 21	1	Springs - boundary		
Spring supports 22	1	Springs - boundary		
Spring supports 23	1	Springs - boundary		
Spring supports 24	1	Springs - boundary		
Spring supports 25	1	Springs - boundary		
Spring supports 26	1	Springs - boundary		
Detail F1_line	2	Glass	Element geometry 5	
Detail F2_line	2	Glass	Element geometry 5	
Detail D1_new	20	Titanium	Element geometry 2	
Detail D2_new	20	Titanium	Element geometry 2	
Detail D3_new	20	Titanium	Element geometry 2	
Detail D4_new	20	Titanium	Element geometry 2	
Glass Detail D 1	19	Glass	Element geometry 7	
Glass Detail D 2	19	Glass	Element geometry 7	
Glass Detail D 3	19	Glass	Element geometry 7	
Glass Detail D 4	19	Glass	Element geometry 7	
Detail A & F	26	Springs	Springs	

Materials

Material: Glass

Name	Value
Material class	Concrete and masonry
Material model	Linear elastic isotropic
Color	grey
Young's modulus	70000 N/mm^2
Poisson's ratio	0.23
Mass density	2.5e-09 T/mm^3

Material: Titanium

Name	Value
Material class	Steel
Material model	Linear elastic isotropic
Color	steelblue
Young's modulus	106000 N/mm^2
Poisson's ratio	0.34
Mass density	4.26e-09 T/mm^3

Material: Detail F

Name	Value
Material class	Interface elements
Material model	Linear elasticity
Color	silver
Type	3D surface interface
Normal stiffness modulus-z	1e+10 N/mm^3
Shear stiffness modulus-x	1e+10 N/mm^3
Shear stiffness modulus-y	1e+10 N/mm^3

Material: Springs

Name	Value
Material class	Springs and dashpots
Material model	Translational spring/dashpot
Color	gold
Spring stiffness	0.5 N/mm
Spring behavior	Force-elongation diagram
Elongation-Force	-5.1 -10000 -5 -2.5 0 0 5 2.5 5.1 10000 mm

Elongation-Force

Material: Springs - boundary

Name	Value
Material class	Mass elements
Material model	Point mass
Color	darkred
Mass/damping behavior	Isotropic translational mass/damping
Concentrated mass	1 T

Material: Material 6

Name	Value
Material class	Interface elements
Material model	Nonlinear elasticity
Color	silver
Type	3D surface interface
Normal stiffness modulus-z	1e+06 N/mm^3
Shear stiffness modulus-x	1e+06 N/mm^3
Shear stiffness modulus-y	1e+06 N/mm^3
No-tension or diagram	No-tension with shear stiffness reduction
Tension reduction parameters	0 0 mm
Reduction parameters in first shear direction	0 0 mm
Reduction parameters in second shear direction	0 0 mm

Geometry

Geometry: Element geometry 1

Name	Value
Geometry class	Sheets
Geometry model	Regular flat shell elements
Thickness	19.2 mm
Orthotropic thickness	False
Shape factor	1.5

Geometry: Element geometry 2

Name	Value
Geometry class	Sheets
Geometry model	Regular flat shell elements
Thickness	10 mm
Orthotropic thickness	False
Shape factor	1.5

Geometry: Element geometry 3

Name	Value
Geometry class	Lines
Geometry model	Shell line interface elements
Thickness	19.3 mm
Shape definition type	Flat
Direction vector	Normal to shell plane
Direction vector normal to shell plane	0 1 0

Geometry: Element geometry 4

Name	Value
Geometry class	Lines
Geometry model	Regular truss element
Cross-section	1 mm^2

Geometry: Element geometry 5

Name	Value
Geometry class	Lines

Name	Value
Geometry model	3D Class-III beam elements
Shape	Rectangle
Dimensions of a filled rectangle	1 1 mm

Geometry: Element geometry 7

Name	Value
Geometry class	Sheets
Geometry model	Regular flat shell elements
Thickness	9.6 mm
Orthotropic thickness	False
Shape factor	1.5

Geometry: Springs

Name	Value
Geometry class	Points
Geometry model	Translation springs/dashpots
Working direction	0 1 0

Supports and loads

Geometry support sets

Detail D

Name	Target	Translation	Rotation
Detail D	LINE	X,Y	

Detail F_z

Name	Target	Translation	Rotation
Detail F_z	LINE	Z	

Geometry load cases

Permanent loads

Name	Target	Type	Direction	DOF	Value	Unit
Self weight	model	WEIGHT				

Wind

Name	Target	Type	Direction	DOF	Value	Unit
Wind A	SURFAC	FORCE	Y		-0.0012	N/mm^2
Wind B	SURFAC	FORCE	Y		-0.00086	N/mm^2
Wind C	SURFAC	FORCE	Y		-0.00065	N/mm^2

Analysis settings

Analysis: Analysis1

Definition

```
Structural nonlinear
 Structural nonlinear
  Evaluate model
   Evaluate elements
    Average nodal normals
     Tolerance angle  = 0.349066
    Evaluate composed elements
   Assemble Elements
    Tolerance  = 1e-06
   Setup matrices
   Setup load vectors
  Nonlinear effects
   Physical nonlinear
    Plasticity
     MMC model
     Tangent stiffness  = First order
     Maximum number of iterations  = 25
     Sub-stepping in internal iteration  = 0.01
     Yield function tolerance  = 0.0001
    Creep
     Creep approximation  = Zero order
     Maximum number of iterations  = 1
     Stress accuracy tolerance  = 0.0001
    Corrosion influence
    Temperature influence
    Concentration influence
    Cracking
     Crack normal stiffness  = Secant
     Threshold angle between cracks  = 60
     Tension cut-off tolerance  = 0.001
    Total strain based cracking
     Crack normal stiffness  = Secant
    Nonlinear elastic material
    Viscoelastic material
    Viscoplastic material
    Maturity dependent material
    Degree of reaction dependent material
    Pressure influence
    Hyperelastic material
    Interface nonlinearity
     Tangent stiffness  = Consistent
     Maximum number of iterations  = 25
     Yield function tolerance  = 0.0001
    Contact
    Material shrinkage
    Material swelling
    Simple soil material
     Tangen  = Linear
    Simple stress dependent material
    Engineering masonry material
    Perfectly matched layer material
    Kotsovos concrete material
   Linear stress/strain determination for linear elements  = False
   Recompute total stress for modified elasticity  = False
  Execute steps
```

```
Execute steps
  Step type  = Load steps
  Load steps
    Load set  = 1
    Steps
      Step size  = Explicit
      Explicit
  Equilibrium iteration
    Maximum number of iterations  = 10
    Continuation method  = False
    Iteration method settings
      Iteration method  = Newton-Raphson
      Newton-Raphson
      Switch  = False
    Convergence criteria
      Simultaneously satisfied criteria  = False
      Force norm
      Displacement norm
  Logging information
    Logging report
      Verbosity  = Brief
      Logging sequence  = Step
    Plasticity information
    Crack information
    Reaction forces information
Solution method
  Method  = Parallel Direct Sparse
  Convergence tolerance  = 1e-08
  Parallel Direct Sparse
    Factorization
Output
  Output
    Device  = DIANA native
    Option  = Binary
    Seltyp  = PRIMAR
    Select
      Blknam  = OUTPUT
      Modsel  = Complete
      Casety  = STEPS
      Steps
        User selection  = ALL
    Primar
```

DCF Commands

```
*NONLIN LABEL="Structural nonlinear"
  BEGIN EXECUT
    TEXT "new execute block 2"
    BEGIN LOAD
      LOADNR 1
      STEPS EXPLIC SIZES 0.05(20)
    END LOAD
    ITERAT METHOD NEWTON
  END EXECUT
  SOLVE PARDIS
  BEGIN OUTPUT
    TEXT "Output"
    BINARY
    SELECT STEPS ALL /
  END OUTPUT
*END
```

Phases

Results

Analysis1
Load-step 20, Load-factor 1.0000
Displacements TDtY
min: -14.28mm max: 1.00mm

Introduction

Project information

Diana project name	Pro_Detail_D/Untitled.dpf
Analysis aspects	['Structural', 'Groundwater flow', 'Design analysis']
Model dimension	['Three dimensional']
Default mesher type	HEXQUAD
Default mesher order	LINEAR
Diana version	Diana 10.5, Latest update: 2022-02-03 13:49:38
System	Windows NT 6.2 Build 9200
Model sizebox	1.0

Dimensions

Axes	Minimum coordinate [mm]	Maximum coordinate [mm]
X	-1.5e+02	20
Y	0	0
Z	-24	0

Project details

Units

The following units are applied

Quantity	Unit	Symbol
Length	millimeter	mm
Mass	ton	T
Force	newton	N
Time	second	s
Temperature	kelvin	K
Angle	radian	rad

Directions

The following directions are defined:

Name	X	Y	Z
X	1	0	0
Y	0	1	0
Z	0	0	1
	0	-1	0

Model characteristics

The model consists of the following shapes, reinforcements, piles and interfaces:

Shapes

Name	Set	Element Class	Material	Geometry	Seeding method	Element size [mm]	Division
Sheet 1	Shapes	FLASHL	Glass	Element geometry 1	ElementSize	0.2	0
Sheet 2	Shapes	FLASHL	Glass	Element geometry 1	ElementSize	0.2	0
Sheet 3	Shapes	FLASHL	Glass	Element geometry 1	ElementSize	0.2	0
SentryGlas sheet	Shapes	FLASHL	SentryGlas	Element geometry 1	ElementSize	0.2	0
Titanium left	Shapes	FLASHL	Titanium	Element geometry 1	ElementSize	0.2	0
Titanium right	Shapes	FLASHL	Titanium	Element geometry 1	ElementSize	0.2	0

Interfaces

Name	Interface Type	Element Class	Material
Titanium left	Unite		
Titanium right			

The Mesh consists of the following parts:

Mesh Sets

Name	# Elements	Material	geometry	Data
Sheet 1	1701	Glass	Element geometry 1	
Sheet 2	2840	Glass	Element geometry 1	
Sheet 3	1802	Glass	Element geometry 1	
SentryGlas sheet	12099	SentryGlas	Element geometry 1	
Titanium left	742	Titanium	Element geometry 1	
Titanium right	210	Titanium	Element geometry 1	

Materials

Material: Glass

Name	Value
Material class	Concrete and masonry
Material model	Linear elastic isotropic
Color	grey
Young's modulus	70000 N/mm^2
Poisson's ratio	0.23

Material: Titanium

Name	Value
Material class	Concrete and masonry
Material model	Linear elastic isotropic
Color	grey
Young's modulus	106000 N/mm^2
Poisson's ratio	0.34

Material: SentryGlas

Name	Value
Material class	Concrete and masonry
Material model	Linear elastic isotropic
Color	grey
Young's modulus	612 N/mm^2
Poisson's ratio	0.449

Material: Interface

Name	Value
Material class	Interface elements
Material model	Nonlinear elasticity
Color	silver
Type	3D line interface (2 shear, 1 normal)
Normal stiffness modulus-y	1e+08 N/mm^3
Shear stiffness modulus-x	1e+08 N/mm^3
Shear stiffness modulus-z	1e+08 N/mm^3
No-tension or diagram	No-tension with shear stiffness reduction
Tension reduction parameters	0 1e-08 mm
Reduction parameters in first shear direction	0 1e-08 mm
Reduction parameters in second shear direction	0 1e-08 mm

Geometry

Geometry: Element geometry 1

Name	Value
Geometry class	Sheets
Geometry model	Regular flat shell elements
Thickness	450 mm
Orthotropic thickness	False
Shape factor	1.5

Geometry: Element geometry 2

Name	Value
Geometry class	Lines
Geometry model	3D line interface elements (2 shear, 1 normal)
Thickness	450 mm
Shape definition type	Flat
Direction vector	Normal to plane
Direction vector normal to plane	0 1 0

Supports and loads

Geometry support sets

Support 1

Name	Target	Translation	Rotation

Name	Target	Translation	Rotation
Support 1	LINE	X,Z,	X

Geometry load cases

Wind

Name	Target	Type	Direction	DOF	Value	Unit
Wind load on D	POINT	FORCE	Z		-4725	N

Analysis settings

Analysis: Analysis1

Definition

```
Structural nonlinear
 Structural nonlinear
  Evaluate model
   Evaluate elements
    Average nodal normals
     Tolerance angle  = 0.349066
    Evaluate composed elements
   Assemble Elements
    Tolerance  = 1e-06
   Setup matrices
   Setup load vectors
  Nonlinear effects
   Physical nonlinear
    Plasticity
     MMC model
     Tangent stiffness  = First order
     Maximum number of iterations  = 25
     Sub-stepping in internal iteration  = 0.01
     Yield function tolerance  = 0.0001
    Creep
     Creep approximation  = Zero order
     Maximum number of iterations  = 1
     Stress accuracy tolerance  = 0.0001
    Corrosion influence
    Temperature influence
    Concentration influence
    Cracking
     Crack normal stiffness  = Secant
     Threshold angle between cracks  = 60
     Tension cut-off tolerance  = 0.001
    Total strain based cracking
     Crack normal stiffness  = Secant
    Nonlinear elastic material
    Viscoelastic material
    Viscoplastic material
    Maturity dependent material
    Degree of reaction dependent material
    Pressure influence
    Hyperelastic material
    Interface nonlinearity
     Tangent stiffness  = Consistent
     Maximum number of iterations  = 25
     Yield function tolerance  = 0.0001
    Contact
    Material shrinkage
    Material swelling
    Simple soil material
     Tangen  = Linear
    Simple stress dependent material
    Engineering masonry material
    Perfectly matched layer material
    Kotsovos concrete material
   Linear stress/strain determination for linear elements  = False
   Recompute total stress for modified elasticity  = False
  Execute steps
```

```
      Execute steps
       Step type  = Load steps
       Load steps
        Load set  = 1
        Steps
          Step size  = Automatic
          Automatic step size
       Equilibrium iteration
        Maximum number of iterations  = 50
        Continuation method  = True
        Iteration method settings
          Iteration method  = Newton-Raphson
          Newton-Raphson
          Switch  = False
        Line Search
          Maximum scale factor  = 1
          Minimum scale factor  = 0.1
          Energy stop criterion  = 0.8
          Regula-Falsi stop criterion  = 0.1
          Maximum number of searches  = 5
        Convergence criteria
          Simultaneously satisfied criteria  = False
          Force norm
          Displacement norm
          Energy norm
       Logging information
        Logging report
          Verbosity  = Brief
          Logging sequence  = Step
        Plasticity information
        Crack information
        Reaction forces information
    Solution method
     Method  = Parallel Direct Sparse
     Convergence tolerance  = 1e-08
     Parallel Direct Sparse
      Factorization
    Output
     Output
      Device  = DIANA native
      Option  = Binary
      Seltyp  = PRIMAR
      Select
       Blknam  = OUTPUT
       Modsel  = Complete
       Casety  = STEPS
       Steps
         User selection  = ALL
      Primar
```

DCF Commands
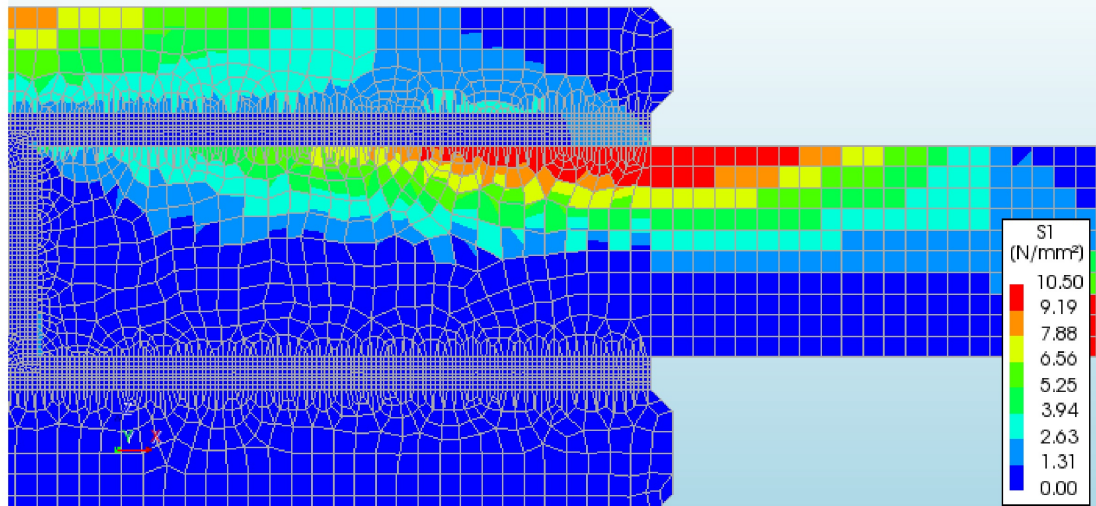
```
*NONLIN LABEL="Structural nonlinear"
  BEGIN EXECUT
    BEGIN LOAD
      LOADNR 1
      STEPS AUTOMA
    END LOAD
    BEGIN ITERAT
      MAXITE 50
      CONTIN ON
      METHOD NEWTON MODIFI
      LINESE
      CONVER ENERGY OFF
    END ITERAT
  END EXECUT
  SOLVE PARDIS
  BEGIN OUTPUT
    TEXT "Output"
    BINARY
    SELECT STEPS ALL /
  END OUTPUT
*END
```

Phases

Results

Analysis1
Load-step 1, Load-factor 1.0000, Wind
Cauchy Total Stresses S1 maximum of 3 layers
min: 0.00N/mm² max: 30.56N/mm²

Analysis1
Load-step 1, Load-factor 1.0000, Wind
Cauchy Total Stresses S1 maximum of 3 layers
min: 0.00N/mm² max: 30.56N/mm²

S1
(N/mm²)

10.50
9.19
7.88
6.56
5.25
3.94
2.63
1.31
0.00